Radome lightning protection - a study of impulse flashover of radar-transparent, lightning diverter strips.

Thesis presented for the degree of Doctor of Philosophy in Electrical Engineering of the University of Strathclyde, Glasgow.

Siew Wah Hoon

Department of Electrical Engineering

June 1982.

PAGE
NUMBERS
CUT OFF
IN
ORIGINAL

SUMMARY

The thesis presents the results of an initial study of the flashover characteristics of segmented - and "Dayton-Granger" - lightning diverter strips, both of which are intended for use as radome protection devices.

The hazards of lightning strikes to or near an aircraft are considered in Chaper 1 and these hazards are related to the various parameters of lightning discharges. The types of discharge are classified into two broad categories, viz. positive and negative. Owing to the complex nature of a lightning discharge, standardised test waveforms, to simulate lightning, have been defined for the purpose of laboratory testing. The last section of the chapter deals with aircraft protection against lightning strikes and with radome protection in particular.

The next chapter reviews the different techniques used in radome protection and the high current; high voltage and radar compatibility tests on segmented strips which have been conducted by researchers in the U.S.A. and the high current tests undertaken in the U.K. The segmented strip consists of a series of conducting segments joined by a resistive layer with the whole assembly mounted on a dielectric substrate. Radar transparency is achieved when the resistive layer has a resistance of at least 260 k ohms/metre and the segments are less than one-eighth of the wavelength of the radar signals.

Chapter 3 reviews the many studies made on surface flashover

characteristics and the mechanisms leading to flashover, both in vacuum and in gases. Although much work has been done, there is still no general agreement on the mechanism of flashover in vacuum. Surface flashover in gases is still being actively studied and much has yet to be learned. Surface flashover along a segmented strip consists of a series of flashovers across very short gaps. A flashover mechanism of such strips is proposed.

The following chapter describes the apparatus and the measuring techniques used in the present study. Various electrodes were designed to hold the strip and to allow the strip length to be varied. In view of the limited heat capacity of the resistive layer in the segmented strip, a parallel chopping gap was designed to operate over a wide range of applied voltages for a fixed gap setting in order to limit the energy input. A current probe, designed to minimise the effect of the displacement current flow between high voltage-and earth-electrodes, is also described. The various apparatus used include a Ferranti-impulse generator; a converter camera/intensifier system for time-resolved photography; a scanning-electron-microscope and X-ray spectroscope, for study of the strip surface, and an automatic recording microdensitometer for analyses of streak-photographs.

Results of preliminary investigations are presented in Chapter 5. The intersegment resistances of the segmented strip were found to be unequal but had an average value of 45 k ohms. These resistances fell after repeated applications of the voltage impulse and this fall is considered to be due to the gradual removal of the initial

high contact resistance existing between each segment and the resistive layer. When this resistance had fallen to a constant value of about 5 k ohms, the strip was considered to be resistance-stabilised. Investigation on the heat capacity of the resistive layer in the segmented strip is also presented. This investigation revealed that damage to the segmented strip is highly probable if it withstood the applied voltage impulse.

In the following chapter, the conditioning characteristics of a segmented strip are presented first. In the course of an 'Up & Down' test, the flashover voltage was found to fall with repeated applications of the voltage impulse. This fall in flashover voltage is unlikely to be due to the process of resistance-stabilisation but could be due to the surface conditioning. In the conditioned state, the fall in flashover voltage ceased. The flashover voltage and time-lag characteristics of a conditioned segmented strip are presented in the next section. The flashover strength of the strip was found to be affected by field non-uniformity in the gap. An approximately proportional relationship with strip length was obtained for a strip situated axially in a uniform field gap but a non-linear relationship was obtained for a strip situated in a non-uniform field gap. Time-lags to flashover are, generally, less than the time-to-crest, 3 microseconds, of the applied voltage impulse. The flashover results indicate that a conditioned strip would be a suitable radome protection device because its flashover strength is much lower than that of the unbridged air gap. Time-resolved photographic studies of the light emission from a developing strip-flashover, for a strip situated

in a uniform field gap, show that discharges were not initiated at one end and then propagated to the other. Instead, various simultaneous discharges were initiated at different points along the strip and then propagated to flashover if the applied voltage was high enough. Current records have revealed that isolated intersegment discharges can occur without propagating to produce a flashover.

Chapter 7 reports the performance of the "Dayton-Granger" strip which is basically a flexible non-conducting strip with a layer of micro-conducting-particles on one surface. As for the segmented strip, the flashover voltage falls to a stable level. In this stable phase, "arrested-flashovers" could occur. An increase in the applied voltage, as low as 1.5%, would cause a flashover to occur if the preceding outcome had been an "arrested-flashover". This stable phase is followed by a deteriorating phase in which the flashover strength increased rapidly with repeated voltage applications. An explanation for such behaviour is presented. Flashover of the strip, in the stable phase, occurs on the wavetail of the applied voltage impulse and time-lag up to 42 microseconds were recorded. Photographic studies of the light emission from a developing flashover showed that discharges could start at different points along a strip. It was also observed that the discharge path of a flashover tends to follow that of the preceding "arrested-flashover".

Conclusions and recommendations for further work are presented in the last chapter. Based on flashover strength, the "Dayton-Granger"

strip is superior to the segmented strip. However, this superiority is offset by its much longer time-lags to flashover. It is suggested that further work be undertaken on the two types of strips to investigate the effects, on their flashover characteristics, of variation of impulse waveshape and polarity and applied field. Recommendations are also made for studies using model segmented strips to investigate the effect of variation of the strip parameters on the flashover characteristics.

Notation of tables, diagrams and appendices

All tables, diagrams and appendices are numbered as Table I.w; figure J.x or Appendix K.y where I, J and K refer to the chapter in which they are first mentioned and w, x and y are numbers, starting from 1, and used to identify the various tables, diagrams and appendices in any one chapter. Hence, for example, figure 5.15 refers to the fifteenth figure in chapter 5 and Appendix 4.3 refers to the third appendix in chapter 4.

Symbols

In general, a voltage level of V_x, where x is a number between 0 and 100, denotes that the probability of flashover or breakdown when a voltage of level V_x is applied is x%.

Other symbols which are used only once are explained in the text.

CONTENTS

1 INTRODUCTION

1.1 General

The consequence of a lightning strike to any unprotected structure is usually disastrous. This has been the motivation for numerous research workers in their investigation of the physics of lightning over very many years. In addition to the measurement of field and current in towers and high buildings[1, 2], recent studies have included airborne measurement of electric field in the vicinity of thunderclouds[3], and initiation of lightning using aircraft and rockets[4, 5]. Although much has been learned, the physics of lightning is still not fully understood. It is, however, generally accepted that the ground-flash or earth flash is the most destructive and protective methods and devices have been introduced with that in perspective.

The problem of protecting aircraft against lightning is becoming ever more complex as more and more sophisticated electronics and light-weight composite structures are used. In particular, radome construction has evolved from the original concept, in which thick solid dielectrics were used, to become a honey-combed structure, having thin inner and outer skins, which makes it more susceptible to lightning puncture. Until the introduction of the segmented lightning diverter strip, radome protection always involved a difficult compromise between the degradation of the radar transmission characteristics and the degree of protection afforded. The present thesis is the result of an investigation into the

flashover characteristics of such a diverter strip.

In the following sections, a general introduction to the hazardous effects of lightning on aircraft and how these hazards can be minimised is provided. Included also are parameters relating to lightning discharges and how these parameters are simulated in a laboratory.

1.2 Effects of lightning on aircraft[6, 7, 8]

If an aircraft is in the vicinity of a thundercloud, then the occurrence of a lightning discharge may have several effects. These will depend on whether the aircraft is struck and on where it is struck.

1.2.1 Thermal effects

The thermal effects include burning and eroding, and the generation of disruptive pressure.

At points on the aircraft where a lightning discharge enters and exits, burning and eroding of the metallic surfaces will occur. The most severe damage occurs when the lightning channel dwells at one point on the aircraft for the total duration of the discharge. This has resulted in holes of up to several centimetres in diameter.

Disruptive pressure is a damage mechanism applicable to composite panels and radomes. When there is a large transfer of energy in

a short time, fast thermal vapourisation of material may result. If this occurs in a confined space, a high pressure may be created which may have sufficient magnitude to cause structural damage.

1.2.2 Mechanical effects

A flow of current in a conductor, in which there is a bend, creates magnetic forces which tend to straighten it. If the magnitude of current in a lightning discharge is sufficiently high, the resultant force can twist or rip structures from rivets, screws or other fasteners.

Another form of mechanical force is also experienced by an aircraft in the immediate vicinity of a lightning discharge. During the return stroke, the lightning channel expands due to the almost instantaneous heating of the channel to a temperature in excess of 30,000°K. The expansion is supersonic and results in a shock wave having initial pressures considerably greater than ten atmospheres.[9]

1.2.3 Electrical effects

The magnetic field associated with a lightning channel can penetrate an aircraft thus giving rise to high overvoltages[10, 11, 12, 13, 14]. These may destroy electronic or other equipment or may cause sparking.

The electronic equipment situated within the radome is, in addition,

vulnerable to damage should a lightning discharge puncture the radome.

1.2.4 Ignition hazards

Fuel vapours and other combustible gases may be ignited by a lightning discharge in several ways:

a) It is possible for a lightning discharge to burn through the thin metallic skin of a fuel tank or to produce a local hot-spot which might cause ignition;

b) a flow of current through a poorly bonded section, for example, a filler cap, can cause sparking and consequent ignition; and

c) sparking, resulting from transient overvoltages induced on electrical wiring within the fuel tank, could also cause ignition.

1.3 Parameters associated with the lightning current

1.3.1 General

The various effects already mentioned are dependent upon different parameters of the lightning current. The most important parameters of the current waveform are the peak value; the rate of rise of current; the total duration; the charge transferred and the action integral ($\int i^2 dt$). These parameters differ between the two basic types of discharge, viz. positive and negative. Differences also exist between the values of lightning currents recorded by different investigators[15]. Typical values are given below for

discharges of both polarities[6].

1.3.2 Positive discharge

In a positive discharge there is usually only one return stroke and this is represented diagrammatically in figure 1.1 Depending upon the geographical location, the positive discharges constitute between 1 and 20% of all flashes. However, positive discharges are more severe than negative ones due to the higher energy content which is related to the action integral. Positive lightning strokes, having action integral values of 10^7 A^2s and charge transfer exceeding 300C, have been recorded.

1.3.3 Negative discharge

A generalised representation of a severe negative discharge is shown in figure 1.2. It is characterised by the occurrence of several strokes of high peak value, indicated by the numbers 1 - 7 in figure 1.2. These high peak current phases are sometimes extended for several milliseconds by intermediate current phases, indicated by the numbers 8 and 9. A low amplitude continuing current phase, indicated by 11, usually occurs after the last stroke.

The initial high peak current phase has a typical magnitude range from 10 - 30 kA but magnitudes as high as 200 kA have been recorded. The rate of rise is typically 10 - 20 kA per microsecond[6].

The intermediate current phase is a low-level decaying current of a few kiloamperes that flows for several milliseconds after the initial more rapid decay from the peak current of some of the strokes.

The continuing current phase usually occurs after the last stroke of a flash. Typical current magnitudes and times of current flow are 100 - 400 amperes and 100 - 800 milliseconds respectively. Consequently, a high charge transfer is realised during this phase and is of the order of 200C for a severe discharge. Charge transfer during the high peak current phase is only a few coulombs.

Restrikes are typical for negative discharges and they occur with an average interval of 50 milliseconds. This interval increases to 145 milliseconds if a continuing current phase, indicated by 10 in figure 1.2, precedes the restrike. The peak value of the restrike is typically one half of that of the initial stroke but its rate of rise is generally greater than that of the initial stroke.

1.4 Laboratory simulation of lightning for aircraft testing

1.4.1 High current test waveform

Owing to laboratory limitations and to the complex variation of the lightning current it has been necessary, for the purpose of high current testing, to

a) define an equivalent test waveform that contains all the

essential features of a lightning discharge,

b) divide the various effects of a lightning discharge on an aircraft into groups, and

c) divide the aircraft into zones.

The test waveform, as defined by the Lightning Studies Unit, Culham Laboratory, UKAEA, is reproduced in figure 1.3[6]. The important parameters of component A are peak amplitude, action integral and time duration; of component B are maximum charge transfer and average amplitude; of component C are charge transfer and amplitude; and of component D are peak amplitude and action integral.

The effects of lightning on an aircraft have been arranged into two groups. Group 1 effects cover metal skin puncture, hot spot formation, mechanical damage, magnetic forces, damage to composite structures, fuel ignition and damage to lightning arresters. Group 2 effects include induced voltages, voltage flashover, sparking and fuel ignition. For group 2 effects, the parameters of component D in the test waveform are changed to peak amplitude, peak initial rate of rise, and duration for which the rate of rise should exceed 25 kA per microsecond.

It has been generally accepted that aircraft surfaces can be divided into three zones according to their lightning attachment and/or transfer characteristics. Zone 1 covers surfaces of the aircraft for which there is a high probability of initial lightning attachment, examples are the nose, wing-tips and tail. Zone 2

encompasses those areas into which a lightning channel has a high probability of being swept from a Zone 1 point of initial attachment, for example, the fuselage. Zone 3 includes all those areas not covered by Zones 1 and 2. All three zones are normally identified from the results of attachment points tests on model aircraft[16, 17, 18].

1.4.2 High voltage test waveform

In the laboratory, the lightning leader is often simulated by the long spark[19, 20]. Long fronted waves (200/2000 microseconds) are used for conducting hardware attachment tests. It is recommended that the test object be earthed and that the test gap be not less than 1 metre[6].

The recommendation for attachment point testing using model aircraft is, however, different and is detailed in Appendix 6 of United Kingdom Atomic Energy Report No: CLM-R 163. This recommendation was made following investigations into the breakdown performance of spark-gaps containing an isolated conducting body[21].

For flashover and puncture testing of dielectric hardware, the standard lightning impulse of 1.2/50 microseconds is recommended[6].

1.5 Aircraft protection

1.5.1 General

The severity of the lightning discharge has been discussed in

relation to its parameters and the effects of such a discharge occurring to, or near to, an aircraft have been outlined. Protection systems and devices have been implemented to minimise the hazards resulting from a lightning discharge.

The established protection criteria[22] include

a) safety of flight,

b) reliability,

and c) maintenance costs.

These and other criteria should be considered individually for each component part of an aircraft at all stages of the design development cycle. However, particularly in commercial aircraft, economics prevail and damage of a non-hazardous nature is sometimes accepted as being more economical than the provision of protection. This applies to areas which would have no effect on flight characteristics or a negligible effect on the aircraft operation and, if destroyed or damaged, will not allow penetration of lightning into the aircraft's interior. For example, damage to trailing-edge plastic fairings on large aircraft would hardly affect their flight characteristics[22].

Fuel system. One of the most important areas to be protected is the fuel system. Here the protection criterion adopted is that no sparking shall be observed when currents or voltages having the relevant test waveforms are applied to an empty fuel tank.

Electrical and avionic circuitry. Protection against electrical

power disruption on board an aircraft and protection of the avionic circuitry are both provided by the use of devices, situated at the possible lightning entry points, such as lightning arresters, spark gaps, zener diodes, metallic oxide varisters, diodes, fuses or shorting stubs.

However, difficulties in providing protection for advanced electronic systems are increasing for the following reasons:

a) Greater vulnerability to lightning-induced voltages due to the greater input impedance and wider bandwidth of advanced digital semiconductor circuits.
b) Greater exposure of electronic systems because of the increasing use of non-metallic skins.
c) Critical dependence on electronic control systems due to increased automation within the aircraft.

Radio interference suppression. Radio interference is caused by electrical discharges at non-metallic surfaces, by sparkover to the main airframe from electrically isolated external metallic conductors and by streamering at aircraft extremities. Suppression of the interference is effected by the use of static discharge devices[22] for aircraft extremities and by the application of anti-static coatings on dielectric surfaces where high-frequency, long range communication is required. The sparkover of electrically isolated metallic conductors is prevented by ensuring that at least some conductance exists between the metallic component and the airframe.

Structures. The basic protective approach for non-metallic structures is the use of metallic coatings, applied over the entire surface or in grid patterns. These coatings include metal foil, fine metal mesh, plasma flame sprayed metal and metallic paints. Fuel savings of up to 15% have been estimated as the potential for new aircraft designs taking full advantage of the use of light-weight composite materials[23]. Undoubtedly, this will add another dimension to the problems of protecting aircraft structures[24]. Continuous or grid-pattern coatings cannot, however, be used on radomes because they would excessively attenuate the on board-radar signals. Therefore, patterns of metallic conductors must be used which do not interfere with the operation of the radar system.

1.5.2 Radome protection

The radome is one of the most damage-prone components of the aircraft. It is constantly subject to damage from bird- and lightning-strikes, hail storms, moisture absorption and collision damage from handling-equipment on the ground[25].

In the area of lightning protection, the basic approach is the provision of external conductors which will provide the initial lightning attachment point and which may be required to conduct the full lightning discharge, with minimal damage, depending on the method used.

If the radar equipment is situated within a radome which forms the

nose of the aircraft then protection can be achieved by the use of a metallic spike protruding from the front of the radome and connected internally to the main airframe by one or more conductors capable of carrying the lightning discharge without damage. The pitot boom usually acts as the spike required.

Other possible methods include:

a) external metallic studs connected, through the radome wall, to an internal conductor which is connected to the main airframe;

b) metallic strips, varying from thin foil to thick conductors, fixed externally on the surface of the radome and connected individually to the main airframe;

and c) segmented strips fixed as in (b) above.

Interaction between the shielding requirements and the necessity for minimal interference with the radar system determines the physical arrangement of these conductors. The basic criterion for the spacing between protection conductors on radomes is that surface flashover, rather than puncture of the radome wall, will always occur.

2 REVIEW OF RADOME PROTECTION TECHNIQUES

2.1 General

In addition to protecting the radar system from damage, the protection method is constrained by several additional requirements. These include minimum radar degradation, minimum drag, minimum risk of radome puncture, ease of manufacture and low susceptibility to moisture penetration. Unfortunately, none of the adopted methods can satisfy all of these requirements.

The nose spike and metallic studs are essentially internally-earthed systems. Consequently, the conductors can be orientated so as to minimise radar degradation without aerodynamic concern. The nose spike method, however, has the disadvantage of higher risk of radome puncture, especially during a swept stroke. The risk of radome puncture is greatly reduced in the metallic studs method by the existence of external attachment points on the radome surface. This method, however, suffers from manufacturing complexity and the possibility of moisture penetration. Repairs would also be costly and complicated.

The continuous and the segmented strips are externally-earthed systems. They do not have the disadvantages of internally-earthed systems but, depending on the method, do present aerodynamic, environmental and radar degradation problems.

The foil strip is typically 0.5mm thick and 10mm wide[26]. Owing to

its flatness, it has the best aerodynamic characteristics. The cross-section area is however not large enough to withstand a full lightning discharge. The strip is vapourised and forms an ionised channel which then carries the full discharge current. (A complete description, operation and physical arrangement, on the radome, of the strip can be found in Patent Number Re 25417 which is reproduced as Appendix 2.1). Therefore, it is sometimes called the vapourising strip. Radar degradation is quite considerable and transmission loss can be as high as 25%[27]. Environmentally, the foil strip has disadvantages too. Cross cracking may occur due to radome wall vibration or rain erosion. When such a crack completely interupts the strip, protection is reduced and noise interference to communication systems may be introduced by static discharges across the crack.

The thick conductor strip or permanent conductor strip is made of aluminium and has typical dimensions of 3mm thick and 10mm wide[28]. It is capable of withstanding a full lightning discharge and, hence, of multi-stroke protection. The larger dimensions result in less desirable drag characteristics than those of the foil strip. Radar degradation is no better than that of the foil strip.

In most commercial aircraft, radar degradation caused by the continuous strips - foil or thick conductor - is acceptable and hence the wide use of either, dependent on the drag characteristics which can be tolerated. When radar degradation is not acceptable, segmented strips are used. These segmented strips are considered to be radar-transparent and to provide multi-stroke protection.

(Description, operation and physical arrangement, on the radome, of the strips can be found in Patent No: 3416027 which is reproduced as Appendix 2.2). Its drag characteristics are, however, not as good as those of the foil strip although better than those of the permanent strip. A review of recent investigations into the performance of the segmented strip is presented in the following sections.

2.2 The segmented lightning diverter strip

2.2.1 Physical construction

The construction of the segmented strip is as shown in figure 2.1. It consists of a series of circular riveted segments, with diameter of 2.44mm, spaced 0.31mm apart[32]. These segments are centrally located along the length of a fibreglass laminate with overall dimensions of approximately 1mm thickness, 10mm width and 1.2m length. The segments are bridged on the reverse side by a layer of resistive material. Amason recommended (Appendix 2.2) that this resistive layer should have a minimum value of 260 k-ohms per metre. The sides of the strip are coated with Neoprene for protection against wind and rain erosion.

2.2.2 Electromagnetic compatibility

Tests have shown that the segmented strip is virtually radar-transparent[28, 33]. Degradation of the antenna radiation pattern is negligible[28] and transmission loss is only about 2% [27] when

segmented strips are used as the protection conductors. In the following paragraphs, the virtual radar-transparent property of a segmented strip is highlighted by considering the problems which can be encountered through the use of continuous-conductor systems.

Generally, the extent of antenna pattern degradation depends on the frequency of operation of the antenna system, on the orientation of the strips/conductors with respect to the antenna polarization, on the location of the antenna, and on the type and length of the protection strips/conductors[28, 33].

When localizer antennae are installed on the forward aircraft bulkhead under the nose radome, continuous strips present a significant problem. The wavelength of the localizer beam is approximately 2.8m and the continuous strips are approximately one-eighth to one-half wavelength. This could cause unacceptable pattern degradation because a grounded quarter-wavelength conductor or an ungrounded half-wavelength strip can radiate quite efficiently. Similar problems are also encountered by the use of glideslope antennae which operate at about one-third of the wavelength of the localizer antennae. In particular, a compromise in the length of the conductors/strips may be required when both the glideslope and the localizer antennae are installed within the same radome.

The pattern degradation caused by the continuous conductors/strips at the weather-radar frequencies of 5.4 GHz and 9.375 GHz is due more to blockage and reflection than to radiation. The width rather than the length of the continuous conductors/strips is the

factor and the objective is to keep the width as narrow as possible.

In terms of radar attenuation during transmission, continuous conductors/strips can attenuate the signal by as much as 25% [27].

2.2.3 Current carrying capability

The current carrying capability of a segmented strip has been a point of controversy among numerous investigators. Investigators in the U.S.A.[27, 34, 35] achieved satisfactory results whereas investigators in the U.K.[29, 30, 31, 32] obtained results which cast doubts on the multi-stroke-high-current carrying capability of a segmented strip.

Amason et al[27] performed high current tests, up to 160 kA peak current, using a 0.4m section of strip and high charge transfer tests, over 200 coulombs, on shorter sections, with satisfactory test results. Both the segmented strip and the end fitting were not damaged by the tests.

Robb et al[34] conducted similar high current tests by combining a 1-MV high voltage impulse and a 200 kA peak current discharge and applying them to a 1-m length of strip. After two such applications, no apparent damage to the strip was observed. Swept stroke tests were also performed by combining 100 kA high current restrikes, initiated by a high rate of rise of 60 kA per microsecond, and a 500- kV impulse component all superimposed on a 200-A continuing current. No damage, other than a slight burnishing of the metal

segments, was observed.

Plumer et al[35] also reported satisfactory results with high current tests up to 200-kA peak and action integrals of 2×10^6 A^2s. Different strips were tested and all tolerated two or more strokes. Testing of each strip was terminated after three or four discharges. It was also reported[35] that segmented strips which had been installed on a Lockheed C-130 hurricane-hunter aircraft diverted a lightning stroke successfully with no damage resulting apart from a slight discolouration of the segments.

High current tests conducted at Culham Lightning Studies Unit, UKAEA, produced results which were not as encouraging[29, 30, 31, 32]. The current applied had two components which were designated as fast and slow. The fast component had a maximum peak value of 200-kA whilst the slow component had a maximum time duration of one second and a maximum charge transfer of 500 coulombs. Instances when the segmented strips were destroyed, after being subjected to high current discharges, were reported[29, 30, 31].

It should be noted that the several experimental arrangements used by the investigators in the U.S.A. were all basically different from that used by the investigators in the U.K. The former ensured that the segmented strip was ionized (evidenced by flashover) before the high current was applied. In the U.K. tests, the high current was applied without any deliberate pre-ionization although the arrangement ensured that the strips were tested in a relatively force-free environment. Hence, any flashover resulting would be as

a consequence of current flow in the resistive layer. However, unless the mechanism of flashover of segmented strips under natural lightning conditions is established, it is debateable which was the more valid arrangement.

2.2.4 High voltage tests

High voltage tests are used to evaluate the efficacy, ie. the shielding effect or capture capability, of any particular lightning protection system. The objective of such tests is to determine an optimum protection system. This would use a minimum number of strips to capture lightning strikes, from all possible directions, and to prevent the lightning channel from puncturing the radome wall. Significant factors influencing the design of protection systems include the thickness and dielectric constants of the radome wall; the surface conductivity of the outer radome wall; and the form and position of the 'earthed' metallic equipment within the radome[26, 27, 28]. It has been stated, however, that for any radome/radar configuration, more segmented strips would be required than if continuous strips were to be used[28]. This has been confirmed in tests performed at British Aerospace, Stevenage[32]. Their results also indicated that the strip was not effective in capturing strikes when it was attached on an anti-static surface having a resistance of 200 k-ohms per square.

High voltage tests conducted by Plumer et al[35] produced an interesting result. Irrespective of the rate of rise of voltage, an apparent constant time-lag to flashover of 0.7 microsecond was

obtained for a strip of 1.2m length (figure 2.2). Their other result shows the relationship between flashover voltage, both polarities, and strip length (figure 2.3). They considered this relationship to be linear inspite of the large variations in flashover voltages obtained.

2.3 Present study

Apart from the results of Plumer et al mentioned in the preceding section, no other publications on the flashover characteristics or the mechanism leading to a flashover of a segmented strip have been produced. Therefore, much has yet to be learned regarding the flashover characteristics and the flashover mechanism of segmented strips. The present study is, therefore, an attempt to satisfy this need.

If the nose radome of an aircraft is in the immediate vicinity of a lightning leader, three consequences are possible, viz. the radome wall may be punctured; the radome surface may be flashed over, or the segmented strip may be flashed over. Therefore, flashover of the segmented strip must always occur for effective protection. If the flashover characteristics of a strip, and of a radome surface, and also the puncture voltage of a radome wall[36] are as shown in figure 2.4, then effective protection will be achieved if the length of each segmented strip does not exceed the critical length shown. However, there is a shortage of detailed information regarding the relationship between flashover voltage and strip length. Hence, the immediate aim of the present study was to establish this relationship

and to confirm, or otherwise, the results of Plumer et al. In addition, the mechanism involved in the development of a flashover discharge on the segmented strip would be studied.

3 REVIEW OF SURFACE FLASHOVER CHARACTERISTICS AND MECHANISMS

3.1 General

The physical construction of the segmented strip was described in section 2.2.1. In the event of a flashover, every intersegment gap between adjacent conducting segments is bridged by a spark channel. It is considered that these spark channels occur in air (the gas medium in this case) and are adjacent to the surface of the dielectric substrate. Therefore, the flashover of a segmented strip is made up of a series of insulator-surface-flashovers between conducting segments which are spaced 0.3 mm apart.

Insulator-surface-flashover between conductors, under different physical conditions, has been studied by various investigators and their results are reviewed in the following sections. Surface flashover in vacuum is included because it has been established that, under vacuum, the discharge develops in a region of desorbed gas.

3.2 Surface flashover in vacuum

Although insulator-surface-flashover between conductors in vacuum has been studied by numerous investigators, the mechanism of this form of flashover is still not well understood.

In most of the mechanisms proposed, the phenomenon of secondary electron emission from the surface was considered to be operative.

Bruining[37] gives a comprehensive treatment of this phenomenon which describes the emission of secondary electrons from a solid when primary electrons of sufficient kinetic energy impinge upon it. The secondary electron yield per primary impinging electron is normally plotted against the energy of the impinging electrons and the general form of the resulting curve is as shown in figure 3.1. In general, the secondary electron yield from an insulator is much higher than that from a metal.

Willis and Skinner[38] measured the secondary electron yield of polymers, viz. P.T.F.E. (Teflon), Polystyrene (Styrafoil), P.E.T. (melinex and mylar) and Polyamide (Kapton), and found that the maximum yield ranged from 2 to 5 at a primary electron energy of about 200 eV.

Sudarshan and Cross[39] investigated the effect of coatings of chromium oxide, which have a maximum yield of less than unity, on the secondary electron yield from alumina spacers and found that the maximum yield of the aluminium spacer had been reduced from greater than six to less than unity.

A mechanism of surface charging by secondary electron emission avalanche was proposed by Boersch et al[40]. In this mechanism, initiatory electrons, supplied by field emission at the triple junction of cathode, insulator and vacuum, are multiplied due to the secondary electron emission phenomenon. This leaves a small area of the surface of the insulator positively charged. Owing to this positive charge, the secondary electrons are attracted back towards the insulator surface thus producing more secondary electrons.

Hence, an avalanche results and a larger area of the insulator surface then becomes positively charged. This mechanism was studied by other investigators[41, 42, 43] and supported by their results.

There is, however, no general agreement regarding a flashover mechanism[44, 45, 46, 47]. The main controversy is about the dependence of the flashover development upon the secondary electron emission avalanche. Nevertheless, most workers agree that field emission of electrons from the triple junction is the initial event in a flashover and that development of the discharge occurs in a region of gas desorbed from the surface of the insulator[46].

As initiatory electrons are assumed to be provided by field emission at the triple junction, field measurements at this junction have been undertaken by various investigators. In the study of Sudarshan et al[43], the junction field was measured using an electronic microforce balance with static voltages applied between uniform field aluminium electrodes. The insulators were in the form of right circular cylinders, 1.27 cm diameter and 1.27 cm long, of uncoated, high density alumina or of high density alumina coated with cuprous oxide or chromium oxide. They found that the higher field enhancement existed at the cathode triple junction for both uncoated alumina and alumina coated with cuprous oxide. Surprisingly, the higher field enhancement was at the anode triple junction for alumina coated with chromium oxide. They also found that, in all cases, if the mean applied field was increased from zero to about 8 kV/cm and then reduced again to zero, the junction field also fell

to zero without exhibiting hysteresis. However, if the mean applied field exceeded 8 kV/cm and was then reduced to zero, the junction field, in all cases, displayed hysteresis and did not fall to zero. This residual junction field took days to decay for uncoated alumina and minutes for alumina coated with either cuprous or chromium oxide.

Measurement of the field along a nylon insulator surface was made by Thompson and Lin[48]. The anode to cathode separation was 1 cm and the voltage waveform applied was a 10 ns pulse with rise and fall times of approximately 3 ns. The field was determined by measuring the Kerr effect in nitrobenzene liquid, which surrounded the hollow, - and evacuated, - interior of the nylon insulator, using a polarization analyzer and a ruby-laser. The results showed that there was higher field enhancement at the cathode triple junction. Similar results were obtained by Thompson et al[49, 50] using potassium-dihydrogen-phosphate (KDP) crystal as the insulating material.

It has been found that the surface flashover voltage is governed by the insulator material, its dimensions and shape, the quality of contact at the triple junction, the presence of an external magnetic field and the duration of the applied voltage pulse. Watson[51] studied the variation of the mean field at flashover with conical angle of an insulating right circular frustrum situated between two flat circular electrodes. The conical angle is defined as the angle between the dielectric surface and the normal to the electrode and this angle is positive if $D_c / D_A > 1$; negative if $D_c / D_A < 1$ and

zero if $D_c/D_A = 1$ where D_c is the diameter of the frustrum at the cathode and D_A is the diameter of the frustrum at the anode. The insulating materials used were urethane-epoxy resin (Lexan) and types 7070 and 7740 Pyrex glass. The conical angles considered ranged from -45 to +45 degrees. Applying voltage pulses of 35 and 75 ns duration, the minimum flashover strength was found to occur at angles between -10 and -15 degrees and maximum flashover strength was obtained for samples with conical angles of +45 degrees.

Sudarshan et al[39] achieved a 40% increase in withstand voltage for 2/50 microsecond impulses; an 80% increase on mains frequency and a 170% increase for static voltages by the application of chromium oxide coatings on alumina spacers. On freshly prepared samples coated with chromium oxide, microdischarges were observed and it was thought that these were due to loosely bound particles of chromium oxide being removed from the surface. Also, after about a hundred flashovers, samples were found to show faint brown 'tree' patterns on the surface but the flashover strength was unchanged.

Miller[46], using voltage pulses of 16 microsecond duration, achieved a 60% increase in withstand voltage by quasi-metallizing the surface of alumina spacers using manganese and titanium in the ratio of 4:3.

Variation of flashover voltage with insulator length was investigated by Blatsios and Hackam[52] testing ceramic alumina (98% pure) under static and alternating voltage conditions. The length was varied by using discs, 12 mm in diameter, of different thickness. In each case, the disc was sandwiched between two 25-mm

diameter electrodes. The flashover voltage increased almost linearly with increasing insulator length up to about 0.5 mm and then followed a power law, in which the index was less than unity, for greater lengths. Similar results were obtained by Avdienko[53] on plexiglas using both microsecond and nanosecond pulses.

The growth of surface flashover has been studied by Cross et al[43], [45, 54, 55] using time-resolved photography. In the most recent study[45] on right cylindrical alumina spacers, 12.5 mm diameter and 12.5 mm long, sandwiched between uniform field electrodes, the camera used had a streak speed of 20 mm/ns. The first visible light emission propagated from the cathode to the anode at an approximately constant speed of 4 to 6 mm/ns. Upon the arrival of the wavefront at the anode, anode and cathode directed discharges were initiated from the electrodes and resulted in complete flashover after a further 0.15 ns. In addition, studies by Anderson[56] have indicated a possible dependence of the velocity of propagation on the conical angle.

To summarise, the flashover strength of a dielectric spacer, in vacuum, is dependent upon both the surface material and the form of the spacer. When this surface material, usually present in the form of a coating, has a secondary electron emission yield of less than unity, the flashover strength is increased considerably. It has also been found that the conical angle affects the flashover strength. Field measurements showed that, in general, field enhancement occurs at the cathode triple junction and this is also supported by time-resolved photographs which show discharges

propagating from cathode to anode.

3.3 Surface flashover in gases

The mechanism of surface flashover in gases is also not fully understood. Various mechanisms of spacer flashover in compressed gases have been proposed[57, 58]. These include initiation by a microdischarge at an imperfect contact on a spacer-electrode interface; by a microdischarge at an imperfection on a spacer surface, or by a particle on or near a spacer surface. Such areas would act as high field sites and cause intense electron emission and ionization. The resulting surface charging of the dielectric spacer would then enhance the ionization process and leads to a flashover. In a recent investigation by Jaksts and Cross[59] in nitrogen at atmospheric pressure, it was proposed that additional electron multiplication could result from photo-ionization of the dielectric surface.

Flashover characteristics in compressed gases[57, 58] were found to be influenced by bad contact between a spacer and the electrodes; by spacer profile; by spacer permittivity and conductivity; by surface imperfections; by the surrounding gas; by the presence of dust on the dielectric or on the electrodes and by the presence of moisture in the gas[60].

Cookson[61] investigated the effect of spacer profile on surface flashover using filtered SF_6 or unfiltered nitrogen as the surrounding gas. The effect of dust particles on spacer flashover in SF_6 was

also investigated. Impulses of 1/50 microsecond waveshape were applied and the gas pressure was 3.5 MN/m^2 and 1.5 MN/m^2 for nitrogen and SF_6 respectively. It was found that surface flashover in filtered SF_6 was not affected by spacer corrugations but was adversely affected by the presence of dust particles. However, in unfiltered nitrogen, spacer corrugations did affect the flashover process and could increase the flashover voltage. It was suggested that the different effect of spacer profile on surface flashover was due to space-charge effects. Space charge conditions in nitrogen hinder an advancing discharge streamer but, in SF_6, space charge helps the flashover.

The effect of dust particles on surface flashover was further investigated by Fleming[62] using perspex spacers in SF_6 at 1.47 MN/m^2 pressure. It was found that conducting particles reduced the flashover strength more than non-conducting particles. The highest reduction, obtained by using steel spheres of 125 - 211 microns diameter was approximately 60% and 25% for positive and negative impulses respectively. The reduction was less for smaller particles and seemingly so for larger particles too. Also, reduction in flashover strength was greater when the particles were placed nearer the inner-electrode of the co-axial system used.

Fleming[63] also investigated the effect of conducting particles, of 125 - 211 microns diameter, on spacer flashover in SF_6 at different pressures. For positive impulses, it was found that the particle contaminated flashover strength increased with increasing pressure over the range 0.46 to 1.47 MN/m^2. However, the difference between

the clean and contaminated surface flashover voltages also increased over this pressure range. For negative impulses, the flashover strength also increased with increasing pressure but the reduction in flashover strength caused by the surface contamination was significant only at pressures above 0.77 MN/m^2. The reduction in flashover strength at the lower pressures was investigated by Mansfield and Fleming[64] by considering surface charging of the insulator for positive and negative impulses under dust-free condition. In this study, they found very little evidence of surface charge when the inner electrode was positive but large regions of negative charge on the spacer surface when the inner electrode was negative. From these results it was inferred that, in cases where dust particles are present on the spacer surface, these regions of negative charge could develop close to the dust particles and hence reduce their field enhancement effect.

More recently, the effects of larger size particles, consisting of aluminium or copper wire particles measuring 3 or 6 mm long by 0.45 mm diameter or of aluminium or copper shavings of less than 0.5 mm dimensions, on the flashover voltage of epoxy resin spacers in SF_6 have been studied by Voss[65]. He used a co-axial arrangement and measured flashover voltages over a range of pressure from 1.5 to 5 bar by applying oscillating switching impulses. As in the results obtained by Fleming[63], albeit under different experimental conditions, there was an increased reduction in flashover strength with increase in pressure. In contrast, however, the reduction, when using negative polarity impulses, was larger.

Laghari et at[66] studied the effect of different surrounding gas mixtures on the static flashover voltage of epoxy resin spacers, 10 mm long by 10 mm diameter, situated in a uniform geometric field at a pressure of 5 atmospheres. The gas mixture consisted of SF_6/air, SF_6/N_2, SF_6/CO_2 and SF_6/He with percentages of SF_6 in the mixtures ranging from 0 to 100%. In the absence of the spacer, the ranking of the mixture breakdown strengths in decreasing order was SF_6/N_2, SF_6/air, SF_6/CO_2 and SF_6/He. The effect of the introduction of the spacer was to reduce the breakdown strength by as much as 30% but the relative ranking of the resulting breakdown strengths remained the same. However, the ranking of the amount of reduction or spacer efficiency, which was defined as the ratio of flashover voltage with spacer present to the breakdown voltage of the gap alone, was in the reverse order. In other words, the highest reductions were obtained with the SF_6/N_2 mixtures. The effect of placing a single aluminium particle of 1 mm diameter, on the spacer surface, midway between the electrodes was also investigated. This further reduced the flashover voltages with the maximum reduction occurring in the range 5 - 10% of SF_6 for each mixture.

The effect of intense light falling on an insulator surface in air at atmospheric pressure was investigated by Bedrin et al[67] using static voltages. A Xenon flashlamp was used as the intense light source and it was found that illumination of the dielectric surface reduced the flashover voltage by a factor of more than twenty. However, this effect did not occur for insulating materials which were not evaporated by the light or which exhibited weak evaporation.

In general, therefore, the effect of a spacer is to reduce the breakdown strength of an insulating gas in which the spacer is situated and this breakdown strength is further reduced in the presence of contaminating particles. The amount of reduction will depend on the insulating gas; the size and shape of the contaminating particles; the material of the dielectric spacer and its profile and on the quality of the contact between the spacer and the electrodes.

3.4 Proposed flashover mechanism for a segmented diverter strip

3.4.1 Voltage distribution along a segmented strip

Figure 3.2 shows the electrical circuit representation of a segmented strip with the intersegment resistances in parallel with intersegment capacitances and the stray capacitance from each segment to earth.

The intersegment resistances of a new strip are of the order of 45 k ohms and the intersegment capacitances are less than 2 pF. Therefore, the time-constant of each parallel combination is less than 90 ns which is much shorter than that of the applied impulse. Hence, the intersegment capacitances have a negligible effect on the voltage distribution along a strip.

When a strip bridges a uniform-field air gap, the high voltage plane electrode acts effectively as a shielding electrode[83] thus producing a uniform field in the immediate neighbourhood of the strip.

This uniform field distribution along the strip is equivalent to the disappearance of stray ground fields associated with the stray ground capacitances shown in the figure. Therefore, when a strip is situated axially and bridges a uniform field air gap, the voltage distribution along the strip is governed only by the intersegment resistances.

When a segmented strip bridges a non-uniform field air gap, i.e. a rod/rod or a rod/plane air gap, the shielding electrode effect is non-existent and this requires the stray ground capacitances to be taken into account. In general, the voltage distribution along the strip will be non-linear[83] and this non-linearity becomes more pronounced with increase in strip length.

3.4.2 Mechanism of flashover

Owing to the presence of the resistive layer, any charge in the gas will be subjected to both a magnetic field and an electric field.

The force due to a magnetic field is given by the product of the charge on the particle and the cross-product of the velocity of motion and the flux density. If we consider the flux to be due to a current, I, flowing in the z-direction of a cylindrical co-ordinate system, the flux density is given by the relationship

$$B = \mu_o H$$

where $H = I/2\pi r$ and H is acting in the θ-direction, and r is the radial distance of the moving charge from the current carrying conductor.

For a strip 0.3-m long, the current flowing at voltages close to $V_{50} \approx 100$ kV would be about 600 mA. Then taking r as 0.1 mm, the magnitude of the flux density would be of the order of 10^{-3} Wb/m^2. Taking the electron velocity to be 10^6 cm/sec, the maximum force on an electron due to the magnetic field would be of the order of 10e Newtons, where e is the electron charge.

As there are 110 intersegment gaps in a 0.3-m strip, the voltage across each intersegment gap would be about 900V which is equivalent to a mean field of 2.7 MV/m. The force on an electron due to this field is then $2.7 \times 10^6 \times e$ Newtons.

Therefore, the effect of the magnetic field is negligible and charge transport can be considered to be due to the electric field.

The following mechanism is suggested for flashover of a segmented strip. When the first intersegment gaps have developed to flashover, the voltage collapse across these gaps will cause overvoltages to be impressed across the remaining gaps. This will cause further gaps to flashover and this regenerative process will lead to the complete flashover after a very short time. Initiatory electrons may be provided by field emission at the triple-junction points or by microdischarges from imperfections on the segments. Also, the discharge may be modified by secondary electron emission due to photoionization of the dielectric surface[59].

For a strip situated in a gap having a uniform geometric field, the maximum withstand voltage will then be given approximately by

$$V_o = NV_w$$

where V_o is the 0% flashover voltage for the strip

N is the total number of intersegment gaps

V_w is the maximum withstand voltage for one gap

and the intersegment resistances are assumed to be equal. The flashover voltage variation should therefore be proportional to the number of intersegment gaps and, since the number of gaps is proportional to the strip length, the flashover voltage should be proportional to strip length. An approximately proportional relationship is shown by the results presented in section 6.2.1.

For a strip situated in a gap having a non-uniform geometric field, the maximum withstand voltage should be different from that given above. Owing to the non-linear voltage distribution along the strip, discharges will be initiated at a lower applied voltage and will develop to give flashover of the strip following the flashover mechanism proposed. In addition, owing to the increased non-linear voltage distribution with increase in strip length, it is expected that the relationship between flashover voltage and strip length would not be proportional. The results presented in sections 6.2.2 and 6.2.3. show a lower flashover voltage and a non-linear flashover voltage/strip length relationship.

4 APPARATUS AND MEASURING TECHNIQUES

4.1 High voltage laboratory

The high voltage laboratory measured 21 x 12 x 11m. A built-in under floor electric heater provided a means of heating the laboratory and the air temperature was controlled by means of a thermostat. The walls and ceiling of the laboratory were covered with electrically conducting acoustic tiles and these were connected to the low voltage end of the potential divider. The plan of the laboratory with the various installations is shown in figure 4.1.

4.1.1 Impulse generator

The circuit diagram of the Ferranti impulse generator is shown in figure 4.2. The generator was a high efficiency Marx-type having distributed wavefront and wavetail resistors and a total of 9-stages. Each stage had a 0.08-microfarad storage capacitor rated at 175 kV d.c. thus providing a maximum stored energy of 11 kJ and a maximum nominal output voltage of 1.5 MV peak.

The output of the generator was connected to the wavefront capacitor via a resistor. The wavefront capacitor consisted of seven similar capacitors connected in series, each of 0.01 microfarad and rated at 200 kV impulse. Two high voltage busbars branched from the top of the wavefront capacitor to the voltage divider and the test-gap.

Firing of the generator was achieved by means of a trigatron spark

gap incorporated in the high voltage electrode in the first stage of the impulse generator. The trigatron spark-gap was triggered to breakdown by a 15 kV pulse from a trigger pulse generator. Breakdown of the trigatron spark-gap caused the breakdown of the remainder of the spark-gaps thus producing the desired impulse voltage. The generator recharged to a predetermined voltage automatically after each firing.

Initially, the voltage to which the generator was charged was monitored using a microammeter connected in series with a 400-M ohms resistor across the first stage of the impulse generator. This method gave an accuracy of $\pm$ 0.3%. Recently, the operation of the impulse generator was automated by incorporating a microprocessor system to work along-with the manual control panel. The charging voltage monitoring system was replaced with a voltage divider across the first stage of the impulse generator. The voltage divider had an upper arm of 400 M ohms and a lower arm of 2 k ohms. The electrical signal from the divider was converted to an optical one and fed to the microprocessor system which could control the charging voltage with an accuracy of $\pm$ 0.1%.

Owing to the use of the image intensifier and converter camera, it was necessary to have the laboratory in complete darkness. This required the prevention of the light emitted from the impulse generator's interstage spark-gaps from illuminating the laboratory. This was effected by enclosing the complete generator with heavy black polythene curtains suspended from the roof.

4.1.2 Trigger-pulse generator

The trigger-pulse generator was essentially a single stage impulse generator and the circuit diagram is shown in figure 4.3a. The blocking capacitor had a capacitance of 5000 pF.

On closing switch S, the circuit could be approximated by the equivalent circuit shown (figure 4.3b). A negative 15 kV pulse would be developed between the trigger electrode and the hemisphere thus initiating breakdown of the trigatron spark-gap.

Production of a positive 15 kV pulse to the trigger electrode of the trigatron spark-gap could be realised by interchanging the rectifier diodes. Cross-over shorting-links were available for this purpose.

4.1.3 Voltage divider

The voltage divider was a capacitive divider with a series damping resistor. The upper arm of the divider consisted of two 65-pF capacitors connected in series and the lower arm consisted of twelve 0.05-microfarad capacitors connected in parallel. The signal from the lower arm was fed to an oscilloscope via a coaxial cable matched at the input end. The oscilloscope used was a Tektronix type 555 with a bandwidth of 30 MHz and it was situated inside a screened room. Additional screening of the coaxial cable was provided by means of a flexible corrugated steel tube which was earthed at the voltage divider.

4.1.4 Screened room

The screened room was a Belling & Lee shielded enclosure with dimensions of 3.4 x 2.2 x 2.2 m high. It was situated on a raised platform 0.8 m high and earthed through the flexible corrugated tube mentioned in section 4.1.3.

Power supply in the screened room was provided by an external generator through shielded cables and an r.f. interference filter, Belling & Lee type L1822. The generator was electrically isolated from the rest of the supplies in the laboratory.

All measuring and recording systems which required electrical power for operation were situated inside the screened room. A porthole was cut in the wall of the screened room facing the test-gap for the purpose of recording using the image converter camera.

Triggering of the impulse generator from inside the screened room was achieved through a pneumatically operated microswitch or by depressing a designated key on the keyboard of the microprocessor control system.

4.2 Impulse waveshape and polarity

Impulse voltages with positive polarity were used throughout the experiments.

On firing the impulse generator, the circuit could be approximated by the equivalent circuit shown in figure 4.4 where C1 is the effective capacitance of the storage capacitors, C2 is the effective capacitance of the wavefront capacitor, R1 is the sum of the distributed wavetail resistance and R2 is the sum of the distributed wavefront resistance plus the external resistance. The impulse waveshape would thus be governed by the values of C1, C2, R1 and R2.

In practice, C1 and C2 were kept constant and the impulse waveshape was altered by changing the values of R1 and/or R2, i.e. R_f and/or R_t - the distributed wavefront and wavetail resistors respectively.

R_f and R_t had values of 28 ohms and 500 ohms respectively for a 1.7/39 - microseconds lightning impulse and values of 6.16 k ohms and 50 k ohms respectively for a 300/2600 - microseconds switching impulse. Only the short-fronted 1.7/39 - microseconds impulse was used for the following reasons:

a) it was recommended in the UKAEA Report[6], Number CLM-R163, that lightning impulses should be used in the testing of radomes. Since the segmented strips are mounted on the surfaces of radomes, it is considered appropriate that lightning impulses be used in tests on segmented strips;

b) if the long-fronted impulse was used, the effective wavetail resistance would be of the same order of magnitude as the resistance of the segmented strip thus altering the waveshape, and

c) as shown in Appendix 4.1, the action integral of a switching impulse up to the time-to-crest is about 5 times the action integral of a full lightning impulse. Since the strips are damaged by the applications of a full lightning impulse, damage to the strips will result before the crest-value is reached if switching impulses are used.

4.3 Gap configuration and electrodes

To establish the effect of the gap configuration on the flashover characteristics, plane-plane, rod-plane and rod-rod geometries were used.

The gap geometry was defined with all the earth electrodes situated 2 m above ground.

Raising the earth electrode had an additional advantage. Focusing of the optical system was made much easier because the camera and the gap were at about the same level above ground.

4.3.1 The plane electrode

The earth-plane in both the rod-plane and plane-plane configurations had a diameter of 1.83 m. It consisted of a 1.8-m diameter aluminium sheet as the plane with a 0.3-m diameter cross-section toroid mounted on the periphery to reduce edge effects. The aluminium sheet was reinforced by a wooden cross-beam on the underside.

A 27.5-mm diameter hole was bored at the centre of the electrode and fitted with an aluminium insert having a slot to accommodate the width and thickness of the segmented strip. This allowed the same strip to be used in the investigation of the variation of flashover voltage with segmented strip length. A leaf-spring was incorporated in the slot to ensure that the segmented strip was earthed.

A wooden tripod was used to maintain the clearance of 2 m above ground for the earth-plane.

The high voltage electrode was an aluminium spinning having the same diameter as the earth plane electrode. A wooden cross-beam was also used to support this electrode so that it could be suspended from the high voltage busbar.

Two holes of 1mm diameter were drilled in the centre of the high voltage electrode to allow the two ends of a nylon thread to pass through. The nylon thread was used to hold the upper end of the segmented strip in contact with the high voltage electrode or to maintain the upper end of the strip with a fixed gap clearance from the surface of the high voltage electrode.

4.3.2 The rod-electrodes

Each rod electrode consisted of a two-metre length of steel tube capped by a hemispherical ended brass rod. The tube and rod each had an outer diameter of 32 mm.

Each brass rod had a slot to accommodate the segmented strip with the excess space filled by a brass insert which kept the part of the segmented strip inserted into the slot at the same potential as the electrode. A countersunk pinch-screw kept the segmented strip and the insert in position. The plan and elevation of the high voltage brass rod is shown in figure 4.5.

The brass rod for the earth electrode was slightly different from that shown in figure 4.5. The length was about 50 mm and the slot ran from end to end. This allowed the same segmented strip to be used in the investigation of the variation of flashover voltage with segmented strip length.

4.4 The chopping gap system

In most test systems, a parallel chopping gap is normally used to dump the stored energy from the impulse generator once it is detected that the total current through the test object has increased beyond a critical level. In the present case, dumping of the stored energy was only desired when flashover of the segmented strip was not likely to occur since this would probably result in the segmented strip being damaged.

The basis of the chopping gap system is as shown in figure 4.6. It was basically a three-electrode gap where the middle electrode was biased to a static potential of V_{dc} and the upper electrode was effectively at ground potential before the application of the voltage impulse. The lower gap was set to withstand the bias

voltage. The capacitor, C3, across the lower gap maintained the static potential of the middle electrode when an impulse voltage was applied to the upper electrode. The upper gap was set to withstand the voltage given by $V_p - V_{dc}$, where $V_p \triangleq nV_{dc}$ and $n > 1$. When the lower gap was triggered to breakdown at or immediately after the peak of the impulse, the middle electrode was brought to ground potential and this effectively overvolted the upper gap by approximately $(100/(n-1))\%$. Provided that the overvoltage exceeded the V_{100} of the upper gap, it would then break down and divert the stored energy of the impulse generator away from the test-gap.

4.4.1 Design of the chopping gap system

To make use of the existing facilities, n was chosen to be 9 (it was later changed to 7 for reasons discussed in the following section) so that V_{dc} was equal to the stage voltage of the impulse generator.

The chopping gap thus adopted is shown in figure 4.7. The capacitor, C3, had a value of 0.01 microfarad and was rated at 200 kVdc. The 2-M ohms resistor prevented appreciable discharge of the capacitor, C3, after the impulse generator had been triggered. For the lower gap, a trigatron was the most obvious triggering device in view of the magnitude of the voltage across it. With $n = 9$, the upper gap would be overvolted by a maximum of 12.5% which dictated the use of a uniform field gap to ensure that the overvoltage exceeded the V_{100} of the upper gap. The use of a pair

of Bruce profile electrodes or similar would be ideal in establishing the uniform field. However, the capacitance between such electrodes would be too large for the system and as a compromise two 1-m diameter sphere electrodes were used (see Appendix 4.2).

4.4.2 Design of the trigger circuit

Preliminary tests performed on the segmented strip indicated that flashover of the strip tended to occur on the wavefront or around the peak of the impulse voltage wave. Therefore, damage to the segmented strip would be prevented if the chopping gap could be triggered to breakdown at a predetermined time after the peak of the applied voltage impulse. Several trigger circuits were considered and tested and the results are given in the following sections.

4.4.2.1 Trigger circuit 1

The circuit diagram of the trigger circuit is shown in figures 4.8a and b. It was designed with the common earth-rail isolated from the earth of the impulse generator because the trigger circuit would be operating in a high voltage impulse environment. The input signal was coupled optically to a non-retriggerable monostable which, when triggered, produced a 3.6-V positive pulse having a pulse width of 10 microseconds. When the two transistors were turned-on, the charged 10-microfarads capacitor supplemented the conduction current of the transistors because the turn-on current required for the silicon-controlled-rectifier was 50 mA.

The purpose of the 3-electrode sphere gap (figure 4.8b) was to attempt to reduce the time jitter to breakdown of the trigatron by increasing the energy in the pulse applied to it [68].

The circuitry was double-screened and placed in a large copper box. Dry-cell batteries were used for the low voltage supplies. The 300-V supply was obtained from an inverter operating from 2 x 1.5-V dry-cell batteries. The 10-kV supply was produced by a diode-capacitor-voltage-tripler from the 250-V mains supplying the impulse generator charging circuit.

This circuit did not perform to expectation due to noise injection via the pulse transformer. In view of the difficulty of operating electronic circuits in a noisy environment, trigger circuit 2 was considered.

4.4.2.2 Trigger circuit 2

The principle involved is explained with reference to figure 4.9. Curve 1 represents the impulse voltage applied to trigger the impulse generator and curve 2 represents the impulse voltage applied to trigger the chopping gap. Both impulses start at the same time. If the minimum trigger voltage level required to operate each trigatron is as shown, the impulse generator will be triggered at time T1 and the chopping gap will be triggered at a later time of T2. Assuming negligible time jitter in the operation of the two trigatrons, then (T2 - T1) will represent the time-to-chop of the applied voltage impulse.

The trigger circuit is shown in figure 4.10. The top half of the circuit provided the trigger pulse for the trigatron in the impulse generator whilst the bottom half provided the trigger pulse for the trigatron in the chopping gap. By using the same static charging-voltage and the same shorting contacts, S, any difference in the starting times of the two trigger voltage impulses was eliminated. Also, the trigatron in the chopping gap was identical to the trigatron in the impulse generator so that there was no difference in the trigger voltage levels. On closing switch, S, each half of the circuit can be represented by an equivalent circuit as in figure 4.3. Therefore, varying the resistance, R3 of figure 4.10, will vary the wavefront of the voltage impulse applied to the trigatron in the chopping gap and hence, the time-to-chop of the applied test voltage.

Surprisingly, the performance of this trigger arrangement was not much better than that of trigger circuit 1. Examination of the physical layout of the system showed that:

a) for a positive impulse generator charging voltage, the trigatron in the impulse generator was anode-triggered whereas the trigatron in the chopping gap was cathode-triggered, and

b) the earth of the trigatron in the chopping gap was not brought directly to the earth of the charged capacitors of the impulse generator but via the earth of the wavefront capacitor which was situated about 2.5 m away.

Several authors[68, 69, 70] have shown that the operating characteristics of anode-and cathode-triggered trigatrons are different. Therefore, it was decided to alter the physical layout so that a) both trigatrons were anode-triggered, and b) the trigatron in the chopping gap had the same 'earth' as the trigatron in the impulse generator.

4.4.2.3 Trigger circuit 3

In the preceding section, it was considered that both trigatrons should be anode triggered and that both should be earthed at the same point. The former requirement could be realised without much difficulty. As for the latter requirement, it should be satisfied by arranging the trigatrons to be as close as possible thus making the earth-connection as short as possible.

Fortuitously, the construction of the impulse generator was such that only minor modifications were required to satisfy both these requirements. Figure 4.11 shows the construction of the first four stages of the 9-stage impulse generator. The storage capacitors are stacked one above another but electrically insulated from one another by isolators of equal dimensions. To limit the height of the resultant vertical column, the complete impulse generator is made up of two columns and the stages are identified as shown in figure 4.11.

The two requirements were satisfied by making SG1 and SG3 the triggered gaps in the chopping circuit and in the modified impulse

generator respectively. The trigatron in SG1 was duplicated in SG3. Complete isolation of the third stage from the first and second stages was achieved by removing the charging-resistor, R_c, between the second and third stage and by connecting the low voltage end of the third stage to ground. The distributed wavetail resistor, R_t, across the first stage was replaced by a shorting-link and the rest of the distributed wavefront, R_f, and wavetail resistors across the first and second stage were removed. The first stage was used as the static bias and the storage capacitor of the second stage served as an additional coupling capacitor between the trigger circuit and the trigatron. The complete circuit of the modified impulse generator and the trigger circuits for the two trigatrons is shown in figure 4.12.

In using the first and second stages for the chopping gap system, an additional advantage was realised. The length of the trigatron spark-gap in the chopping circuit was automatically adjusted in tandem with the length of the interstage spark-gaps of the impulse generator - a feature not readily available when the trigatron in the chopping circuit was remote from the impulse generator. The sacrifice was, of course, a reduction in the maximum impulse voltage to 7/9th of that previously available.

The system was tested for different times-to-chop of the applied test voltage and performed satisfactorily. For a fixed gap setting, the times-to-chop, as observed on an oscilloscope, were found to be consistent to within $\pm$ 0.4 microsecond. The time-to-chop was finally set at 5 microseconds for future tests.

4.5 Probe for current measurement

The pre-flashover current was recorded by means of a probe shown in figures 4.13a and b. The measuring probe was isolated from the earth electrode to prevent measuring the displacement current of the gap. The clearance of approximately 1 mm between the brass insert and the earth electrode was essentially a protective spark-gap in parallel with the measuring resistor and operated when flashover occurred across the segmented strip. The measuring resistor consisted of six 100-ohms resistors in parallel and the sum of this value and R4 was equal to the characteristic impedance of the coaxial cable.

4.6 Optical systems

4.6.1 Image converter camera

Time resolved photographs were obtained using an Imacon converter camera model 790 manufactured by Hadland Photonics Ltd. The tube had a photocathode with S20 spectral response and an UV transmitting window. The light gain was 40 times per unit area for white light (50 times at 440 nm). The total gain was four times the above figures because the image size at the output was twice that of the photocathode which was 9 mm high by 8 mm wide. The output image was displayed on a P11 medium persistence phosphor screen having a fibre optic output for direct contact recording on film. The mode of operation of the camera was set by the type of plug-in used. The two modes of operation used were:- framing and streak.

Framing mode. In the framing mode, individual frames of a discharge were produced as shown in figure 4.14. The number of frames could be continuously varied from 8 to 16. The two plug-ins used had framing rates of 2×10^6 frames per second and 2×10^7 frames per second. These gave exposure times of 100 ns and 10 ns and time between frames of 400 ns and 40 ns respectively. The framing sequence was initiated by a single trigger pulse from a separate pulse generator.

Streak mode. In the streak mode, the image at the output was swept from left to right at a speed determined by the streak speed. For the plug-in used, one of the four preset speeds of 1 ns, 2 ns, 5 ns and 10 ns per mm could be selected. The trigger pulse required also came from the separate pulse generator.

4.6.2 Image intensifier unit

The unit used was the image intensifier system type T2001 manufactured by EMI Industrial Electronics Ltd. The 4-stage intensifier tube was air-cooled and had a typical gain of 10^6 at 33 kV. The input photocathode was of the bialkali type (SbNaK) which gives exceptionally low electron dark current - a typical maximum being 10 counts/cm^2/s. The window of the tube was of sapphire which gave a response at wavelengths down to less than 200 nm. The disadvantage of the sapphire window was to increase the electron dark current by a factor of two because of scintillations occurring in the window due to cosmic rays and natural radioactivity.

4.6.3 Pulse generator

The trigger pulse generator was a type PG-75A manufactured by Lyons Instruments Ltd. Figure 4.15 shows the input/output connections to the generator. The cathode-ray-oscilloscope was triggered by the signal from the high voltage divider and the oscilloscope's gating pulse was used to trigger the trigger pulse generator. The output pulse from the generator was delayed before being applied to the Imacon converter camera. The amount of delay could be varied and depended on the inherent delay in the triggering of the converter camera. A typical delay setting was approximately 0.5 microsecond.

4.7 Additional analytical aids

4.7.1 Philips scanning-electron-microscope

A Philips scanning-electron-microscope, PSEM 500, equipped with a Links System 860 for spectroscopic detection and quantitative analysis of elements, was used for the observation of the surface of the strips and for analysing the elements present in the strips.

4.7.2 Automatic recording microdensitometer

Owing to the short development time of the discharge, it was difficult to interpret the streak photographs without bias. For this reason, a MK III CS double-beam automatic recording microdensitometer manufactured by Joyce, Loebl & Co., Ltd. was used

to produce image-density/time curves.

4.8 50% flashover voltage, V_{50}, and mean voltage at flashover

4.8.1 50% flashover voltage, V_{50}

There are two generally accepted method of estimating the 50% flashover voltage. In the first method, voltage impulses having a constant prospective peak value, say V_{est}, are applied r times. If, as a result of these r applications, there are s flashovers then the probability of flashover at the level V_{est} is given by s/r. In this way, by changing the applied voltage levels, a range of probability between 0 and 1 can be obtained. The results are then plotted on probability paper and a best straight line drawn through the points. The values of V_{50} and its 95% confidence levels can then be estimated [71, 72, 73]. However, this method requires many voltage applications and is not suitable for the present study due to the tendency of the segmented strip to be damaged.

The other method requires many fewer voltage applications to be made and is known as the 'Up & Down' method[74]. A likely value of V_{50} is chosen and a voltage impulse having this amplitude is then applied. If a flashover occurs, the next applied voltage will be reduced by $\triangle V$. If a withstand results, the next applied voltage will be increased by $\triangle V$. This decision-making process is also applied for the remainder of the voltage applications. A detail description of the method and the formulae used to compute the V_{50} and its 95% confidence levels are given in Appendix 4.3.

In the 'Up & Down' method, the applied voltage levels should oscillate about the actual V_{50} level. Hence, this oscillatory characteristic should be achieved in any tests on the segmented strips for any mathematical computation arising therefrom to be valid. This oscillatory characteristic is exhibited when a length of segmented strip has been conditioned and is termed the stable-phase in section 6.1.

4.8.2 Mean voltage at flashover

If, for each application of an impulse voltage which is at a level giving 50% probability of flashover, the voltage at the instant of flashover is then recorded then the mean voltage at flashover is given by the arithmetic mean of these values.

5 PRELIMINARY INVESTIGATION ON THE SEGMENTED STRIP

5.1 Physical properties

5.1.1 Construction and material composition

The strip is made up of a series of conducting segments which are joined by a resistive layer. These were fabricated on a dielectric substrate and the physical dimensions are as shown in figure 2.1. That the segments are made of nickel-plated copper was confirmed by X-ray analysis, figure 5.1. The resistive layer is formed from carbonised-resin and the dielectric substrate is a fibreglass laminate. For rain erosion prevention, the side surfaces are coated with neoprene or a polycarbonate layer. X-ray analysis of the dielectric medium revealed a significant proportion, 88%, of titanium (figure 5.2). This could be present as TiO_2 which is used commercially both as a filler and a white pigment[75] and the strip is actually glossy white. Carbon, hydrogen and oxygen were not detected because the lightest element which could be confidently detected was magnesium.

5.1.2 Intersegment capacitance

Attempts were made to measure the intersegment capacitance using a Wayne-Kerr bridge. However, due to the low conductance presented by the resistive layer, the best estimate was approximately 2pF. A simple check using the equation, $C = A\epsilon_o\epsilon_r/d$, for the capacitance of two parallel plates gave the intersegment capacitance as 1.5 pF

assuming A = 1 mm x 10 mm, $\epsilon r = 5$, d = 0.3 mm and $\epsilon o = 8.854 \times 10^{-12}$ F/m. Therefore, it is likely that the intersegment capacitance is not greater than 2pF.

5.1.3 Intersegment resistance

The intersegment resistances were measured using a low direct-voltage source. Measurements were undertaken using two unused segmented strips of 1.2-m length and the results are presented in figures 5.3a and 5.3b and in figures 5.4a and 5.4b.

The values of intersegment resistance for one strip ranged from 15 k ohms to 330 k ohms with a majority, 145 out of 442, laying between 30+ and 40 k ohms (figure 5.3b). The values for the other ranged from 24 k ohms to 185 k ohms with a majority, 124 out of 442, also laying between 30+ and 40 k ohms (figure 5.4b). Except for the extreme values the distributions of intersegment resistances in the two strips are similar, albeit non-uniform.

Also, a discrepancy was noted between the measured resistance of a 1.2-m length of strip and the sum of the individual intersegment resistances. The corresponding values for one strip were 14.58 M ohms and 19.75 M ohms and for the other strip were 15.6 M ohms and 21.15 M ohms. As the resistive layer was basically brushed on, this discrepancy could be due to the contact resistance between the resistive layer and each conducting segment. The brushed-on method of producing the resistive layer may also be the cause for the tendency of higher values of intersegment resistance to be

concentrated on one half of the strip (figures 5.3a and 5.4a).

With reference to the proposed flashover mechanism (section 3.4), it would be possible to predict the point of initiation of flashover if the intersegment resistances remained constant thus maintaining the spatio-relationship. However, owing to the possible existence of contact resistance, the intersegment resistances may change. These possibilities are investigated in the next section.

5.2 Change in intersegment resistances with repeated applications of voltage impulse (Full wave)

5.2.1 Using voltage impulses at levels below V_o

The experimental arrangement was as shown in figure 5.5. The length of segmented strip used was 0.14m. Before commencement of the test, the intersegment resistances were measured. A voltage of 91.8 kV prospective peak was then applied to the strip without causing a flashover. The intersegment resistances were measured again and the values were found to have been reduced. The second impulse applied had a higher voltage of 97.6 kV prospective peak and a flashover resulted. The intersegment resistances were again measured with evidence of further reduction in value. The third, fourth and fifth impulse applied had values of 91.8 kV prospective peak and the intersegment resistances were measured after each application of the voltage impulse.

The spatial plot of the intersegment resistances in log-linear

scale is shown in figure 5.6a and in linear-linear scale in figure 5.6b. As high-lighted in figure 5.6b, the intersegment resistances were reduced considerably after the application of only one voltage impulse and after five applications of the voltage impulse, the non-uniformity of the intersegment resistances was greatly improved. At this stage, the ratio between successive intersegment resistances was still as high as 3:1 (figure 5.6c). Figure 5.6d shows histograms of the intersegment resistances, each corresponding to one set of the results shown in figure 5.6b. After only 5 applications of the voltage impulse, all intersegment resistances had been reduced to less than or equal to 24 k ohms with a majority between 10+ and 12 k ohms.

5.2.2 Using voltage impulses at levels above V_{100}

A new 0.14-m length of strip was used and the procedure and experimental arrangement were as in section 5.2.1. The voltage impulse applied had a 120.5-kV prospective peak value and the intersegment resistances were measured before the test; after the eleventh application of the voltage impulse and after the twenty-second application of the voltage impulse.

The results are shown in figures 5.7a to d which, like those of figures 5.6a to d, revealed a tendency for the intersegment resistances to be reduced with repeated applications of a voltage impulse. In this investigation, all intersegment resistances were reduced to less than or equal to 12 k ohms with a majority between 4+ and 6 k ohms.

5.2.3 Using voltage impulses at levels between V_o and V_{100}

The experimental arrangement was as shown in figure 5.5 and a new 0.3-m length of strip was used. In this test, the impulse applied had a prospective peak of 200.9 kV which was estimated to lie between V_o and V_{100} for this length of strip. The estimate made was based on the results of section 5.2.1.

Before commencement of the test, the intersegment resistances and the strip-resistance were measured. As expected, there was a discrepancy between these two values with the sum of the individual intersegment resistances being greater than the strip resistance. Impulses were then applied to the strip which caused a sequence of flashovers and non-flashovers. The test was terminated when 100% flashover was obtained between the 45th and the 62nd impulse application. The strip resistance was again measured and found to be 0.65 M ohms compared with an initial value of 0.96 M ohms.

It was observed that on the rear of the segmented strip (i.e. the side on which the resistive layer was situated) the dielectric coating had been removed and the resistive layer exposed. Apparently, this damage was the cause of the 100% flashovers. Flashover was evident due to the presence of burn-marks in the immediate vicinity of the damaged area (figures 5.9 and 5.10).

As a result of the flashovers across the front surface there were 'carbon' deposits between segments as shown in figure 5.8. Removal of these deposits increased the strip-resistance from 0.65 M ohms

to 0.675 M ohms, i.e. by about 4%. The intersegment resistances were again measured.

Table 5.1 shows the results of the measurements taken and the observations made. As expected, the values of the intersegment resistances were reduced from an average value of 18 k ohms to an average value of 6 k ohms. The results appear to confirm the possibility that high contact resistances exist between each segment and the resistive layer. Before the application of impulses to the strip, the sum of the individual intersegment resistances was approximately 2 M ohms and the strip resistance was 0.96 M ohms. After the application of impulses, the difference between these resistances was negligible with the sum being 0.678 M ohms and the strip-resistance 0.675 M ohms. In addition, it appeared that the flow of current through the resistive layer improved the conductivity of the layer too. This was shown by the reduction of the strip-resistance from 0.96 M ohms to 0.675 M ohms. Also, it appeared that the intersegment resistances of damaged areas were relatively higher than those of undamaged areas. These higher values probably result from some inevitable removal of material comprising the resistive layer.

The reduction in intersegment resistances appeared to result from the better electrical contact achieved between each segment and the resistive layer after a flow of current through it. The contact resistance falls with every application of a voltage impulse and finally became negligible when the intersegment resistances stabilised at values between 4 and 6 k ohms. As discussed in

section 3.4, flashover voltage of a segmented strip is dependent upon the intersegment resistances. Therefore, it would be necessary to resistance-stabilise a segmented strip by repeated applications of a voltage impulse before any test was made.

Apparently, damage occurring on the rear of a segmented strip reduced the withstand voltage. Investigations on the cause of damage and on methods to prevent the occurrence of damage are reported in the following sections.

5.3 Rate of deterioration of segmented strip with repeated impulse applications (Full wave)

5.3.1 With voltages less than the flashover value

The experimental arrangement is shown in figure 5.5. A partially damaged 546-mm long segmented strip was used. This, however, was of no consequence as the aim of the test was to establish whether more intersegment surfaces at the rear would be damaged by the application of impulse voltages at less than the flashover value. The voltage level applied was 160 kV peak and the frequency of application was one impulse every 50 seconds. After the application of 70 impulses, flashover occurred on every subsequent impulse. The level of the applied voltage was then reduced to 150 kV peak for the remainder of the test which was terminated after about 2 hours. Observation of the strip revealed that an additional 119 intersegment surfaces had been damaged. These results are tabulated in Table 5.2.

5.3.2 With voltages higher than the flashover value

The experimental arrangement is shown in figure 5.5. For the reason mentioned in the preceding section, a partially damaged 0.14-m long segmented strip was used. The voltage level of the impulse applied was 160 kV which was about 1.5 times the V_{50} flashover value. The frequency of impulse application was one every 40 seconds and the duration of the test was about two and three-quarter hours. At the end of the test, no additional damage to the intersegment surfaces on the rear of the strip was evident. The results are tabulated in Table 5.3.

It appeared that no damage to the resistive track occurred if the applied voltage was such as to produce flashover of the strip. Damage only occurred if the strip withstood a voltage in excess of a critical value.

5.3.3 With voltages between V_o and V_{100}

The experimental arrangement is shown in figure 5.5. A new 0.3-m length of segmented strip was used. An estimate of the 50% flashover-voltage level was obtained by performing the 'Up & Down' test on the strip for a total of 18 impulses. The estimate of V_{50} resulting from this test was 192.2 kV and no damage to the intersegment surface at the rear was observed. For subsequent application of impulse-voltages, the voltage level was fixed at 192.2 kV and the rear surface of the strip was inspected for damage after every fifth flashover. The test was terminated when it became clear that

flashover would result on each application of the impulse-voltage.

Table 5.4 is a tabulation of the results obtained. It shows that the applied voltage level of 192.2 kV was higher than the 50% level and was close to the 100% level after the application of the 62nd impulse. At this point, 11 intersegment surfaces were damaged out of the total of 111 and 'burn' marks were to be seen in the vicinity of 3 of them. With the application of the next 22 impulses, 9 additional intersegment surfaces were damaged and 'burn' marks appeared on another 13 intersegment gaps. There was an apparent correlation between reduction in the withstand level of the strip and damage to the intersegment surfaces at the rear.

Figure 5.11 shows the complete rear view of the segmented strip. Scanning-electron-microscope photographs of the damaged area are shown in figure 5.12. Evidence of arcing between the segments at a damaged intersegment surface was revealed by metal erosion on the segments and also by the formation of a channel between the segments probably due to vapourisation of the carbonised-resin.

Scanning-electron-microscope photographs of the front of a segmented strip are shown in figures 5.13 and 5.14. The former figure shows the surface structure of the segments and the surface between them on a new length of segmented strip and the latter figure shows corresponding regions on a strip which has been flashed over. As a result of the flashover, melting was evident although confined to the section of the segments nearest to the intersegment gap. The dielectric surface between the segments contained particles which

appeared to have come from the segments. The 'carbon' deposits were situated around the intersegment gaps on the dielectric surface as well as on the segments. X-ray analysis of the deposits (figure 5.15) on the dielectric surface produced results which were not much different from those of a dielectric surface of a new segmented strip (figure 5.2). This showed that the deposit contained mainly elements which are below magnesium in the periodic table. However, quantitative analysis of the same region showed the presence of 0.7 - 1.4% of nickel. The corresponding value for a new segmented strip was 0%. Quantitative analysis of the intersegment surface outside the area of the deposit also showed the presence of nickel in the same order of magnitude. Tentative results from an Auger analysis[76] gave the composition of the dielectric as 95% carbon; 2.5% oxygen; 1.9% titanium and 0.6% sulphur, and the compsition of the conducting segment as 79.1% carbon; 10.7% oxygen; 5% titanium; 4.1% nickel and 1.1% sulphur. It should be noted that the samples used in the X-ray and Auger analyses were not the same although both were taken from used strips. From the X-ray results it can be concluded that, very probably, a small amount of nickel had been eroded from the segments and deposited on the intersegment surfaces.

Figure 5.16 shows the location of the 'carbon' deposit on the strip surface. Although a high percentage of carbon was detected in the deposit outside the segments, it was not possible to conclude the presence of carbon in the deposit because the dielectric surface was carbon based. However, the detection of a high percentage of carbon in the deposit on the segments did indicate that the deposit

was indeed carbon because the segments were made of nickel-plated copper.

Integrated photographs of the light emission from the discharges on the strip were taken both 'face-on' and 'side-on'. Only two intersegment gaps were observed for reasons of spatial resolution and the rear surface of one of the gaps had been damaged. This was arranged in order to investigate whether flashover was still occurring on the front of the intersegment gap while there was damage at the rear. The results are shown in figures 5.17 and 5.18. Flashover only occurred across the front when the rear surface was not damaged and only occurred across the rear when the rear surface was damaged. The latter observation was interesting in view of the fact that the separation between the square segments at the rear is 5 times that between the corresponding circular segments at the front. The implication here is that segments having high stress points, e.g. corners of a square, have a higher probability of initiating a flashover. Hence, a reduction in the withstand voltage of a segmented strip is expected when the strip is damaged and these high stress points are no longer covered by the insulating layer. The light emission due to the flashover at the rear appeared to be more active than that of the front. In general, the discharge was a single channel between the segments. However, in one case there seemed to be two discharge channels which were parallel and displaced from the axis of the intersegment gap.

5.4 Behaviour of segmented strips when mounted on a dielectric

In practice, the segmented strip is normally mounted on a radome

surface. This condition was simulated in the laboratory by mounting the segmented strip on transparent perspex or by applying a thick layer of adhesive to the back of the strip. This simulation was undertaken to determine whether damage to the strip could be prevented.

The experimental arrangement is shown in figure 5.5. Four new lengths of segmented strip, each 0.14m long, were used and were prepared in the following manner.

a) The first segmented strip was stuck on to a piece of clear perspex, using two component quick drying adhesive, and the circular conducting segments were left exposed.

b) The second was prepared in a similar manner but using the recommended two component epoxy adhesive provided by the Royal Aircraft Establishment, Farnborough, U.K.

c) The third was coated on the back with a 1mm thick layer of two component quick drying araldite adhesive.

d) The fourth was prepared in a similar manner as the third but using the recommended two component epoxy adhesive.

An 'Up & Down' test was performed on each of the strips and the test was terminated for each when it became apparent that further applications of impulse voltages would cause 100% flashover. The results of the tests are shown in figures 5.19 to 5.22. At the end of the tests, the condition of the segmented strips was as follows.

a) The first strip had separated from the perspex except for about 30 mm at the earthed end. It was evident that the araldite was not suitable for bonding to the segmented strip because the araldite remained on the perspex surface over most of the

separated section and left no traces of araldite on the surface of the segmented strip. In addition, 22 of the 51 intersegment surfaces had been damaged by the application of 24 impulses.

b) The second strip also separated from the perspex except for a 10 mm portion at the high voltage end. The insulation layer which was detached from the rear surface of the segmented strip remained glued on to the epoxy adhesive which was still intact on the perspex surface. This observation indicated that the epoxy adhesive had formed a good bond between the perspex and segmented strip surfaces. Altogether, 42 of the 51 intersegment gaps were damaged after the application of 35 impulses.

c) The extent of damage to the third and fourth strips were similar to that of the first and second respectively.

The results indicated that neither mounting the segmented strip on an insulating surface nor coating the rear of the strip with a thick layer of insulating adhesive prevented the occurrence of damage to the back of the segmented strip but indeed appeared to increase the rate at which damage occurred.

5.5 Attempts to obtain a stable strip-flashover characteristic

The results so far indicated that the withstand voltage of a segmented strip would be reduced as a result of damage to the intersegment surfaces at the rear. This would undoubtedly alter the flashover characteristics of the strip and this was not desired.

Two approaches to this problem were:-

a) to maintain the withstand voltage of the strip by some means, even though it was damaged, and

b) to prevent it being damaged at all.

5.5.1 'Repair' of segmented strip

The first option was attempted by applying a layer of silicon grease on to the damaged area. It was considered that the silicon grease layer should restore the dielectric strength of the damaged area thus preventing discharging at this point on the strip and hence maintaining the flashover strength. The term 'repair' is used to identify such an attempt.

Using the experimental arrangement shown in figure 5.5, and a new 0.14-m length of segmented strip, an 'Up & Down' test was performed with the magnitude of the first voltage applied being 91 kV. The strip was examined for any possible damage after each time that it withstood the applied impulse voltage. If damage had occurred, the damaged area was 'repaired' before continuation of the test.

It was noted that arcing across the damaged area was prevented by the 'repair' but that the flashover strength was not maintained as shown by the results in figure 5.23. After having withstood 11 impulses, the first damage was observed as shown by point 'a' in the figure. That this damage reduced the withstand level of the strip is evident from the six successive flashovers following the initial damage. At the reduced withstand level, more damage occurred

(point 'b') and reduced the withstand level further. More damage were observed at points 'c' to 'i'.

Air-holes were also visible in the silicon grease layer. The presence of these air-holes indicated the escape of gas or gases due to intense heating at the damaged areas. It appears that although the silicon grease did prevent flashovers across damaged areas, the silicon grease is not capable of maintaining the withstand level and hence the flashover characteristic of a strip. After 60 applications of the voltage impulse, the withstand level had decreased by about 20%. The other possibility is that the silicon grease is effective in preventing flashovers across damaged areas and the reduction in withstand level is due to some other factors, e.g. conditioning characteristic of section 6.1.

5.5.2 Application of chopped impulses

In section 5.3.2, it was shown that no damage to the strip resulted when the applied impulse caused a flashover. This could be made use of to prevent strip damage during testing. From voltage records obtained during an 'Up & Down' test on a segmented strip, the maximum time-lag to flashover was determined to be about 3 microseconds. Time-lag is as defined in figure 5.24 . Therefore, if the applied impulse was chopped at a time of, say, 5 microseconds, the probability of damage to the strip would be much reduced. Table 5.5 shows the effect of chopping time on the action-integral of impulses. For chopped impulses having a time to chop[77] of 5 microseconds, the energy deposited per metre into the resistive

layer would be only 10% of that deposited by a full impulse.

The chopping gap system used was described in section 4.4. The 'Up & Down' test was performed on a new 0.5-m length of strip bridging a rod/plane gap. The strip was examined for damage after every fifth impulse and the test was terminated after a total of 66 impulses had been applied. No visible damage to the strip was observed throughout the test.

In view of the results obtained, a parallel chopping gap system was preferred to the silicon-grease 'repair' technique.

5.6 Summary of results and discussion

The intersegment resistances of a new length of segmented strip varied over a wide range of values. This large variation of intersegment resistance was apparently caused by high contact resistance between each conducting segment and the resistive layer. The contact resistance could be greatly reduced with any of the procedures described in section 5.2 and such resistance-stabilisation would be desirable if it was assumed that the flashover characteristics of the segmented strip was dependent upon the intersegment resistances. The result of the stabilisation was to reduce the intersegment resistances to about 5 k ohms.

The probability of damage occurring to the intersegment surfaces at the rear was greatly increased when the strip withstood the voltage applied. The consequence of such damage was to reduce the withstand

voltage level of a segmented strip thus altering the flashover characteristics. Mounting the strip on to a dielectric did not prevent damage occurring to the strip nor did the prevention of arcing across damaged areas between segments appear to maintain the withstand voltage level. The application of chopped impulses did prevent damage to the strip and this technique was used in all further experiments.

In addition, there was no difference in the flashover results obtained with the strip unmounted or mounted on a perspex sheet and hence, all future experiments were conducted with unmounted strip.

6 EXPERIMENTAL RESULTS AND DISCUSSION

6.1 Conditioning characteristics

It was shown in the previous chapter that repeated applications of an impulse voltage considerably reduced the intersegment resistance. It was also noted that a segmented strip would need to be resistance-stabilised by repeated application of an impulse voltage if the flashover voltage was affected by the values of the intersegment resistances.

In order to examine the effect of repeated voltage application on the strip flashover voltage, a 0.3-m length of segmented strip was tested using the experimental arrangement shown in figure 6.1. This was the only arrangement used in the tests described in this section. The voltage chopping system was set to give a time-to-chop of approximately 5 microseconds. An 'Up & Down' test was performed on the strip, starting with an applied voltage of 111.5 kV and using changes in the level of the applied voltage of 2.2 kV. The test was terminated when both the withstand and flashover voltage levels reached constant values. The procedure was repeated for new strips, having lengths of 0.5 m and 0.75 m, but with changes in the level of the applied voltage of 4.5 kV and initial applied voltages of 182.9 kV and 379.1 kV respectively.

The results obtained are shown in figure 6.2. Conventionally, in the presentation of 'Up & Down' test results, flashovers were indicated by crosses and non-flashovers or withstands by noughts.

However, owing to the number of impulses applied for each test, it was considered appropriate to present the results as straight lines joining all the applied voltage levels sequentially. Whether a flashover or a withstand occurred at any point on the curve can then be determined from the sign of the slope of the line from that point to the next point. The results show that repeated flashovers tended to reduce the flashover strengths of the strips. The reduction in flashover strength was however a gradual process, comprising a series of diminishing withstand and flashover voltage levels, and a relatively stabilised condition was considered to have been achieved when this process ended. At this point, the strip is considered to be conditioned. Earlier results have shown that a segmented strip would be resistance-stabilised after about 50 impulse applications. Therefore, the reduction in flashover strength is unlikely to be due to the intersegment resistances but to other causes.

In general, the results could be represented by the curve shown in figure 6.3. Two distinct regions can be distinguished, viz. the conditioning-phase and the stable-or conditioned-phase. The stable-phase covers the region where the response was fairly consistent while the region before it is the conditioning-phase. For the purpose of investigating the variation of flashover voltage with strip length, it was therefore reasonable to obtain flashover data from the stable phases.

6.2 Mean voltage at flashover and time-lag characteristics

6.2.1 For a strip bridging plane/plane electrodes

The experimental arrangement is shown in figure 6.1. The 1.01-m segmented strip used had already had 0.75 m of its length conditioned in the tests described in the previous section. The earthed-end was solidly connected and the upper-end was in touch-contact with the high voltage electrode. The chopping gap system was set to give a time-to-chop of 5 microseconds. The 'Up & Down' procedure was then performed on the strip until the stable phase had been attained. Further impulses were applied to obtain data for calculation of the mean voltage at flashover and its 95% confidence level using the standard statistical treatment for random data having a t-distribution[78]. For flashovers occurring on the wavetail, the flashover voltage was considered to be equal to the peak value[77]. For flashovers occurring on the wavefront, the flashover voltage was given by the voltage at the instant of voltage collapse. This voltage was determined by using the time at flashover, t, in the expression $V_i = 1.08U (\exp(-0.0211t) - \exp(-1.4528t))$ which represented the applied impulse voltage (U = 1 for unity peak voltage and t is in microseconds). The error on the computed voltage is a maximum of $\pm 1.5\%$ over the range of breakdown times measured. The time-lags to flashover were determined from the voltage oscillograms. The procedure was repeated for segmented strip lengths of 0.75 m, 0.5m and 0.3 m and the values of the mean voltage at flashover and the time-lags to flashover are shown in figures 6.4 and 6.5 and Table 6.1. The 50% flashover voltages and their 95% confidence levels were calculated using the equations as given by Dixon and Mood[74] and an illustration of this technique is

given in Appendix 4.3.

Figure 6.4 is a graph showing the relationship between flashover voltage and strip length. The straight line through the origin is is a least-square fit to the results and gives the mean field at flashover as 380 kV/m.

There was scatter in the time-lags to flashover at each strip length considered. The scatter was largest at the shortest length and smallest at the longest length. The minimum time-lag to flash-over was 0.8 microsecond at 1.01m and 1.2 microseconds for the other three lengths tested.

Table 6.2 shows the comparison of experimental results and reference values for different strip lengths. The reference value at the various strip lengths is given by the product of the flashover voltage of a 0.3-mm uniform field air-gap and the total number of 0.3-mm intersegment gaps. The flashover voltage of the uniform field air-gap was computed using the expression $V_s = 24.4\rho d + 6.53\sqrt{\rho d}$ where V_s is in kV, d is in cm and ρ is the air density-correction factor. The expression[81] is for a uniform field and valid for gap lengths between 0.01 and 20 cm under static or alternating voltage stress. Impulse breakdown data by Aked[79] for 0% breakdown with 1/50-microseconds waves were within 1.5% of the formula over the range 1 to 5 cm. Therefore, the computed voltage is the withstand voltage for lightning impulses. The maximum flashover values (column 5, Table 6.2) were obtained from the conditioning results of section 6.1. The experimental

results were smoothed using a least-square fit and comparisons are made between the smoothed values and the computed values.

The comparisons show that the reference values bore constant ratios to both sets of least-square approximated values. The values of the mean voltage at flashover were about 56% of the reference values and the maximum flashover values were about 19% above the reference values. Therefore, it is considered that the flashover voltage of a new length of segmented strip is given by the product of the breakdown of a 0.3-mm sphere/sphere air-gap and the number of intersegment gaps. However, this relationship would have to be investigated in further studies using arrangements having one intersegment gap; two intersegment gaps; three intersegment gaps and so on. Thus, the flashover voltages for one, two, three, ... gaps in series could be compared.

In chapter 3, it was reported that the flashover strength of an air gap is always higher than when the same gap is bridged by a dielectric surface. This effect was only apparent on a conditioned segmented strip and not on a new strip. This may be explained with reference to figure 6.6 which shows the profile of an intersegment gap in a new strip and the assumed profile of an intersegment gap in a conditioned strip. The recessed dielectric surface between the segments in a conditioned strip may result from vapourisation of the dielectric material during a flashover. A typical field line between the segments is shown dotted in each of the profile. Therefore, for a given breakdown strength, the flashover voltage of a new strip should be higher than that of a conditioned strip. In

addition, the effect of the dielectric surface on the flashover strength of a new strip may also be negligible. Table 6.2 shows that the effect of the dielectric surface was to reduce the flashover strength to about 60% of the reference value. It is assumed here that the one major factor for the reduction in flashover strength is the presence of the dielectric surface between the segments. Future studies using strips where the variables, like segment protrusion; surface roughness; dielectric constant and intersegment resistance; for example, are under control might identify other possible factors.

The corollary is that the maximum flashover strength of a segmented strip should be used in the determination of the critical length (see chapter 2) which is the maximum length of strip that can be used and at the same time prevent puncture of the radome wall or flashover of the radome surface. Owing to non-availability of the relevant data, numerical determination of the critical length is not yet possible.

6.2.2 For a strip bridging rod/plane electrodes

The experimental arrangement was as shown in figure 6.7 and the segmented strip used was the same one as that described in section 6.2.1. The chopping gap system was set at a time-to-chop of about 5 microseconds.

The ends of the strip were solidly connected to the high voltage and earthed electrodes respectively - arrangement 1. With the effective

strip length set at 0.3m, the 'Up & Down' procedure was performed on the strip and oscillograms of each applied impulse voltage were obtained. The mean voltage at flashover and its 95% confidence levels were determined as in section 6.2.1.

The procedure was repeated for effective strip lengths of 0.5m, 0.75m and 1.01m.

Mean voltages at flashover and time-lags to flashover were also determined for these lengths of segmented strip, using the same procedure but in an arrangement in which there was a 2-mm gap between the upper end of the segmented strip and the surface of the rod electrode - arrangement 2.

The results obtained are shown in figures 6.8 and 6.9. The results pertaining to arrangement 2 have been plotted with the vertical axis shifted 2 mm to the right of the vertical axis for arrangement 1. This is to provide clarity and ease of comparison.

Apart from the fact that at a strip length of 0.75m where the mean voltage at flashover for arrangement 2 was about 25% higher than that for arrangement 1, there was no other significant difference in the levels of the mean voltage at flashover between the two arrangements for the lengths of segmented strip considered. Inspite of the anomalous behaviour, it is still apparent that the relationship between strip length and mean voltage at flashover is not linear. This non-linearity may be attributed to the divergent geometric field of the rod/plane gap (c.f. results for plane/plane gap,

figure 6.4).

There was scatter in the time-lags to flashover, for each strip length, and the magnitude of the scatter varied from one length to another. At the shortest length of 0.3m, the scatter in the time-lags to flashover was much larger than that at 1.01m. However, the minimum time-lag to flashover measured for each strip length lay between 0.8 and 1.2 microseconds.

In the investigation of Plumer and Hoots[35], the experimental arrangement was basically a point/plane configuration with the laboratory floor acting as the plane. The segmented strip used was 1.22m long and was mounted on a fibreglass panel, 1.22m square. The lower end of the strip was attached to an earthed-bar along the bottom edge of the panel and the high voltage point was a few centimetres from the upper end of the strip. With the strip length kept constant, voltages ranging from about 700 kV peak to greater than 1600 kV peak were applied. The results obtained are shown in figure 2.2. A fairly constant time-lag to flashover of 0.7 microsecond was obtained for the segmented strip while the time-lag to flashover of an equal length of air gap, without the presence of the strip, varied as shown, for the same range of applied voltages. This latter is typical of an air gap stressed at different overvoltages.

The apparent contradiction between Plumer and Hoots' observed time-lags to flashover and those of the author is, however, only superficial. The time-lags to flashover presented by the author were observed as a result of the application of voltages each of

which had a probability of 0.5 of causing a flashover. In addition, the mean voltage at flashover obtained by the author was about 104 kV for a 1.01m length of strip. The minimum voltage applied by Plumer and Hoots was about 700 kV peak which is at least six times greater than the expected V_{50} value for a length of 1.22m. In short, the time-lags to flashover obtained by Plumer and Hoots were measured under experimental conditions different from the author's. They obtained an approximately constant time-lag to flashover of 0.7 microsecond under overvoltage conditions. In comparison, the range of time-lags observed by the author for a strip length of 1.01m was from 0.8 to 1.0 microsecond for arrangement 2. Therefore, it is probable that the scatter would be negligible under overvoltage conditions thus making the measured time-lags to flashover an approximate constant of 0.8 microsecond.

6.2.3 For a strip bridging rod/rod electrodes

The experimental arrangement was as shown in figure 6.10 and the tests were carried out on the same segmented strip as was used in the previous measurements described in sections 6.2.1 and 6.2.2. The special electrodes used were described in section 4.3.2 and the earthed electrode allowed for the effective length of the strip to be altered by having a section of the strip (shown dotted in figure 6.10) situated within it. To reduce the effect of the laboratory floor on the geometric field, the tip of the earth electrode was set 2m above floor-level. The parallel chopping gap system was again set at a time-to-chop of about 5 microseconds.

The upper end of the strip was kept at a distance of about 2mm from the tip of the high-voltage electrode, i.e. the strip partially bridged the rod/rod gap - arrangement 3. With the effective length of the strip set at 0.3m, the 'Up & Down' procedure was performed on the strip and oscillograms of each applied impulse voltage were made. The mean voltage at flashover and its 95% confidence levels were determined as before.

The procedure was repeated for effective strip lengths of 0.5m, 0.75m and 1.01m respectively and also at 0.3m, 0.5m, 0.75m and 1.01m for the experimental arrangement having the upper end of the strip solidly connected to the high voltage rod electrode - arrangement 4. The results obtained are shown in figures 6.11 and 6.12.

The mean voltage at flashover measured for each strip length did not differ very much between the two arrangements except at 0.5m, where the mean voltage at flashover for arrangement 3 was significantly lower than that for arrangement 4. Nevertheless, it is apparent that the relationship between the flashover voltage and strip length was again non-linear. As in section 6.2.2, this non-linearity is probably due to the non-uniform geometric field.

Scatter in the time-lags to flashover was apparent for each strip length and as in the previous results, the scatter varied from one length to another. The scatter in the time-lags was again largest at the shortest strip length of 0.3m. The scatter also tended to reduce with increasing strip length for both arrangements except for arrangement 3 with a strip length of 0.5m. This result had a

negligible scatter and had the lowest time-lag to flashover - 0.7 microsecond. Minimum time-lag to flashover for the other results ranged from 1.0 to 1.6 microseconds.

Table 6.3 summarises the results obtained for strips in a non-uniform geometric field.

The flashover voltage results are not in agreement with the conclusions of Plumer and Hoots[35] who claimed an approximately linear relationship between flashover voltage and strip length. The experimental arrangement used by them is shown in figure 6.13. The strip lengths tested were 0.87m, 1.07m and 1.75m and different strips were used for each length tested. Their assumption was that different strips would possess similar flashover characteristics. For each strip length tested, the magnitude of the applied voltage was kept constant at about 700 kV peak. The result is reproduced in figure 2.3. It is the author's view that the relationship between the flashover voltage and strip length should not be determined by the application of constant magnitude voltages for different strip lengths. By applying a constant magnitude voltage, the shortest length tested would be subjected to the highest rate of rise of electric field and vice versa. Instead, the probability of flashover, resulting from the application of a voltage across any length of strip tested, should be approximately equal, preferably having the value of 0.5. Also, Plumer and Hoots presented results obtained from the applications of both positive and negative impulses in the same figure. This is unsatisfactory and does not give a true picture of the flashover voltage/strip length relationship for a segmented strip.

Another point which might have caused a change in the test-conditions is that the test voltage was taken from the second bottom stage of a 14-section voltage divider. In doing so, the source impedance would be high and if this was of the same order as that of the strip resistance, the applied waveform and voltage magnitude would be different from those expected.

With the effective strip length at 1.01m, the author has investigated the possibility of a constant time-lag to flashover under overvoltage conditions. Voltages having prospective peaks of up to three times the V_{50} value were applied and the time-lags to flashover remained relatively constant at 0.6 microsecond (figure 6.14). This confirmed the suggestion made in the last paragraph of section 6.2.2.

6.2.4 Comparison of strip flashover voltages with breakdown voltages of air gaps

As no breakdown voltage data for a rod/rod configuration similar to that used by the author were available, these data were obtained experimentally.

The experimental arrangement is shown in figure 6.15 with the two rod electrodes situated on the same axis. The gap length was altered by raising or lowering the high voltage electrode. The parallel chopping gap system was in-circuit but made ineffective by having a large sphere/sphere gap.

The 'Up & Down' procedure was performed for each of the four gap

lengths considered (0.3m, 0.5m, 0.75m and 1.01m) and oscillograms of each applied voltage impulse were obtained. Since every breakdown occurred with a time-lag which corresponded to a point on the wavetail of the applied impulse, the breakdown voltage is considered to be the peak value of the applied impulse as recommended by IEC 60[77]. Hence, the 50% flashover voltage was calculated as described in Appendix 4.3. The results are shown in figures 6.16 and 6.17. The straight line through the origin in figure 6.16 is the least-square fit to the experimental data and gives a mean field at V_{50} of 630 kV/m.

For the rod/plane air gap, Paris and Cortina[80] obtained a mean field at V_{50} of 540 kV/m which is in agreement with results of earlier investigators[81]. This value of 540 kV/m was used to compute the breakdown voltages required in the comparison.

Owing to the limited output voltage of the impulse generator, the breakdown voltages of a uniform field air gap at different gap lengths were calculated using the expression for static and alternating voltage stress[82]. The computed and measured results for all three electrode configurations are given in Table 6.4.

Figure 6.18 shows a graphical comparison between the flashover voltage characteristics of a segmented strip and the breakdown voltage characteristics of air gaps for the three electrode configurations. Two observations are immediately apparent. Irrespective of the electrode configuration, the mean field at flashover of a conditioned segmented strip is always lower than the

mean field at V_{50} of an air gap of equal length. In other words, the introduction of a segmented strip into an air gap reduces the breakdown voltage considerably. Assuming a linear flashover voltage/strip length relationship for a strip bridging a uniform field gap, the reduction in breakdown voltage is approximately 84%. As the plane electrodes used had an effective diameter of 1.83m, a uniform field at the central region of these electrodes will exist as long as the gap length is not greater than the radii of the electrodes. Therefore, at the gap length of 1.01m, a non-uniform field situation arises and results in an actual breakdown voltage which will be less than the estimated value. Hence, the reduction in breakdown voltage due to the introduction of a strip at this length would be less than 84%. When a strip bridges a rod/rod gap, the reduction is about 50% at a strip length of 0.3m and about 82% at a strip length of 1.01m. The corresponding values are 55% and 80% when a strip bridges a rod/plane gap. Owing to the saturation effect, which causes the proportional increase in flashover voltage to be considerably less than the corresponding increase in strip length for non-uniform geometric fields, the reduction in breakdown voltage could be as high as 90% at a strip length of 2m. The saturation effect can be seen from the results of all the tests which are shown in figure 6.19. It is also evident that the flashover voltage is related to the geometric field in which a strip is situated. For positive impulses, the breakdown voltage of a plane/plane gap is greater than that for a rod/rod gap which in turn exceeds that of a rod/plane gap[80]. This relative order is maintained even when the gaps are bridged by segmented strips.

The other observation, and perhaps the more important, is the magnitude of the flashover voltages required by an unconditioned strip in a uniform geometric field. These flashover values are about 30% of the breakdown values of uniform field air gaps and this figure is rather surprising in view of the fact that about 90% of the gap is bridged by the conducting segments in the strip. Notwithstanding this, the ratio of the flashover values of an unconditioned strip in a rod/rod or rod/plane gap to the breakdown values of the air gap may not be as low as 30% due to the possibly less significant effect of the strip in gaps having non-uniform geometric fields. This possibility should be examined in future studies for the following reason. If the lightning leader is assumed to be equivalent to a rod electrode and the field distribution non-uniform, then this would imply that a newly installed segmented diverter strip protection system might be ineffective. The alternative implication is that only conditioned segmented strips should be used because of their lower flashover voltage. The lower flashover voltage of a conditioned strip also implies that such a strip would have a better capture capability than a new strip. This was shown by tests undertaken at British Aerospace[32] (formerly British Aircraft Corporation), Stevenage. In the tests, a discharge was initiated from a high voltage electrode situated above and mid-way between two segmented strips, one of which was new. The results showed a definite bias towards the used strip in terms of the number of discharges captured.

6.3 Time-resolved photographic study of the propagation of the intersegment flashovers

The experimental arrangement was as shown in figure 6.1 and the effective length of the segmented strip was set at 0.3m. The strip was the same one that had been used for the tests described in the previous section and the parallel chopping gap system was set for a time-to-chop of about 5 microseconds.

A 105-mm lens was used to focus the entire length of the strip on to the photo-cathode of an image converter camera. The triggering of the converter camera is described in section 4.6.3. Owing to the wide scatter in the time-lags to flashover when the applied impulse was at the V_{50} level, there were synchronisation difficulties. These difficulties were reduced by applying impulses which were greater than the V_{100} level thus producing an almost constant time-lag to flashover of about 1 microsecond. With the camera operated at a framing speed of 2×10^6 frames per second, the results obtained indicated that a better time resolution was required. However, results obtained with the camera operated at the highest framing speed of 2×10^7 frames per second showed similar results. As the time between frames is 50 ns, when the camera is operated at this highest framing speed, the total intersegment flashover propagation time was less than 50 ns. The camera was then operated in the streak-mode to give better time resolution. Results obtained with streak speeds of 10ns/mm and 5ns/mm still showed inadequate resolution. Owing to the synchronisation difficulties when the camera was operated at streak speeds of 1ns/mm and 2ns/mm, only

three useful results were obtained and these are shown in figures 6.20 to 6.22. Although the spatial resolution is insufficient to resolve the individual intersegment gaps, it is still evident that the wave of intersegment flashovers did not propagate from anode to cathode or vice versa. The records also show that flashovers were initiated in different gaps along the strip and that in approximately 10ns all the intersegment gaps had flashed over. At the instant of discharge initiation, discharge free sections are seen to punctuate the whole strip and such sections were as long as 30mm. To investigate the possibility that some of the faint discharges had not been recorded on the film, the output of the converter camera was intensified by an image intensifier which was operated with a nominal gain of 10^6. The results obtained however were similar to those obtained when using the converter camera alone.

Better spatial resolution was achieved by focusing only on a few intersegment gaps, using a combination of two lenses. The two lenses used had focal lengths of 508mm and 105mm with the former nearer the segmented strip. Examples of framing records obtained at a framing speed of 2×10^7 frames per second are shown in figures 6.23 to 6.26. Owing to the high propagation speed of the wave of intersegment flashovers, most of the records obtained were similar to that shown in figure 6.23. Nevertheless, figures 6.24 to 6.26 indicate that there was no dominant direction of propagation, i.e. anode to cathode or vice versa.

Streak records obtained at a speed of 1ns/mm showed better time resolution. Figure 6.27 shows the streak record of discharges which

occurred in three intersegment gaps. The discharge associated with each intersegment gap is identified either as discharge A, B or C with discharge A nearest the earth-electrode. Considerable synchronisation difficulties were experienced during these measurements but sixty five synchronised records were obtained. As a considerable number of the time delays in discharge initiation among the three gaps were less than 1 ns (which corresponds to 1mm on the record), a double-beam, automatic recording microdensitometer was used to analyse all the records in order to prevent the possibility of human bias in the analysis. To cater for the possibility that the strip might not be physically perpendicular to the line of streak or that the discharges might not lie on a line perpendicular to the line of streak, integrated photographs of the discharges and still photographs of the short section of strip containing the three intersegment gaps were taken at intervals throughout the tests. These records were also analysed, using the microdensitometer, and the results used to establish the range of uncertainty in the time estimations for the purpose of determining the sequence of discharge initiation.

As each image of the discharge on the streak records was about 1.5mm wide, the window of the analyser probe was adjusted to give a slit of 0.05 mm width by 2mm length. The slit length of 2mm allowed the start of the image on the records to be determined accurately and, as shown in figure 6.28, also allowed a smooth trace to be produced. Figure 6.28 shows the microdensitometer analysis of the record shown in figure 6.27. The reference density (that of unexposed film and shown by the relatively straight horizontal trace

in the figure) is the same for the three discharges but has been shifted vertically in the figure. The instant of discharge initiation in any one record is shown by the start of a permanent deviation of the trace from the reference level. As indicated on the figure, the discharge sequence is determined as B $\approx$ C, A. The symbol $\approx$ is used to denote instances when the time difference between the two discharges lies within the range of uncertainty. Hence, either discharge B or C could have occurred first but discharge A definitely occurred last.

A tabulation of the analysis of the 65 recordings is shown in Table 6.5. In the determination of the discharge sequence, only a discharge which has a time separation, from each of the other two discharges, lying outside the range of uncertainty can have its position in the sequence identified. Brackets down the left of the table encompass rows of results which were obtained from consecutive frames of the negative. Examination of the bracketed results shows that the discharge sequence may change from one flashover to the next (brackets 1 and 3). This change agrees well with the proposition that the voltage distribution along the segmented strip is dependent upon the intersegment resistance (as shown in figures 5.6a and 5.7a, the intersegment resistance changes with applied impulses and it is probable that the status of neighbouring intersegment resistances may be interchanged, i.e. the higher intersegment resistance become the lower). More examples of this change in discharge sequence become evident if the range of uncertainty for the time separations among discharges is ignored.

The results, displayed in the form of a histogram in figure 6.29, show that there was no predominant sequence of discharges and this substantiates earlier streak and framing records (figures 6.20 to 6.26). Although the discharge sequence of only three intersegment gaps was determined, it is still evident that there was no dominant tendency for the wave of intersegment flashovers to propagate from the anode electrode to the cathode electrode or vice versa.

Figure 6.30 shows microdensitometer analyses of three consecutive integrated photographs of the 3 intersegment flashover discharges. Only one core of discharge, indicated by one trough, is identifiable in discharges A and B but two (shown arrowed in the figures) are identifiable in discharge C. In figure 6.30b, the two cores produce almost equal brightness and, if enlarged optically, would produce a photograph similar to that of figure 5.17b. This condition of equal brightness was not maintained as shown in the next frame (figure 6.30c) where the core on the right dominated in intensity. The double-core phenomenon may be due to two pairs of highly stressed points which were subjected to erosion during each discharge. Hence, the cyclic tendency in dominance of one over the other as shown in figures 6.31a and 6.31b from later frames. However, it is unlikely that the two cores of discharge would be occurring simultaneously.

6.4 Current measurement

The experimental arrangement is shown in figure 4.13a. The current

probe, the construction and characteristics of which are fully described in section 4.5, was connected in series with the segmented strip at the low voltage end. The segmented strip used was the one described in section 6.3 but cut to 0.3m length to accommodate the current probe. The parallel chopping gap system was set at a time-to-chop of about 5 microseconds.

Initial measurements of the current flowing through the resistive track of the segmented strip produced results similar to that shown in figure 6.32. The waveform of the current flow in the resistive track is as expected except for the presence of superimposed oscillations. These oscillations were damped by inserting a resistor between the output of the impulse generator and the high voltage electrode. Various resistances were used and the damped waveform for each is shown in figures 6.33a to 6.33f. Approximately critical damping was obtained for resistances between 0.4 and 1.5 k ohms. The value chosen for the remainder of the test was 400 ohms.

The 'Up & Down' procedure was then performed and oscillograms of the total current, i.e. the sum of the ohmic component due to the resistive layer and the gap-discharge component due to discharges in the intersegment gaps, were obtained. Figure 6.34 is an oscillogram of the total current with no apparent discharge development, i.e. the ohmic current only. From the 'Up & Down' test records, oscillograms showing the current growth to flashover were chosen for impulses having the same prospective peak values and are shown in figures 6.35 to 6.39. Each of these records was compared with the corresponding record (figure 6.34) showing only ohmic current, to

determine the gap discharge development time. Where the waveform of the total current first deviates from the waveform of the ohmic current determines the instant of discharge initiation. The instant of flashover is determined by the point on the record where there is a step change in current magnitude with the final value lying beyond the limit of the oscillogram. The gap discharge development time is then given by the time from the instant of discharge initiation to the instant of flashover. The oscillogram shown in figure 6.40 resulted from an applied voltage of 106 kV and, for the purpose of determination of the gap discharge development time, the ohmic current which would flow at this applied voltage was estimated by extrapolating the waveform of figure 6.34.

The gap discharge development times ranged from less than 0.1 microsecond to about 2 microseconds. However, the majority (75%) are less than, or equal to 1.0 microsecond with slightly less than 50% being less than, or equal to, 0.5 microsecond (figure 6.41). The single case of a 3-microsecond development time is exceptional. This may be due to an increased withstand capability for, as noted in figure 6.40, the applied voltage was 106 kV and this was the maximum level applied during the test. Subsequent development times were all less than 1.0 microsecond except for two out of nine, which were greater than 1.0 microsecond but less than 2.0 microseconds.

Figure 6.42 to 6.44 show some of the cases where isolated intersegment discharges might have occurred. Flashover did not occur and each voltage impulse was chopped by the operation of the parallel chopping gap system. However, deviations from the ohmic current

waveform (figure 6.34) are obvious and thus imply that the gap discharge current did not develop to flashover. It is not probable that a possible flashover had been suppressed as a result of the operation of the parallel chopping gap system because most of the flashovers tended to occur on the wavefront of the applied impulse, even when the parallel chopping gap was not present, as was the situation in some of the early measurements (see section 5.5.2).

In the analyses of the current records, it has been assumed that the values of the intersegment resistances are time-invariant. However, perhaps due to the heating effect (see section 5.5.1), the values may change with time during the period of the applied impulse. If this change is significant, then meaningful current measurements could only be made when the intersegment resistances are under control.

6.5 Summary of results and discussion

The conditioning characteristic of a new length of segmented strip, subsequent to resistance stabilisation, shows that there are two distinct regions, viz. the conditioning phase and the stable phase (figure 6.3). Therefore, to obtain consistent and reproducible results, flashover characteristics of a segmented strip should be obtained from a conditioned strip.

The variation of flashover voltage with strip length for a segmented strip bridging a uniform field gap is approximately linear (figure 6.4). The linear relationship gives a mean field at flashover of

about 380 kV/m. However, the relationship when a segmented strip bridged a rod/plane or a rod/rod gap was non-linear (figure 6.19). The non-linearity is probably due to the effect of the non-uniform geometric field between the high voltage and earth electrodes. This effect could be investigated by making time-resolved studies of the light emission from the discharges on a strip situated in a non-uniform geometric field. Unfortunately, the demand on the converter camera from other researchers, both in the department and in a co-operating institution, was so great that there was only an opportunity for studying the discharges in uniform-field air gaps.

The flashover voltage of a new length of segmented strip is given approximately by the product of the breakdown voltage of a 0.3-mm sphere/sphere air gap and the number of intersegment gaps (Table 6.2). This flashover strength is approximately double that of a conditioned strip.

When an air gap is bridged by a segmented strip, its effect is to reduce the breakdown voltage. The amount of reduction is dependent upon the geometric field of the air gap and also upon whether the strip is conditioned or otherwise. In the context of lightning protection, a conditioned strip should be able to perform effectively because the amount of reduction is at least 50%. The performance of an unconditioned strip or a new strip is however doubtful, particularly in a non-uniform geometric field.

There is scatter in the time-lags to flashover for each length considered and the scatter is reduced with increase in strip length

(figures 6.5, 6.9 and 6.12). The tendency is apparent in the results obtained for the three electrode configurations considered. It is not clear why the scatter is reduced with increase in strip length. Nevertheless, it is unlikely that the geometric field is a factor because similar characteristics were observed for strips bridging all three electrode configurations.

High speed photographs of the luminous discharge show that the wave of intersegment flashovers did not propagate from the anode electrode to the cathode electrode or vice versa. Instead, discharges were initiated from different points along the strip and discharge-free sections, which punctuated the entire length of the strip at the instant of discharge initiation, could be as long as 30mm. In addition, there was no predominant sequence of intersegment flashover. The absence of a predominant sequence further supports the proposal that the voltage distribution along a segmented strip is dependent upon the intersegment resistances which tend to change with each applied impulse and the change is such that the relative status of neighbouring intersegment resistances may be interchanged, i.e. a higher intersegment resistance may become the lower one when compared to its neighbour. Further studies using strips where the intersegment resistance can be kept constant could be used to test this proposition.

The development times from discharge initiation to strip flashover - determined from measurements of the total current - range from less than 0.1 microsecond to about 2.0 microseconds with the majority less than, or equal to, 1.0 microsecond. The current records obtained also show a probable occurrence of isolated intersegment discharges

which were initiated but did not lead to flashover of the strip. As light emission was not detected by the naked eye under these circumstances, confirmation of such occurrences would require the current measurements to be complemented by simultaneous photomultiplier measurements and such measurements should be undertaken in any future study.

7 PERFORMANCE OF THE DAYTON-GRANGER STRIP

7.1 General

Investigation was also undertaken on the most recent device introduced for lightning protection. This diverter strip is made by the Dayton-Granger division of Dayton System International Inc. and will be referred to as the Dayton-Granger strip. The Dayton-Granger strip appeared to be a more viable proposition in the context of current carrying capability due to the absence of an embedded resistive layer. Its electromagnetic compatibility should be better than that of the segmented strip due to the high resistivity. However, the experience of other investigators of the characteristics of segmented and continuous strips suggests that the high resistivity of the Dayton-Granger strip may reduce its capture capability. The ranking of each form of strip, based on the number required for the protection of any particular radome, would be, in order of increasing numbers:- continuous, segmented and Dayton-Granger strips. Its rain-erosion capability also appeared to leave much to be desired due to the powdery form of the strip coating. These observations require, of course, to be subjected to experimental verification. To the knowledge of the author, no publications of any kind on the Dayton-Granger strip have appeared and it is the aim of the author to compare the flashover characteristics of the Dayton-Granger and the segmented strip.

7.2 Physical properties

The physical appearance of the Dayton-Granger strip is not unlike that of any other foil tape. Figure 7.1 shows a photograph of a section of a strip. The physical dimensions are approximately 0.1mm thick and 13mm wide. It is grey in colour and has a powdery coating on one side. As shown by the scanning-electron-microscope photographs in figures 7.2 to 7.4, the coating consists of particles of various shapes and sizes ranging from less than 10 micrometre to about 100 micrometre. The particles are randomly distributed on the surface, with no fixed orientation. X-ray analysis of the surface revealed that the coating contained mainly aluminium. This aluminium is present in the form of alumina but the oxygen was not detected by the X-ray analysis. This is not surprising since the system uses the energy dispersive method of detection. In using this method, the detectability for light elements is so poor that the smallest atomic number element which can be confidently detected is magnesium.

The static resistance of a 0.3-m length of the strip was measured, using a Myria-megohmmeter, and found to be approximately 8×10^{10} ohms.

7.3 Flashover voltage and time-lag characteristics

7.3.1 Characteristics of unmounted strip

A 1.01-m length of strip was arranged to bridge a pair of uniform

field electrodes and was secured as described in section 4.3.1. In view of the absence of an embedded resistive layer in the Dayton-Granger strip, the chopping gap system was not used as such but was kept in the circuit for all the tests conducted with the Dayton-Granger strip. A slightly modified 'Up & Down' test was then undertaken.

Normally, an 'Up & Down' test commences with the application of a voltage level estimated to be the 50% value. Since there was no indication, from any source, of what this level could be, the initial voltage level applied was 80.3 kV which was considered to be far below the flashover value. The change in voltage level applied was $\pm$ 4.5 kV depending on whether the preceding impulse caused a flashover or not. This change was increased to $\pm$ 9 kV when the voltage applied was in excess of 334.8 kV. The results of this test are shown in figure 7.5 and Table 7.1. Owing to the number of impulses applied, the results are presented as before with all the points being joined together by straight lines. The occurrence or non-occurrence of a flashover at any point is implied by the negative or positive slope of the line joining that point to the next point. The entire test was performed in three sessions on different days and at different times of the day. For succeeding sessions, the first voltage level applied was dependent upon whether flashover or withstand had resulted from the final impulse applied in the previous session - it was assumed that changes in the ambient air conditions would have a negligible effect on the results.

As expected, no flashover resulted from the application of the first impulse. In fact, the strip withstood all subsequent voltage applications until the 58th impulse, which corresponded to an applied voltage having a peak of 334.8 kV. This first flashover occurred with a time-lag to flashover of 1.5 microseconds. Following this there was a series of flashovers and the next voltage withstand did not occur until the 118th impulse when the voltage level had been reduced to 67 kV. The time-lags to flashover in this series ranged from 0.5 microsecond to 17 microseconds and the distribution was such that the shorter times occurred at the higher voltage levels. After the 118th impulse, there followed a series of alternate flashovers and non-flashovers before the start of a general gradual increase and then a subsequent steep increase in flashover strength. The time-lags to flashover in this part of the test sequence ranged from 0.8 to 30 microseconds with a similar distribution to that described above. The test was terminated after a total of 314 impulses when the flashover voltage had increased to 670 kV which was the maximum output from the modified impulse generator.

Preliminary tests, using a Megger-insulation-tester, on the Dayton-Granger strip by the Culham Lightning Studies Unit had indicated a positive effect of surface disturbance of the Dayton-Granger strip on the strip resistance. Similar tests undertaken by the author produced results which were in agreement with those obtained by the Culham Lightning Studies Unit. The output from a 500-V Megger-insulation-tester was applied across the surface of the strip and the separation between the contacts was about 1mm. As

shown by figure 7.6, the resistance of the strip was initially greater than 10^7 ohms but dropped to a very low value at a certain applied voltage as the voltage was increased - indicated in the figure by solid lines with single arrows which show the path followed. Subsequent to this happening, the resistance remained very low for further tests - indicated by solid lines with double arrows. However, if the surface of the strip between the contacts was then disturbed by rubbing with a piece of paper before applying the voltage again, the strip reverted to exhibiting a high resistance again and the characteristic path was repeated. After disturbing the surface, the resistance was not as high as the initial value and the fall in resistance occurred at a lower voltage - indicated by the dashed lines.

After the 'Up & Down' tests it was observed that the strip had a wavy profile and it was considered that this wavy profile might have affected the flashover characteristics. The strip was therefore mounted on a tube to maintain its flat profile. This also prevented movement of the strip during flashover which could conceivably have affected its performance.

7.3.2 Characteristics of strip mounted on SRBP tube (1.01m)

The strip was mounted on a tube made of synthetic resin bonded paper (SRBP) using double-sided adhesive tape. The length of the SRBP tube was equal to the effective length of the Dayton-Granger strip, i.e. 1.01m. The actual length of the strip was a few millimetres longer so that the end could be held between the tube and the

electrodes thus eliminating the possibility of the strip peeling off. Before mounting the strip, the flashover strength of the SRBP tube was tested by applying the maximum voltage (670 kV) across the tube which withstood all ten impulses applied. Hence, any flashovers occurring subsequent to the mounting of the strip would be due to the strip.

The experimental arrangement was as shown in figure 7.7. with the tube kept vertical by resting the high voltage electrode lightly on the end of the tube. The procedure described in section 7.3.1 was then repeated but with a lower initial voltage of 67 kV. The results obtained are shown in Table 7.2 and figure 7.8. These do not differ significantly from those of section 7.3.1.

The first flashover occurred at the 13th impulse with an applied voltage magnitude of 120.5 kV and the corresponding time-lag to flashover was 2 microseconds. The minimum flashover voltage was equal to that of the previous test and this minimum level was maintained for more impulses than in the previous test before the flashover strength of the strip started to increase significantly. As in the previous section, the test was terminated when the applied voltage reached the maximum of 670 kV. This occurred after 387 impulses.

The outstanding difference between the two sets of results was the phenomenon of arrested flashover observed in the second. The term arrested flashover is used to describe the situation where faint discharges, evident by light emission, occur along the strip but

without being accompanied by any detectable fall or collapse of the applied impulse voltage. This phenomenon was not observed in the first test and this could have been due to the relatively poor electrical contact between the strip and the high voltage electrode. Arrested flashover commenced immediately after the minimum flashover voltage was attained and was considered as a "withstand" for the purpose of the 'Up & Down' test. When the arrested-flashovers ceased the flashover strength of the strip began to increase significantly.

As in the previous results, the time-lags to flashover ranged widely - from 0.8 to 31 microseconds - with the shorter time-lags occurring at the higher voltage levels. The static resistance of the strip was measured after the test and was found to have fallen to 1.5×10^{11} ohms from an initial value of "infinity" as indicated by the meter (i.e. $\gg 2 \times 10^{11}$ ohms, the maximum scale indication on the meter).

The experimental procedure was then repeated using a new 1.01-m length of Dayton-Granger strip for two reasons, viz (a) to ascertain that the arrested flashover phenomenon was reproducible, and (b) to study the form of the arrested flashover. The results are shown in Table 7.3 and figure 7.9. Not all results between the start of arrested flashovers and their cessation were obtained by an 'Up & Down' procedure. At some stage, the procedure was modified so that integrated and time-resolved photographic studies could be undertaken and this procedure will be described in section 7.4. Apart from this and the value of the initial flashover voltage, the

results were similar to those of the previous tests. The minimum flashover voltage was relatively constant at approximately 71.4 kV and the range of time-lags to flashover was from approximately 1 to 40 microseconds.

7.3.3 Characteristics of strip mounted on SRBP tube (0.3m)

The procedure of section 7.3.2 was repeated for a new length of strip measuring 0.3m. The results were as shown in Table 7.4 and figure 7.10 with the first flashover occurring at 50.4 kV after 95 impulses. The minimum flashover voltage was 22.3 kV which corresponds to a mean stress of 74.3 kV/m which agrees well with the value of 70.7 kV/m for a 1.01-m length of strip. Time - lags to flashover were of the same order of magnitude as those for the 1.01-m strips. The strip resistance, measured after the test, was 2×10^9 ohms giving a reduction of 97.4% from its original value of 7.8×10^{10} ohms.

A summary of the results is given in Table 7.5. The table should be read in the following manner:- Corresponding to each horizontal and vertical heading there is a rectangular region with four rows. This rectangular region, as defined at the bottom of the table, contains the results of all the strips tested and in the order indicated. To facilitate ease of reference and comparison, the results in each rectangular region are presented along the main diagonal from top-left to bottom-right. Hence, results for any one strip could be read by looking up or down a vertical line in each headed column and horizontally along the relevant row.

The flashover characteristics or, more appropriately, the conditioning characteristics of the Dayton-Granger strip can thus be generalised as shown in figure 7.11. The response can be divided into three distinct regions, viz the conditioning phase; the plateau or stable phase; and the deteriorating phase. The conditioning phase covers the response from the first impulse applied up to the point when arrested flashover commenced, i.e. it is conditioned to the point when further impulse applications produce an approximately normal distribution of flashover probability. The dashed-line represents the form that the response would take if the first applied impulse was high enough to cause a flashover. The stable or plateau phase is self-explanatory and covers the region from the start of arrested-flashovers to their cessation. The remaining region is the deteriorating phase and is so defined because of the loss of its desired flashover performance as evidenced by the rapid increase in flashover voltage.

Figure 7.12 shows a comparison of the flashover characteristics of the segmented strip and the Dayton-Granger strip to a base of strip length. Prospective peak values are shown for the maximum flashover voltages and the values of the other voltages are either peak values or actual voltages at flashover depending on the magnitude of the time-lag to flashover[77]. The results show that the mean voltage at flashover of a segmented strip is at least four times the minimum flashover voltage of a Dayton-Granger strip of equal length. A similar ratio was evident when the maximum flashover voltage levels of both strips were compared. Therefore, it would appear that the Dayton-Granger strip is a more desirable protection device based on

the longer critical length (see section 2.3) that it would have. The critical length is defined as that length of strip for which puncture of the radome-wall, or flashover of the radome surface, has the same probability as flashover of the strip.

In all the tests, faint brown regions were observed along the surface of the strip after the flashovers. Examination of the surface structure using a scanning-electron-microscope did not, in general, reveal any significant differences from that of an unused strip. Figures 7.13 to 7.15 show photographs of three areas which did however appear to show some differences. These were the only three areas and amounted to less than 0.1% of a total scanned area of $1cm^2$. The difference noted is the existence of more holes in the particles on the surface. X-ray analysis of this sample produced a result identical to that of a new strip which had a peak for aluminium (figure 7.16). Tentative results from an Auger[76] analysis indicated that the surface contained a high percentage of carbon which might have been vapourised from the substrate of the strip. Therefore, the discolouration of the strip surface could be due to the presence of this carbon.

7.4 Integrated and time-resolved photographic studies

Integrated and time-resolved photographic studies were made of both arrested flashovers and complete flashovers on a Dayton-Granger strip conditioned as described in section 7.3.2.

Integrated photographs of the alternate complete-and arrested-flash-

overs were obtained as a result of applying changes of ±4.5 kV at the plateau phase of the flashover characteristic. Two cameras were used, one loaded with a high speed film and the other with high contrast recording film which effectively has a much lower ASA number. The camera loaded with the high speed film was used to record only the arrested flashovers while the other was used to record both complete-and arrested-flashovers. Photographs were taken of the entire length of the strip using different lens apertures.

The photographs, taken at full aperture, using the high speed film showed that discharges were occurring along the entire length of the strip even under arrested flashover conditions. However, these records were overexposed thus giving poor image resolution due to fogging. At the smaller apertures, better resolution was achieved and then the discharges appeared to be discontinuous, as shown in figure 7.17, apparently having non-luminous sections. The discontinuous images of the arrested-flashover discharges were also visible on the slow-speed film (figure 7.18). It is evident from the form of the flashover, arrested or complete, that the discharges were occurring along the strip surface and were tortuous over their entire length.

A large aperture, 508-mm lens was used on the camera loaded with the high speed film to achieve better spatial resolution thus allowing the faint discharges at the apparently 'non-luminous' sections to be studied. Arrested flashover records, covering 250mm of the strip, are shown in figures 7.19a to 7.19e. The

results showed that the faint discharges at the 'non-luminous' sections consisted of multiple discharge paths which were only faintly luminous because of the reduced current in each channel. The discharge paths followed by the arrested flashovers were different from each other and their tortuous nature was confirmed. It should be noted that the arrested-flashover records were obtained while performing an 'Up & Down' test procedure and therefore alternated with complete flashovers.

To investigate the effect of a preceding flashover on an arrested-flashover and vice versa, every discharge was optically recorded using high contrast recording film and a 300-mm lens viewing 285mm of the strip. The results are shown in figure 7.20 where the time sequence is from left to right. These records were taken with alternate occurrence of flashovers and arrested-flashovers and were achieved through changes in applied voltage of $\pm$4.5 kV. Reduction of the voltage changes to $\pm$1.1 kV (1.5%) still produced the desired alternating occurrences. The results show that the discharge path of an arrested flashover immediately following the occurrence of a flashover is unlikely to be identical to that of the flashover whereas the discharge path of a flashover following the occurrence of an arrested falshover is much more likely to be similar to that of the preceding discharge. For example, discharges a and b in figure 7.20 show the similar paths followed by an arrested-flashover and the subsequent flashover; discharges c and d in the same figure show the dissimilar paths followed by a flashover and its subsequent arrested-flashover.

The effect of having a few arrested flashovers preceding a flashover was also investigated and the results are shown in figure 7.21. The tendency for the discharge path of a flashover to follow that of the preceding arrested-flashover was still evident, although not in all cases. The records also indicate that the discharge paths followed by successive arrested-flashovers might or might not be similar. Note the dissimilar forms in discharges e, f, g and the similar forms in discharges h, i, j.

A plausible explanation of the mechanism involved may be briefly described as follows. If an electric field is applied across the strip then the effect of the various micro-protrusions, inherent in the construction of the strip, is to cause localised field enhancement. Discharges would then be initiated from these dominant high field points but these might fail to develop to flashover if the applied field was not high enough, i.e. an arrested-flashover would occur. The occurrence of multiple discharge paths is evidence of discharge initiation at many points on the strip surface. If the micro-protrusions were relatively unaffected by the low current in the arrested-flashover then re-application of the electric field would result in a similar pattern of discharge initiation and hence a similar discharge path, particularly if the voltage had been increased so that full flashover resulted. The high current resulting from a flashover appeared to affect the dominant high field points in such a way that they tend to be superseded by other protrusions which, for a subsequent voltage application, will then produce discharges which will result in a discharge path dissimilar to that of the preceding

flashover. Depending on the current magnitudes in repeated arrested-flashovers there may result changes in the discharge paths. The consequence of the flashovers is that eventually, for the particular value of the applied stress, all the active high field points would be removed and hence there would be a resulting increase of flashover strength.

Time resolved photographs of a flashover discharge were obtained, but because of synchronisation difficulties, as discussed in section 6.3, only two synchronised records were obtained and these are shown in figures 7.22 and 7.23. Owing to the size of the photocathode, only a 75-mm section of the strip was photographed. Figure 7.22 shows a record taken at 2×10^6 frames per second with a time between frames of 500 ns and an exposure duration per frame of 100 ns. Figure 7.23 shows a record at 2×10^7 frames per second with a time between frames of 50 ns and an exposure duration per frame of 10 ns. The luminous discharge development time can be estimated to lie between 200 and 500 ns for the section of strip considered. The records show that almost simultaneous discharges were initiated, at different sections along the strip surface, and developed to flashover. The inference is that discharges were not initiated at the anode and propagated to the cathode or vice versa.

7.5 Summary of results and discussion

In performing the 'Up & Down' procedure on a length of Dayton-Granger strip, the resulting characteristic response to the impulses

applied may be catergorised into three distinct regions, viz the conditioning phase; the plateau phase and the deteriorating phase (figure 7.11). If application of the first impulse produces a flashover, the dashed-line response will apply. The conditioning phase covers from the first applied impulse to the commencement of arrested-flashovers. As implied in the terminology used, the strip would be conditioned during this phase to produce subsequent responses where the probability of flashover could be considered to be approximately normally distributed. Arrested-flashover is a term used to describe discharges - evidenced by light emission - along sections of the strip but not accompanied by, or followed by, a detectable fall or collapse in the applied impulse voltage. The arrested-flashover is thus equivalent to a withstand in the context of the 'Up & Down' test. The plateau phase covers the region from the start of arrested-flashovers to where they ceased. The remaining region is the deteriorating phase which shows a sharp increase in flashover strength, i.e. the strip had deteriorated from its desired flashover performance in the plateau phase.

The variation of flashover voltage with strip length can be approximated to by a straight line through the origin. The flash-over voltage for the Dayton-Granger strip was less than one-quarter of that of an equal length of segmented strip (figure 7.12). Consequently, the critical length, which is defined as the minimum length for which puncture of the radome-wall or flashover of the radome surface rather than flashover of the strip is more likely, would be longer and hence the Dayton-Granger strip should be the better device for lightning protection of aircraft radomes.

Integrated photographic studies of arrested-flashover and complete flashovers indicated that:-

a) the discharge paths were tortuous,

b) initiation of discharges appeared to occur simultaneously at different points on the strip. Hence the discharges did not initiate at one end and propagate to the other,

c) parallel discharges may occur along the same section of strip under arrested flashover conditions,

d) the discharge path of a flashover tended to follow that of the preceding arrested-flashover but the converse was not apparent, and finally

e) the discharge paths could be different in a succession of arrested-flashovers.

A plausible explanation on the likely mechanism involved may be summarised as follows. Application of a uniform field stress will result in local field enhancement at the various micro-protrusions inherent in the construction of the strip. Discharges then initiate from the dominant high field points but may not develop to flashover, i.e. an arrested-flashover occurs. If the dominant micro-protrusions are relatively unaffected by the low current in the arrested-flashover then re-application of the electric stress will result in a similar pattern of discharge initiation and hence a similar discharge path particularly if the voltage had been increased so that flashover results. The high currents resulting from flashover appear to affect the dominant high field points in such a way that they tend to be superseded by other protrusions which, for a subsequent voltage application, will then produce discharges having

paths dissimilar to that of the preceding flashover. Depending on the current magnitudes in repeated arrested-flashovers, changes in the discharge paths may result. The consequence of the flashovers is that eventually, for the particular value of applied stress, all the active high field points would be made inactive and hence there is a resulting increase in flashover strength which, perhaps, is improved by the presence of a carbon layer on the surface as indicated by an Auger analysis.

8 CONCLUSIONS AND RECOMMENDATIONS FOR FURTHER STUDIES

8.1 Segmented strip - Conclusions

The present investigation has revealed much about the segmented strip and its flashover characteristics. It has been found that the intersegment capacitance is not more than 2pF and that the intersegment resistance of a new length of segmented strip has an average value of approximately 45 k ohms. The intersegment resistances tend to fall in value with each application of impulse voltage and it is possible for the status of neighbouring intersegment resistances to be interchanged, i.e. the intersegment resistance which was the higher can become the lower. Nevertheless, the general trend is for the intersegment resistances to fall to a lower value of about 5 k ohms. The change in intersegment resistance is still evident regardless of whether the applied impulse voltage is withstood or not.

Owing to the limited energy dissipation capacity of the resistive layer of the segmented strip, it is highly probable that, if the strip withstands an applied impulse, at a level close to V_{50}, it will be damaged, i.e. layers of material on the mounting-surface and between conducting segments will be dislodged. Existence of such damage will provide preferential flashover paths and thus alter the flashover characteristics. In the present work, damage to the segmented strip was prevented by applying impulses which were chopped after a time-lag of about 5 microseconds which is longer than the time-lag to flashover of any length of segmented

strip.

A linear relationship has been found to exist between the flashover voltage and strip length when a segmented strip is situated in a gap having a geometric uniform field. The results reflect the approximately uniform distribution of intersegment resistances in a resistance-stabilised strip where it is assumed that the flashover voltage would be proportional to the number of inter-segment gaps, and hence strip length, if each intersegment resistance is approximately equal in value. The mean field at flashover, however, differs between unconditioned and conditioned strips. For strips which are not conditioned but which have been resistance-stabilised, the value is 750 kV/m but for conditioned strips, the value is 380 kV/m. The former value, being considerably higher than the latter, implies that only conditioned strips should be used in the protection of radomes against lightning because of the increased value of the critical length.

For a conditioned strip situated in a gap having a non-uniform geometric field, the relationship between flashover voltage and strip length is non-linear. This non-linearity, due probably to the non-uniform geometric field, does not pose any problem in the context of radome protection because the maximum voltage at flashover is at most 50% of that of an unbridged air gap. However, the reduction in flashover voltage, from that of an unbridged gap, for a resistance-stabilised strip in a non-uniform geometric field is not yet known and should be investigated in future studies. If the electric field ahead of a lightning leader is considered to be

non-uniform, then the results of such an investigation would reveal the efficacy or otherwise of such strips as lightning protection devices. The effects of the non-uniformity of the geometric field could be further investigated by making time-resolved studies of the discharge development on segmented strips situated between electrodes giving a wide range of geometric field factors (defined as the ratio of maximum to mean field).

Generally, time-lags to flashover were found to be less than the time-to-crest, 3 microseconds, of the applied lightning impulse. Such short time-lags are, without doubt, desirable in any protective device. In particular, the time-lag to flashover approaches a constant value of about 0.6 microsecond when the strip is overvolted which is most likely under natural lightning conditions.

The results of time-resolved photographic studies of the light emission resulting from flashovers were consistent with the proposed mechanism of flashover. The discharge does not propagate from the anode-electrode to the cathode-electrode nor vice versa but discharges are initiated at a number of different intersegment gaps. Two or more of these discharges may be initiated 'simultaneously', i.e. within the limit of time-resolution which was achieved in the present measurements, viz. $\pm$0.5 ns. There is also no pre-dominant sequence of intersegment flashovers and this is expected due to the tendency of the intersegment resistances to change with each applied impulse.

Comparison of the total current, which comprises the ohmic current

due to the resistive layer of the strip and the intersegment gap discharge current, with the ohmic current enables the strip flashover time to be determined. The vast majority of these times lay within 2 microseconds with the majority falling within 1 microsecond for a strip length of 0.3m in a uniform field. The phenomenon of isolated intersegment discharges may occur when a strip withstands an applied impulse. This phenomenon should be further investigated by making simultaneous photomultiplier and total current measurements.

Although much has been learned from the present investigation, the mechanism leading to a flashover of the strip is still not fully understood. Many variables, associated with the strip itself or the environment, may affect the flashover performance. Hence, further studies are required as recommended below.

8.2 Further work on segmented strips

8.2.1 Negative impulse measurements

Positive lightning impulses were used throughout the present investigation. In view of the fact that a majority of lightning impulses are of negative polarity, it is desirable that the performance of the strip under negative impulses be studied. Unfortunately, the impulse voltage chopping system developed does not function as required under negative impulse conditions due to, perhaps, the fact that the trigatrons then changes to being cathode triggered. Therefore, either an alternative chopping system must

be designed or a major alteration of the impulse generator must be undertaken in order to maintain anode-triggering of the trigatrons.

8.2.2 Measurement of intersegment resistances using a potential bridge

It is considered that high contact resistance exists between each segment and the resistive layer. This view is satisfactorily justified by the present results. However, the existence of such high contact resistances can be further investigated by measuring the intersegment resistances using a potential bridge which will allow the effect of the contact resistances to be eliminated.

8.2.3 Measurements in a non-uniform geometric field

If the field ahead of an approaching lightning leader is considered to be non-uniform, then a radome protection system consisting of conditioned segmented strips could be expected to perform satisfactorily. This is because the flashover voltage of a conditioned segmented strip, situated in a non-uniform geometric field, is much lower than the breakdown voltage of the bridged air-gap alone. However, it is likely that only new strips will be used in any protection system and therefore it is necessary to investigate the flashover characteristic of a new strip situated in a non-uniform geometric field in future studies. In addition, the apparent effect of a non-uniform geometric field on the flashover characteristics of a strip should be further investigated by undertaking time-resolved photographic studies under these conditions.

8.2.4 Measurements with strips under different field conditions

In a practical situation where an aircraft is flying under a thundercloud and in the vicinity of an approaching lightning leader, each segmented strip comprising the protection system will be operating under different field conditions. These conditions depend upon the relative positional orientation of each strip to the thundercloud and the lightning leader. In other words, the static field due to a thundercloud and the time varying field due to a lightning leader would both be different for all the strips on a radome surface. Future studies should therefore investigate the effect of an impulse field, superimposed on a static ambient field, on the performance of a strip and also on how the performance is affected by different strip orientation, relative to these applied fields.

8.2.5 Photomultiplier measurements

The current records which have been obtained to date indicate that isolated intersegment discharges may be occurring. This should be further investigated by complementing the current measurements with photomultiplier measurements.

8.3 Future studies using model strips

8.3.1 Proposed design for a model strip

In the present study, only commercially available segmented diverter

strips were used. The use of such strips meant that the strip parameters could not be varied and thus the dependence of the flashover characteristics on these could not be investigated. These parameters include, for example, segment size and shape; segment material and surface finish; intersegment resistance; intersegment gap length; material and surface finish of the dielectric; the ratio of segment size to intersegment gap and the height of the segments above the surface of the dielectric substrate. It is proposed that a model be used in future work in order that all of these factors may be varied. The investigation of the effect of the various factors on the performance of model strips will enable a better understanding of the mechanism leading to segmented strip flashover to be achieved.

Figure 8.1 shows the proposed design of one such model strip. Basically, it consists of two dielectric sections, front and rear, and two conducting ends to allow electrical contact to be made with the high voltage and earth electrodes. The front section would contain the conducting segments and in the rear section there would be a channel to contain a liquid, say salt solution, which would serve as a resistive layer. The effect of size, shape, material, surface finish of the segments; of intersegment gap length; of the ratio of segment size to intersegment gap and of the height of segments above the surface of the dielectric substrate could thus be investigated by having a series of different front sections containing the various segment arrangements to be tested. The material used for making the dielectric sections could also be varied to investigate its effect on flashover performance. The

effect of strip resistances could be studied by changing the resistivity of the salt solution and the effect of the relative magnitude of the intersegment resistances could also be studied by having different liquids, say oil and salt solution, in different sections of the channel. If necessary, provision could be made on the model for automatic or remote replacement of the liquid in the channel so that any effect due to appreciable heating of the liquid resulting from a prolonged test session could be eliminated. However, automatic or remote replacement might not be possible if the resistive layer is composed of several sections containing different liquids.

In all the different model arrangements resulting from the various front sections, it is expected that the intersegment capacitances will be larger than those of the commercially available strip. However, these larger values are of no consequence provided that the discharge-time-constant of each parallel combination of intersegment resistance and capacitance is much lower than the wavefront times of the impulses applied.

8.3.2 Measurements using switching impulses

Owing to the magnitude of the action integral associated with switching impulses, even if chopped at the peak, (see section 4.2) the tests in the present investigation were undertaken using only chopped lightning impulses. On model strips designed to give increased energy dissipation, it would be possible to investigate the effect of variation of the impulse voltage waveshape. From the

results of such investigation the effect of impulse waveforms on the performance of segmented strips might be inferred.

8.3.3 Measurements with model strips having fixed numbers of intersegment gaps per unit length

If the relative magnitudes of the intesegment resistances are fixed, this would enable the correlation between the discharge sequence and intersegment resistance to be determined with confidence. Control of the intersegment resistances would also allow the dependence, if any, of the flashover characteristics upon the absolute value of intersegment resistance to be investigated.

Investigations on spacer flashover in compressed gases by other researchers have shown the dependence of flashover upon spacer material and profile and have thus contributed to more efficient spacer design. Similarly, model strip tests in which the effects of dielectric material and its surface finish on flashover characteristics could possibly lead to the design of more efficient diverters.

It was observed, during the present investigation, that after the rear intersegment surface had been damaged, probably by excessive heating of the resistive layer, flashover occurred across this damaged surface rather than across the undamaged front surface. This occurred despite the fact that the rear intersegment gap, between 1.25-mm square cross-section conductors, is five times that of

the gap between the 2.44-mm diameter circular segments on the front surface. Therefore, it would be valuable to investigate the effect of size, shape, material composition and surface finish of the segments and of the ratio of segment size to intersegment spacing on the flashover characteristics. The possibility of having the resistive layer form the front surface also might be considered.

The effect of the amount of protrusion of the segments above the dielectric surface on the flashover characteristics is an interesting aspect to investigate. The results from such an investigation might confirm the proposition that the lower flashover voltage of a conditioned strip, compared to that of an unconditioned but resistance-stabilised strip, is due to surface erosion of the dielectric between the segments thus increasing the segment protrusion.

Researchers have found that the presence of contaminating particles on spacer surfaces in compressed gases adversely affected the flashover characteristics of the spacer. In the present study, post-flashover carbon deposits on the strips was observed but whether the presence of these deposits significantly affected the flashover characteristics is not known and should be investigated using model strips.

It was found that there was a significant scatter in the time-lags to flashover of a segmented strip and that this scatter was reduced with increase in strip length. The reason for this is not yet clear and it is considered that the results of the studies recommended

above would help to explain this tendency.

8.3.4 Measurements with models having different numbers of intersegment gaps per unit length

Present results are in agreement with the proposal that the flashover strength of a segmented strip, situated axially in a uniform field air gap, is equivalent to the sum of the individual flashover strengths of the intersegment gaps. This proposal could be further investigated by using model strips where the flashover strength of one, two, three or more series - connected intersegment gaps could be measured.

It has been estimated that about 90% of the strip length is bridged by the conducting segments in the type of strip studied to date. It would be useful to measure the effect on the flashover strength, of a fixed length model strip, of varying the number of segments on the strip arranging that in every case the segments bridged 90% of the strip length. The cross-section of the segments could be varied from super-elliptical, for the single segment case, to circular, corresponding to the commercially available strip.

The effects of bridging an increasing portion of a given strip length by conducting segments could also be studied by having different numbers of similarly sized and shaped segments uniformly spaced along a fixed length model strip.

8.4 Dayton-Granger strip

The characteristic response of a Dayton-Granger strip when subjected to voltage impulses can be categorised into three distinct regions, viz. the conditioning phase, the plateau phase and the deteriorating phase. In the plateau phase, the phenomenon of arrested flashover occurs. Optical studies have shown that this phenomenon is accompanied by light emission from short sections of the surface of the strip but there is no collapse of the applied voltage. Optical studies have also revealed that:

a) the discharge paths are tortuous,

b) initiation of discharges appear to occur simultaneously at different sections of a strip, i.e. it is not initiated at one end of a strip and then propagates to the other,

c) parallel discharges may occur along sections of the strip under arrested flashover conditions, and

d) the discharge path may vary in a succession of arrested flashovers but the discharge path of a flashover tends to follow that of the preceding arrested flashover.

The relationship between flashover voltage and strip length is approximately linear and the mean field at flashover is less than one quarter of that of a segmented strip. The lower field at flashover results in a longer critical length which implies that the Dayton-Granger strip should be the better device. This advantage is, however, offset by the much longer time-lags to flashover of the Dayton-Granger strip in the plateau phase.

Although in the present study, the Dayton-Granger strip was only briefly examined, the results obtained were extremely interesting and also encouraging in the context of lightning protection. Its ability to withstand hundreds of impulses without any apparent damage, as evidenced by the scanning-electron-microscope photographs, warrants further investigation. This strip also has the advantage that during the plateau phase, in which, for a considerable number of applied impulses, the flashover strength remains low, approximately 71 kV/m or about 20% of the flashover strength of a conditioned segmented strip.

The existence of the plateau phase of low, and approximately constant, flashover strength appears to indicate that the Dayton-Granger strip might be capable of multi-stroke protection. The assumption here is that the flashover strength of the strip would not be affected by the passage of a high current discharge. An investigation of the validity of this assumption could form part of a future comprehensive study of the electrical characteristics of the Dayton-Granger strip.

In this study, the effects of impulse waveshape and polarity on the flashover characteristics should be investigated along with those resulting from variation of field distribution and strip orientation - because, in the present investigation, the flashover characteristics were studied only with the strips situated axially in a uniform field gap.

Further time-resolved photographic studies, complemented by current

measurements, especially under the arrested-flashover condition, could be included.

Dielectric surface charging has been found to occur in situations where a spacer bridges two electrodes in vacuum or in compressed gases. It is therefore not unreasonable to consider that surface charging of the Dayton-Granger strip might also exist in air at atmospheric pressure. The magnitude of this charge and its effect on the flashover characteristics is not yet known and should be investigated in the future. In view of the fact that air is not a pure gas, which complicates the matter further, an initial step could be the study of such strips in a pure gas, such as nitrogen. This study could be easily undertaken in the future because two of the research projects presently being undertaken in the Department are concerned with dielectric surface charging and flashover in compressed gases.

Results from the above recommended studies should provide a better understanding of the performance of Dayton-Granger strips. In the final analysis, perhaps the ultimate protection strip could result from a marriage of the desirable properties from both the segmented - and the Dayton-Granger - strips.

ACKNOWLEDGEMENTS

The support and encouragement given by Professor D.J. Tedford throughout the period of the present study is very much appreciated.

Thanks and appreciation are also given to Dr. A. Aked for his invaluable advice and useful discussion and for his unending support and encouragement during the course of the present study.

Thanks and appreciation are also due to:-

The Procurement Executive of the Ministry of Defence, U.K. for their financial support;

Dr. J.E. Matthews, Dr. D.T.A. Blair, Mr. I.A. Sommerville and other members of staff for their views and discussion;

Dr. J. Bishop of R.A.E., Farnborough and Dr. P.F. Little and Mr. A.W. Hanson of Culham Laboratory, UKAEA for their views and suggestions during the various progress-meetings;

Miss J. Baird for typing all the progress reports produced during this investigation;

Mr. J. Dickson and his staff for workshop and other assistance provided;

Miss E. Aird for her assistance in printing the photographs; and

last but not least, my wife, Linda, for her patience throughout and for her effort in typing this thesis which is additional to the demands on her as mother of our recently born son.

REFERENCES

1. Gorin, B.N., et al, "Lightning strokes on Ostakinsk tele-tower in Moscow, Electric Technology, USSR, No. 3, (1977), 45 - 55

2. Clifford, D.W., et al, "A case for sub-microsecond rise time lightning current pulses for use in aircraft induced-coupling studies", IEEE ELM-CS, (1979)

3. Nanevicz, J.E., et al, "Airborne measurement of the electromagnetic environment near thunderstorm cells", IEEE ELM-CS, (1977), 232 - 6

4. Shaeffer, J.F., Weinstock, G.L., "Aircraft initiation of lightning strikes", IEEE Electronics and Aerospace systems convention, (1972), 70 - 6

5. Fitzgerald, D.R., "Aircraft and rocket triggered natural lightning discharges", L.S.E.C. 1970, (1971), 3 - 9

6. Phillpott, J., "Recommended practice for lightning simulation and testing techniques for aircraft", UKAEA Report, (1977), CLM - R163

7. Electrical Research Association, "An aircraft lightning strike test facility - a study of requirements", (1971), ERA 71 - 167

8. James, T.E., Phillpott, J., "Simulation of lightning strikes to aircraft", UKAEA Report, (1971), CLM - R111

9. Uman, M.A., "Lightning", McGraw Hill, (1969), 228

10. Burrows, B.J.C., "Induced voltages, measurement techniques and typical values", L.S.E.C., (1975)

11. Clifford, D.W., "Laboratory tests for undesired conducted currents and surge voltages caused by lightning", Conference on certification of aircraft for lightning and atmospheric electricity hazards, (1978)

12. Clifford, D.W., Zeisel, K.S., "Evaluation of lightning induced transients in aircraft using high voltage shock excitation techniques", IEEE ELM-CS, (1979)

13. Braithwaite, N.ST.J., Cooke, M.J., "A survey of the high frequency effects associated with the lightning discharge", University of Oxford, England, (1979)

14. Little, P.F., "A survey of high frequency effects due to lightning", UKAEA Culham, CLM - R201, (1979)

15. Golde, R.H., "Lightning", Academic Press, (1977), 309 - 344

16. Phillpott, J., Little, P., White, E.L., Ryan, H.M., Powell, A. Reyrolle & Co., Dale, S.J., Aked, A., Tedford, D.J., Waters, R.T., "Lightning strike point location studies on scale models", L.S.E.C. 75, Session I, No. 5

17. Galczak, J., Aked, A., "Distribution of lightning strike point location on aircraft - The reliability of scale model tests", (1981), University of Strathclyde, Report No: ET/2065/031/4

18. Clifford, D.W., "Laboratory tests to determine lightning attachment points with small aircraft models", Conference on Certification of Aircraft for lightning and atmospheric electricity hazards, (1978)

19. Jones, B., Ross, J.N., "The physics of the long spark", CEGB Research, October, (1978), 27 - 36

20. Uman, M.A., "A comparison of natural lightning and the long laboratory spark with application to lightning testing", Westinghouse Res. Lab. Report No: FAA-NA-69-27, (1970)

21. Dale, S.J., "Breakdown in spark gaps containing an isolated metallic body", Proc. Int. Conf. Gas Discharges, IEE Publication No: 143, (1976), 295 - 298

22. Golde, R.H., "Lightning", Acadamic Press, (1977), 659 - 96

23. Hodge, K.E., "Research developments for aircraft safety", Aircraft Engineering, (1980), 52, No: 1, 10 - 15

24. Kung, J.T., Amason, M.P., "Electrical conductive characteristics of graphite composite structures", IEEE ELM-CS, (1977), 403 - 9

25. Himsley, D., Hoare, R.G., "The repair of glass-fibre reinforced plastic radomes", Aircraft Engineering, (1971), 43, No: 2, 29 - 30

26. Conti, D.A., Cary, R.H.J., "Radome protection techniques", L.S.E.C.,(1975)

27. Amason, M.P., et al, "Aircraft applications of segmented-strip lightning protection systems", L.S.E.C. 75 Session IV, No. 9

28. Amason, M.P., Cassel, G.J., "Radome lightning protection techniques and their electromagnetic compatibility", IEEE ELM-CS, (1970), 12, 286

29. Phillpott, J., "Preliminary evaluation of button and foil radome protection strips for BAC, Stevenage", Culham Lightning Studies Unit, CLSU Memo 7, (1973)

30. Hanson, A.W., Little, P.F., "Further evaluation of button strip protection on radomes for BAC, Stevenage", Culham Lightning Studies Unit, CLSU Memo 21, (1974)

31. Hanson, A.W., "Results of the third series of tests on button strip protection for radomes", Culham Lightning Studies Unit, CLSU Memo 26, (1975)

32. Phillpott, J., Hanson, A.W., "Summary of work on button strip protection for radomes", Culham Lightning Studies Unit, CLSU Memo 32, (1975)

33. Hoots, L.C., Moorefield, S.A., Stahmann, J.R., Amason, M.P., "Lightning protection for advanced aircraft radomes based on the segmented lightning diverter strip", 12th Symposium on electromagnetic windows, (1974), 138 - 43

34. Robb, J.D., Chen, T., Cook, P.L., "Lightning tests of segmented diverter strips for protection of aircraft radomes", LTRI, ICALP, (1976), LTRI Report No. 632

35. Plumer, J.A., Hoots, L.C., "Lightning protection with segmented diverters", IEEE/EMC Symposium, (1978)

36. Bishop, J., "The application of button strips to radome protection", R.A.E. (1977)

37. Bruining, H., "Physics and applications of secondary electron emission", Pergamon Press Ltd., London, (1954)

38. Willis, R.F., Skinner, D.K., "Secondary electron emission yield behaviour of polymers", Solid State Communications, (1973), 13, 685 - 88

39. Sudarshan, T.S., Cross, J.D., "The effect of chromium oxide coatings on surface flashover of alumina spacers in vacuum", IEEE Trans. Elect. Insulation, (1976), E1 - 11, No. 1, 32 - 35

40. Boersch, H., Hamisch, H., Ehrlich, W., Z. Agnew Phys., (1963), 15, 518

41. De Tourreil, C.H., Srivastava, K.D., "Mechanism of surface charging of high voltage insulators in vacuum", IEEE Trans. Electrical Insulation, (March 1973), E1-8, No. 1, 17 - 21

42. Bergeron, K.D., "Theory of the secondary electron avalanche at electrically stressed insulator-vacuum interfaces", Journal of Applied Physics, (1977), 48, No. 7, 3073 - 80

43. Sudarshan, T.S., Cross, J.D., Srivastava, K.D., "Prebreakdown processes associated with surface flashover of solid insulators in vacuum", IEEE Trans. Electrical Insulation, (1977), E1 - 12, No. 3, 200 - 208

44. Anderson, R.A., "Mechanism of fast surface flashover in vacuum", Applied Phys. Letters, (1974), 24, No. 2, 54 - 56

45. Cross, J.D., "High speed photography of surface flashover in vacuum", IEEE Trans. Electrical Insulation, (1978), E1 - 13, No. 3, 145 - 48

46. Miller, H.C., "Improving the voltage hold-off performance of alumina insulators in vacuum through quasimetallizing", IEEE Trans. Electrical Insulation, (1980), EI - 15, No. 5, 419 - 428

47. Avdienko, A.A., Malev, M.D., "Surface breakdown of solid dielectrics in vacuum. II Mechanism for surface breakdown", Sov. Phys. Tech. Phys., (1977), 22, No. 8, 986 - 91

48. Thompson, J.E., Lin, J., "Electro-optical surface flashover measurements", Applied Phys. Letters, (1980), 37, No. 6, 574-6

49. Thompson, J.E., Lin, J., Mikkelson, K., Kristiansen, M., "Investigations of fast insulator surface flashover in vacuum", IEEE Trans. Plasma Science, (1980), PS-8, No. 3, 191 - 7

50. Thompson, J.E., Hyslop, D., Sudarshan, T.S., "Electro-optical measurement of insulator surface preflashover fields in vacuum", Conf. on electrical insulation and dielectric phenomena, (1979), 334 - 45

51. Watson, A., "Pulsed flashover in vacuum", Journal of Applied physics, (1967), 38, No. 5, 2019 - 23

52. Blatsios, J.A., Hackam, R., "Dielectric strength of solid insulators in vacuum", Conf. electrical insulation and dielectric phenomena, (1979), 297 - 303

53. Avdienko, A.A., "Surface breakdown of solid dielectrics in vacuum. I Characteristics for breakdown of insulators along the vacuum surface", Sov. Phys. Tech. Phys., (1977), 22, No. 8, 982 - 5

54. Cross, J.D., Srivastava, K.D., "High speed photography of surface flashover of solid insulators under impulse voltages in vacuum", App. Phys. Letters, (1972), 21, No. 11, 549 - 51

55. Cross, J.D., Sudarshan, T.S., "High speed photography of surface flashover across high density alumina in vacuum under direct and impulse voltages", IEEE Trans. electrical insulation, (1976), EI-11, No. 2, 63 - 6

56. Anderson, R.A., "Propagation velocity of cathode-initiated surface flashover", Journal of App. Phys., (1977), 48, No. 10, 4210 - 4

57. Cookson, A.H., "Electrical breakdown for uniform fields in compressed gases", Proc. IEE, (1970), 117, No. 1, 269 - 80

58. Cookson, A.H., "Review of high voltage gas breakdown and insulators in compressed gases", Proc. IEE, (1981), 128, Part A, No. 4, 303 - 12

59. Jaksts, A., Cross, J., "The influence of a solid dielectric spacer on electron avalanches in nitrogen at atmospheric pressure", Canada Elect. Eng. Journal, (1981), 6, No. 2, 14 - 18

60. Frisco, L.J., Chapman, J.J., "The flashover strength of solid dielectrics", AIEE, (1956), 77 - 83

61. Cookson, A.H., "High voltage flashover of spacers in compressed SF_6 and N_2", CERL Report No. RD/L/N44/68, (1968)

62. Fleming, S.P., "Impulse flashover of insulation: Effect of dust particle size", CERL Report No. RD/L/N170/70, (1970)

63. Fleming, S.P., "Impulse flashover of insulation: Effect of dust at various gas pressures", CERL Report No. RD/L/N86/71, (1971)

64. Mansfield, M.W.D., Fleming, S.P., "Impulse flashover of insulation: Effect of surface charge", CERL Report No. RD/L/N95/71, (1971)

65. Voss, H.J., "The flashover of spacer surfaces in SF_6 caused by conducting particles under oscillating switching impulse voltage", Gas Discharges and their applications, IEE Conf. Pub. No. 189, Part 1, (1980), 247 - 50

66. Laghari, J.R., Qureshi, A.H., "Flashover voltages of cylindrical insulators in gas mixtures", Gas Discharges and their applications, IEE Conf. Pub. No. 189, Part 1, (1980), 240 - 2

67. Bedrin, A.G., Lavrentyuk, V.E., Podmoshenskii, I.V., Rogovtsev, P.N., "Photo-induced surface discharge", Sov. Phys. Tech. Phys., (1979), 24, No. 10, 1181 - 5

68. Kurimoto, A., et al, "Breakdown mechanism of trigatron spark gap in air", Nagoya Institute of Technology, (1974)

69. Broadbent, T.E., "The characteristics of the trigatron spark-gap at very high voltages", IEE Monograph, (1960), No. 364M, 213 - 5

70. Sletten, A.M., et al, "Characteristics of the trigatron spark-gap", IEE Monograph, (1956), No. 193M, 54 - 61

71. Gallet, G., Leroy, G., "Up & Down testing modalities using fully automatic equipment application at Les Renardieres to the study of large air gaps", IEEE Power Engineering Soc. Summer Meeting, San Francisco, California, (1972)

72. Brown, G.W., "Determination of critical flashover voltage and standard deviation from flashover probability data", IEEE Trans. Power Apparatus and Systems, 88, No. 3, (1969), 189 - 94

73. Brown, G.W., "Method of maximum likelihood applied to the analysis of flashover data", IEEE Trans. Power Apparatus and Systems, 88, No. 12, (1969), 1923 - 30

74. Dixon, W.J., Mood, A.M., "A method of obtaining and analysing sensitivity data", Journal of the American Statistical Association, (1948), 43, 109 - 26

75. Lubin, G., "Handbook of fibreglass and advanced plastics composites", Van Nostrand Reinhold Company, (1969), 287 & 818

76. Partridge, J., Correspondence on Auger analysis of Dayton-Granger strip and segmented strip, May 1981

77. International Electrotechnical Commission, Publication 60, (1973)

78. Murray R. Spiegel, "Theory and problems of statistics", Schaum Publishing Co., N.Y., (1961), 89 - 92

79. Aked, A., Ph.D. Thesis, Glasgow University, (1964)

80. Paris, L., Cortina, R., "Switching and lightning impulse discharge characteristics of large air gaps and long insulator strings", IEEE Trans. Power Apparatus and Systems, (1968), 87, No. 4, 947 - 57

81. Meek, J.M., Craggs, J.D., "Electrical breakdown of gases", Oxford University Press, (1953)

82. Matthews, J.E., Tedford, D.J., "Spark gap measuring techniques", Harwell High voltage Technology Course, (1973)

83. Schwab, A.J., "High voltage measurement techniques", (1972), MIT Press, Cambridge, Massachusetts and London, England

84. Siew, W.H., "Progress report on radome protection techniques", University of Strathclyde, A54a/363/1, (Dec. 1978)

85. Siew, W.H., "Progress report on radome protection techniques", University of Strathclyde, A54a/363/2, (April 1979)

86. Siew, W.H., "Progress report on radome protection techniques", University of Strathclyde, A54a/363/3, (July 1979)

87. Siew, W.H., "Progress report on radome protection techniques", University of Strathclyde, A54a/363/4, (Jan. 1980)

88. Siew, W.H., "Progress report on radome protection techniques", University of Strathclyde, A54a/363/5, (July 1980)

89. Siew, W.H., "Progress report on radome protection techniques", University of Strathclyde, A54a/363/6, (Nov. 1980)

90. Siew, W.H., "Progress report on radome protection techniques", University of Strathclyde, A54a/363/7, (Feb. 1981)

91. Siew, W.H., "Progress report on radome protection techniques", University of Strathclyde, A54a/363/8, (Sept. 1981).

Table 5.1

Variation of intersegment resistance with repeated applications of impulses between V_0 and V_{100} voltage levels.

Intersegment resistance before test, k ohms	Intersegment resistance after test, k ohms	Condition of strip surface at the rear of the strip at the point corresponding to the intersegment.
30	4	
18	5.2	
18	9.5	damaged plus evidence of flashover
16	6	
16	6.8	
16.5	10	
16	9	
16	9	
50	7.2	
25	4.6	
140	4.8	
16.5	4.5	
16.5	5.8	
17	5.2	
17	5.9	
18	6.1	
18	6.5	damaged plus evidence of flashover
17.5	7.9	damaged plus evidence of flashover
17.5	6.2	damaged plus evidence of flashover
17	5.3	
16	5.9	
16.5	5.8	
16.5	5.8	
17	5	
19	5	
16	5.6	
16	5.2	
16	4.4	
16	5.9	
16	5.9	
16	6.1	
16.5	6	
16	5.8	
16.5	5.4	
16	4.8	
16	5.7	
18.5	9.7	damaged plus evidence of flashover
17	6.8	
16	7	damaged but no evidence of flashover
15.5	10.5	damaged plus evidence of flashover
17	6.3	
16	5.7	
15	4.4	
16	5.7	
15.5	5.6	

Table 5.1 (continued)

16	6	
17	5.2	
16	5.7	
16	5.8	
16.5	6.8	
16	5.2	
15.5	4.6	
16	4.8	
16	4.3	
15.5	5	
16	5.3	
16	6	
16	6.6	
16	5.8	
16	5	
15.5	4.9	
16	4	
16	5.4	
16.5	4.9	
17	5.8	
17	5	
17	5.8	
17	8.2	damaged plus evidence of flashover
17	5.7	
16	5	
16.5	8.3	damaged plus evidence of flashover
17.5	7.7	damaged plus evidence of flashover
16.5	5	
17	5	
16	5.2	
17	5.6	
18.5	9.5	damaged plus evidence of flashover
17	6	damaged but no evidence of flashover
17	6.2	
16	9	damaged plus evidence of flashover
16.5	6.6	
17	8	
16	5.8	
17	8.5	damaged but no evidence of flashover
16	6	
15.5	5.2	
16.5	6.6	
17	7.8	
17	6.2	
16	6.2	
17	6.2	
17	6.4	
17	6.6	
17	5.6	
17	6.2	
16.5	6.6	
17.5	10	damaged plus evidence of flashover

Table 5.1 (continued)

16	6.6	
15.5	5.7	
15.5	5.9	
15	5.3	
15	5.4	
16	5.2	
15.5	4.3	
17	5	
16	4.9	
16	5.9	
16	4.5	
17	8	damaged but no evidence of flashover
15.5	5	
15.5	5.2	

sum of individual intersegment resistance before test = 2 M ohms
strip-resistance before test = 0.96 M ohms
strip-resistance after test = 0.65 M ohms

strip-resistance after test and after removal of 'carbon' deposit between segments on front surface = 0.675 M ohms
sum of individual intersegment resistances after test and after removal of 'carbon' deposit = 0.678 M ohms

Table 5.2

Effect of applied impulses at less than the flashover level

Number of damaged intersegment surfaces before commencement of test	49 out of 204
Magnitude of impulse voltage	160 kV*, 150 kV
Frequency of impulse application	once every 50 seconds
Duration of test	2 hours
Number of impulses applied	144
Number of damaged intersegment surfaces after test	168

* 160 kV was applied for the first hour.
After the 70th impulse application, flashover occurred for every subsequent impulse applied and the voltage level was reduced to 150 kV.

Inference: Damage occurred at an additional 119 intersegment surfaces.

Table 5.3

Effect of applied impulses at voltages higher than the V_{100} flashover value.

Number of damaged intersegment surfaces before test	19 out of 51
Magnitude of impulse voltage	160 kV ($\triangleq 1.5V_{50}$)
Frequency of impulse application	once every 40 seconds
Duration of test	2.75 hours
Number of impulses applied	248
Number of damaged intersegment surfaces after test	19

Inference: No additional damage to the intersegment surfaces was evident.

Table 5.4

Rate of deterioration of a segmented strip.

Total number of flashovers B	Total number of shots applied, S	% flashover (B/S)x100%	$\frac{\Delta B}{\Delta S}$ x100%	Observations
10	18	56		No visible damage
15	28	54	50	No visible damage
20	35	57	71	4 nearly equally spaced 'swellings' were seen on the intersegment surfaces at lower half of strip.
25	44	57	56	White insulating layer removed from intersegment surface at middle of strip but no 'burn marks' (did not occur at swelling points observed at shot 35).
30	54	56	50	(a)'burn marks' appear at point where white insulating layer was removed from shot 44, thus indicating arcing. (b)White insulating layer removed from largest of the 4 swellings.
35	62	56	63	(a)White insulating layer removed from 9 more intersegmentsurfaces. (b)2 additional arcing points observed.
40	68	59	83	(a)White insulating layer removed from 1 more intersegment surface. (b)4 additional arcing points observed.
45	74	61	83	(a)White insulating layer removed from 5 more intersegment surfaces. (b)3 additional arcing points observed.
50	79	63	100	(a)White insulating layer removed from 1 more intersegment surface. (b)3 additional arcing points observed.
55	84	65	100	(a)White insulating layer removed from 2 more intersegment surfaces. (b)3 additional arcing points observed.

Total number of intersegment surfaces = 111
Total number of intersegment surfaces with insulation removed = 20
Total number of intersegment surfaces with 'burn marks' = 16
Total number of intersegment surfaces with both insulation removal and 'burn marks' = 14

Table 5.5

Action integral for a lightning impulse.

100% corresponds to the complete impulse,

i.e. when there was no chopping.

Time-lag to chop μs	Action integral %
2	3.9
5	11.6
10	23
20	41.7
50	75

Table 6.1

Flashover voltage and time-lag results for a strip bridging a uniform field gap.

Strip length m	50% flashover voltage and 95% confidence levels, kV	Mean voltage at flashover and 95% confidence levels, kV	Time-lags to flashover, μs
0.3	118.3 113.2 to 123.3	107.5 103.9 to 111.1	1.2 to 2.0
0.5	190.6 178.4 to 202.7	171.3 166.3 to 176.2	1.2 to 1.9
0.75	353.8 338.9 to 368.7	315.0 305.0 to 325.0	1.2 to 1.6
1.01	479.0 456.6 to 501.3	370.2 350.5 to 390.0	0.8 to 1.0

Table 6.2 Flashover voltages of a strip in a uniform field

Strip length m	Method of determination of flashover voltages				
	Mean voltage at flashover values, kV	Least-square fit to mean voltage at flashover values, kV	Reference values * kV	Maximum flashover-values, kV	Least-square fit to maximum flashover values, kV
0.3	108	115 (57% of R.V.)	202	196	241 (119% of R.V.)
0.5	171	190 (56% of R.V.)	340	442	401 (118% of R.V.)
0.75	315	285 (56% of R.V.)	507	593	602 (119% of R.V.)
1.01	370	380 (56% of R.V.)	684		811 (119% of R.V.)

Maximum flashover value for a strip length of 1.01 m is not known due to limited output of the impulse generator.

R.V. = Reference value = NV_s where N = number of intersegment gaps

* Values were calculated using $V_s = 24.4 \rho d + 6.53 \sqrt{\rho d}$ kV with d in cm and ρ = relative air density[81]

Table 6.3 Flashover voltages of a strip in a non-uniform field

Electrode configuration	Strip length, m							
	0.3		0.5		0.75		1.01	
	a	b	a	b	a	b	a	b
Rod/plane without air gap between strip and rod	79 71 to 75	1.2 to 4.0	93 81 to 83	1.2 to 1.5	115 85 to 91	0.8 to 0.9	119 104 to 108	1.0 to 1.5
Rod/plane with air gap between strip and rod	78 71 to 76	1.1 to 2.8	102 82 to 95	1.0 to 2.1	136 108 to 112	0.8 to 1.1	133 99 to 108	0.8 to 1.0
Rod/rod with air gap between strip and upper rod	103 97 to 100	1.5 to 3.0	130 85 to 88	0.7	129 107 to 110	1.0 to 1.2	132 111 to 115	1.1 to 1.3
Rod/rod without air gap between strip and upper rod	102 102 to 104	1.6 to 4.0	108 104 to 106	1.3 to 2.2	116 112 to 114	1.5 to 2.4	121 109 to 113	1.3 to 1.5

a - 50% flashover voltage and 95% confidence levels corresponding to the mean voltage at flashover, kV

b - Range of time-lags to flashover, μs

Table 6.4

Breakdown voltages of air-gaps.

Gap length	Breakdown voltages, kV		
m	Rod/rod gap	Rod/plane gap	Uniform field gap
0.3	211 95% C.L.=209 & 213	162	760
0.5	333 95% C.L.=331 & 336	270	1251
0.75	477 95% C.L.=474 & 480	405	1882
1.01	620 95% C.L.=618 & 622	545	2522

C.L. = Confidence levels

Table 6.5

Table of time-delay among discharges A, B and C.

	T_{AB}	T_{AC}	Discharge sequence		
			1st	2nd	3rd
	0.55	0			B
	0.1	0.1			
	0	0			
	-0.9	-0.3	B		
1	0.2	-0.6	C		
	0.8	0.1			B
	-0.1	-0.6	C		
	0.3	-0.1			
	1.0	0.5			B
	0	0			
	1.0	0.2			B
	0	0.5			
	0	-1.0	C		
	0.3	0			
	0.5	0.2			
	1.2	0.3			B
3	-2.0	-2.0			A
	0.7	0			B
	1.0	0.5			B
	0	1.3			C
	-0.8	0.1	B		
	0.5	0			B
	0.2	0			
	-0.4	-1.5	C	B	A
	1.0	1.0	A		
	-2.1	-3.4	C	B	A
	-0.4	0.2	B		
	0	1.0			C
	-2.0	-3.0	C	B	A
	0	0			
	-0.7	-0.1	B		
	2.3	2.5	A		
	-7.0	4.5	B	A	C
	0	0.1			
	-0.5	-0.5			A
	0.4	0.1			
	-1.2	-0.9			A
	0.5	0.2			
	0.6	1.0	A	B	C
	0	-1.0	C		
	6.5	6.5	A		
	-5.9	-5.9			A
	-6.9	-6.5	B	C	A
	-1.4	-4.0	C	B	A
	-6.2	-3.7	B	C	A
	-8.1	-7.9			A
	-5.0	-0.5	B	C	A

Table 6.5 (continued)

-9.0	-7.5	B	C	A
-7.0	-5.7	B	C	A
-3.5	-1.0	B	C	A
1.8	5.8	A	B	C
0	0			
0	0.5			
2.4	1.3	A	C	B
1.2	0.9	A		
-1.5	-0.8	B	C	A
-1.8	0	B		
2.3	2.3	A		
-1.0	2.5	B	A	C
-0.9	2.2	B	A	C
0	0.1			
-1.0	-0.9			A
0.8	0.1			B
-2.5	-2.8			A
2.5	3.0	A	B	C

1) T_{AB} - Time delay in μs between discharge initiation in gaps A and B with A as reference.

2) T_{AC} - Time delay in μs between discharge initiation in gaps A and C with A as reference.

3) When the time-delay between two discharges falls within the range of uncertainty, the discharge sequence for the discharges in question are not determined.
Range of uncertainty for T_{AB} is -0.25 to 0.43 μs,
for T_{AC} is -0.34 to 0.5 μs
and for T_{BC} is -0.35 to 0.33 μs where T_{BC} is the time delay in μs between discharge initiation in gaps B and C with B as reference.

4) Bracketed rows indicate results from consecutive frames of the negative.

Table 7.1

Results for 1.01-m Dayton-Granger strip with strip not mounted on SRBP tube.

Stage of test attained	Voltage applied at stage considered, kV	Range of time lags observed from preceding stage to stage considered, μs	Total number of impulses applied
Start	80.3	Not Applicable	1
1st flashover	334.8	1.5	58
Minimum flashover	71.4	0.5 to 17	117
End	670	0.8 to 30	314

Table 7.2

Results for 1st 1.01-m Dayton-Granger strip - strip mounted on SRBP tube.

Stage of test attained	Voltage applied at stage considered, kV	Range of time lags observed from preceding stage to stage considered, μs	Total number of impulses applied
Start	67	Not Applicable	1
1st flashover	120.5	2	13
Minimum flashover	71.4	2 to 18	24
1st arrested flashover	67	Not Applicable	25
Last arrested flashover	80.3	11 to 31	163
End	670	0.8 to 14	387

Table 7.3

Results for 2nd 1.01-m Dayton-Granger strip - strip mounted on SRBP tube.

Stage of test attained	Voltage applied at stage considered, kV	Range of time lags observed from preceding stage to stage considered, μs	Total number of impulses applied
Start	67	Not Applicable	1
1st flashover	200.9	2	51
Minimum flashover	71.4	1.3 to 29	80
1st arrested flashover	67	Not Applicable	81
Last arrested flashover	70.3	12 to 42	232
End	670	1 to 14	465

Table 7.4

Results for 0.3-m Dayton-Granger strip - strip mounted on SRBP tube.

Stage of test attained	Voltage applied at stage considered, kV	Range of time lags observed from preceding stage to stage considered, μs	Total number of impulses applied
Start	19.1	Not Applicable	1
1st flashover	50.4	3.5	95
1st arrested flashover	21.7	Not Applicable	140
Last arrested flashover	23.6	7 to 37	346
End	191	1 to 15	872

Table 7.5

Summary of flashover results for Dayton-Granger strip.

Stage of test attained	Mean stress at stage considered kV/m	Range of time lags observed from preceding stage to stage considered, μs	Total number of impulses applied
Start	79.5 66.3 66.3 63.7	Not applicable NA NA NA	1 1 1 1
1st flashover	331.5 119.3 198.9 168	1.5 2 2 3.5	58 13 51 95
Minimum flashover	70.7 70.7 70.7 74.3	0.5-17 2-18 1.3-29 2.2-26	117 24 80 139
1st arrested flashover	Not observed 66.3 66.3 72.3	NA NA NA NA	NA 25 81 140
Last arrested flashover	Not observed 79.5 69.6 78.7	NA 11-31 12-42 7-37	NA 163 232 346
End	663.4 663.4 663.4 636.7	0.8-30 0.8-14 1-14 1-15	314 387 465 872

LEGEND

Results of strip 1	- 1.01-m length. Strip not mounted on SRBP tube.
Results of strip 2	- 1.01-m length. Strip mounted on SRBP tube.
Results of strip 3	- 1.01-m length. Strip mounted on SRBP tube.
Results of strip 4	- 0.3-m length. Strip mounted on SRBP tube.

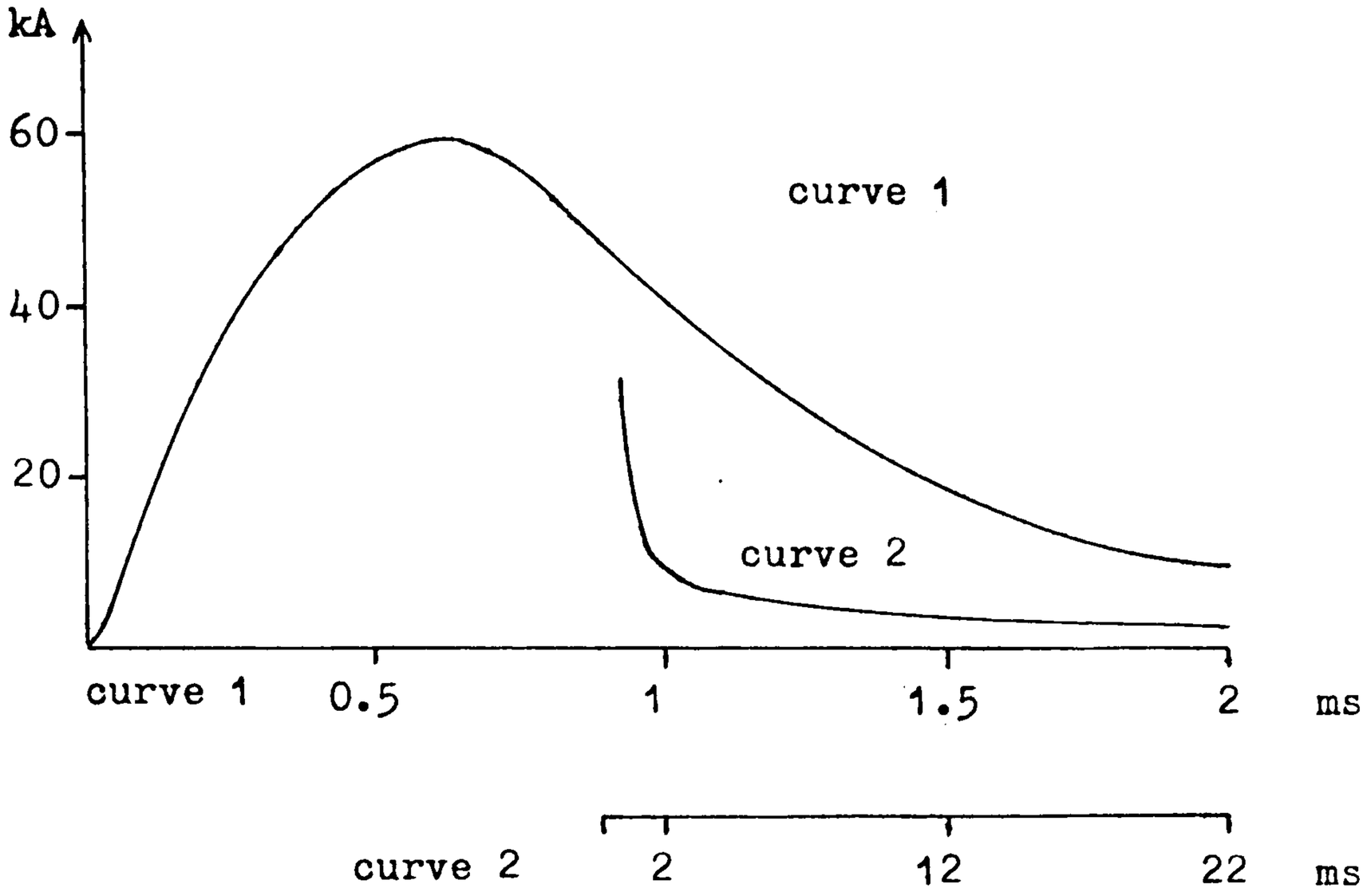

Fig. 1.1 Typical current waveform for positive-flash to ground (based on reference 6).

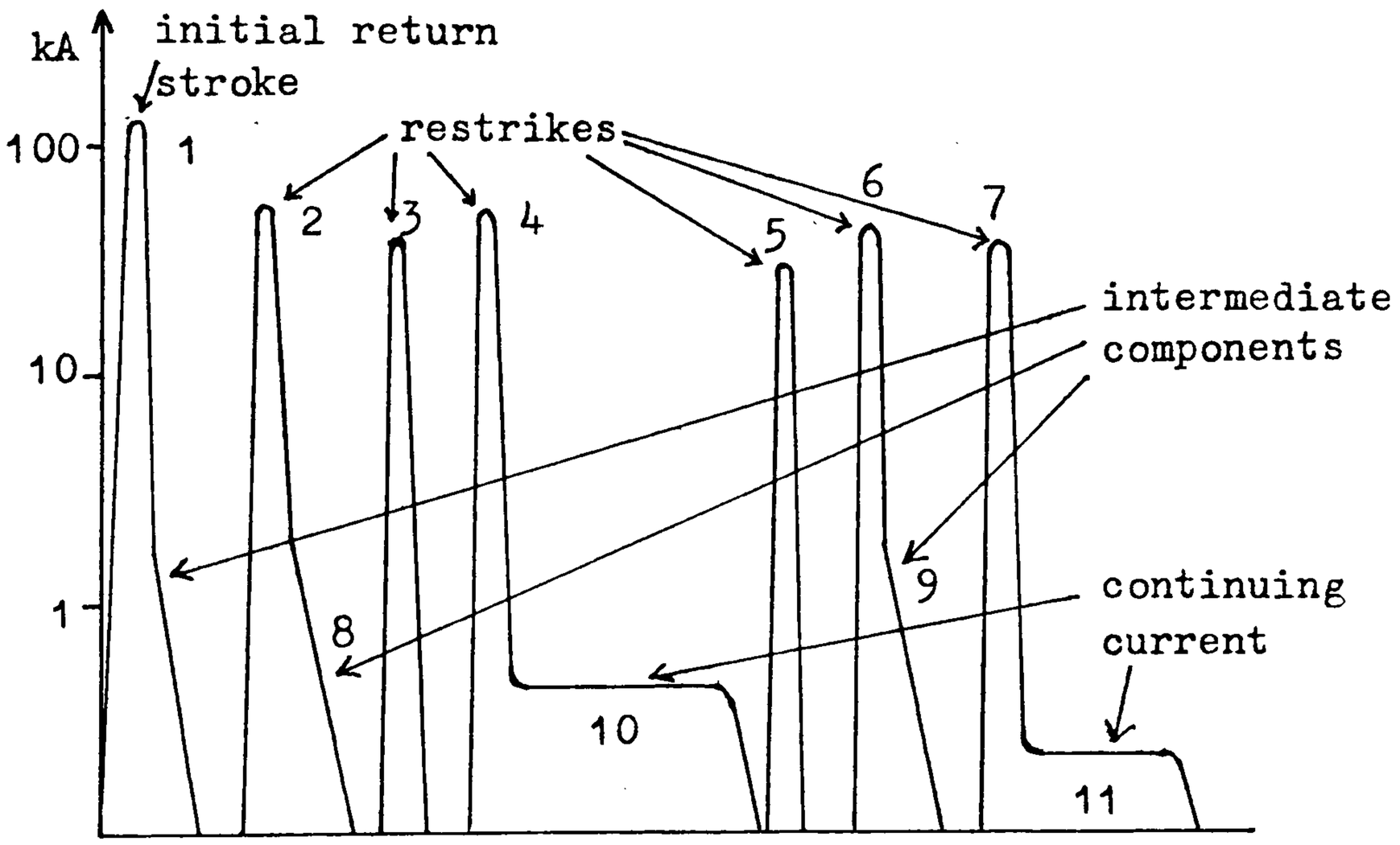

Fig. 1.2 Severe negative-flash current waveform (based on reference 6)

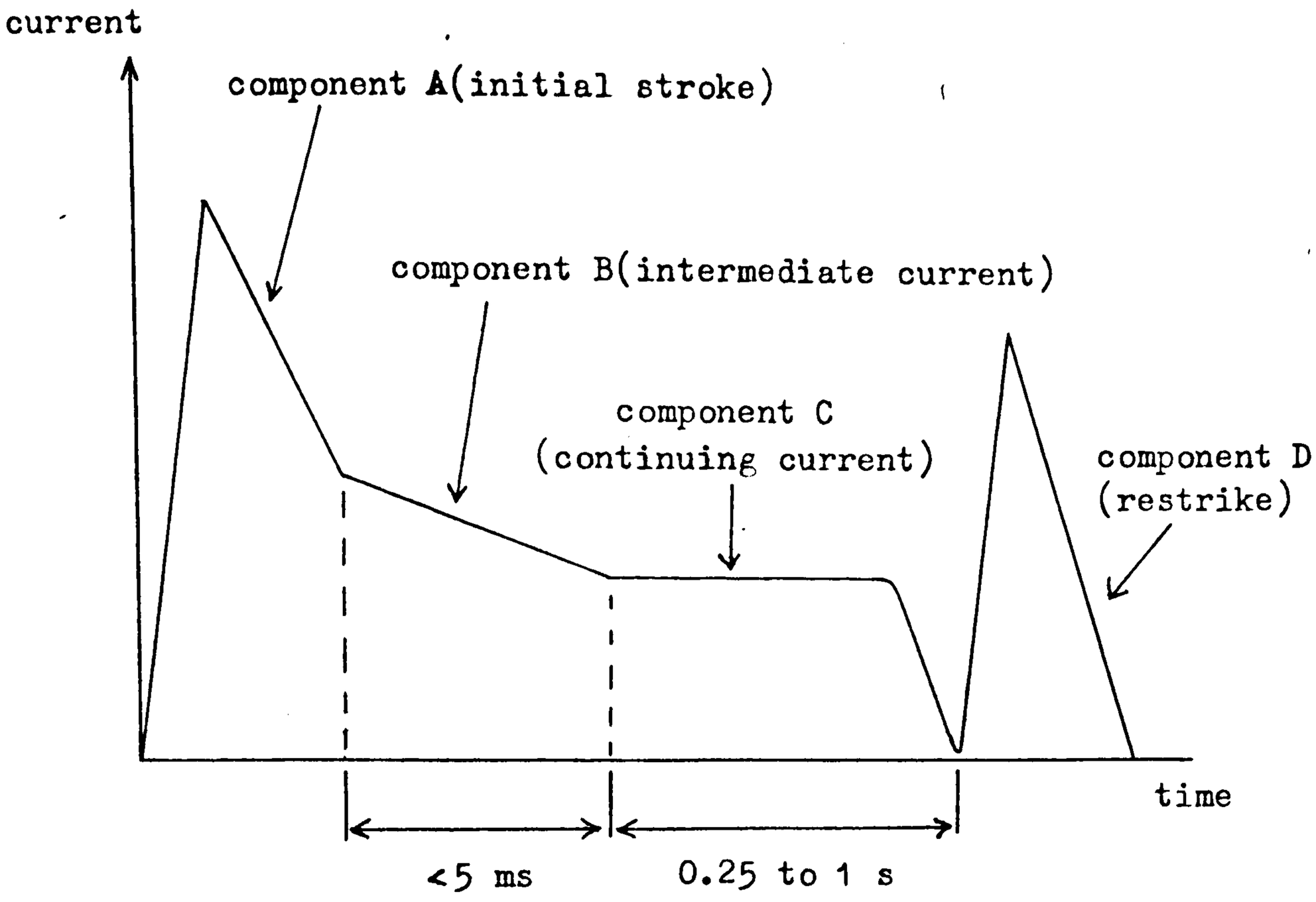

component A: peak amplitude 200 kA ± 10%
action integral 2×10^6 A^2s ± 10%
time duration <500 μs

component B: maximum charge transfer 10C
average amplitude 2 kA ± 10%

component C: charge transfer 200C ± 20%
amplitude 200-800 A

component D: peak amplitude 100 kA ± 10% } Group 1 effects
action integral 0.25×10^6 A^2s ± 10% }
peak amplitude 100 kA ± 10% } Group 2 effects
peak initial rate of rise of current 100 kA/μs ± 10% }
time for which di/dt should exceed 25 kA/μs 0.5 μs ± 10% }

Fig. 1.3 Idealised current test waveform[6].

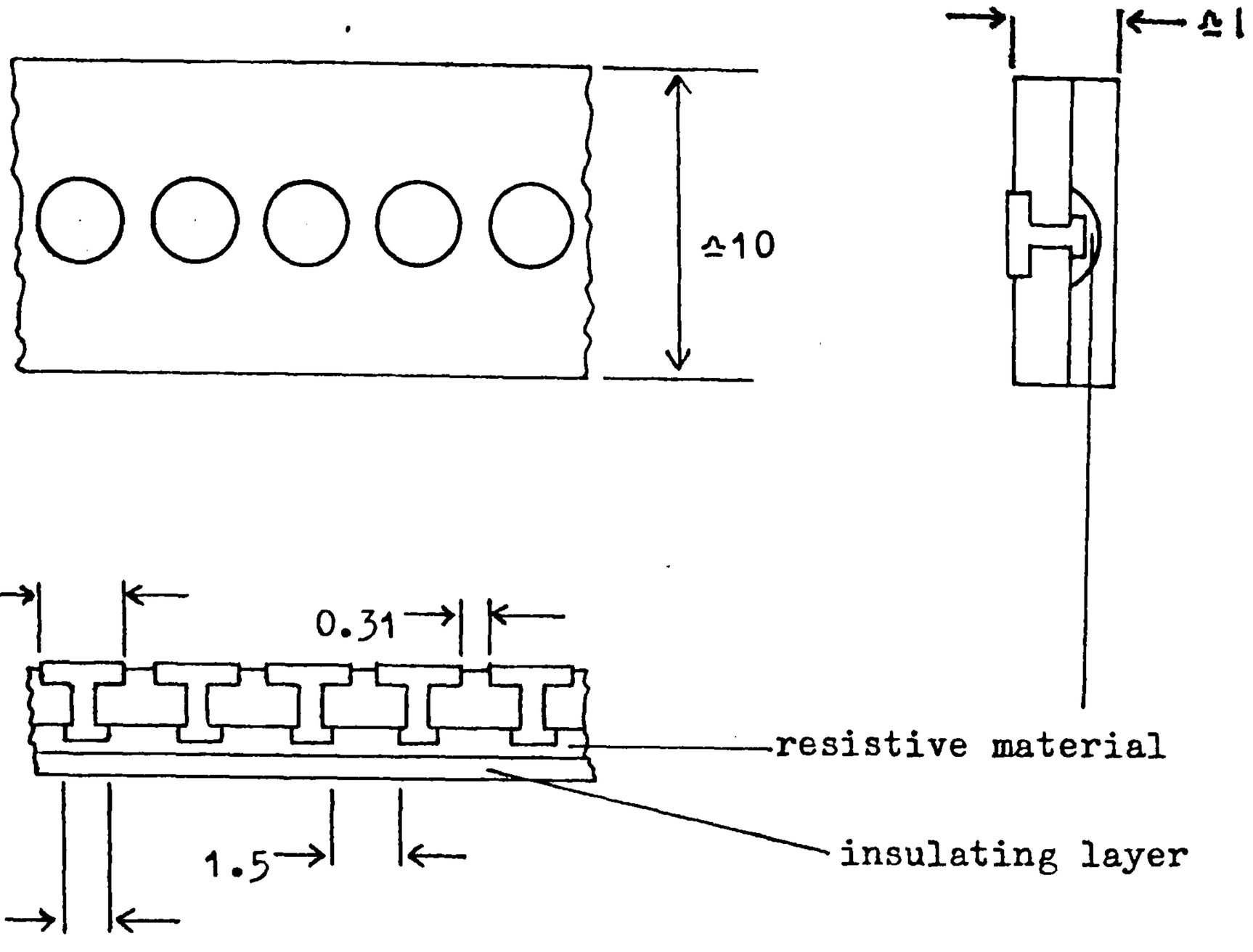

All dimensions in mm

Fig. 2.1 Segmented diverter strip.

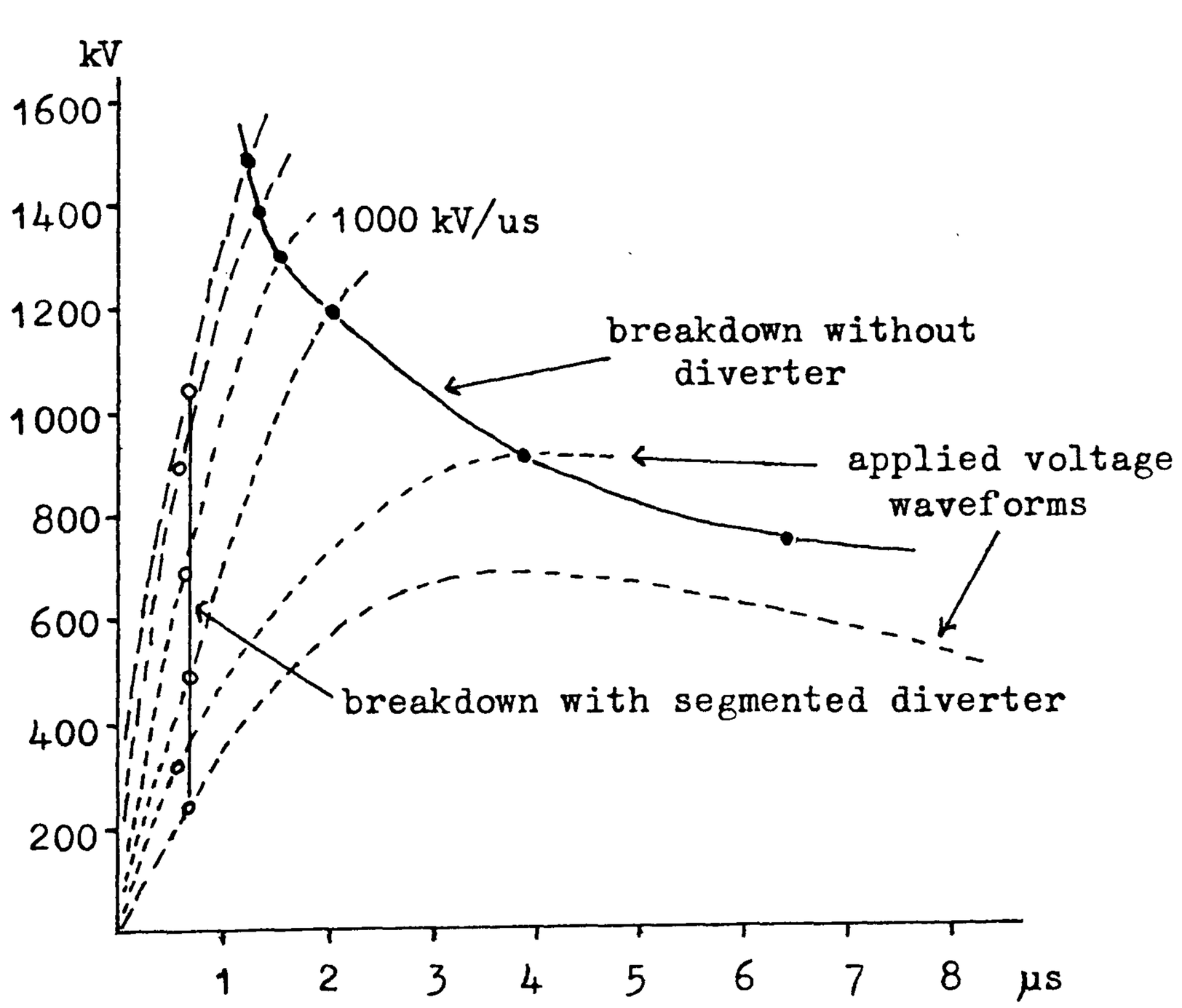

Fig. 2.2 Breakdown voltage vs. time to breakdown across 1.2m radome wall with and without segmented diverter[35].

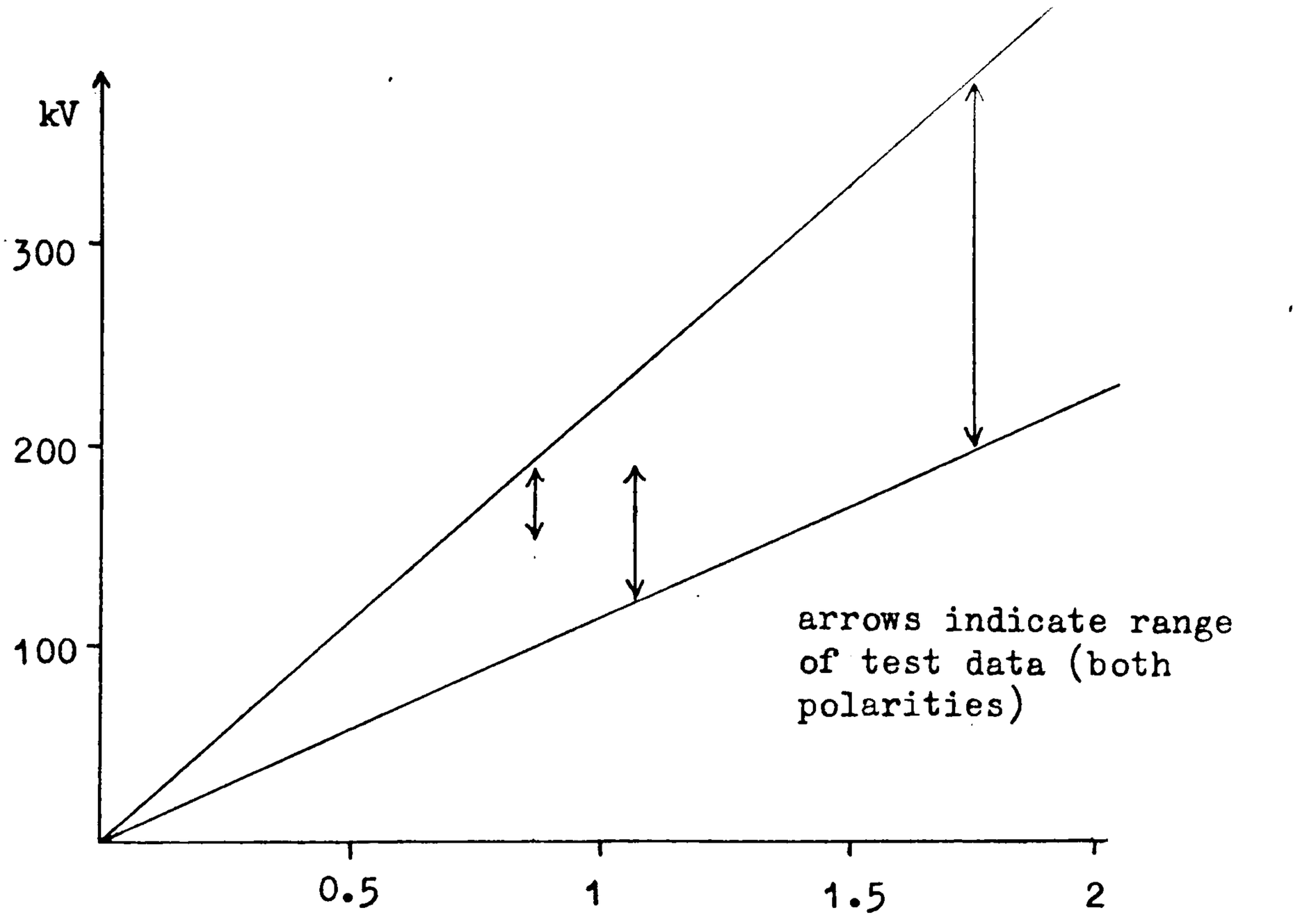

Fig. 2.3 Segmented strip flashover voltage vs. strip length at 200 kV/μs rate of voltage rise[35].

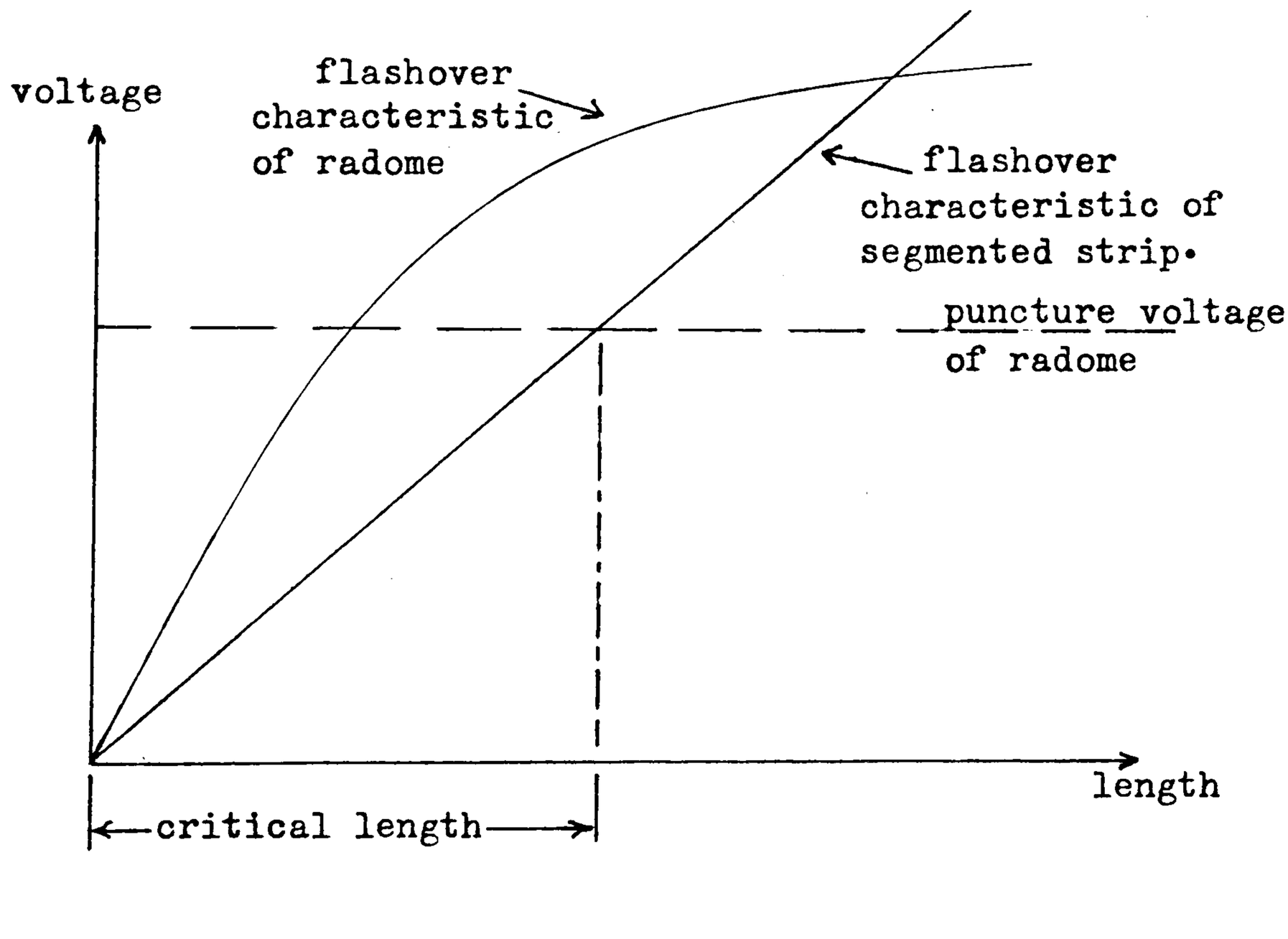

Fig. 2.4 Determination of the maximum strip length permissible[36].

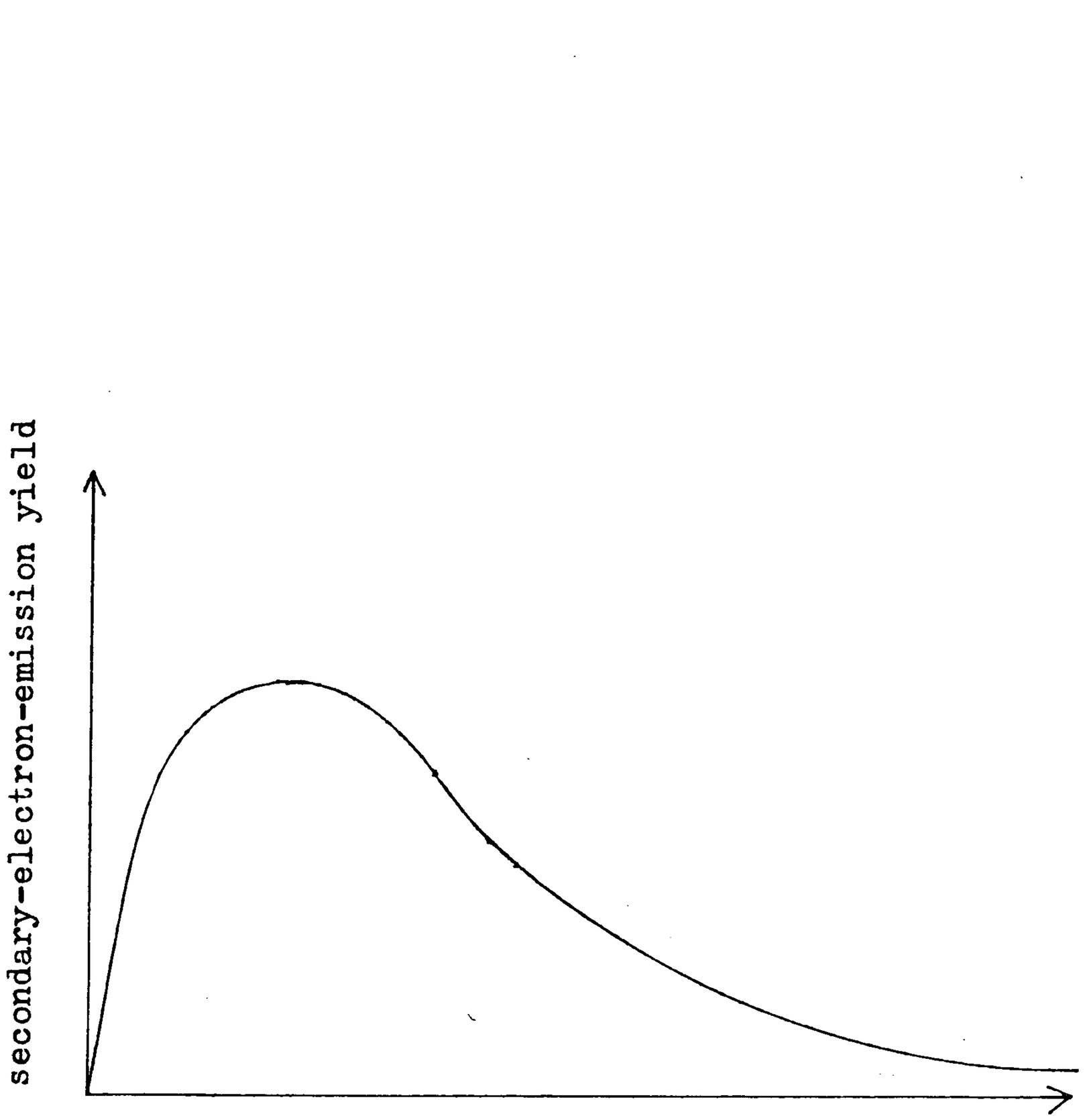

Fig. 3.1 Typical form of a secondary-electron-emission yield curve.

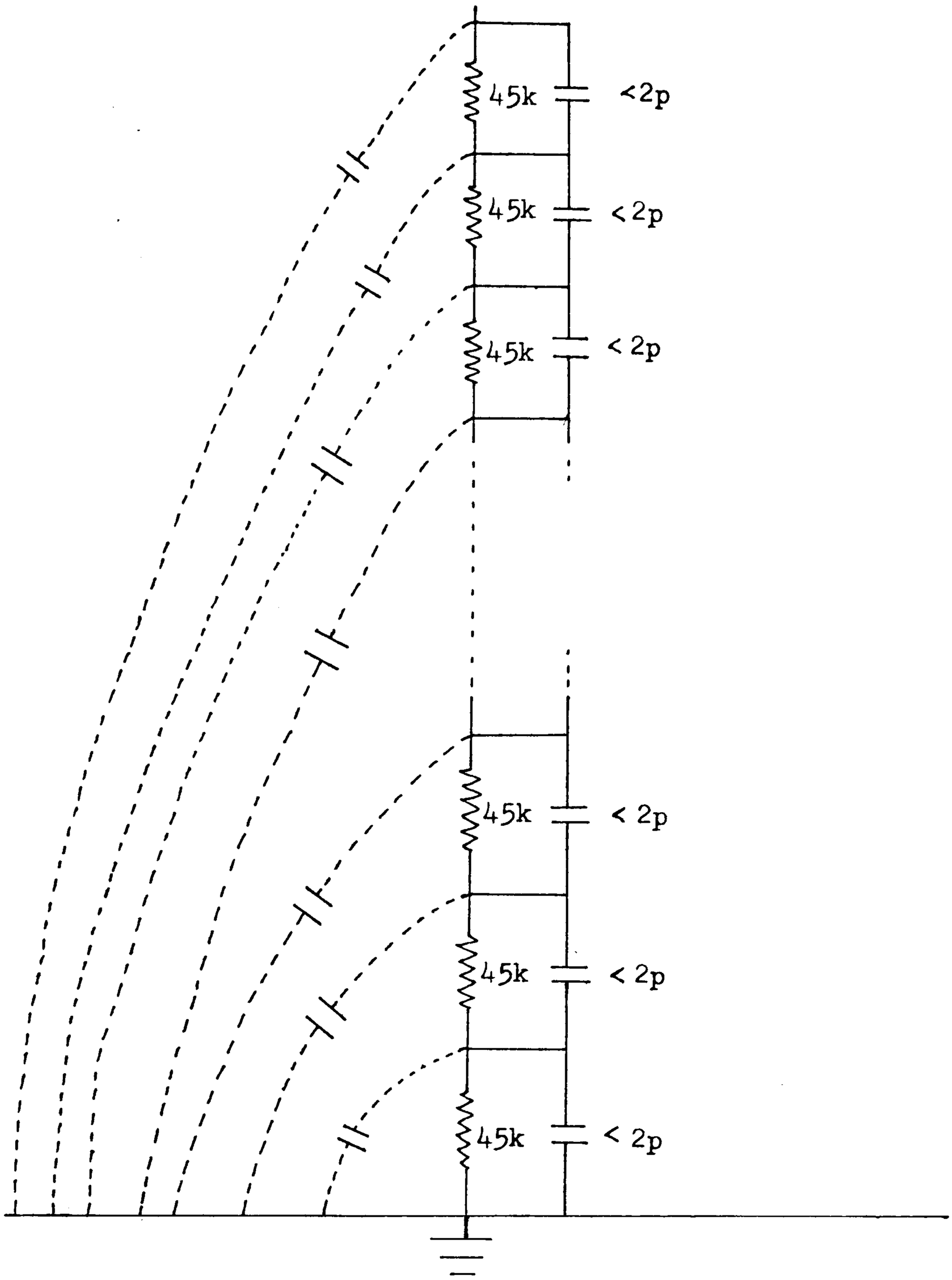

Fig. 3.2 Equivalent circuit of segmented strip.

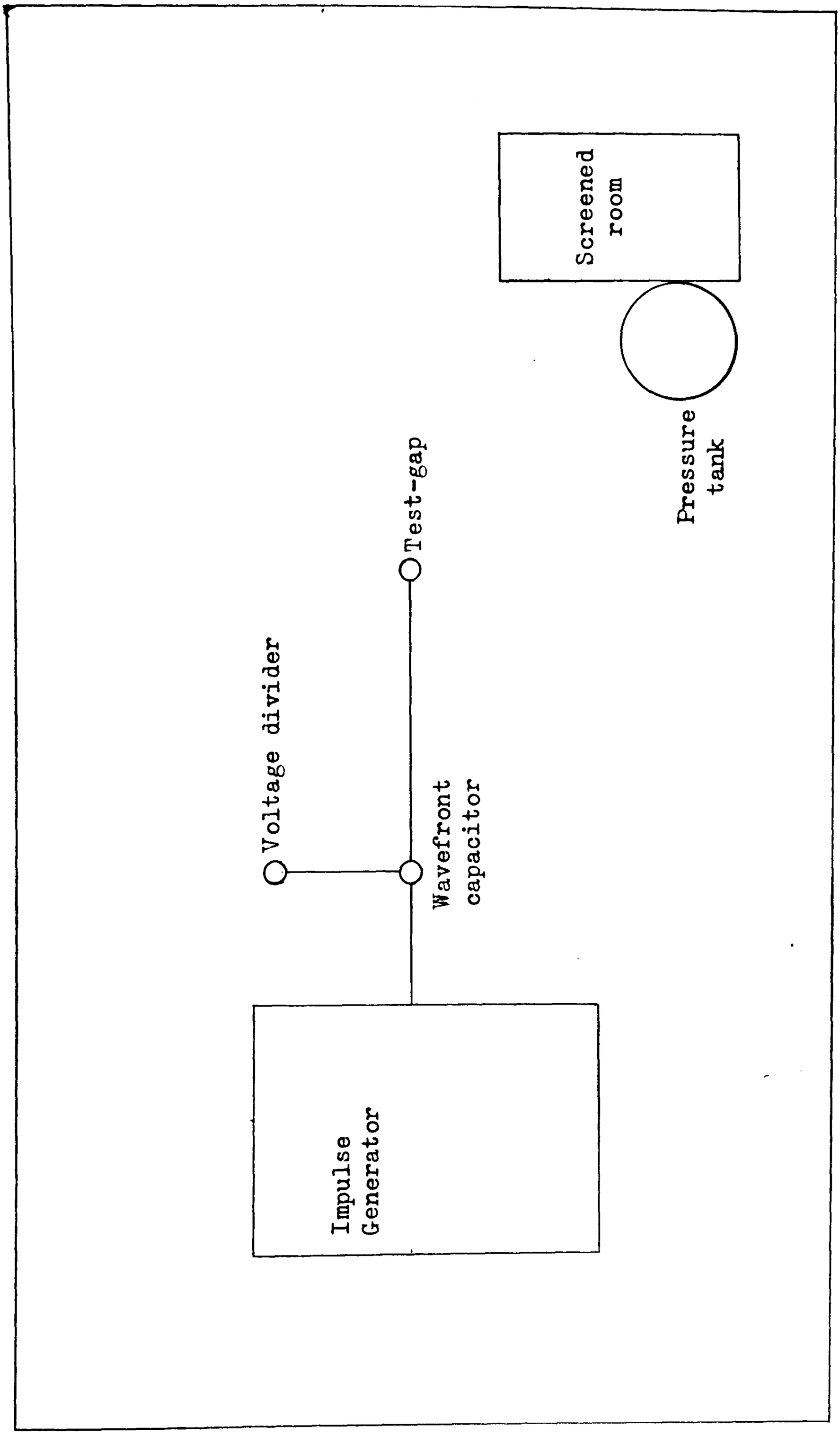

Fig. 4.1 Plan of the High-voltage laboratory.

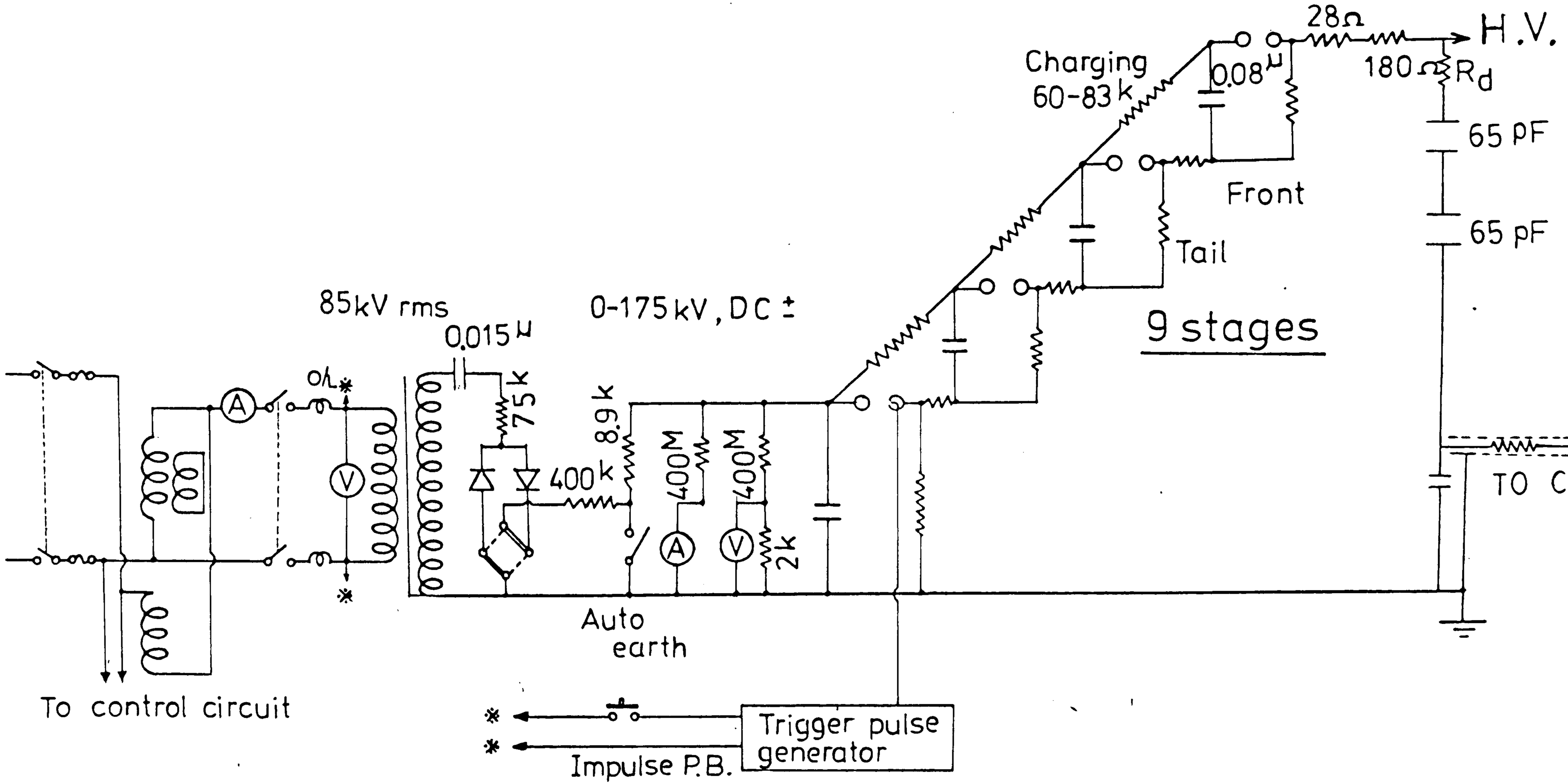

Fig. 4.2 Impulse generator : Main circuit (175 kV, 9 stages)

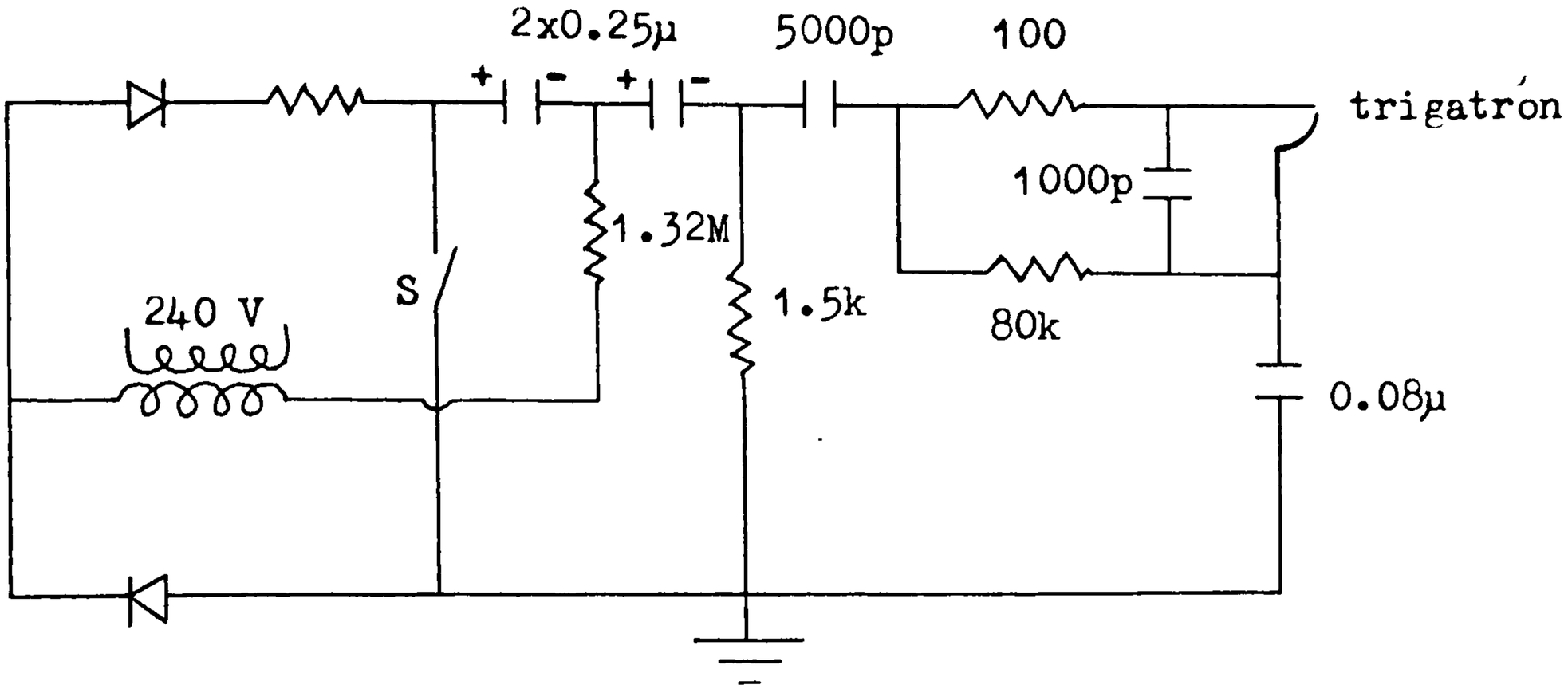

(a)

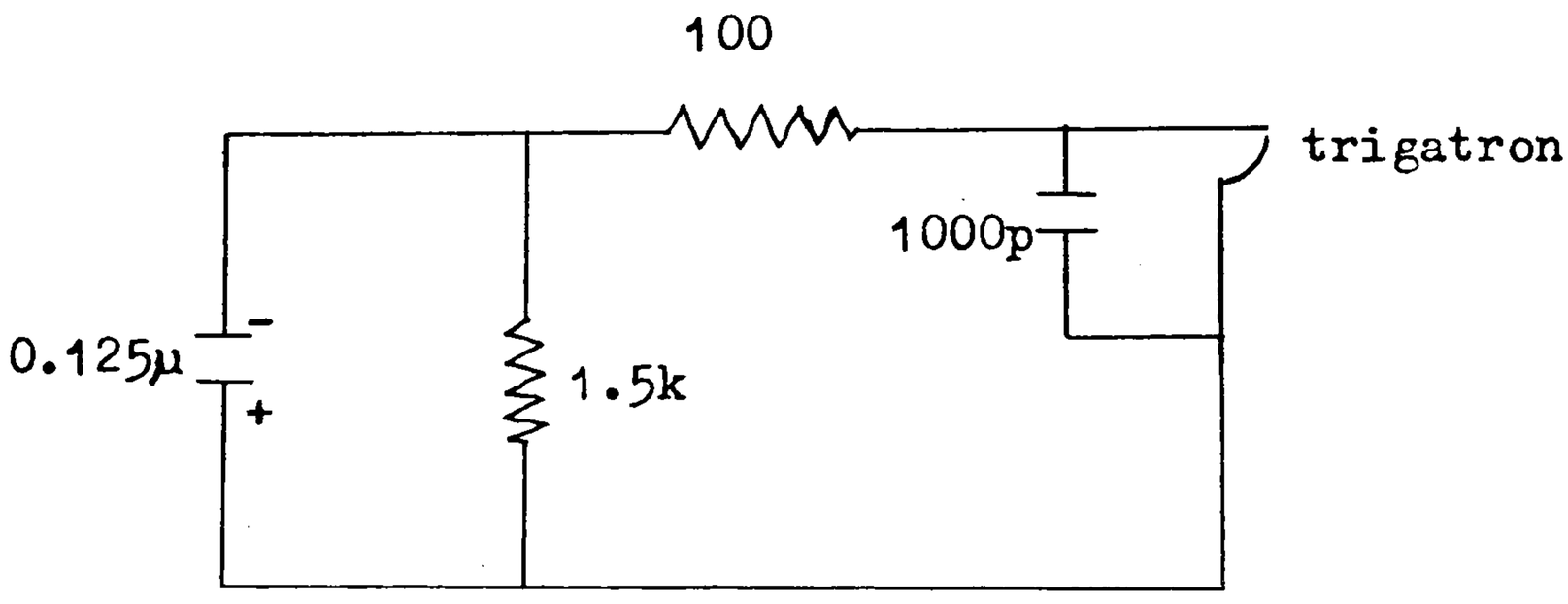

(b)

Fig. 4.3 (a) - Actual circuit

(b) - Equivalent circuit after switch S is closed.

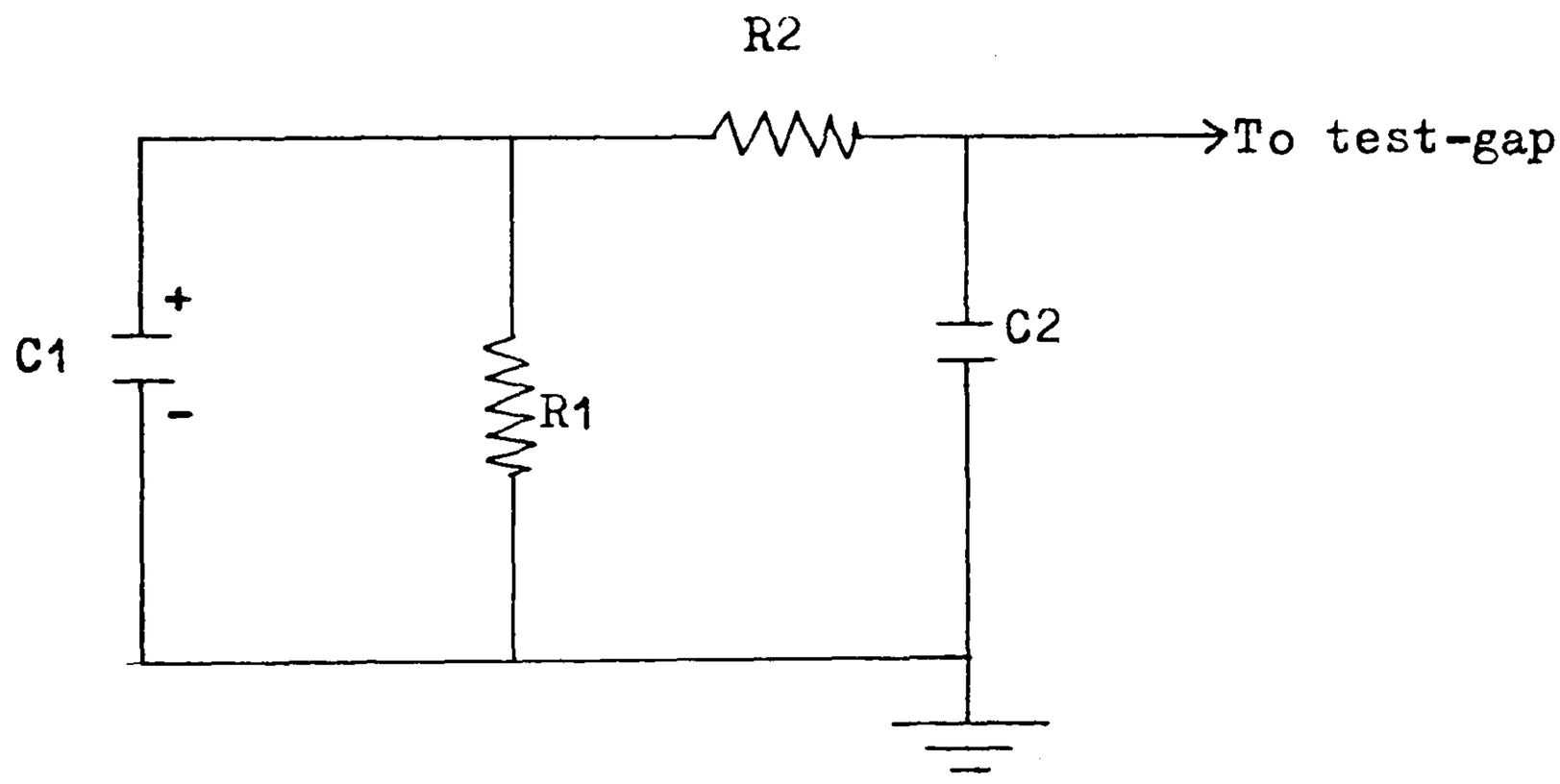

Fig. 4.4 Equivalent circuit of impulse generator.

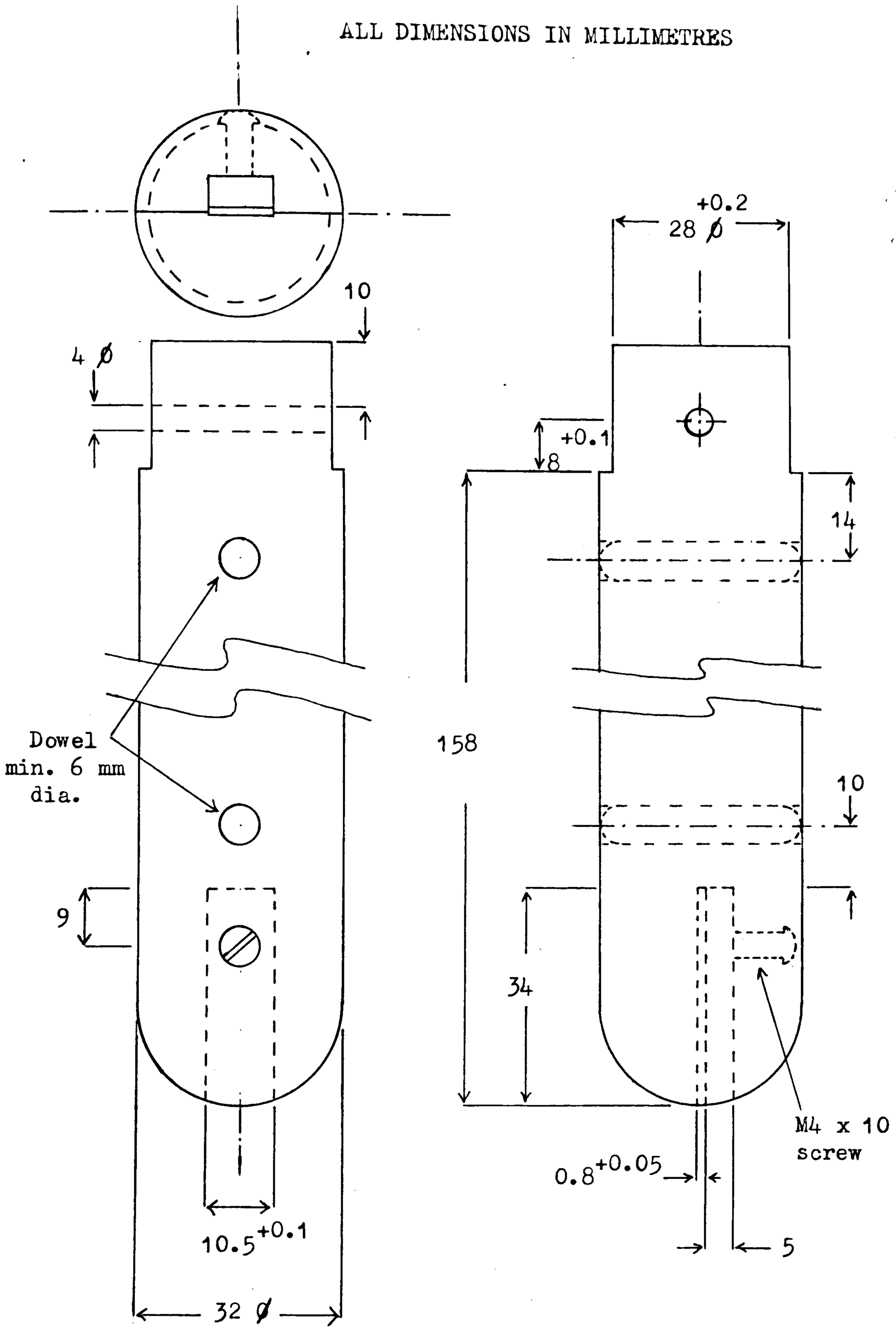

Fig. 4.5 Plan and elevation of brass rod electrode.

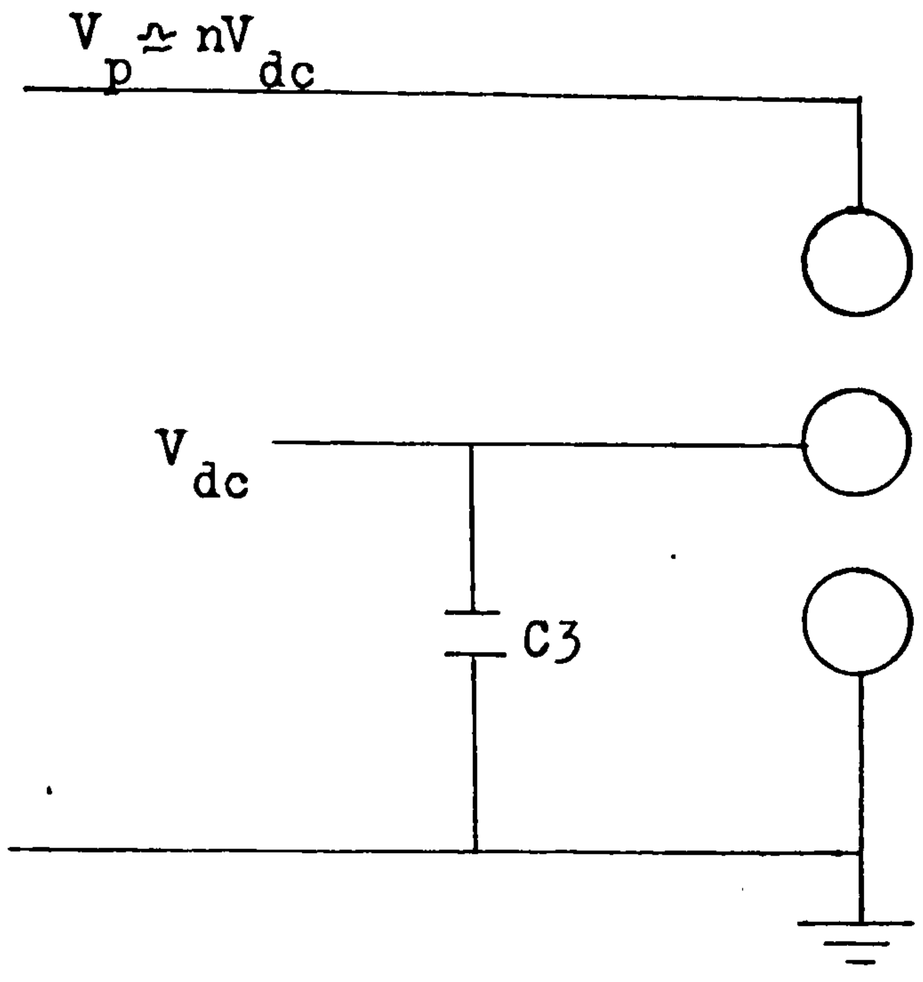

Fig. 4.6 Basis of chopping gap system.

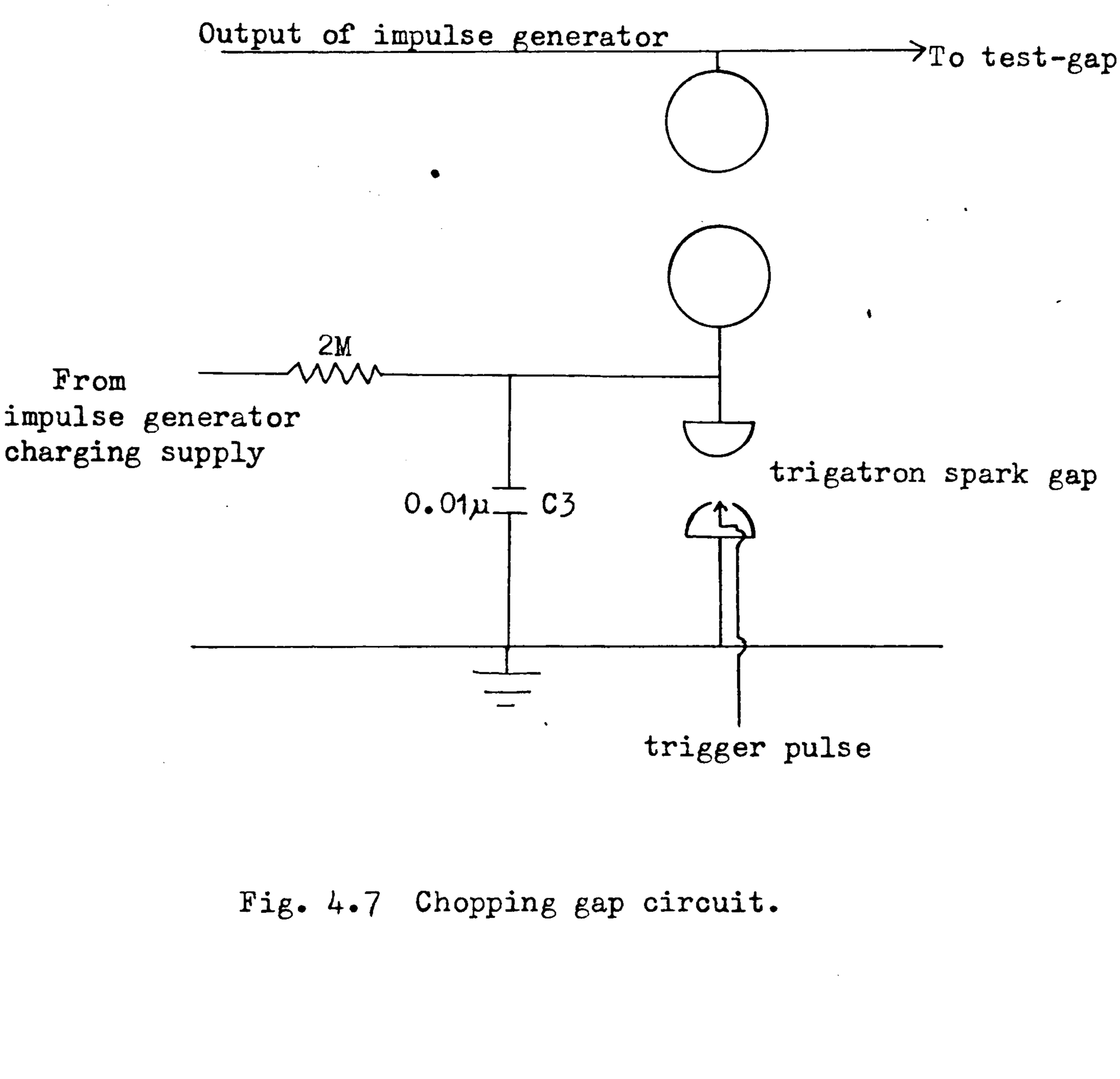

Fig. 4.7 Chopping gap circuit.

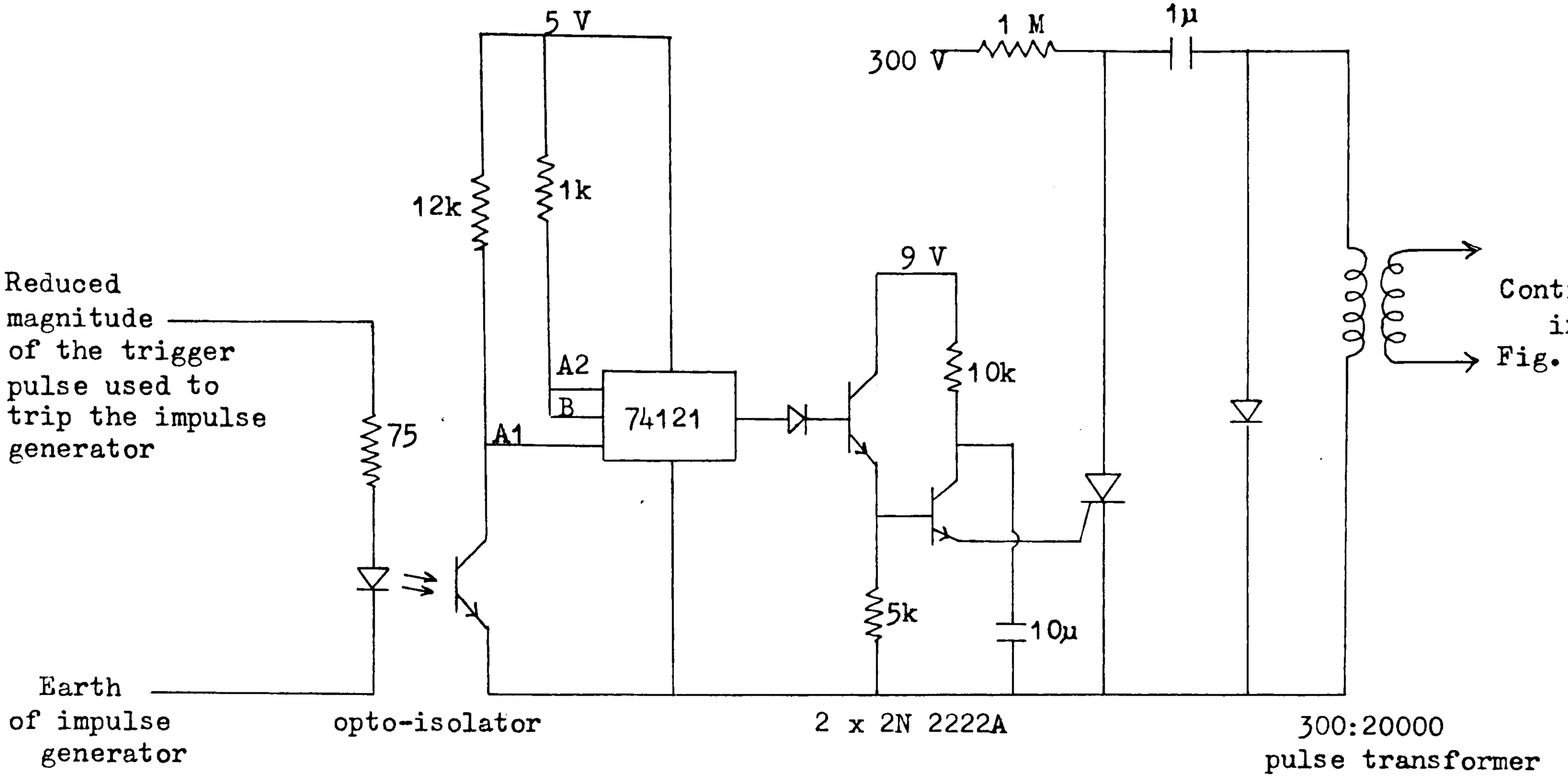

Fig. 4.8a Trigger circuit 1

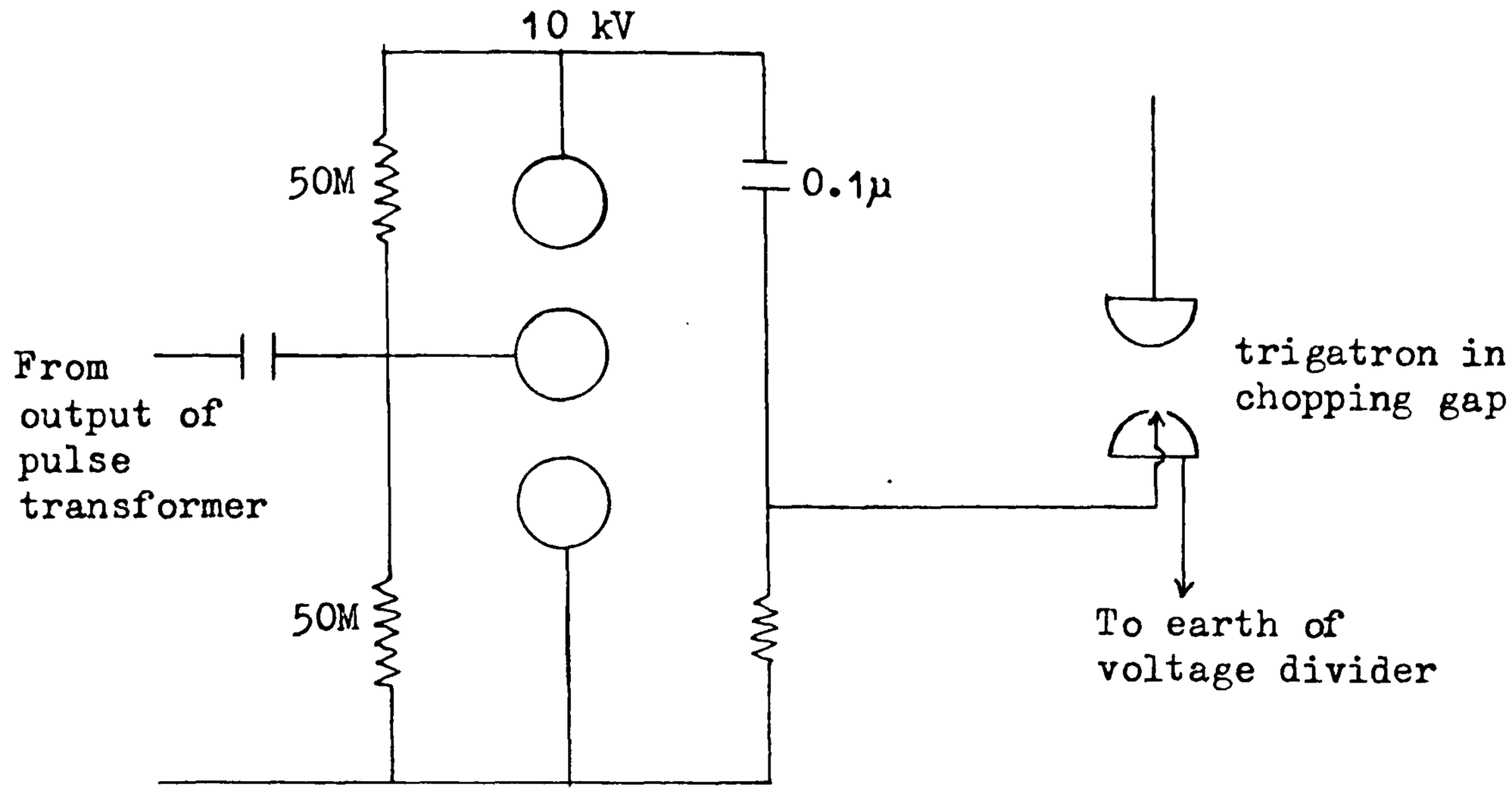

Fig. 4.8b Trigger circuit 1 (continued)

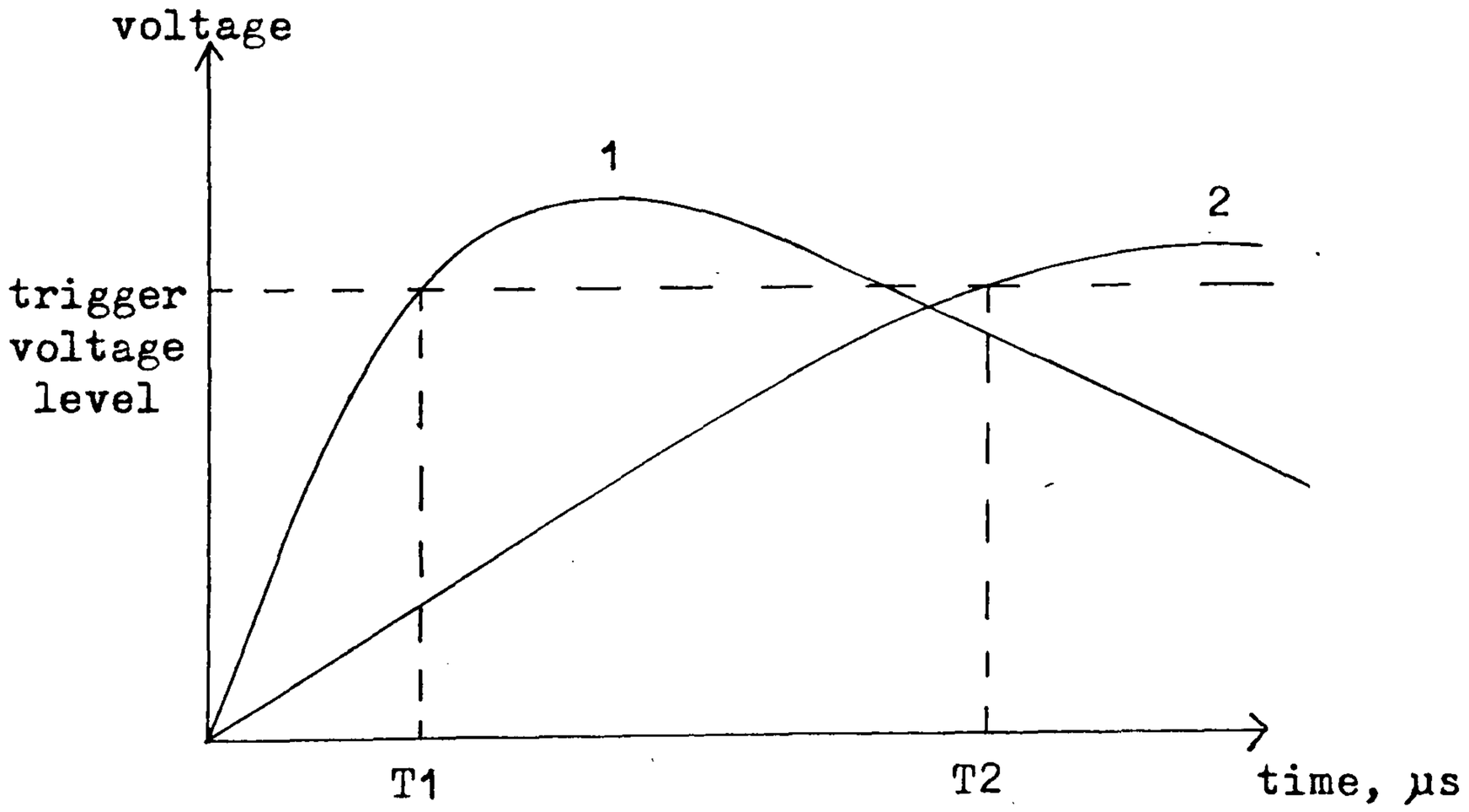

Fig. 4.9 Principle of delayed triggering for trigatron in chopping gap.

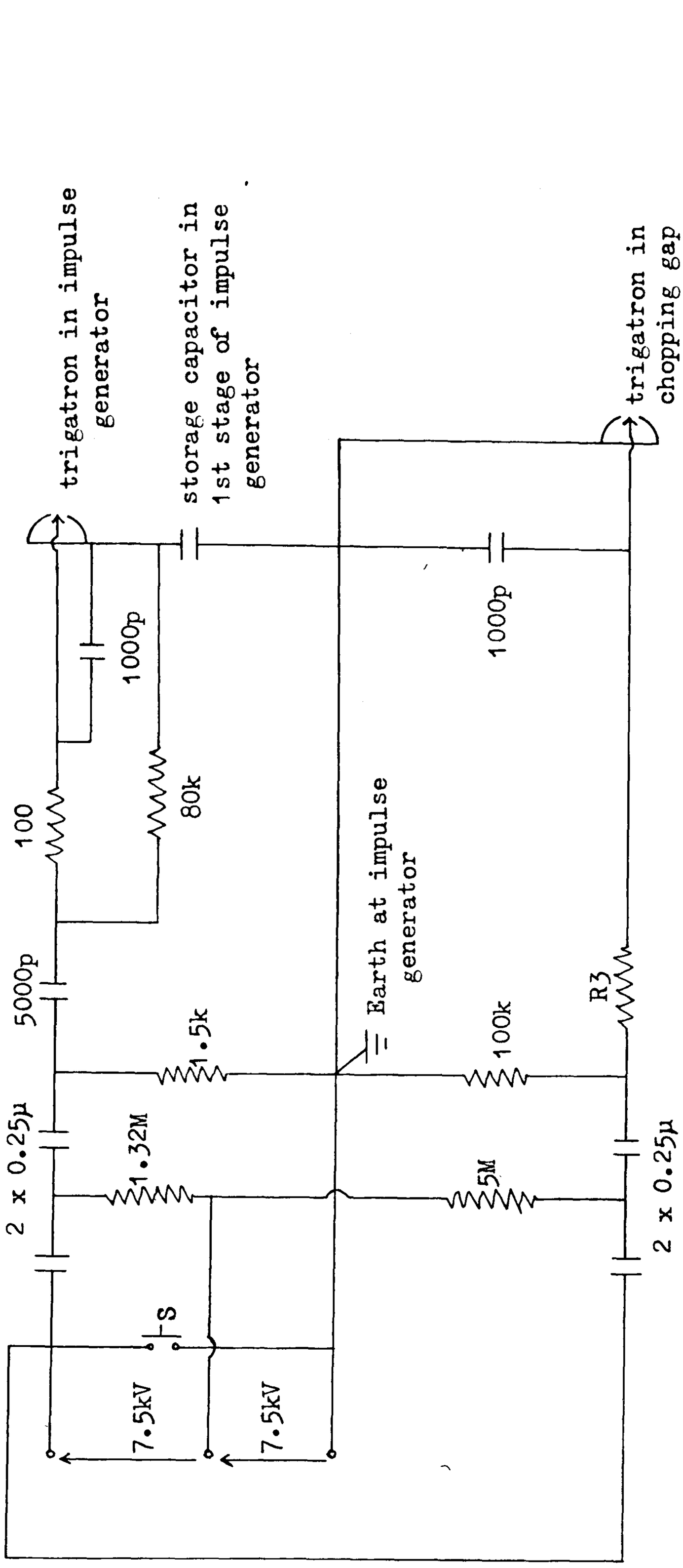

Fig. 4.10 Trigger circuit 2

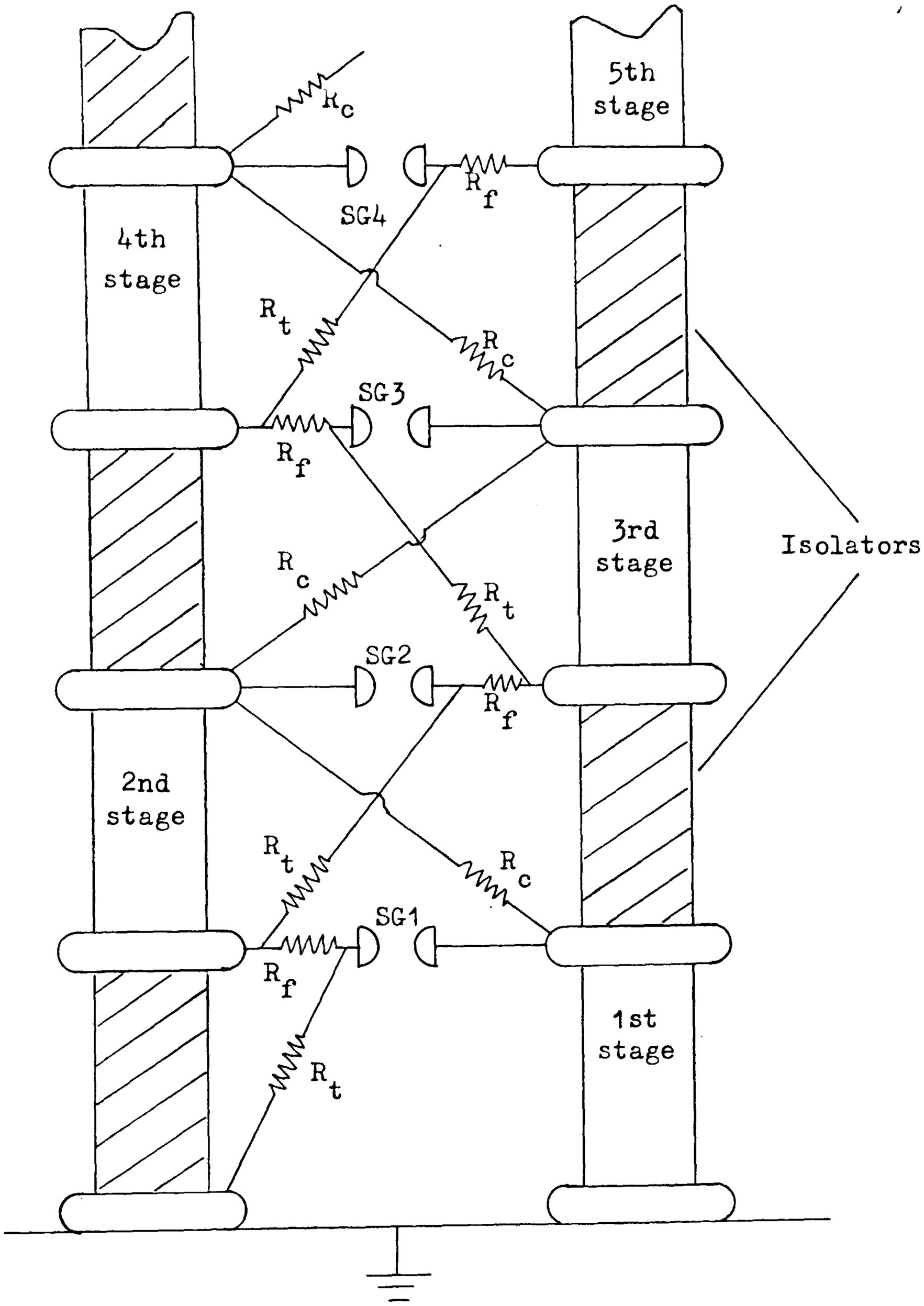

Fig. 4.11 Construction of impulse generator (only 4 stages shown)

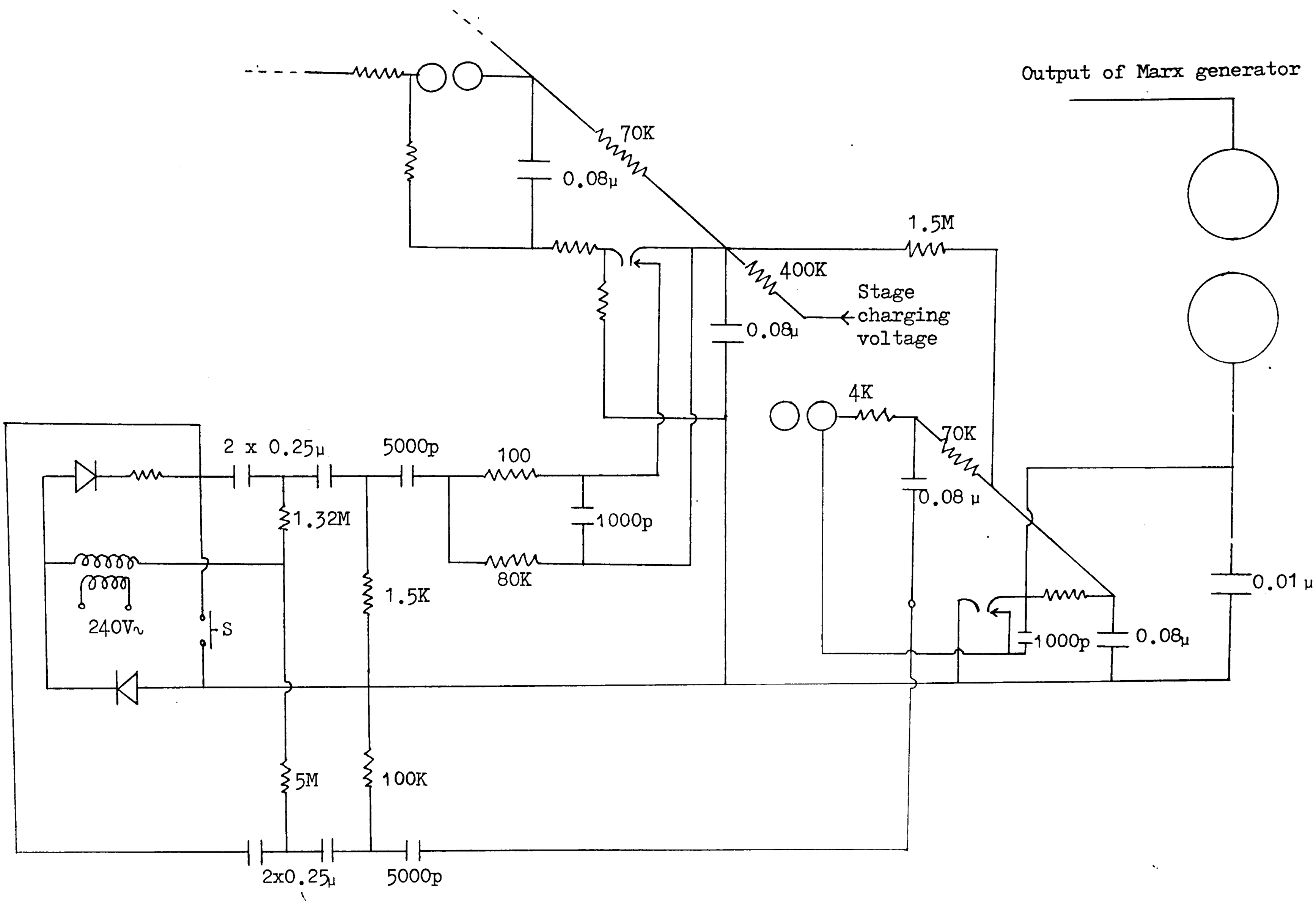

Fig. 4.12 Trigger Circuit 3

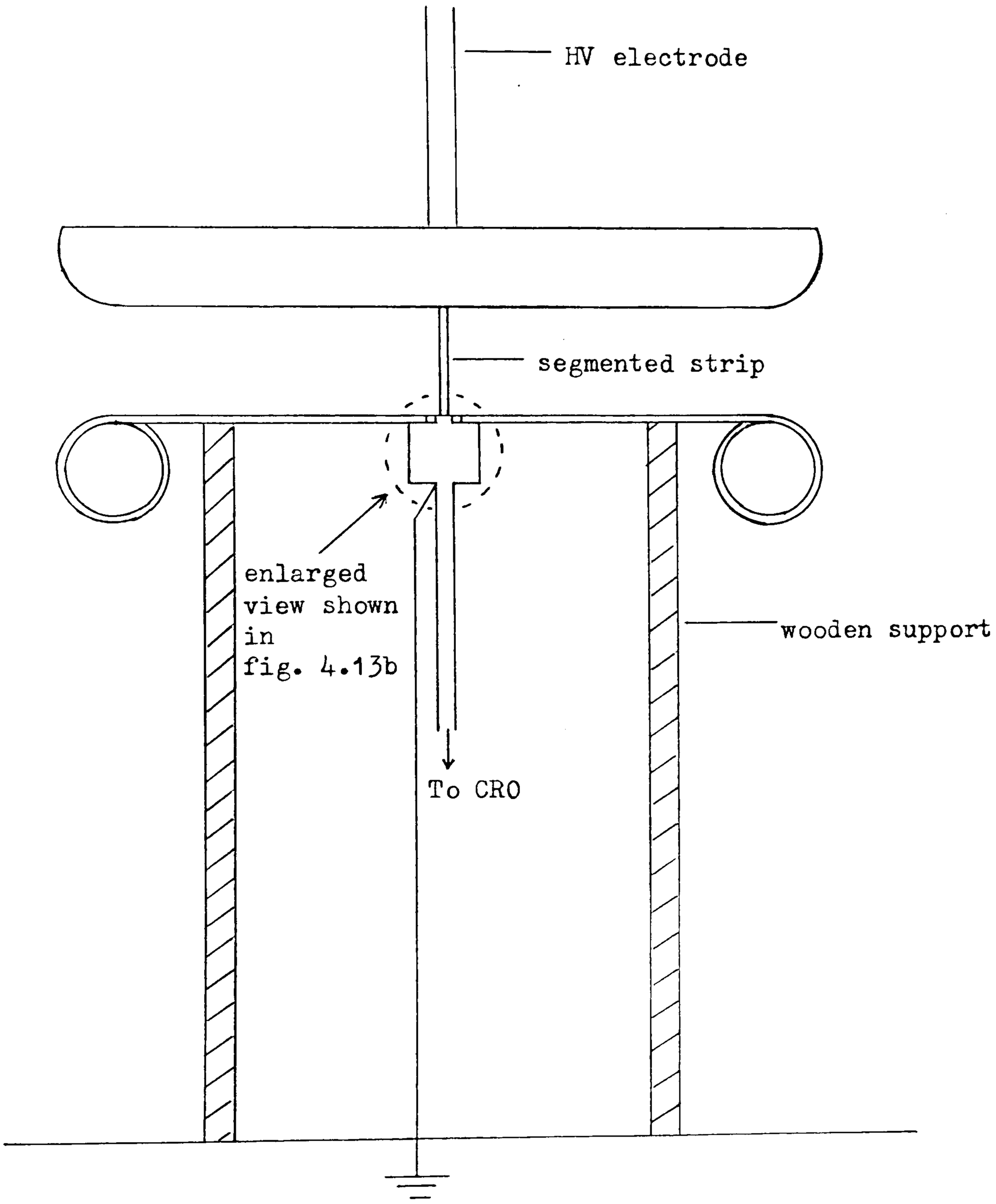

Fig. 4.13a Current measuring probe.

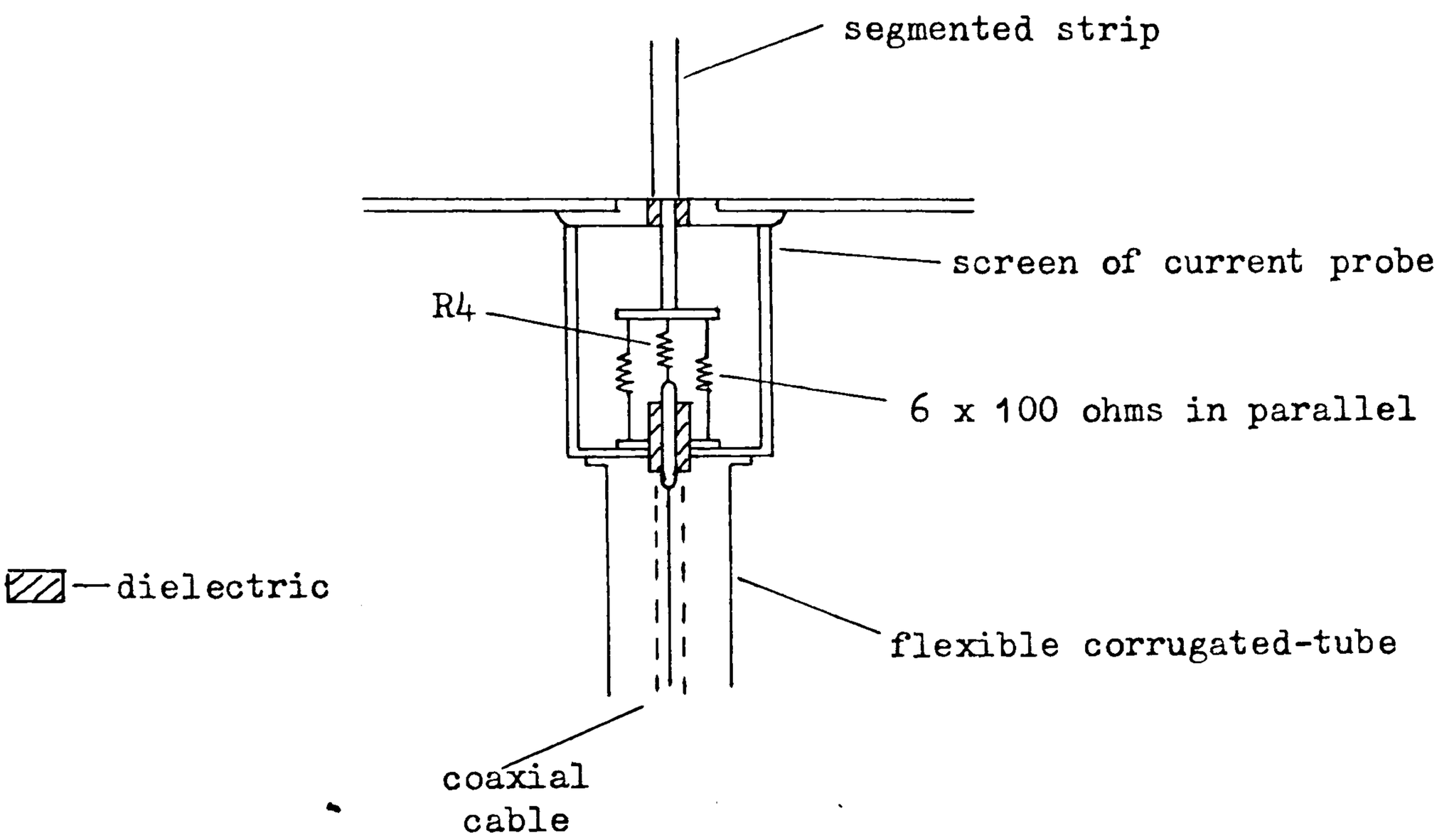

Fig. 4.13b Current measuring probe in detail.

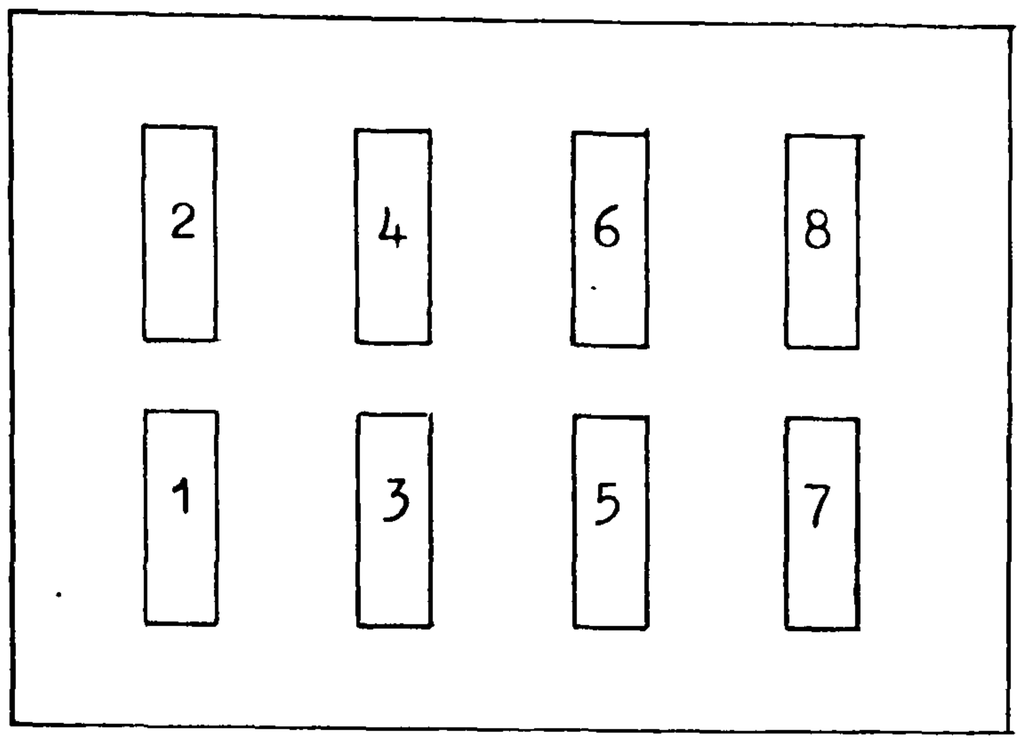

Fig. 4.14 Framing sequence.

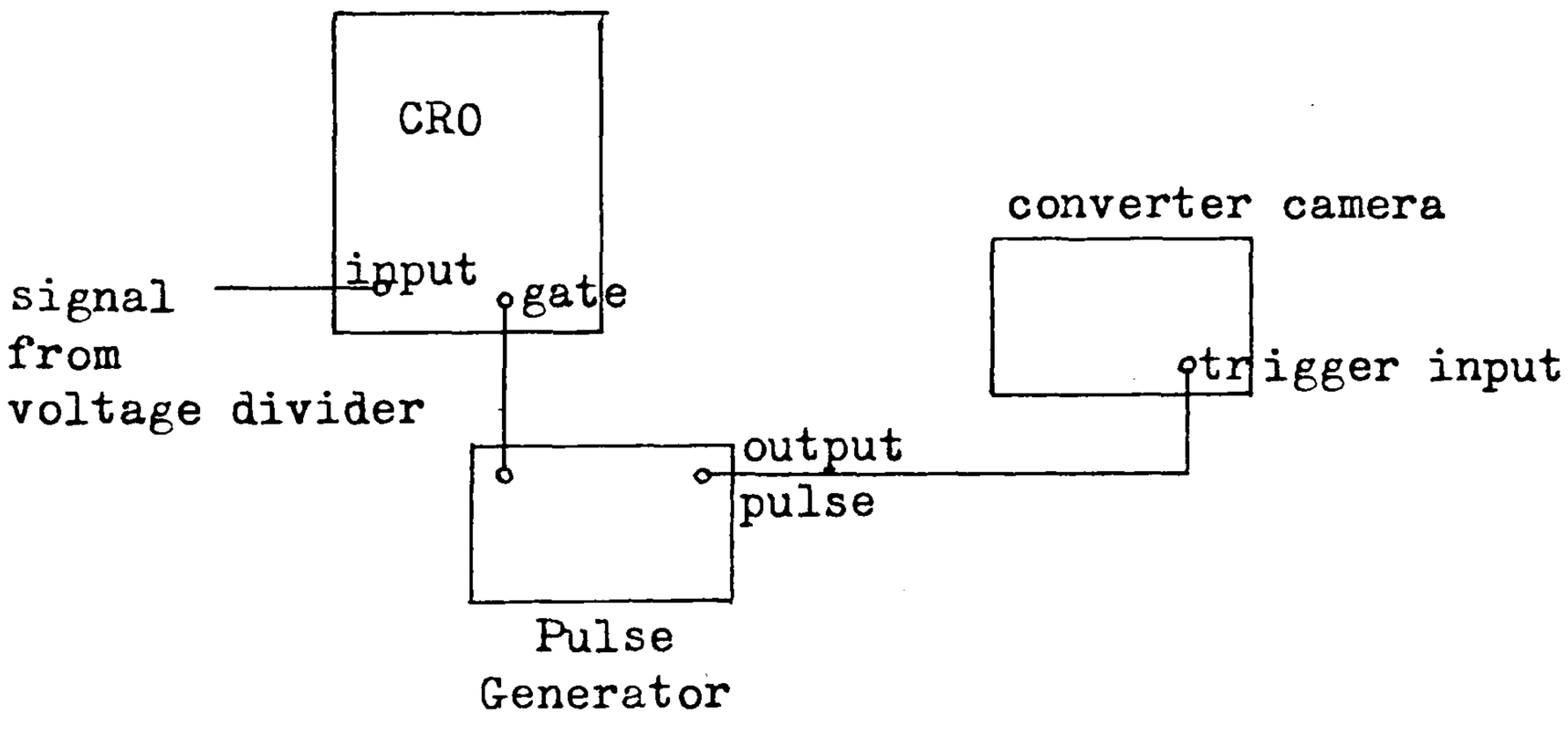

Fig. 4.15 Trigger arrangement for time-resolved photography.

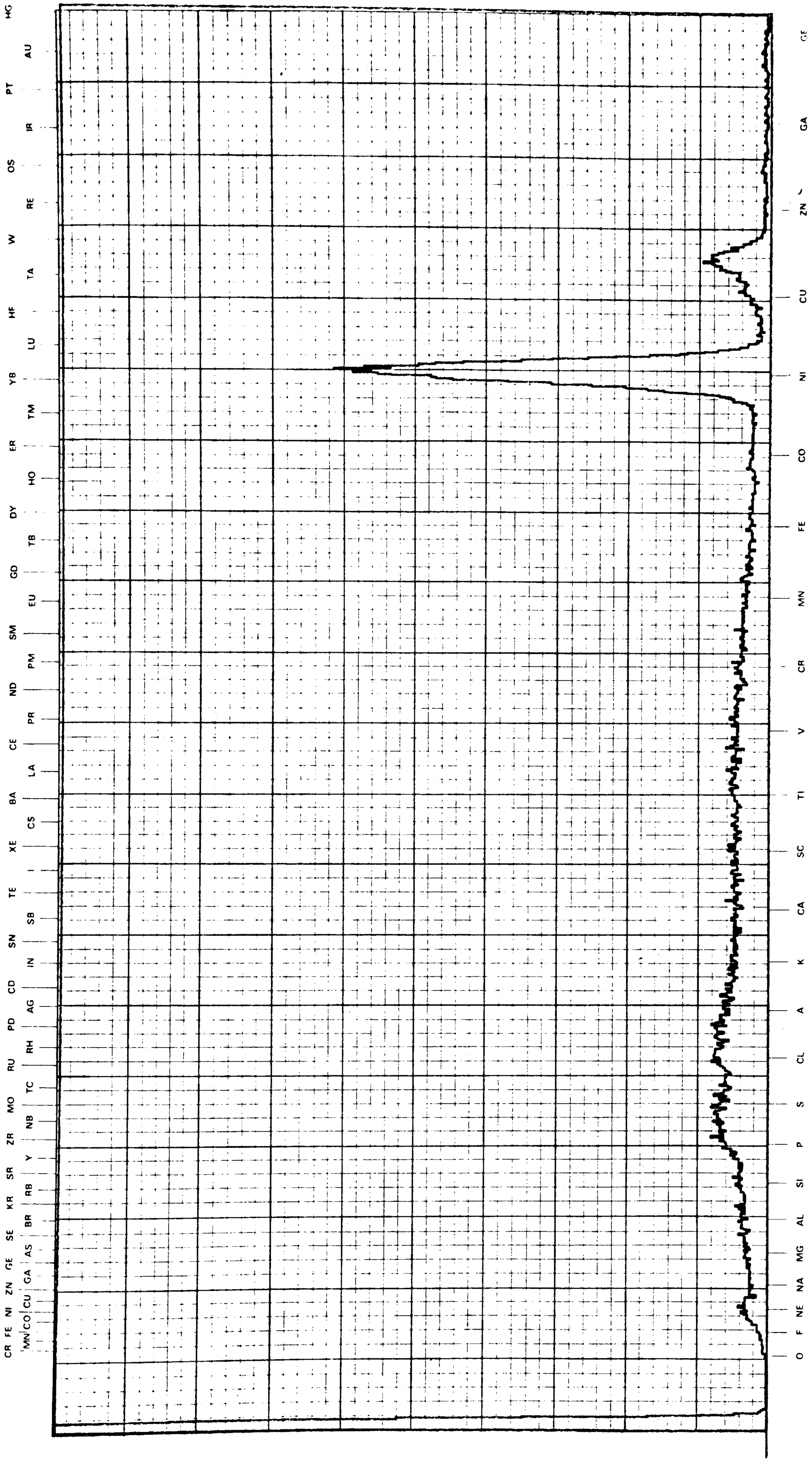

Fig. 5.1 X-ray analysis of metallic segment in segmented strip.

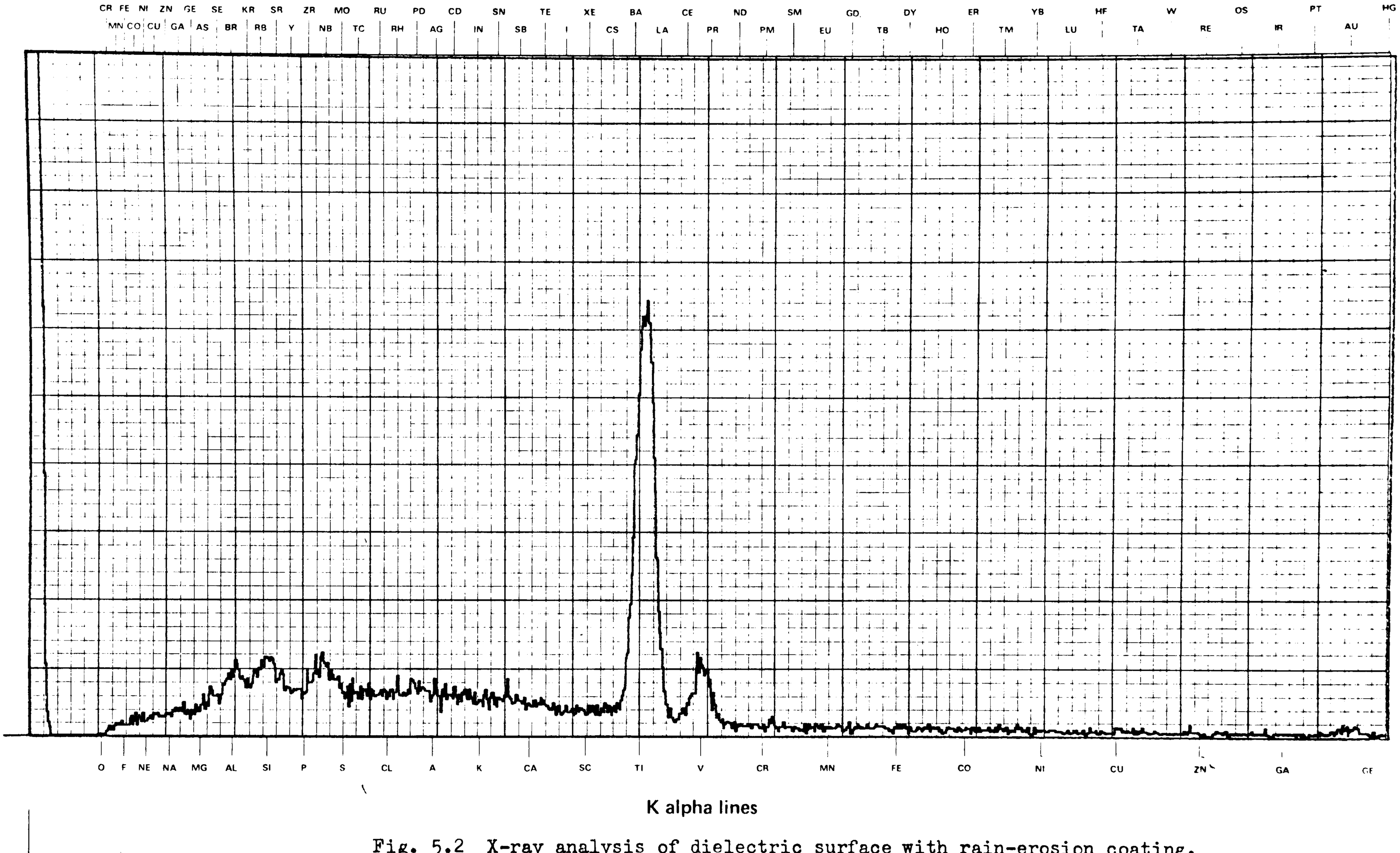

Fig. 5.2 X-ray analysis of dielectric surface with rain-erosion coating.

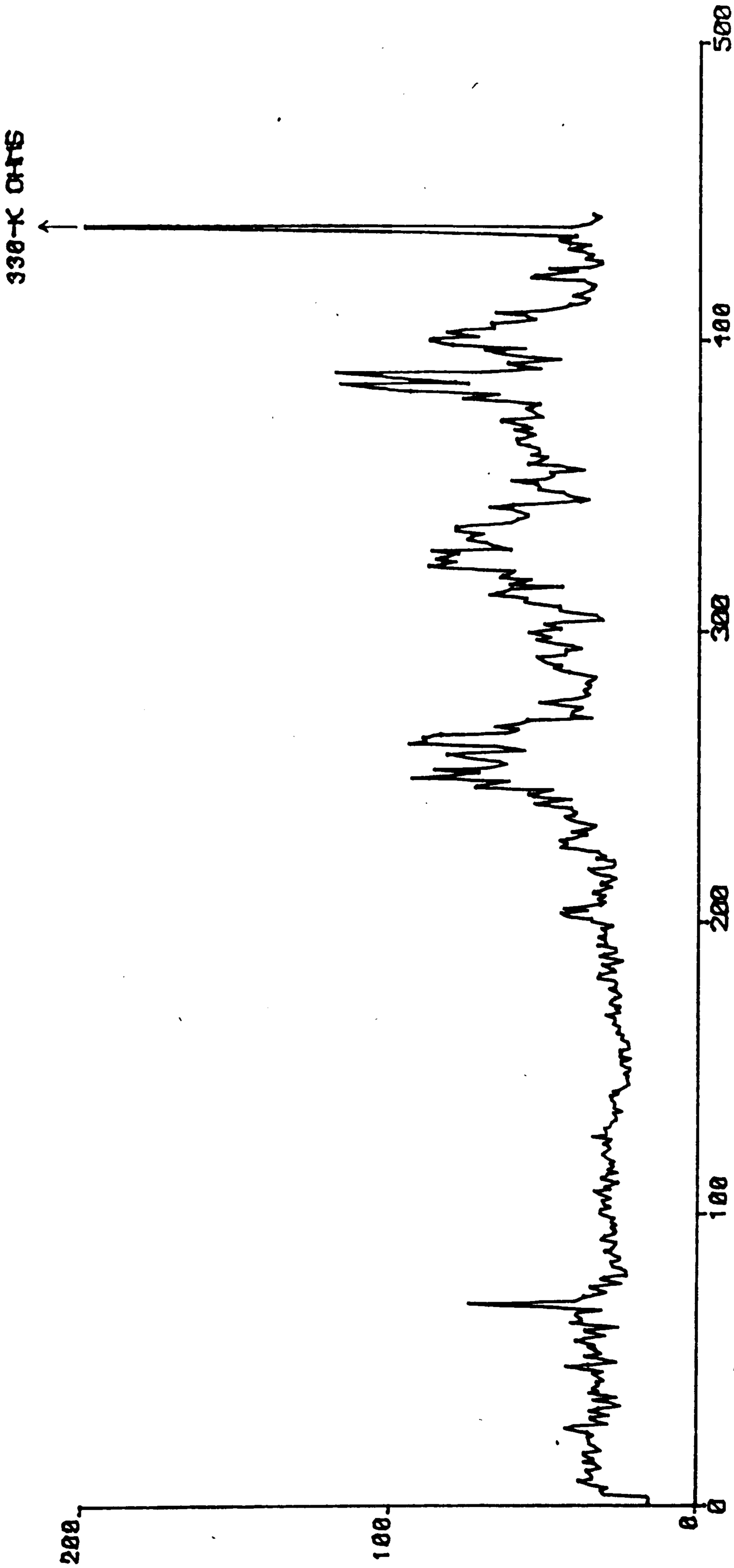

FIG. 5.3a SPATIAL PLOT O

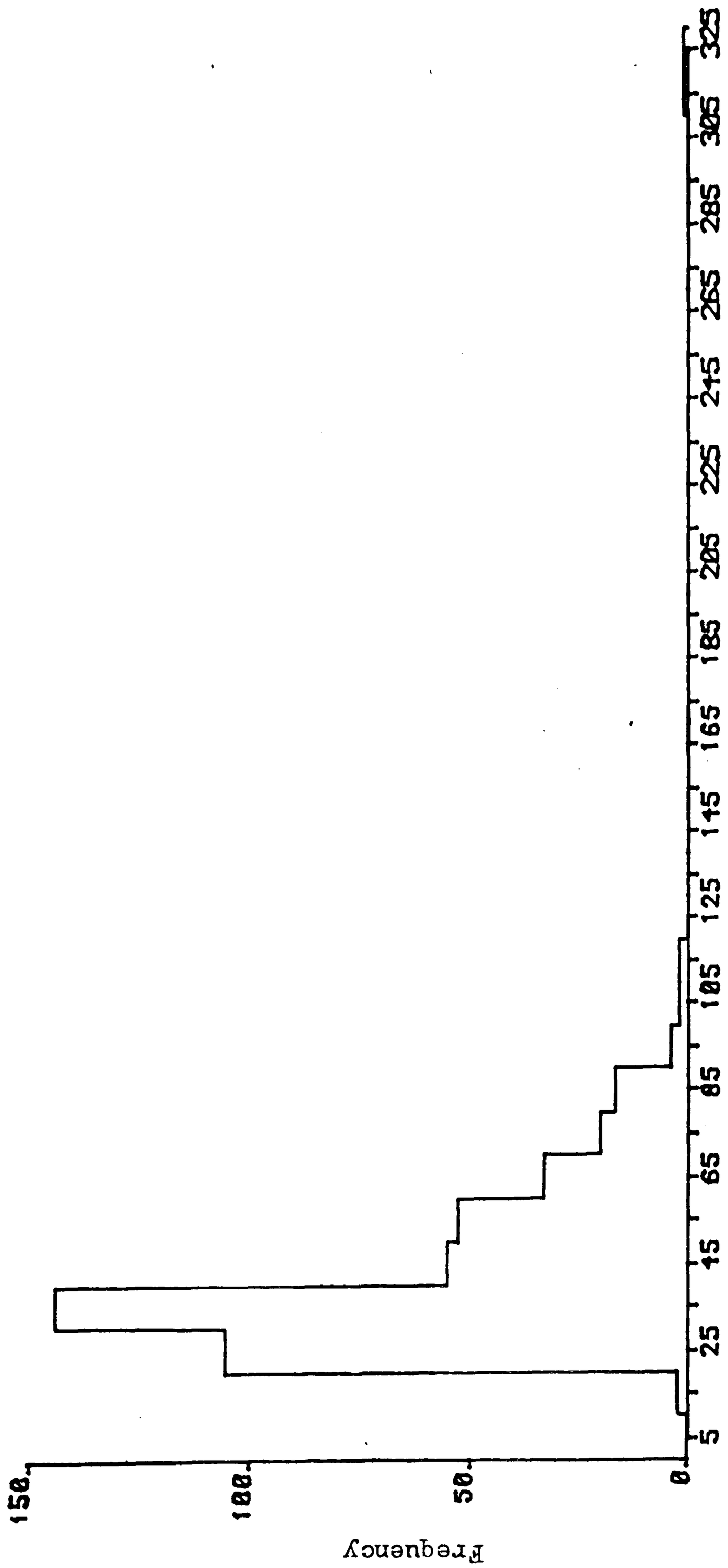

Fig. 5.3b Histogram of intersegment resistance for an unused strip.
(Note: Two resistances at 320-330 k ohms)

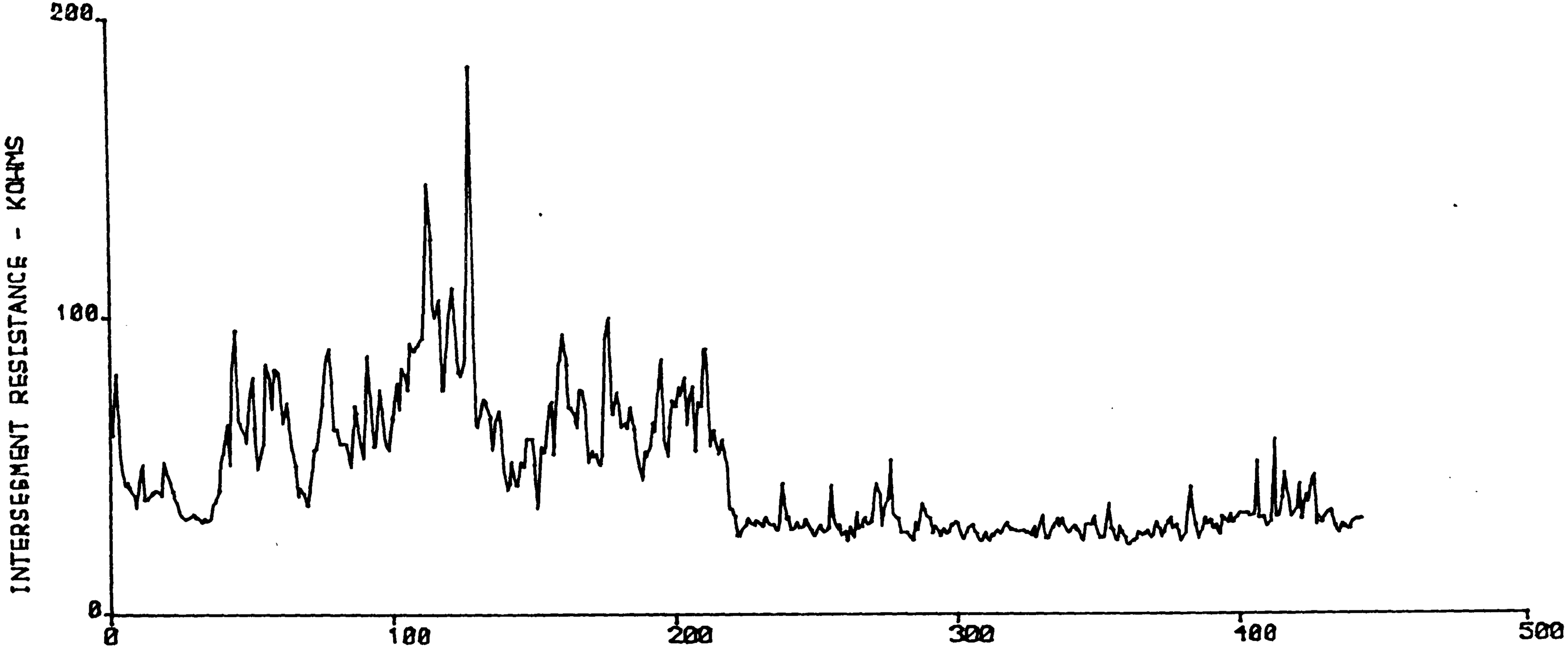

FIG.5.4a SPATIAL PLOT OF INTERSEGMENT RESISTANCE

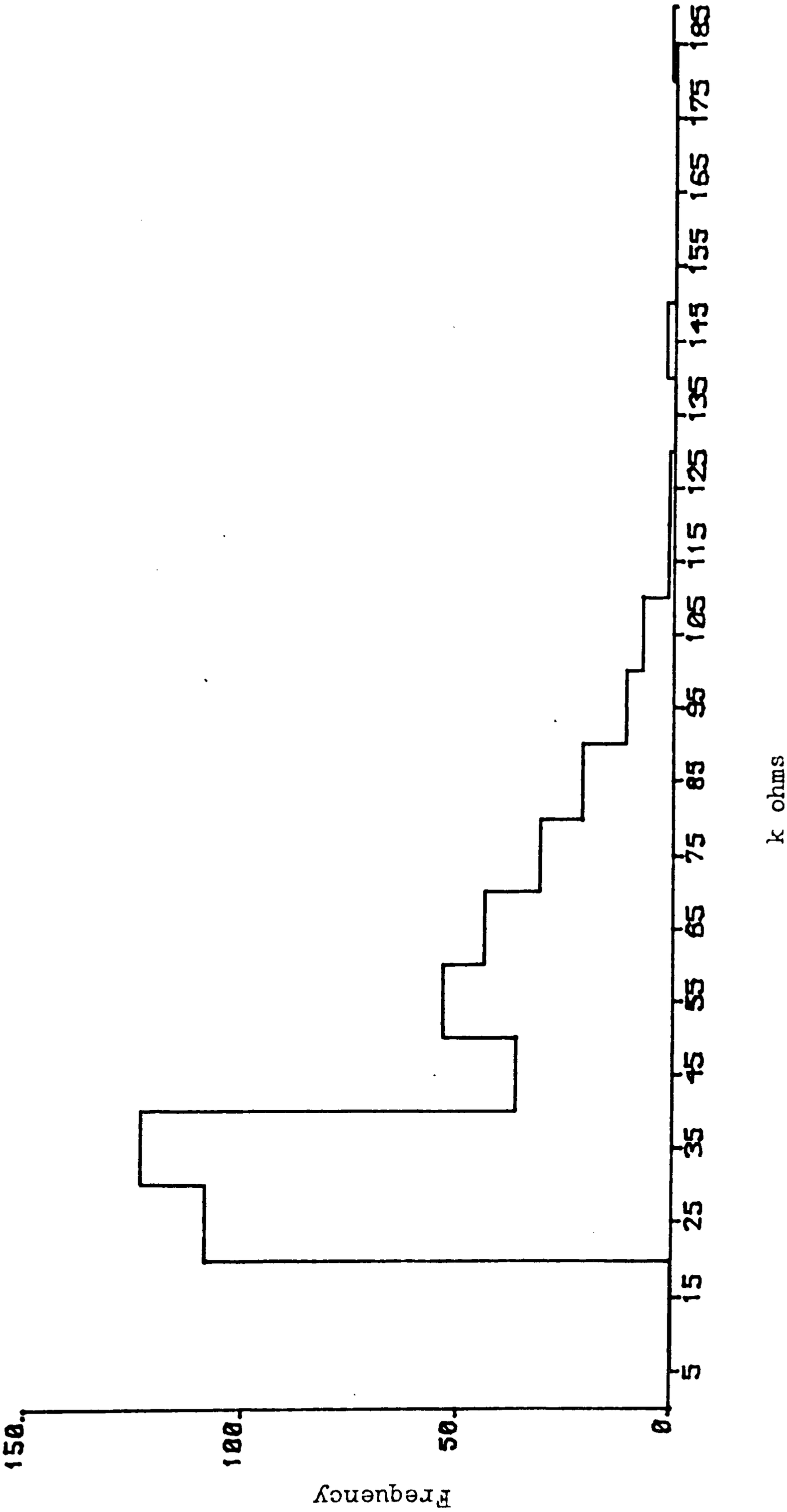

Fig. 5.4b Histogram of intersegment resistances for an unused strip.

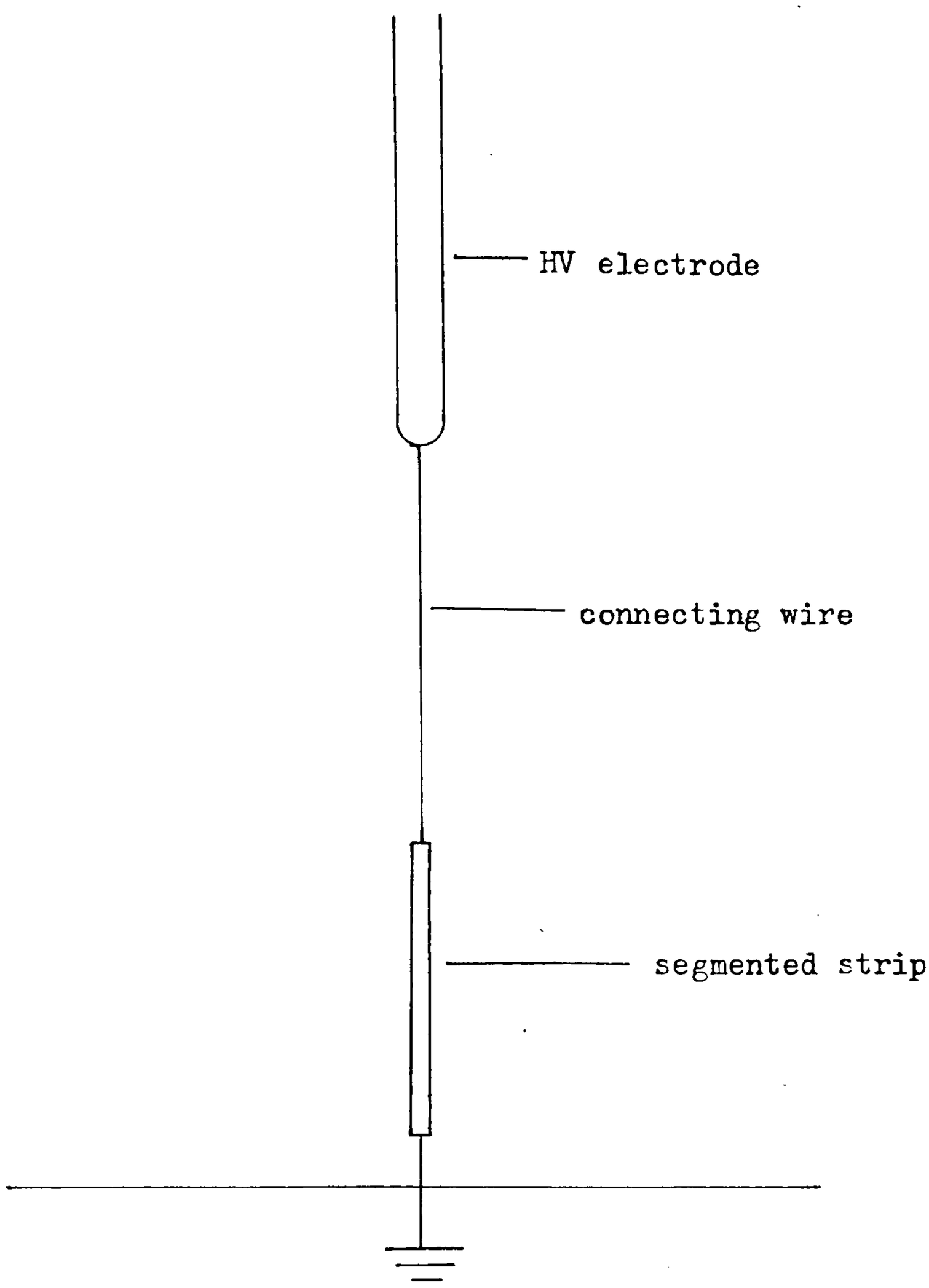

Fig. 5.5 Experimental arrangement.

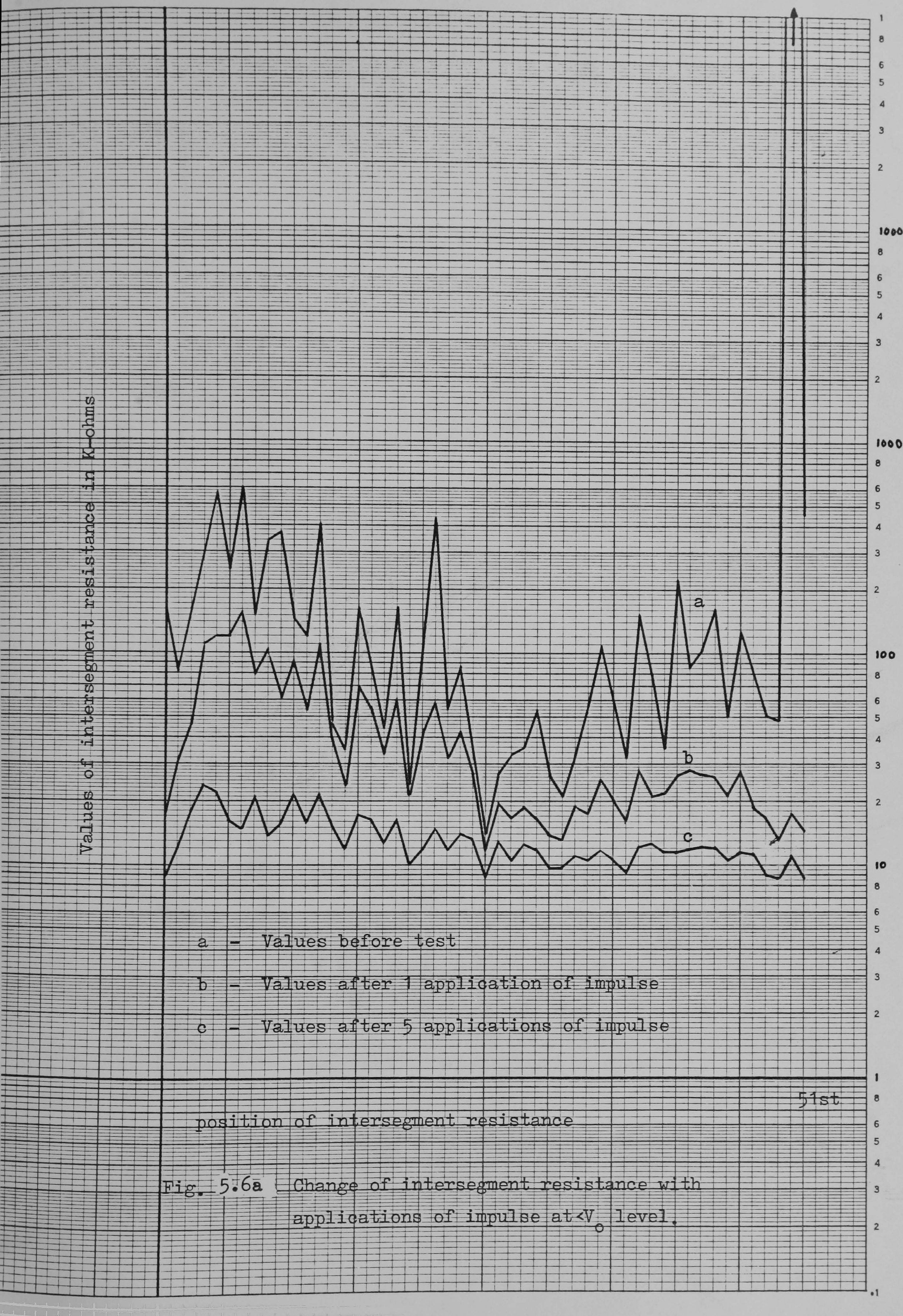

Fig. 5.6a Change of intersegment resistance with applications of impulse at $<V_o$ level.

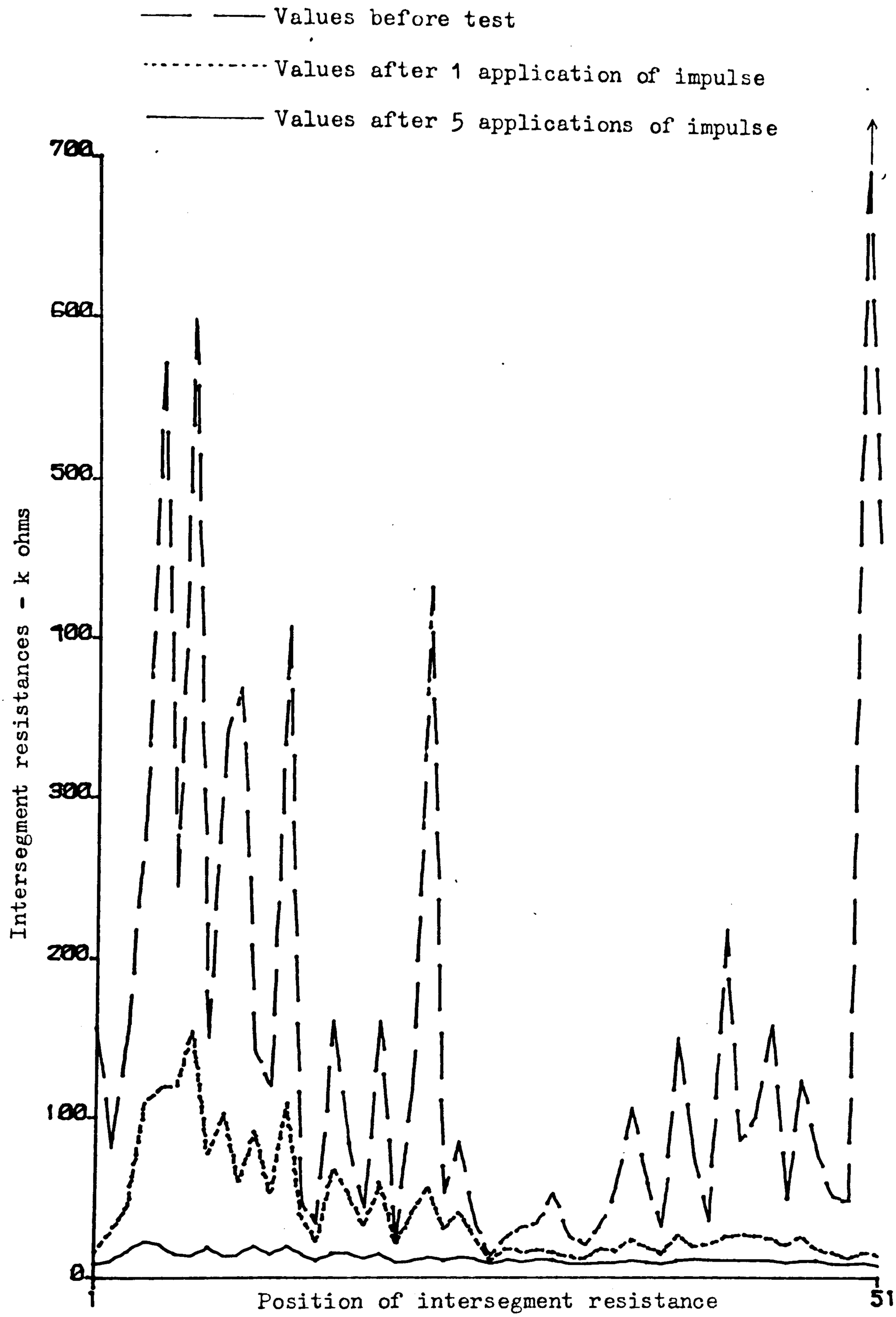

Fig. 5.6b Change of intersegment resistance with applications of impulse voltages at a level below V_0.

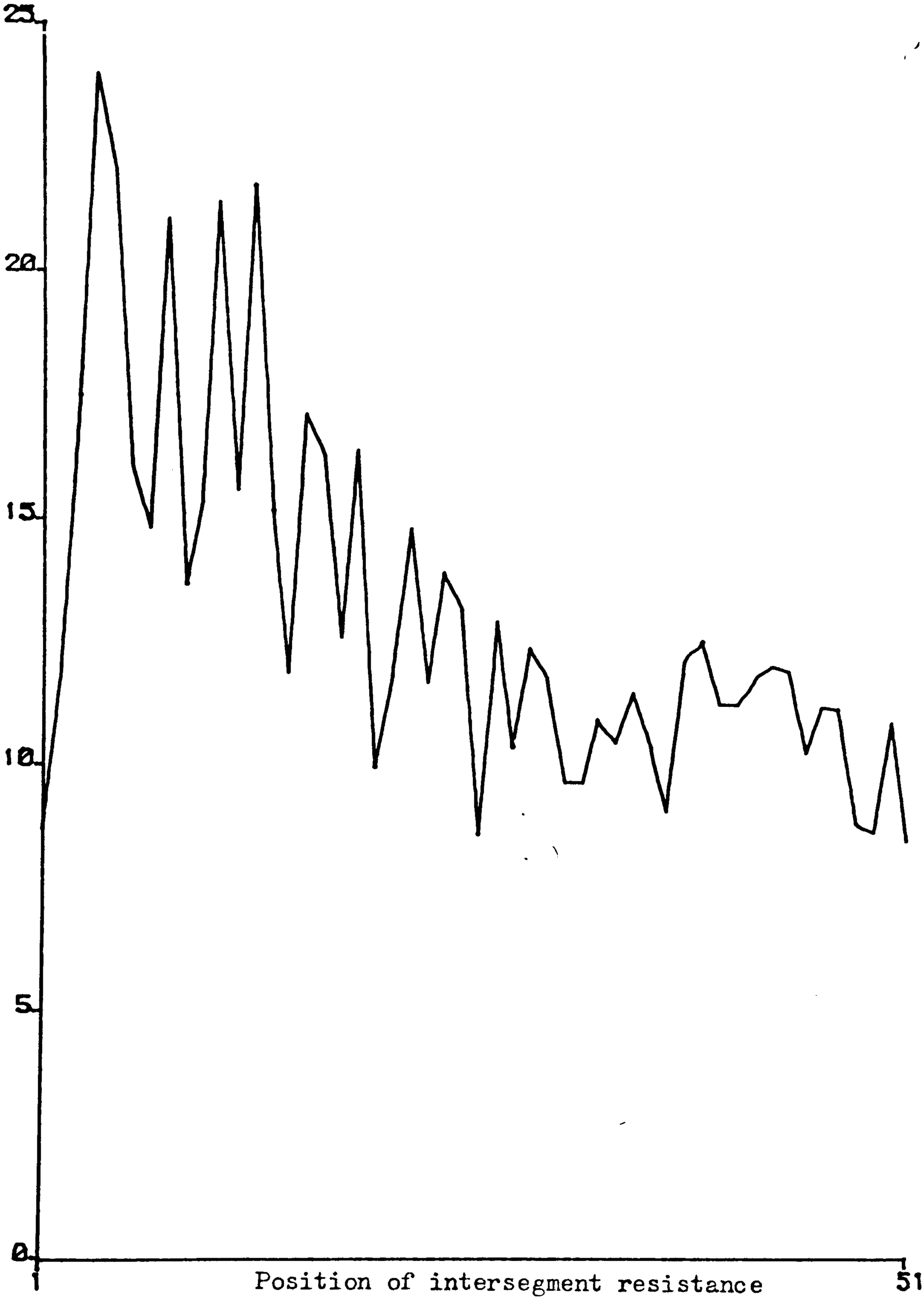

Fig. 5.6c Intersegment resistances, after 5 voltage applications (solid line curve in fig. 5.6b).

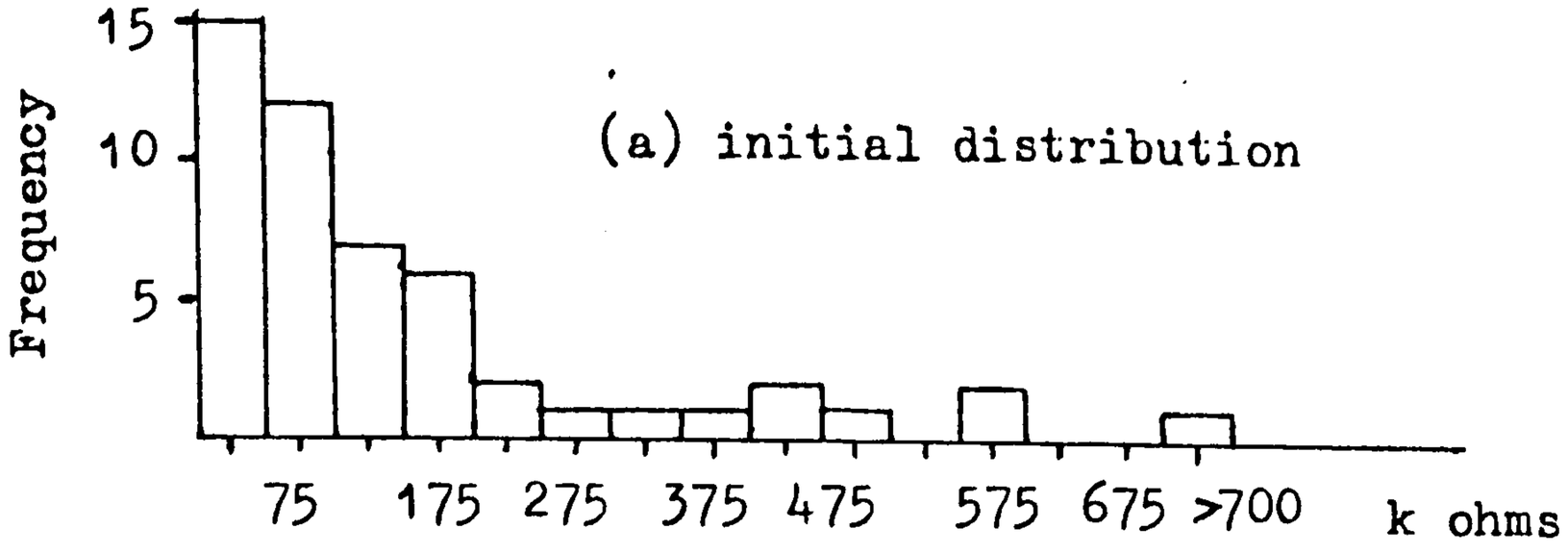

(a) initial distribution

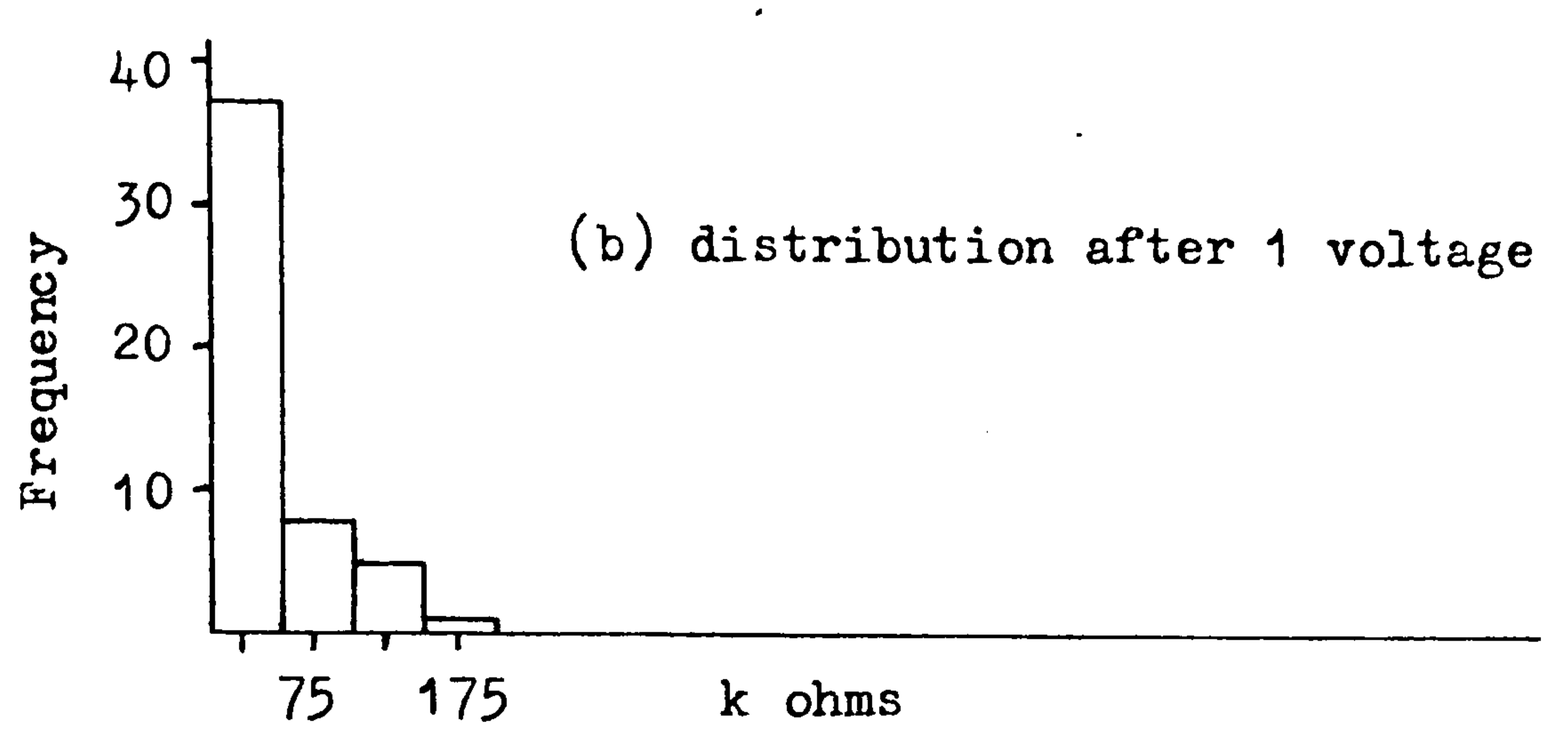

(b) distribution after 1 voltage impulse

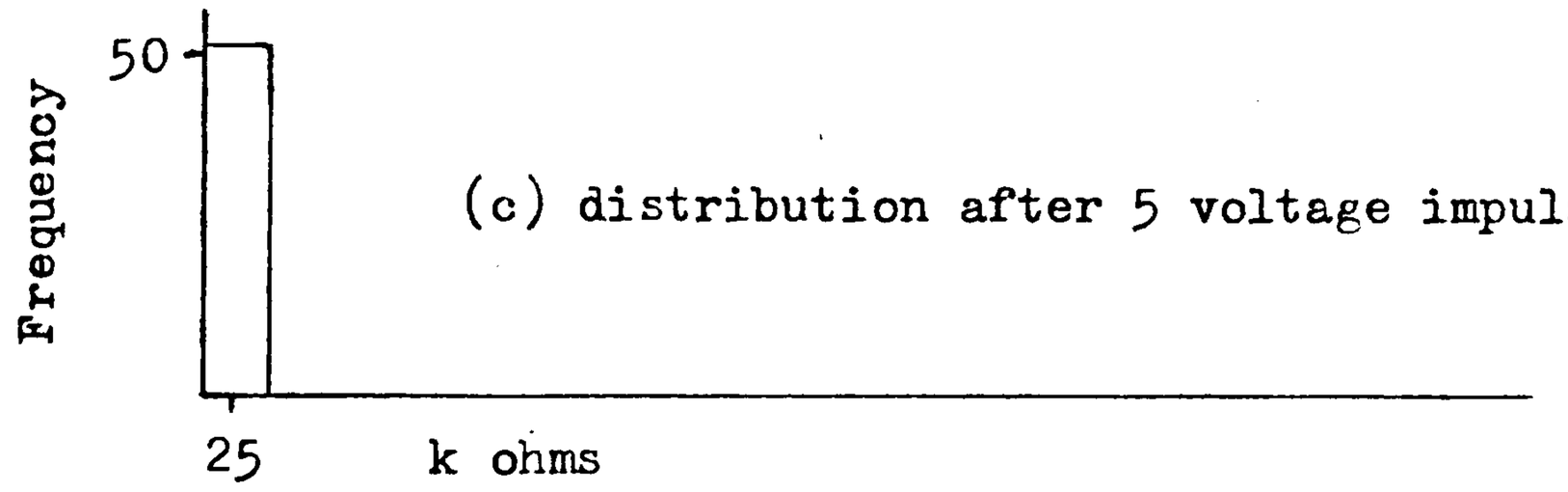

(c) distribution after 5 voltage impulses

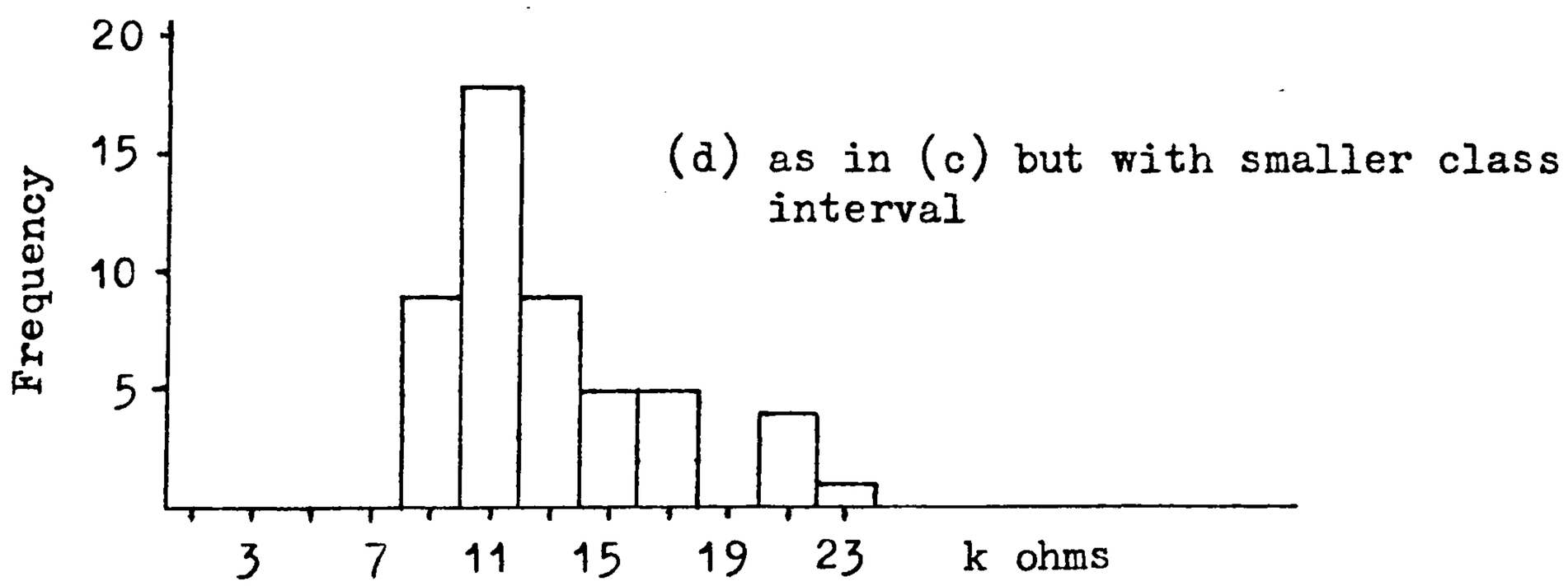

(d) as in (c) but with smaller class interval

Fig. 5.6d Effect of applied voltage impulses at levels below V_0 on intersegment resistance distribution.

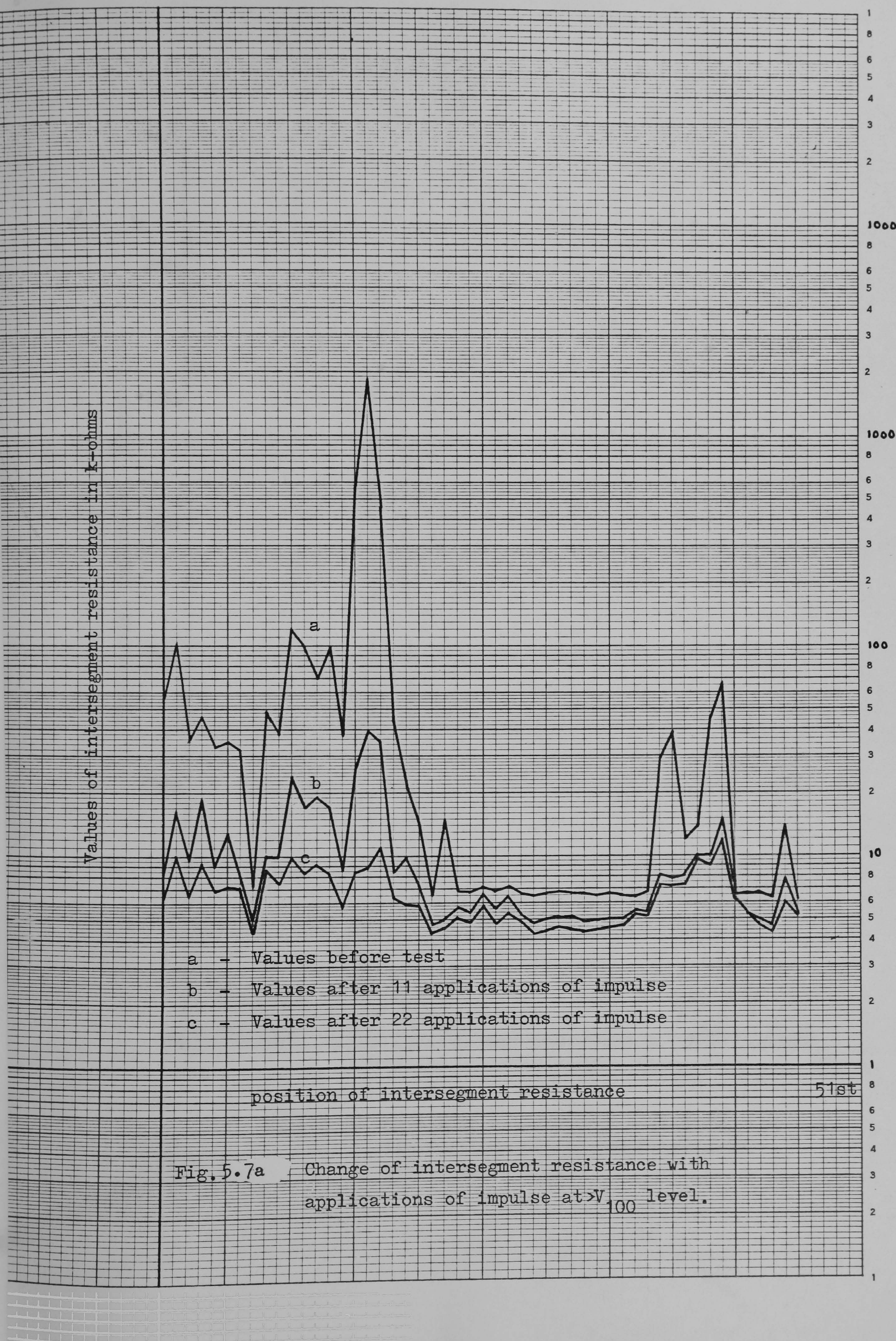

Fig. 5.7a Change of intersegment resistance with applications of impulse at $>V_{100}$ level.

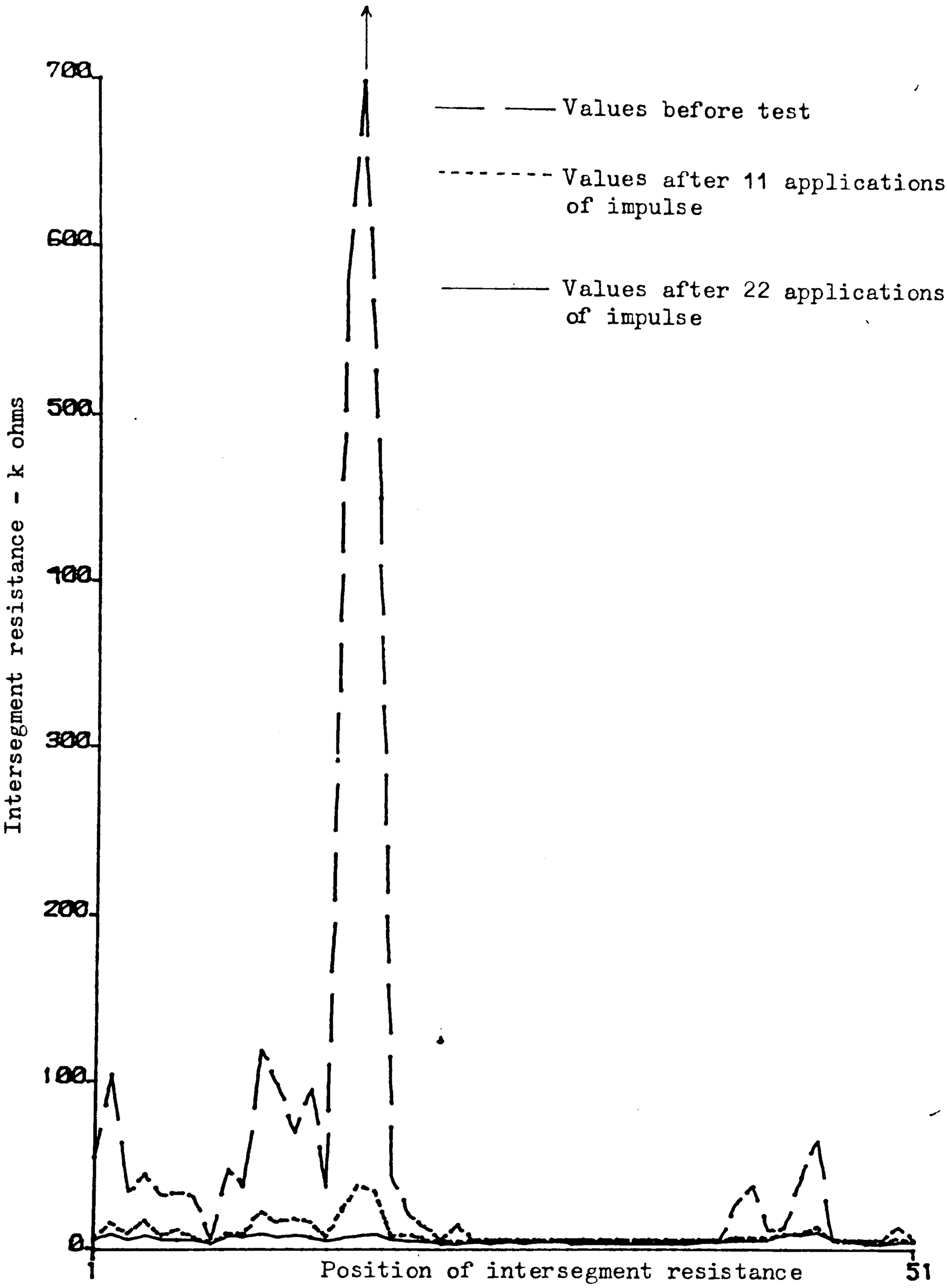

Fig. 5.7b Change of intersegment resistance with applications of impulse at voltage levels above V_{100} .

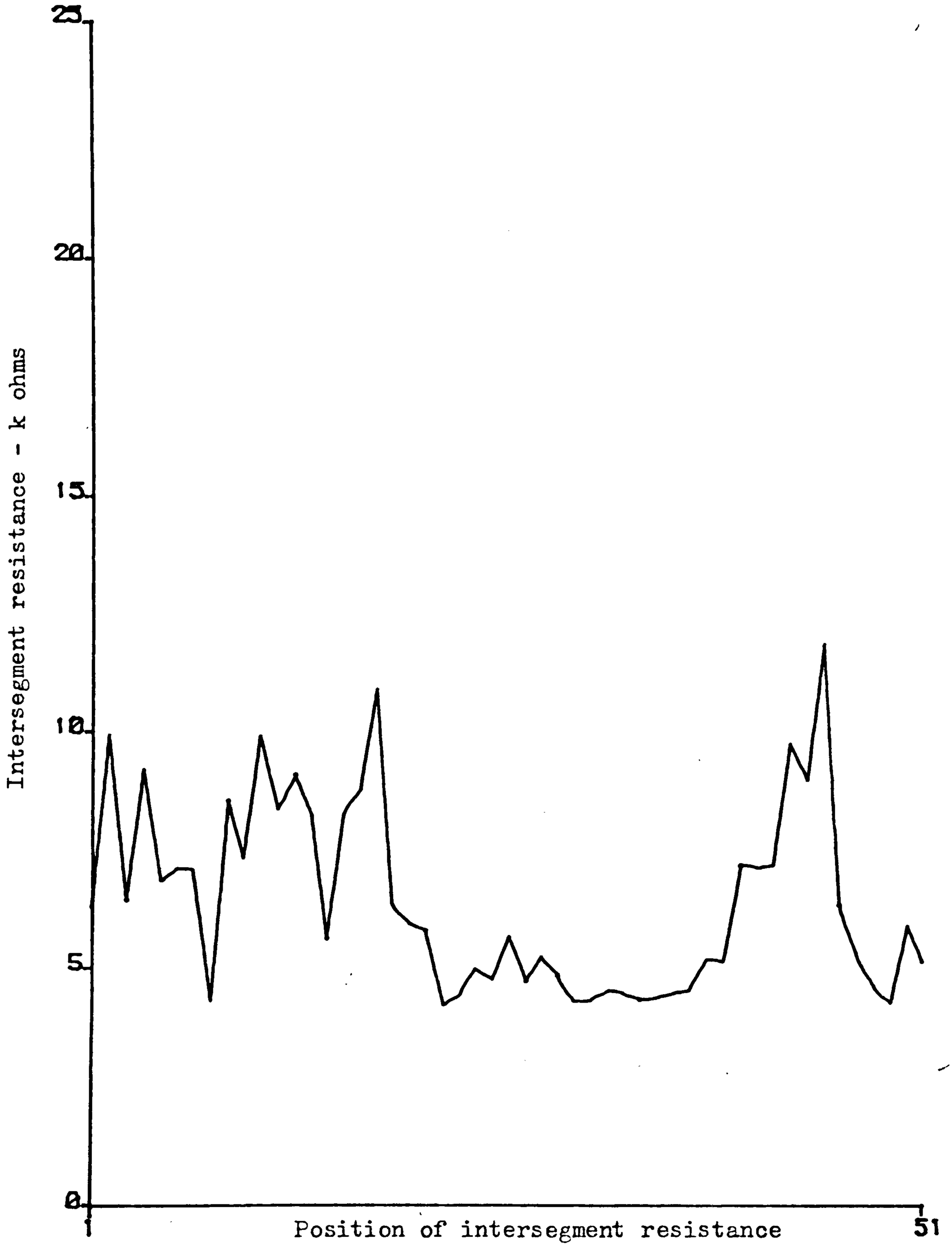

Fig. 5.7c Intersegment resistances after 22 voltage applications (solid line curve in fig. 5.7b).

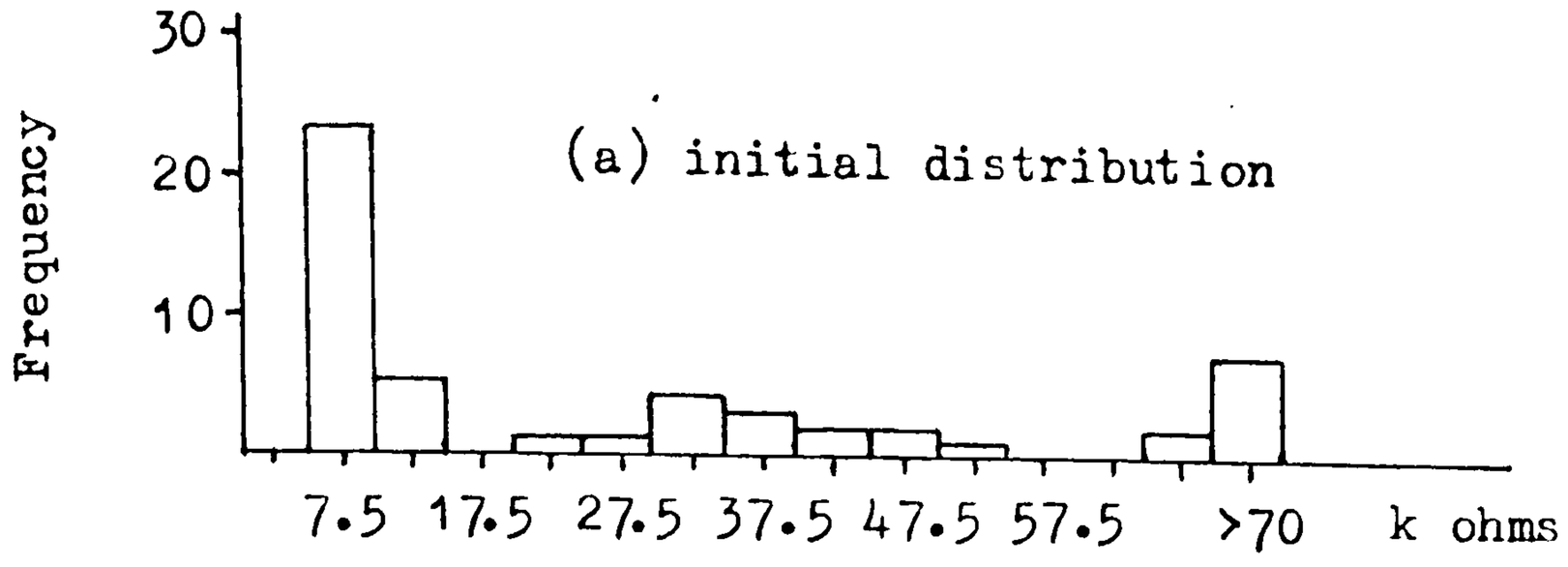

(a) initial distribution

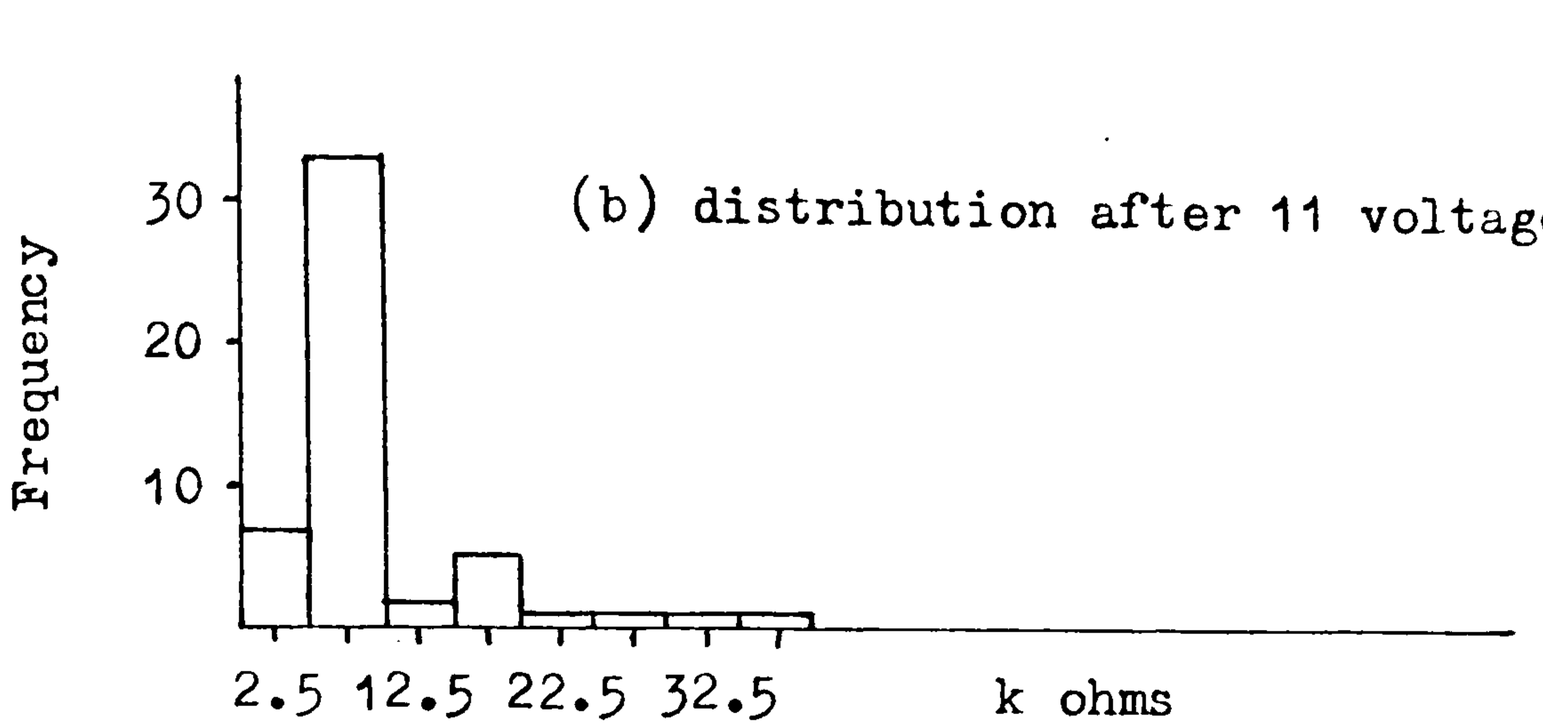

(b) distribution after 11 voltage impulses

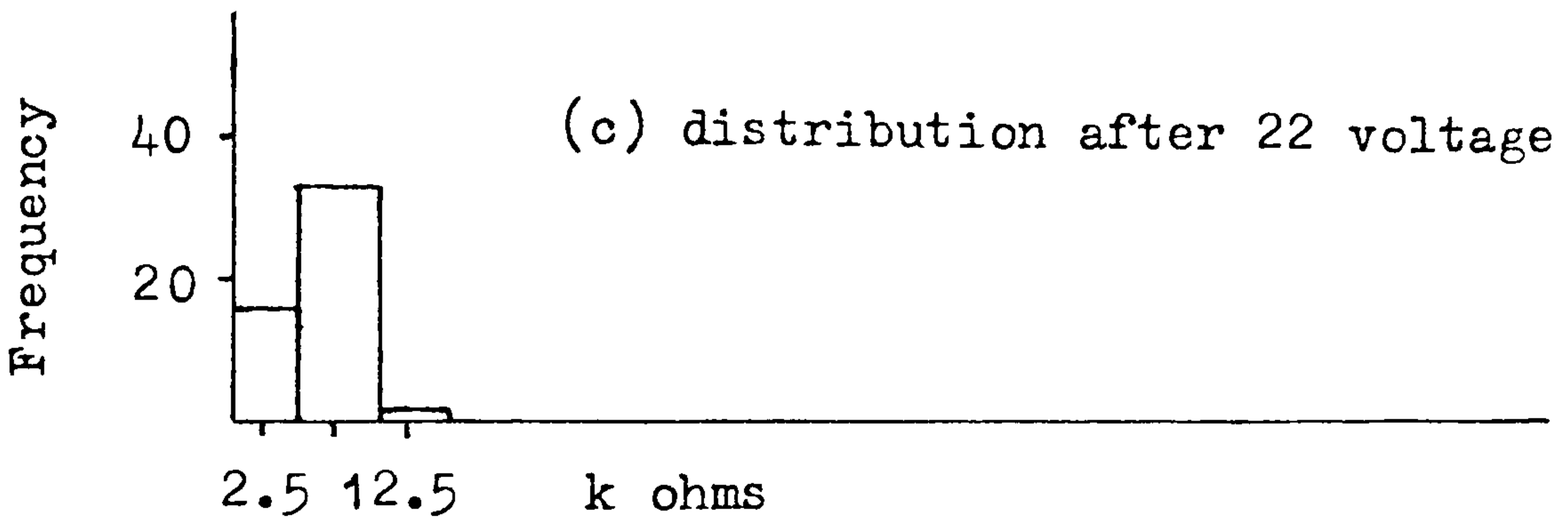

(c) distribution after 22 voltage impulses

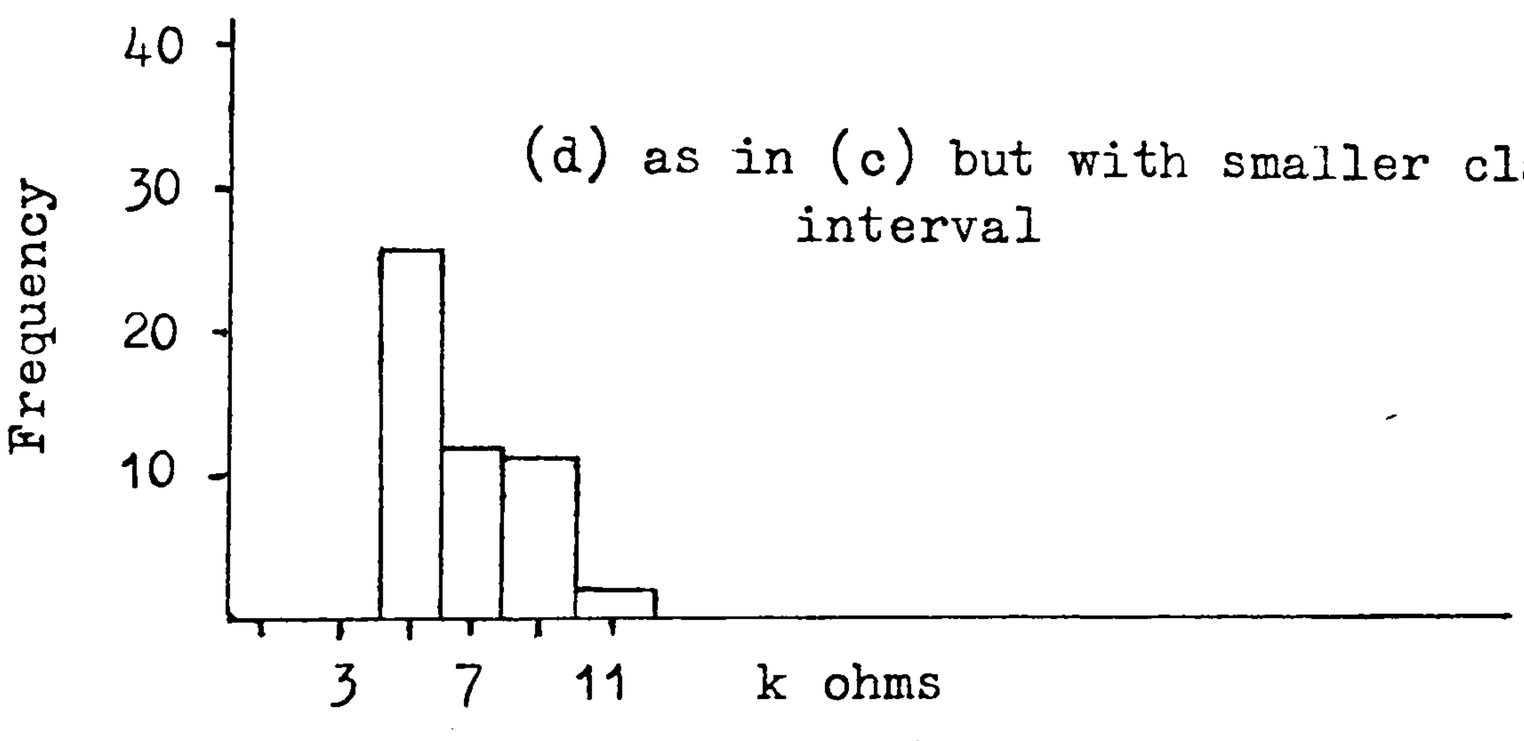

(d) as in (c) but with smaller class interval

Fig. 5.7d Effect of applied voltage impulses at levels above V_{100} on intersegment resistances.

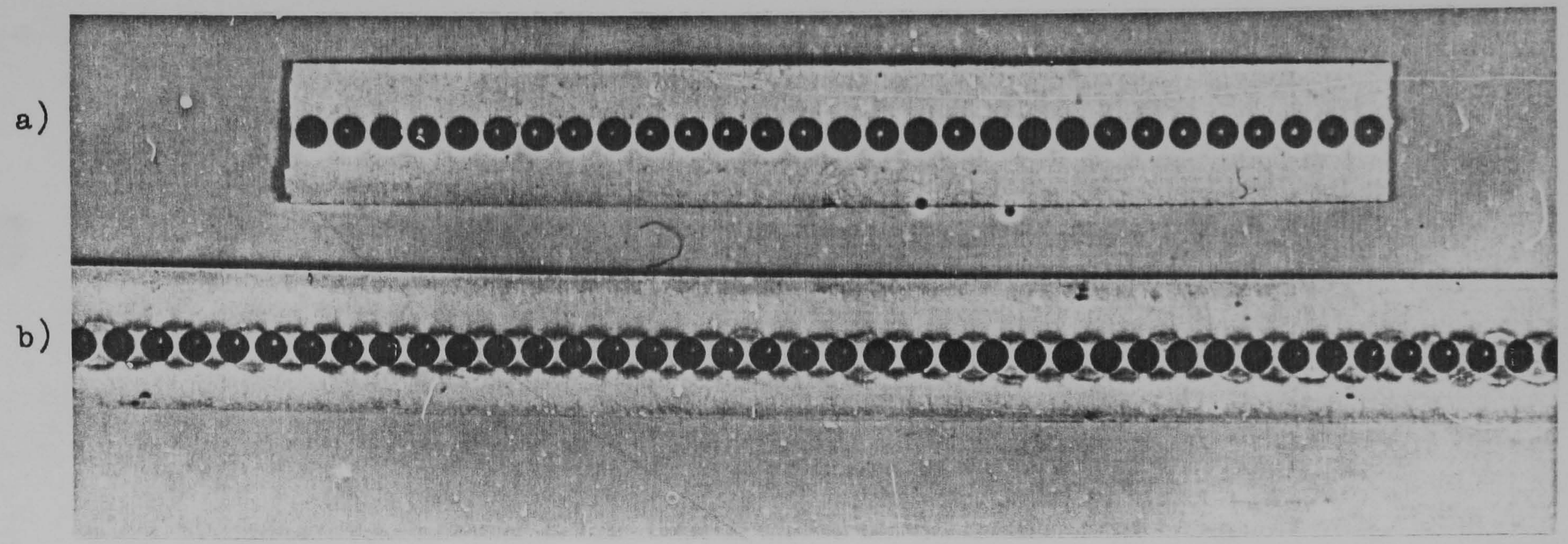

Fig. 5.8 Front view of segmented strips
a) a new strip
b) a used strip (not the strip shown in (a))

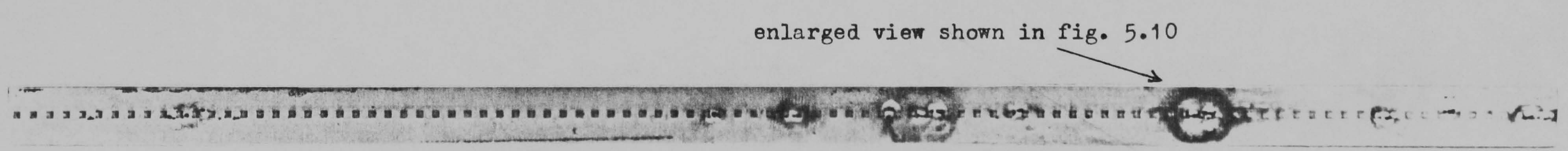

Fig. 5.9 Rear view of a section of a damaged segmented strip

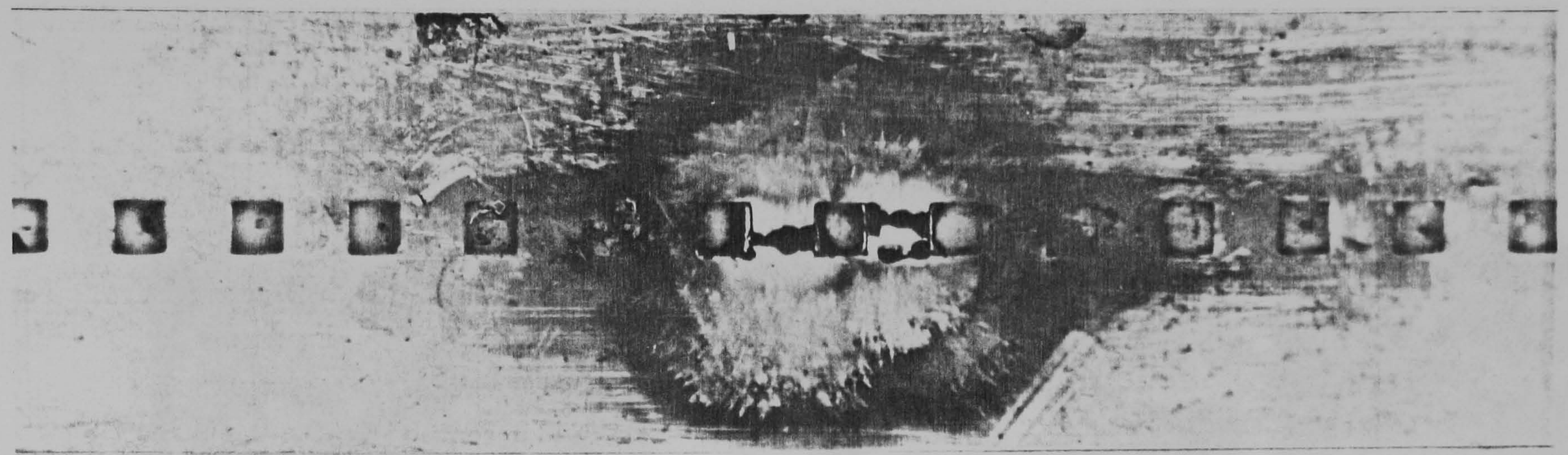

Fig. 5.10 Enlarged view of the damaged area indicated in fig. 5.9

Fig. 5.11 Rear view of a second damaged segmented strip

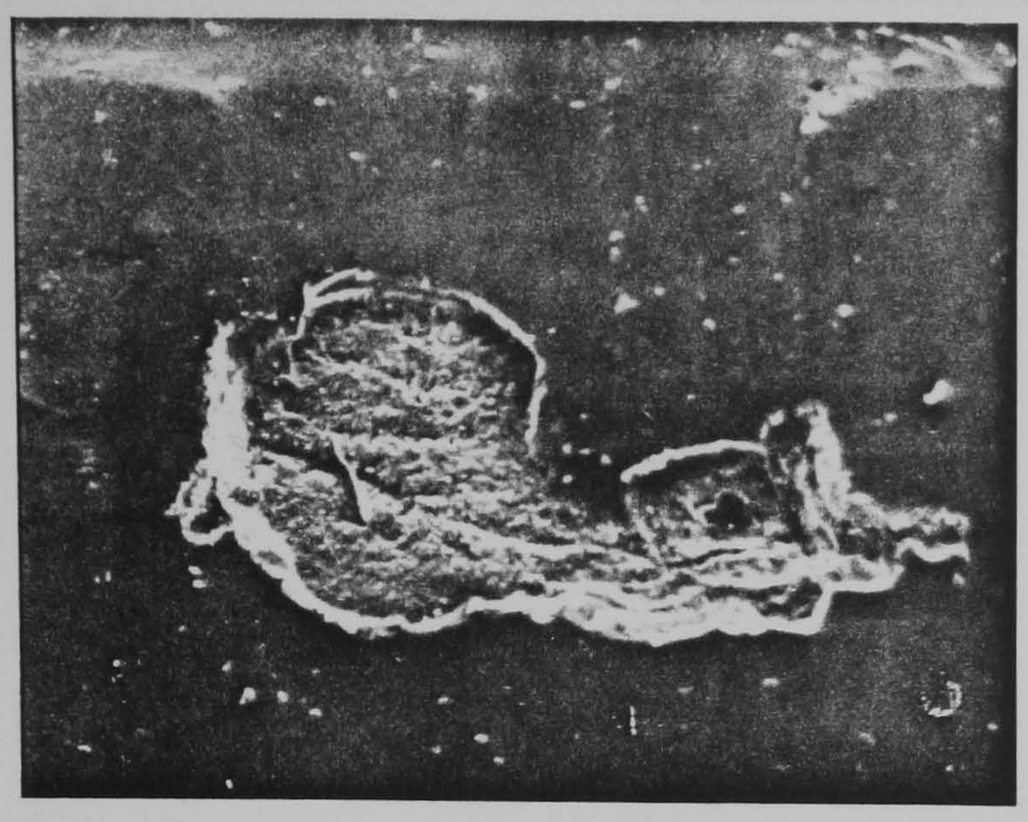

Magnification 40X

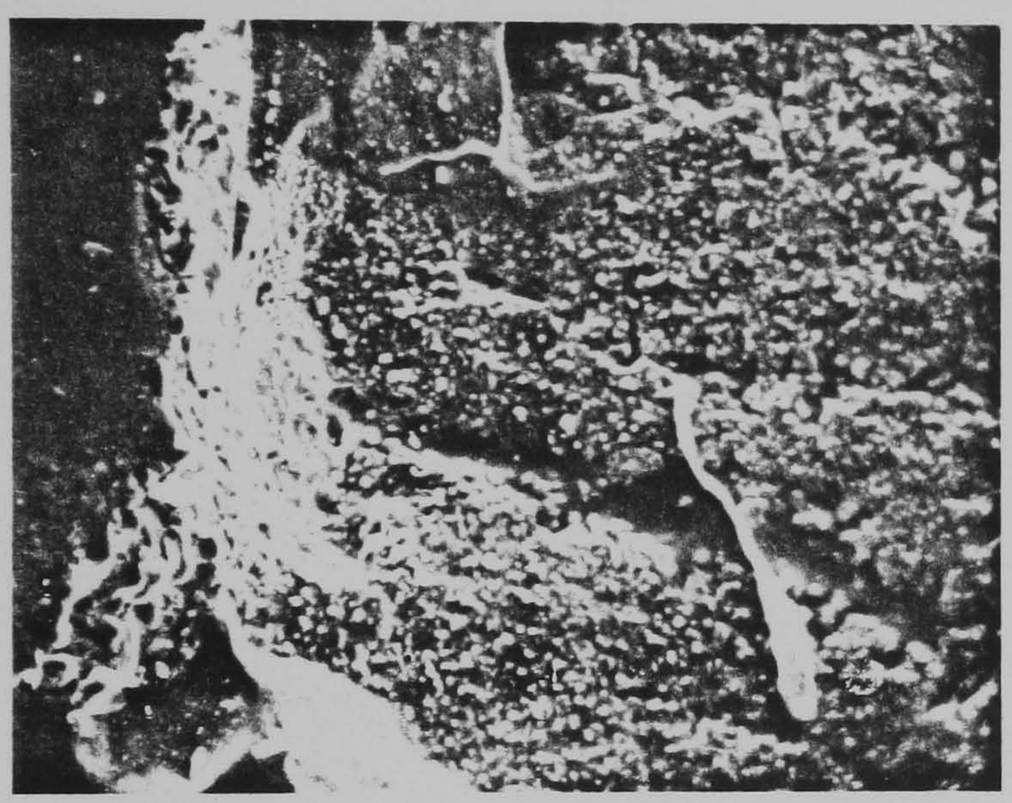

Magnification 160X

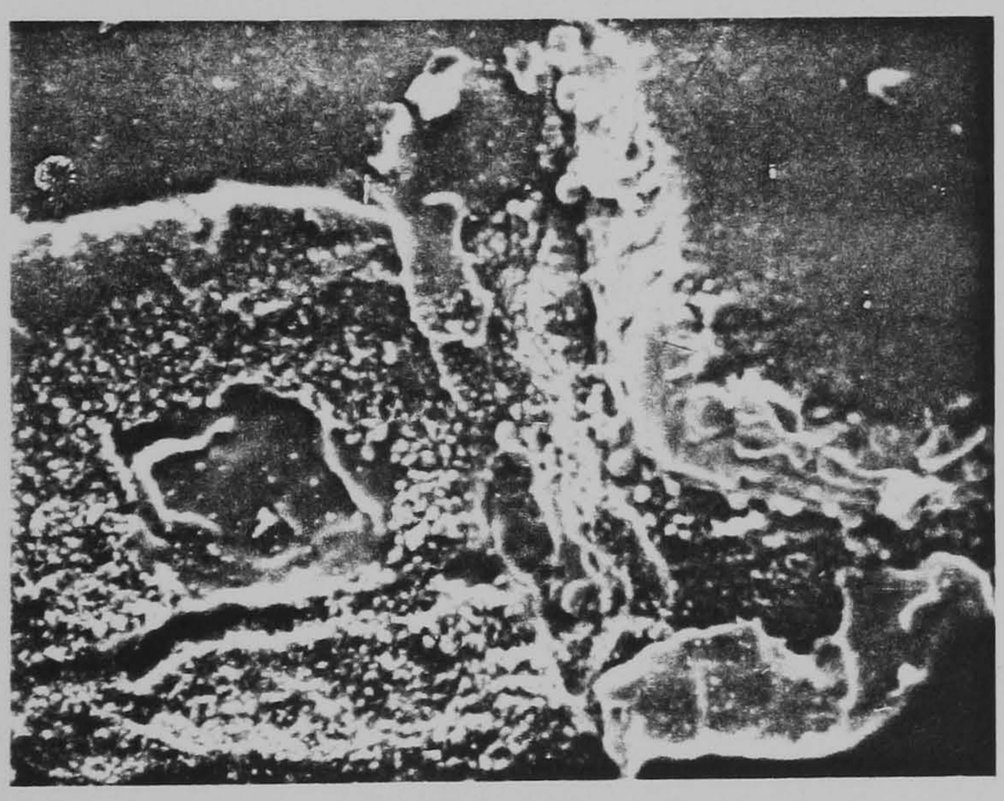

Magnification 160X

Fig. 5.12 Scanning electron microscope photographs of a damaged intersegment surface

Fig. 5.13 Scanning electron microscope photographs of front surface of a new segmented strip.

a) photograph of intersegment surface shown with 100-micron markers

b) photograph of conducting segment shown with 100-micron markers

Fig. 5.14 Scanning electron microscope photographs of front surface of a used segmented strip.

a) photograph of intersegment surface shown with 100-micron markers

b) photograph of left portion of (a) and shown with 10-micron markers

c) photograph of right portion of (a) and shown with 10-micron markers

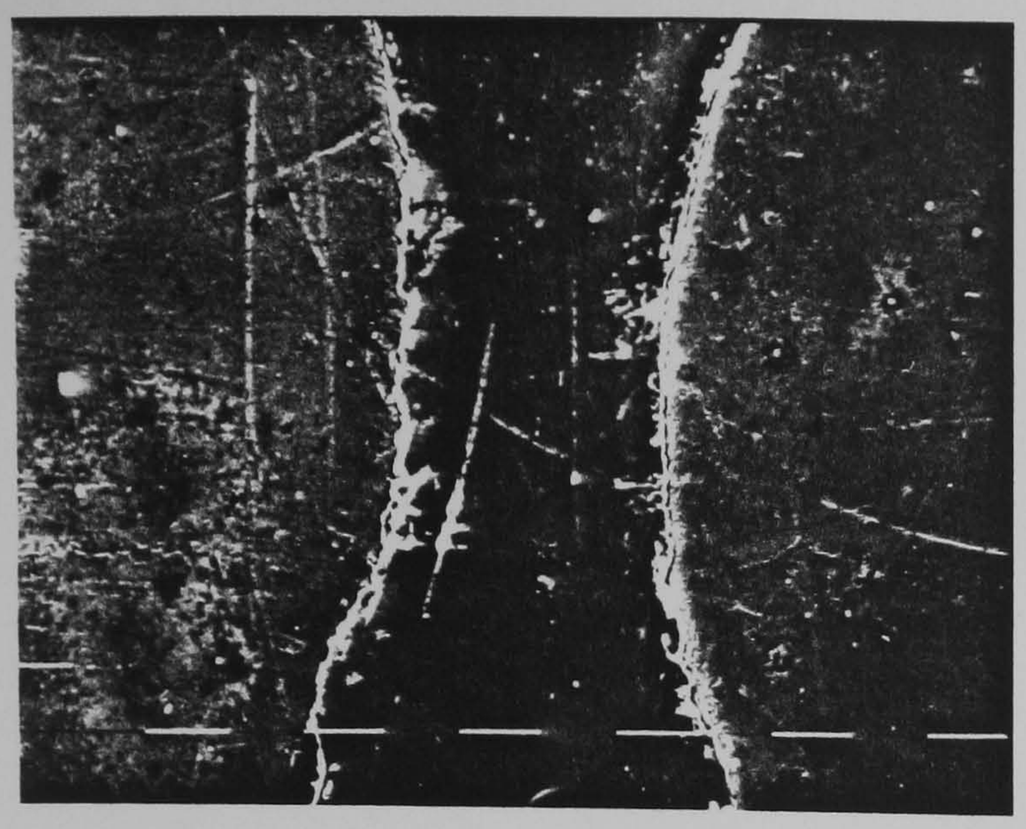

(a)

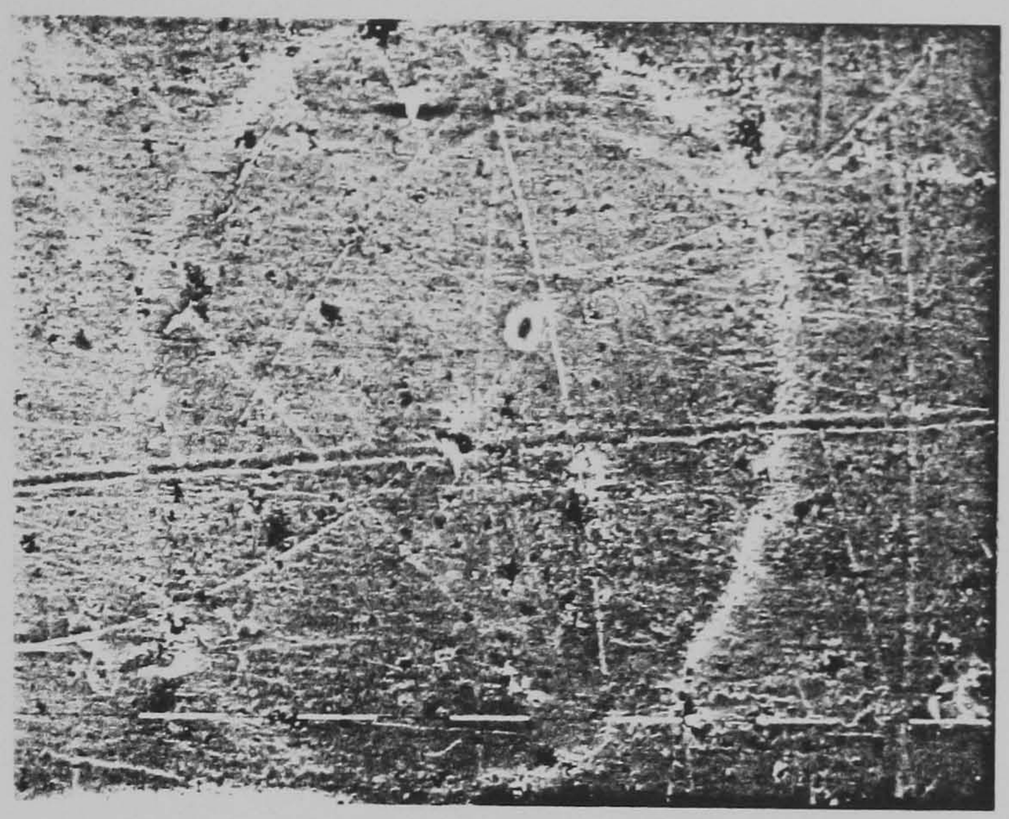

(b)

Fig. 5.13

(a)

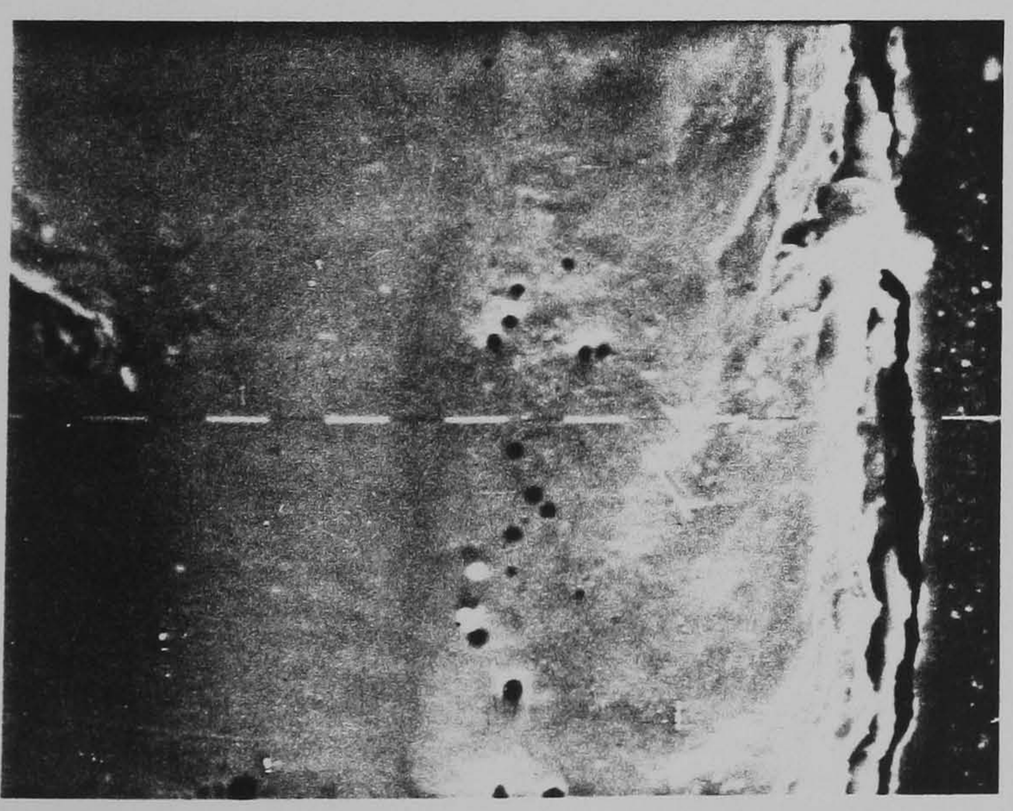

(b)

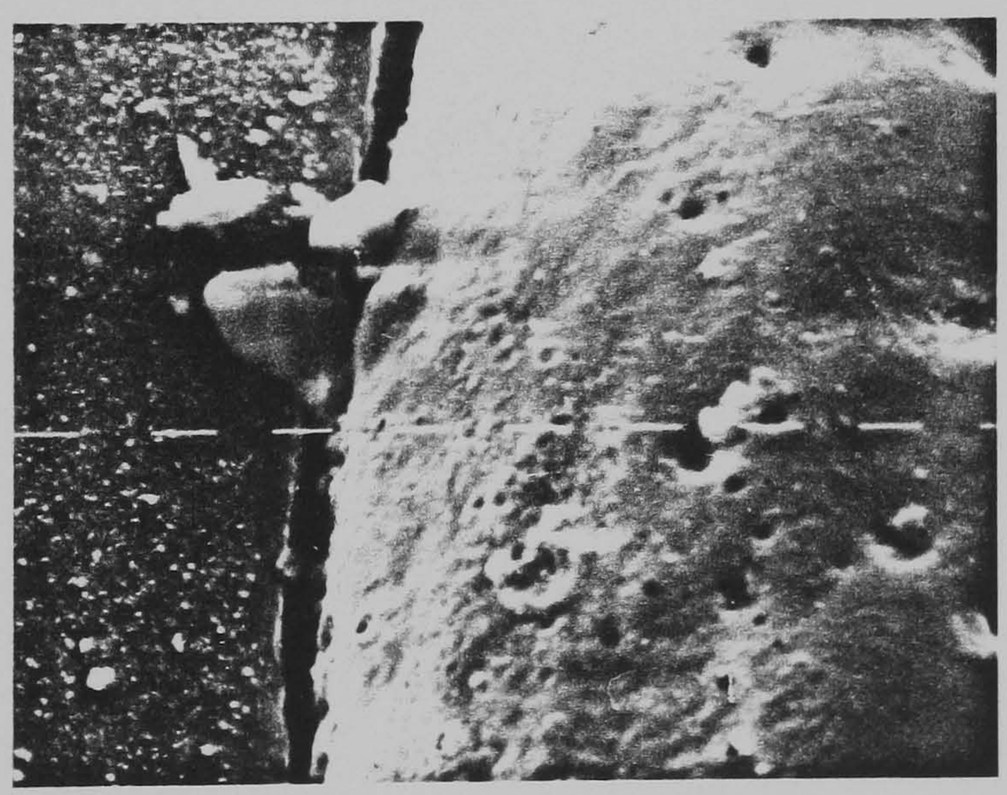

(c)

Fig. 5.14

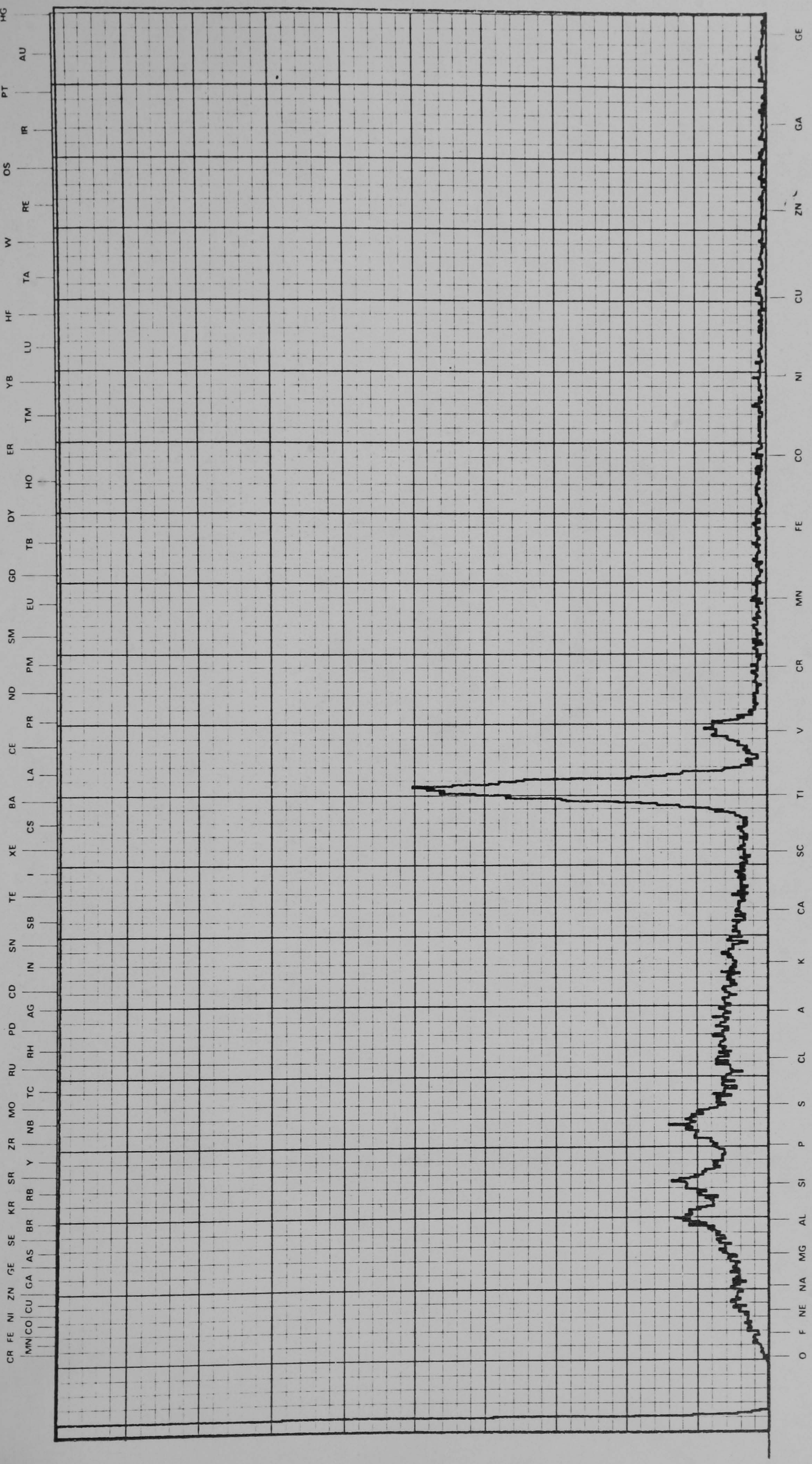

Fig. 5.15 X-ray analysis of 'carbon' deposit on front surface of segmented strip.

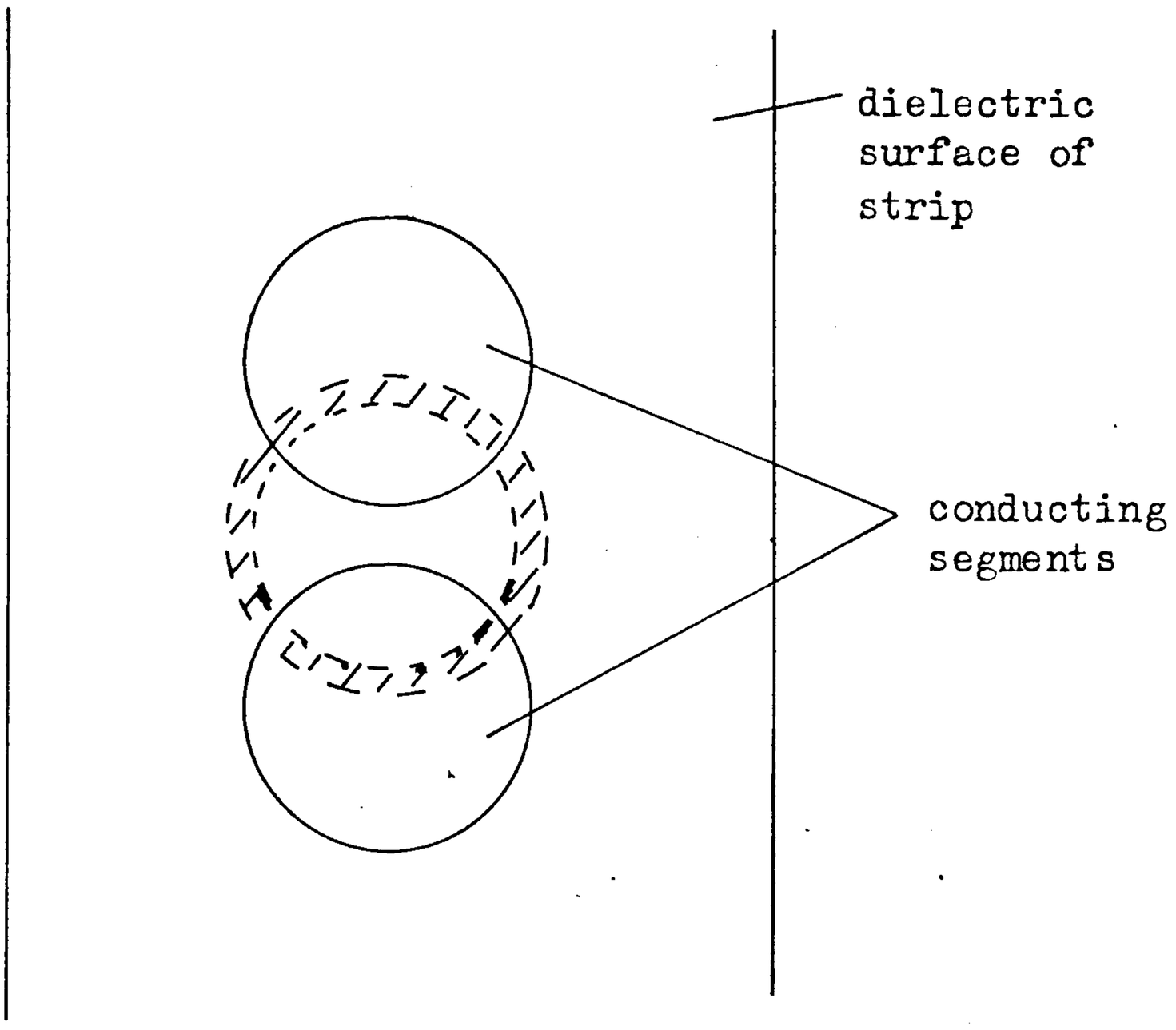

▨ - 'carbon' deposit

Fig. 5.16 Location of 'carbon' deposit on strip surface.

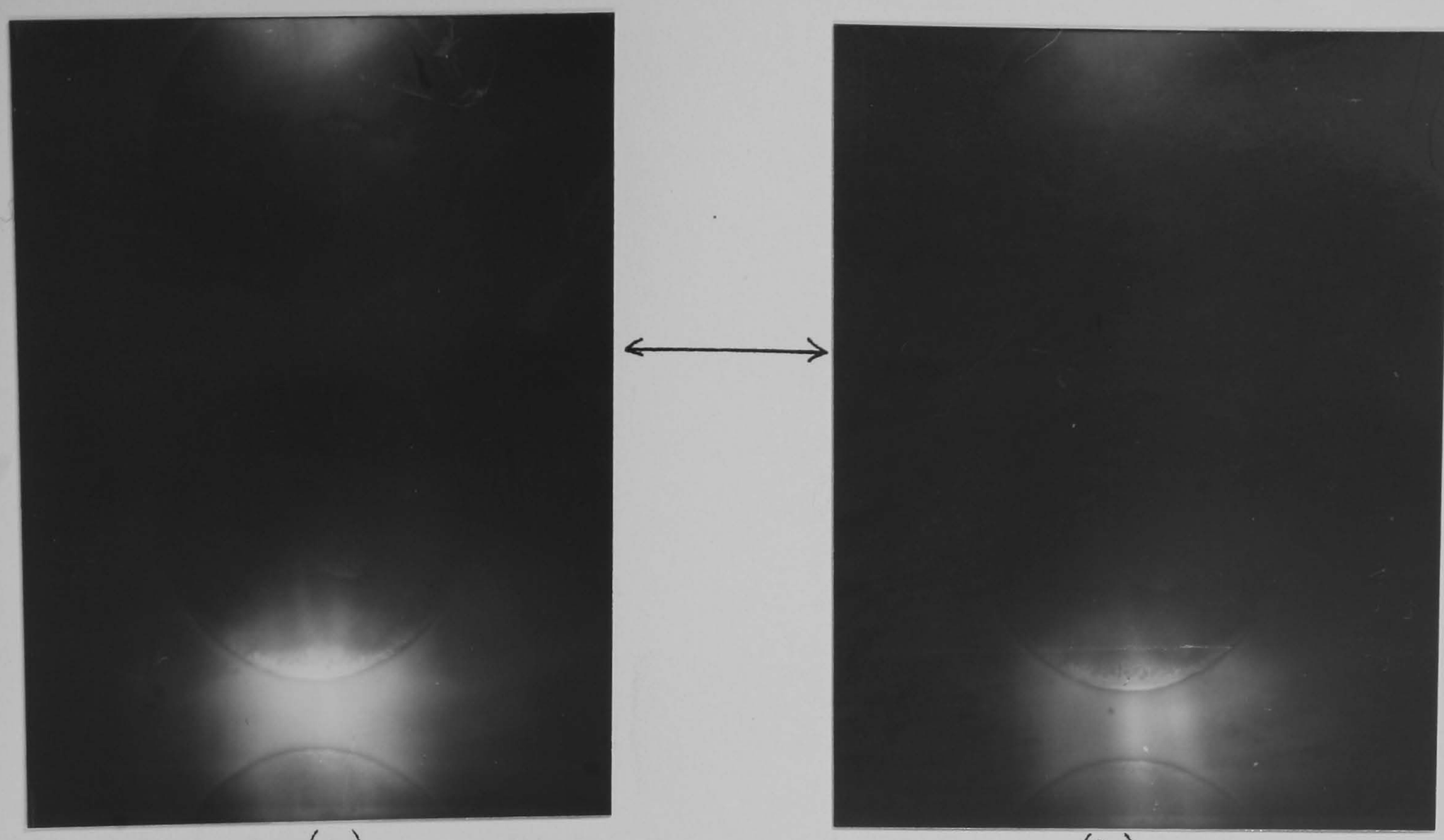

(a) (b)

Arrow shows gap where rear surface was damaged

Fig. 5.17 a) Front view of strip showing flashover between two segments
b) Front view of strip showing flashover between the same segments as in (a) but having 2 cores in the discharge

Fig. 5.18a Side view of a strip with intersegment discharges on both surfaces.

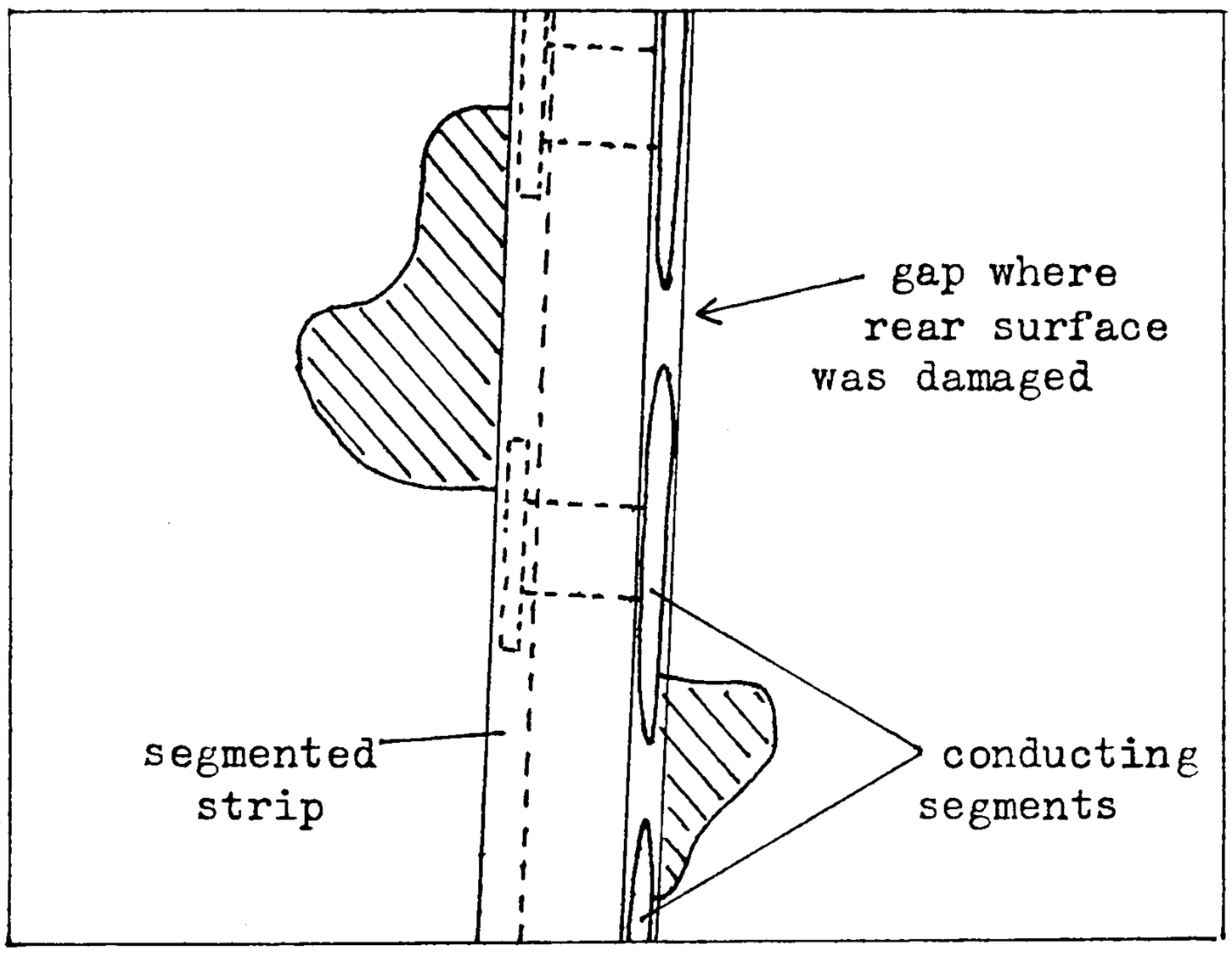

Shaded area shows optical form of the discharge

Fig. 5.18b Sketch corresponding to fig. 5.18a.

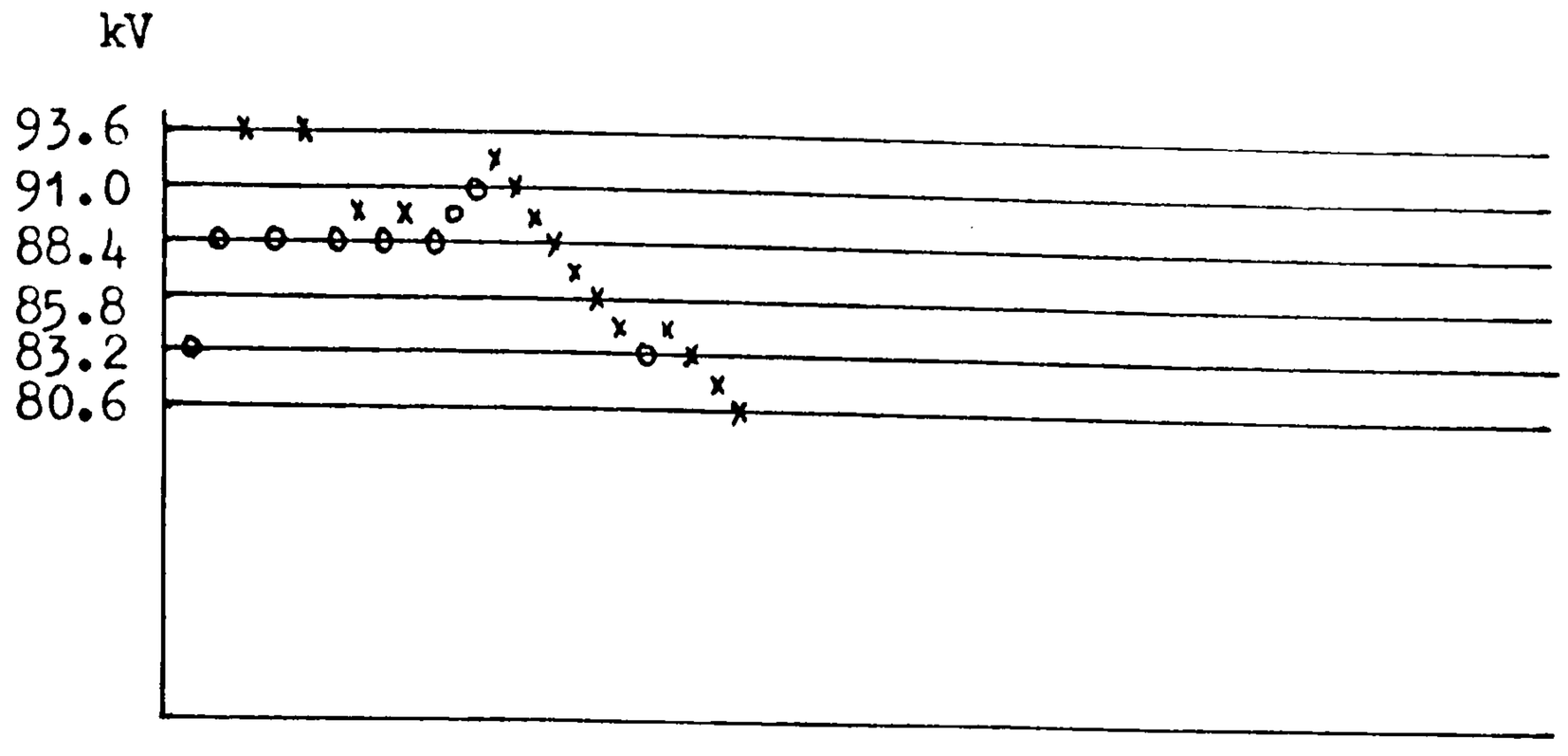

Fig. 5.19 'Up & Down' test results for segmented strip stuck on to perspex with araldite.
Full impulse voltage waves applied

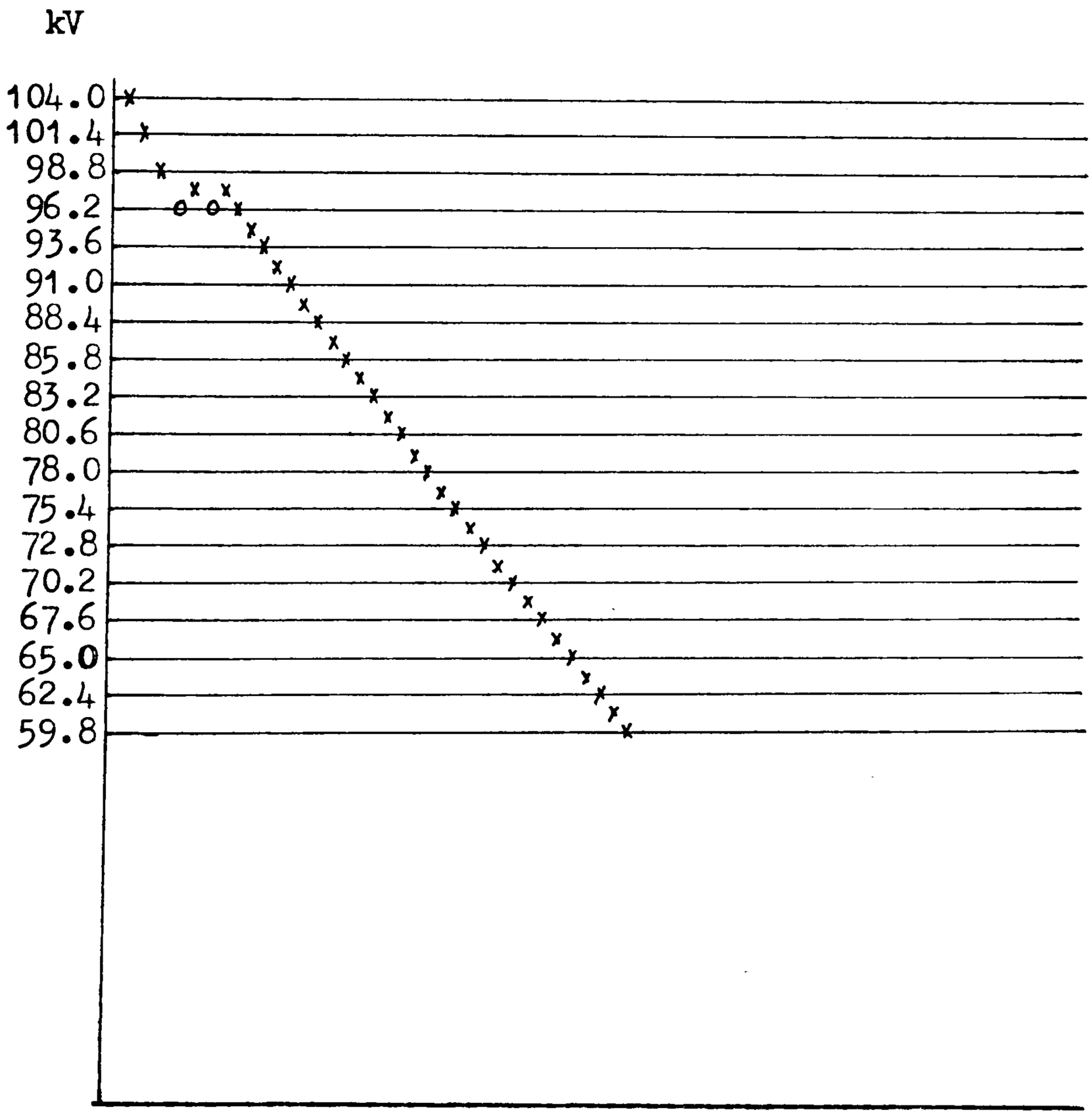

Fig. 5.20 'Up & Down' test results for segmented strip stuck on to perspex with epoxy adhesive.
Full impulse voltage waves applied

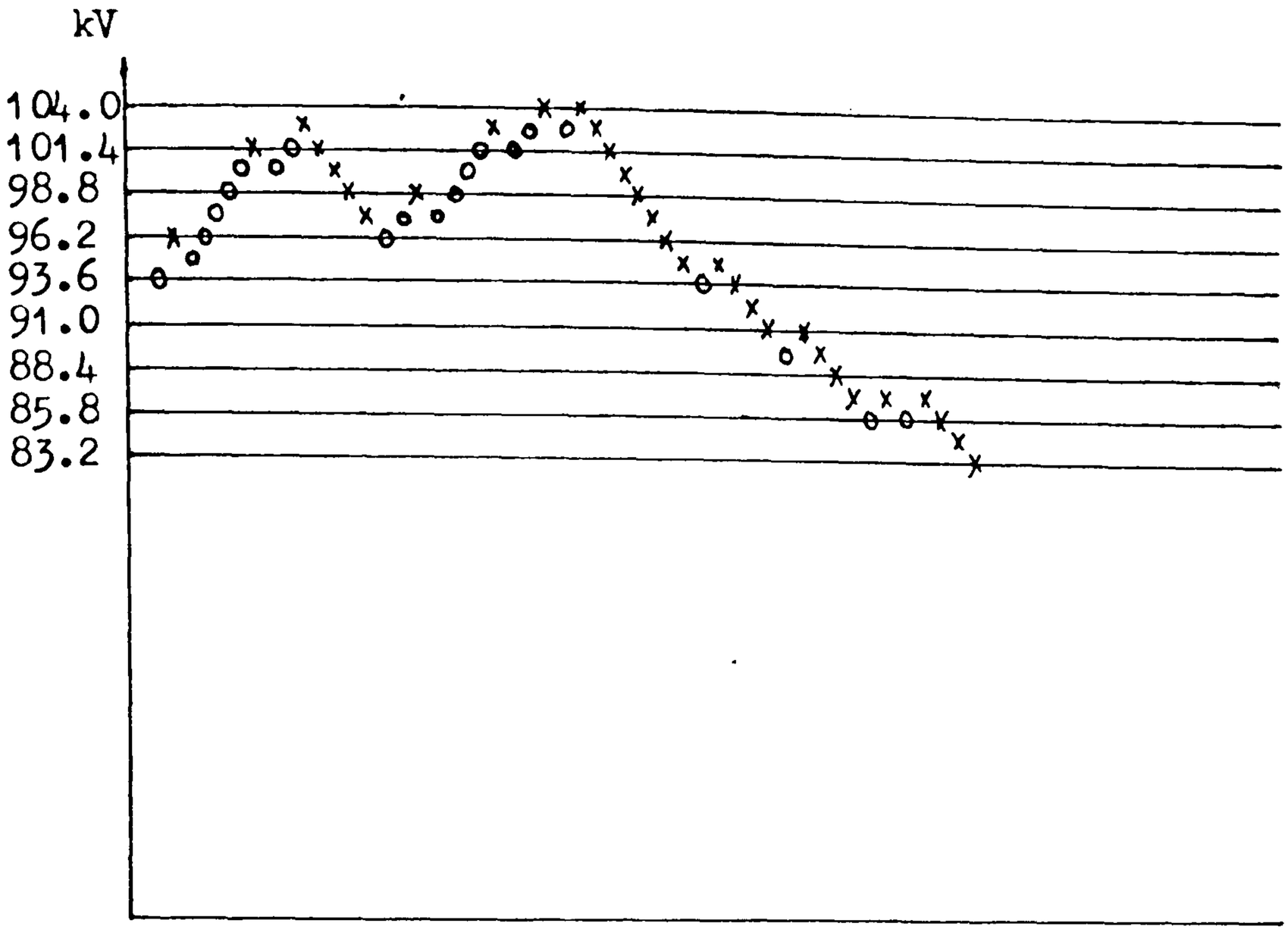

Fig. 5.21 'Up & Down' test results for segmented strip coated on the rear surface with araldite adhesive. Full impulse voltage waves applied

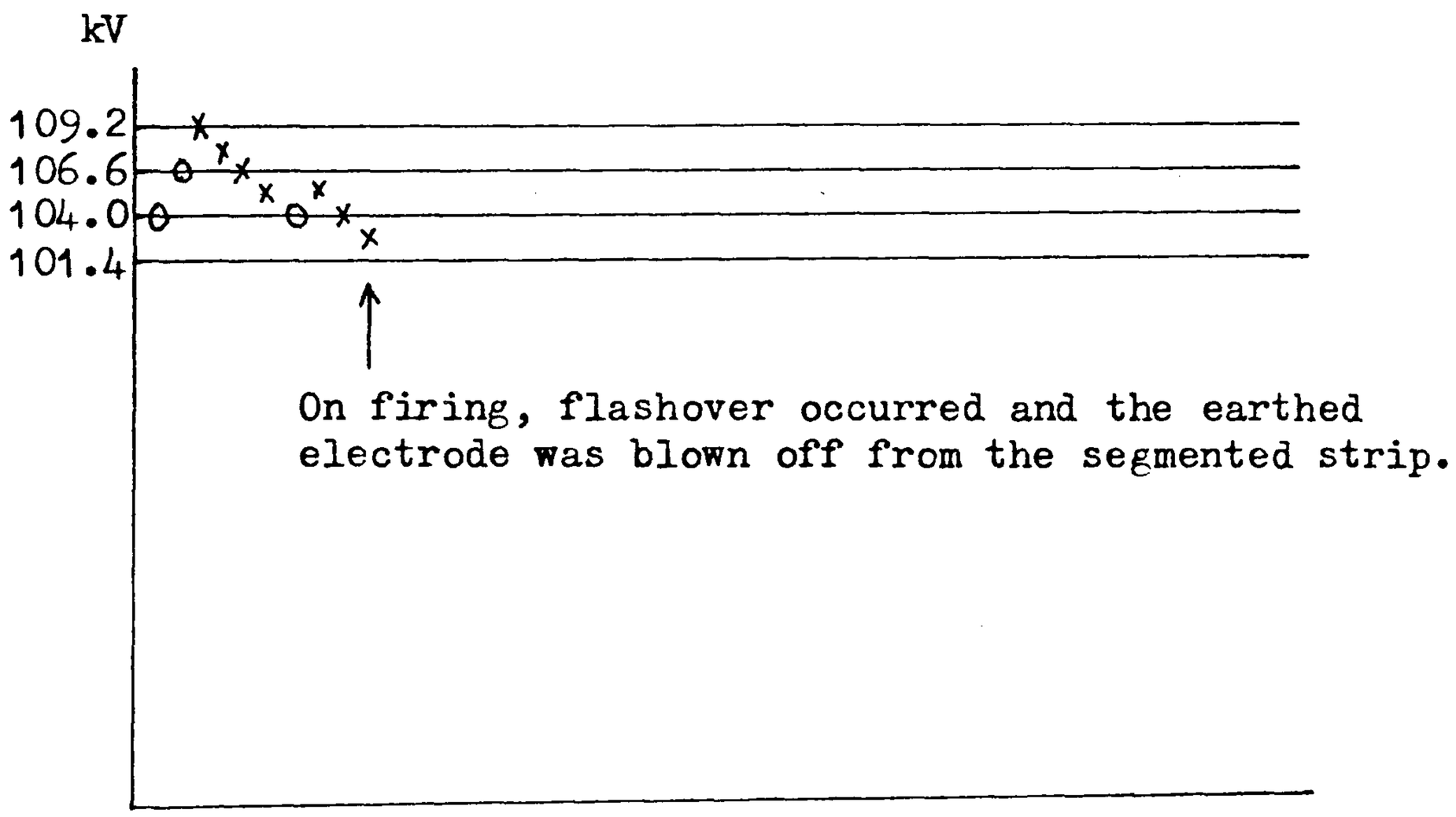

Fig. 5.22 'Up & Down' test results for segmented strip coated on the rear surface with epoxy adhesive. Full impulse voltage waves applied

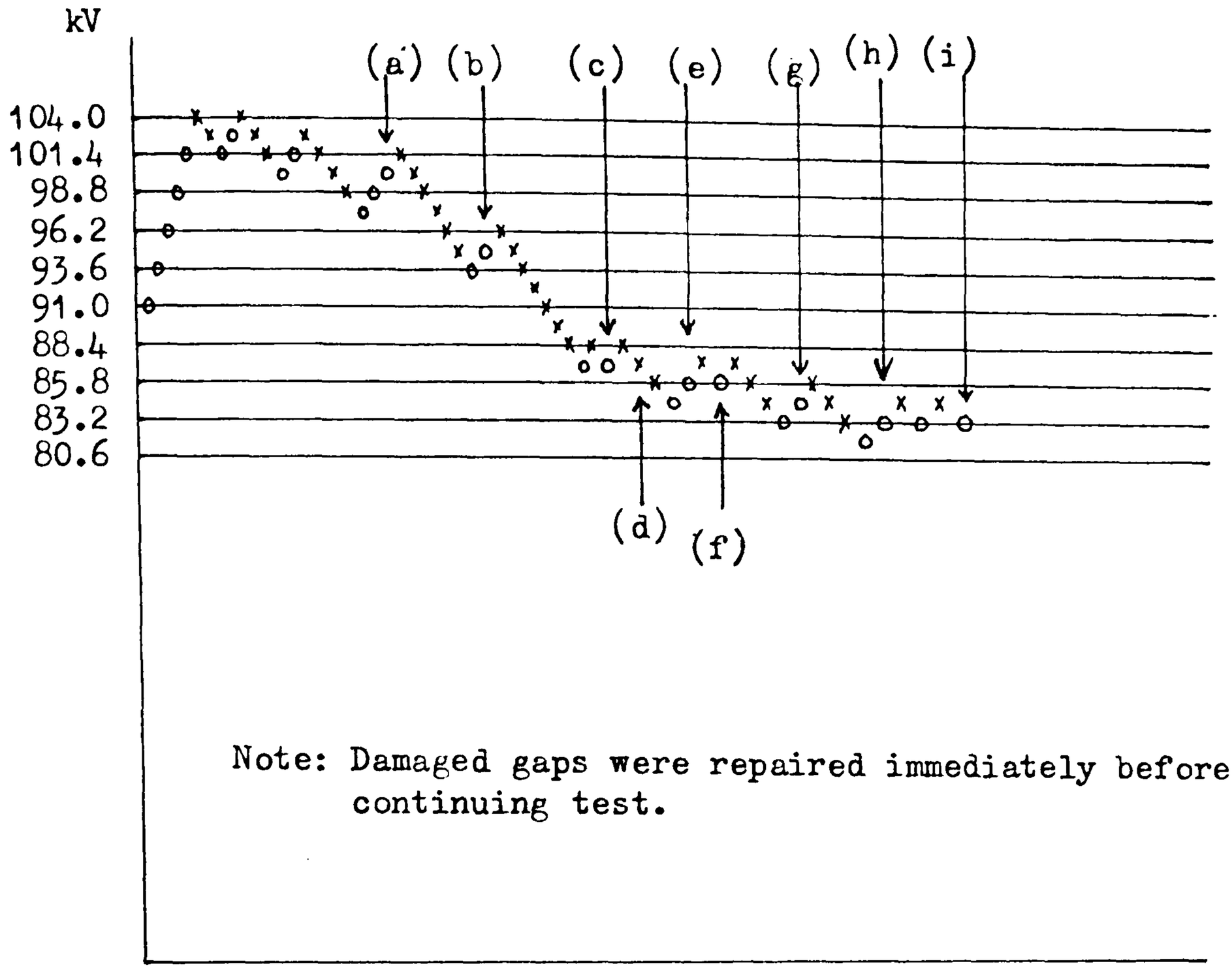

Note: Damaged gaps were repaired immediately before continuing test.

Observations at

(a) Orange spark and 1 intersegment gap was damaged.

(b) Orange spark and 2 additional gaps were damaged.

(c) Orange spark and 3 additional gaps were damaged.

(d) White spark and 1 additional gap was damaged.

(e) Orange spark and 2 additional gaps were damaged.

(f) Orange spark and 1 additional gap was damaged.

(g) Orange spark and 1 additional gap was damaged.

(h) Orange spark and 5 additional gaps were damaged.

(i) Orange spark and 3 additional gaps were damaged.

Fig. 5.23 'Up & Down' test results for segmented strip when damaged intersegment gaps were 'repaired' immediately with silicon grease.
Full impulse voltage waves applied

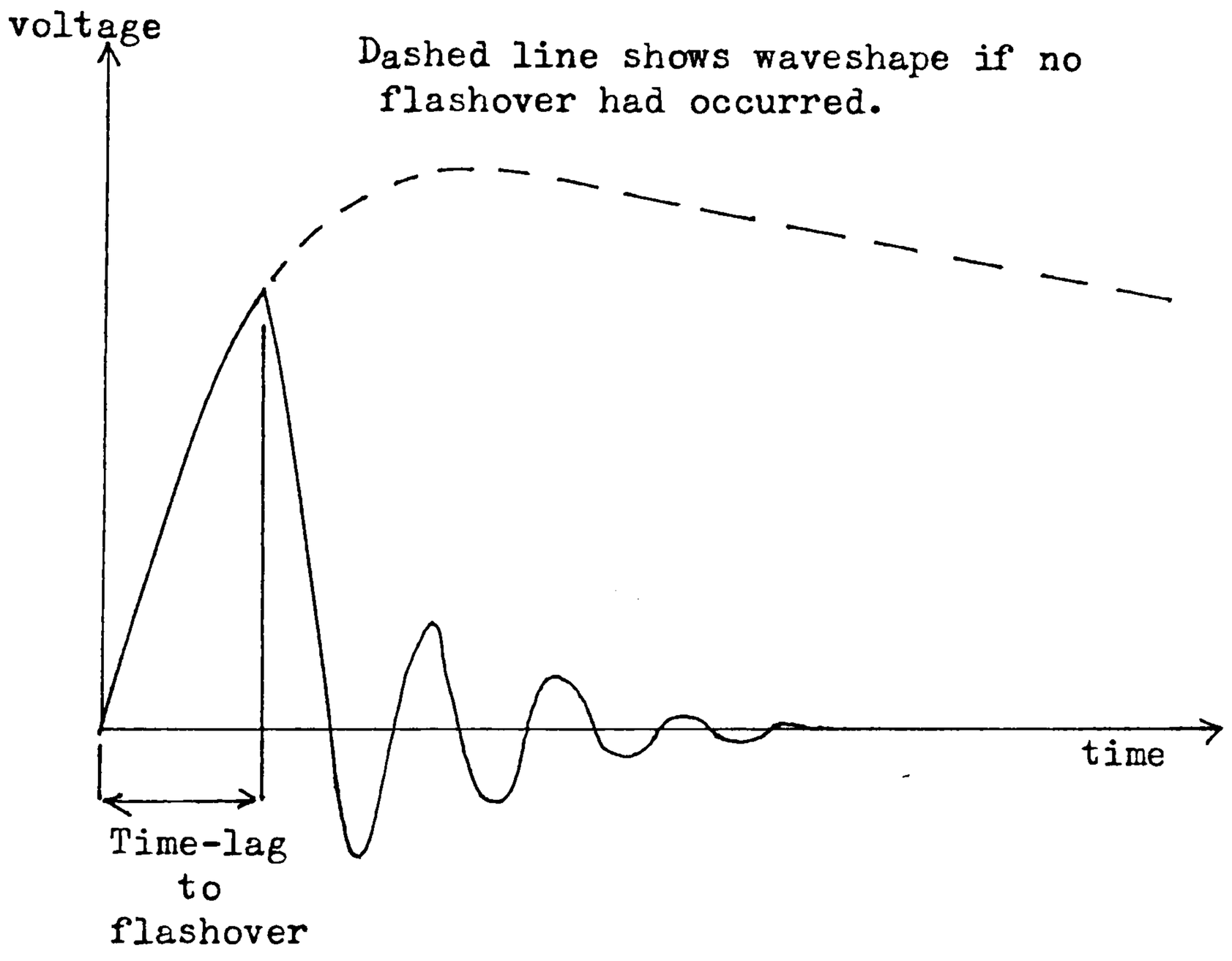

Fig. 5.24 Definition of time-lag to flashover.

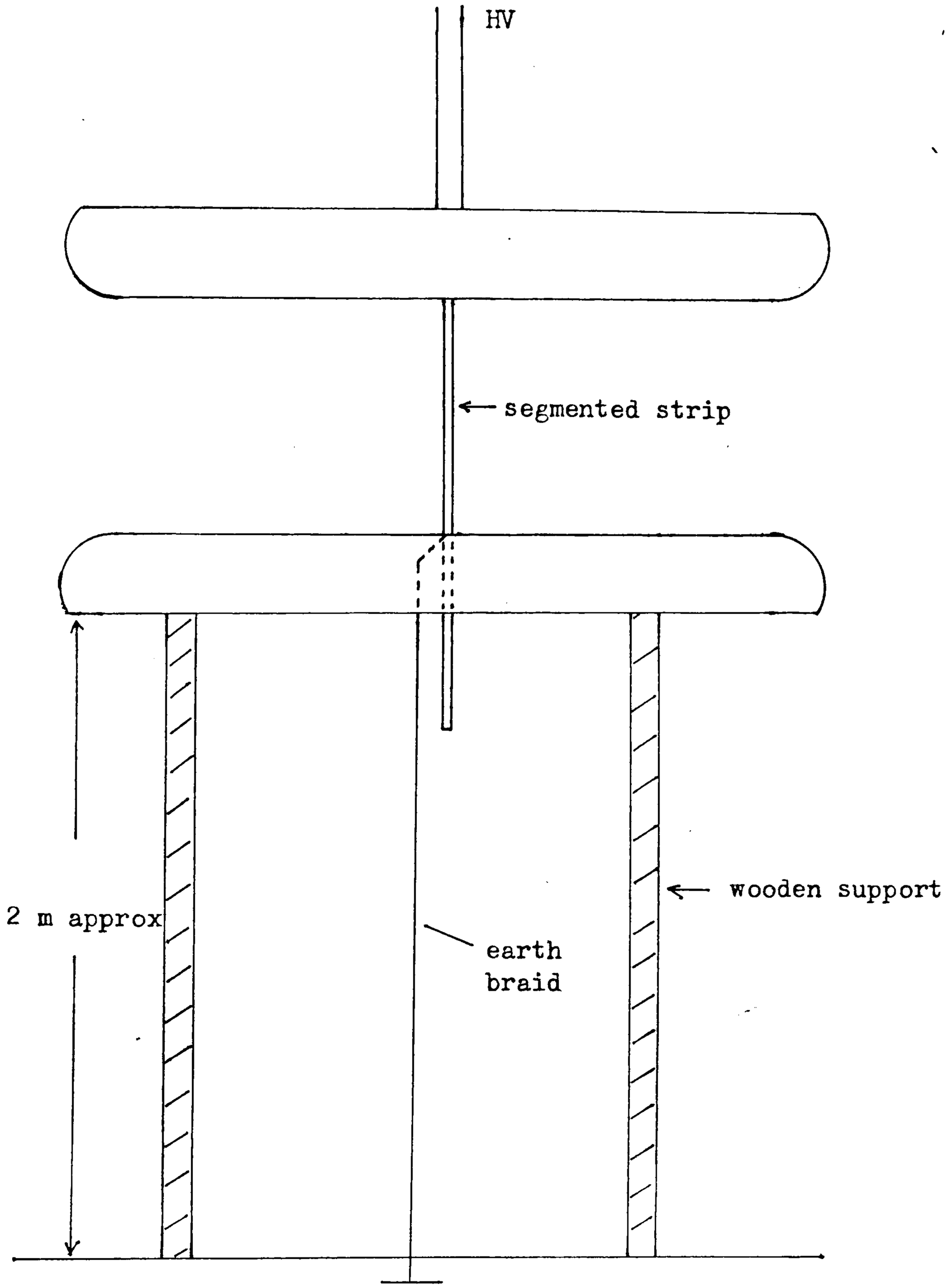

Fig. 6.1 Experimental arrangement for tests on a strip situated in a uniform field air gap.

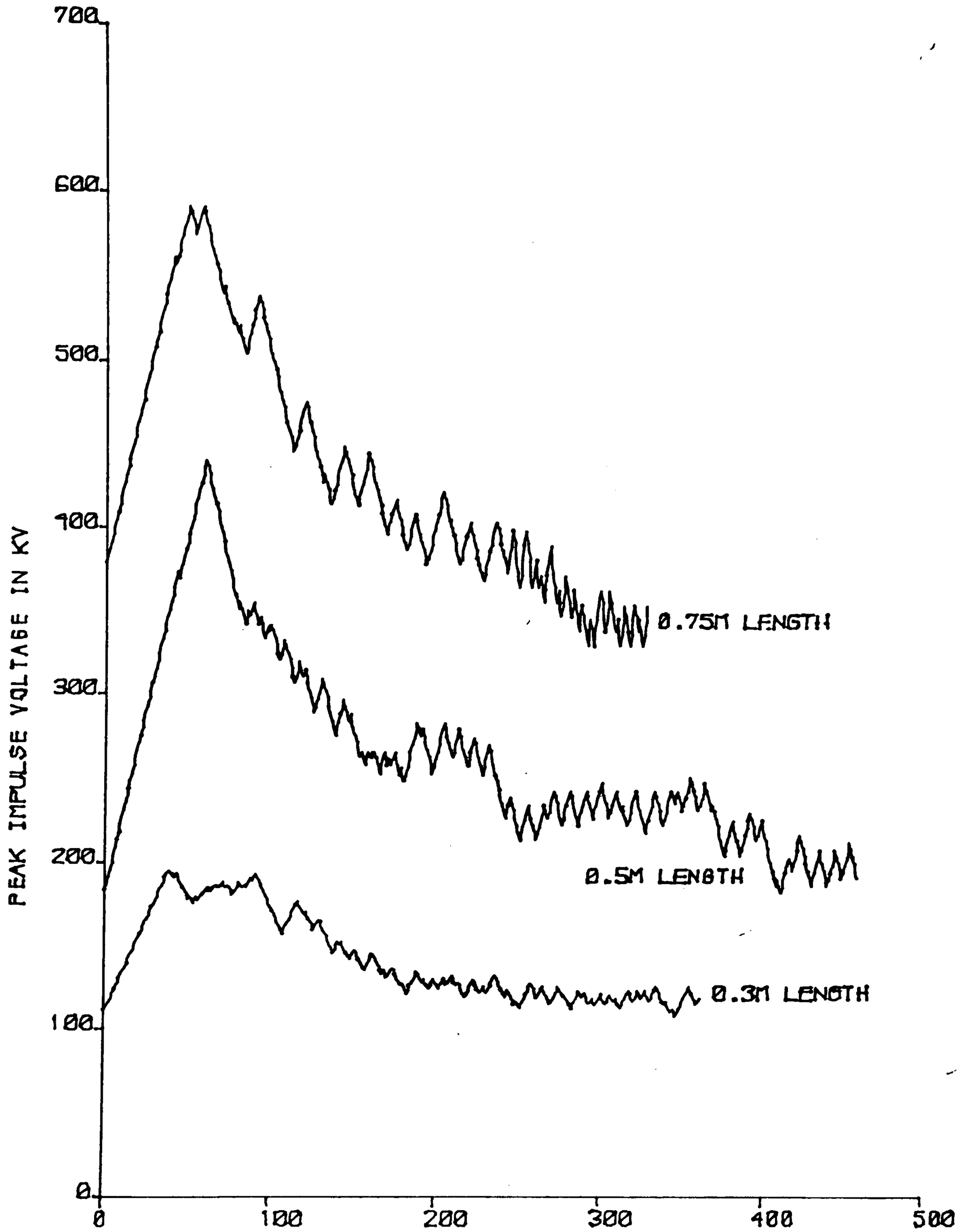

FIG. 6.2 UP & DOWN TEST RESULTS FOR SEGMENTED STRIP

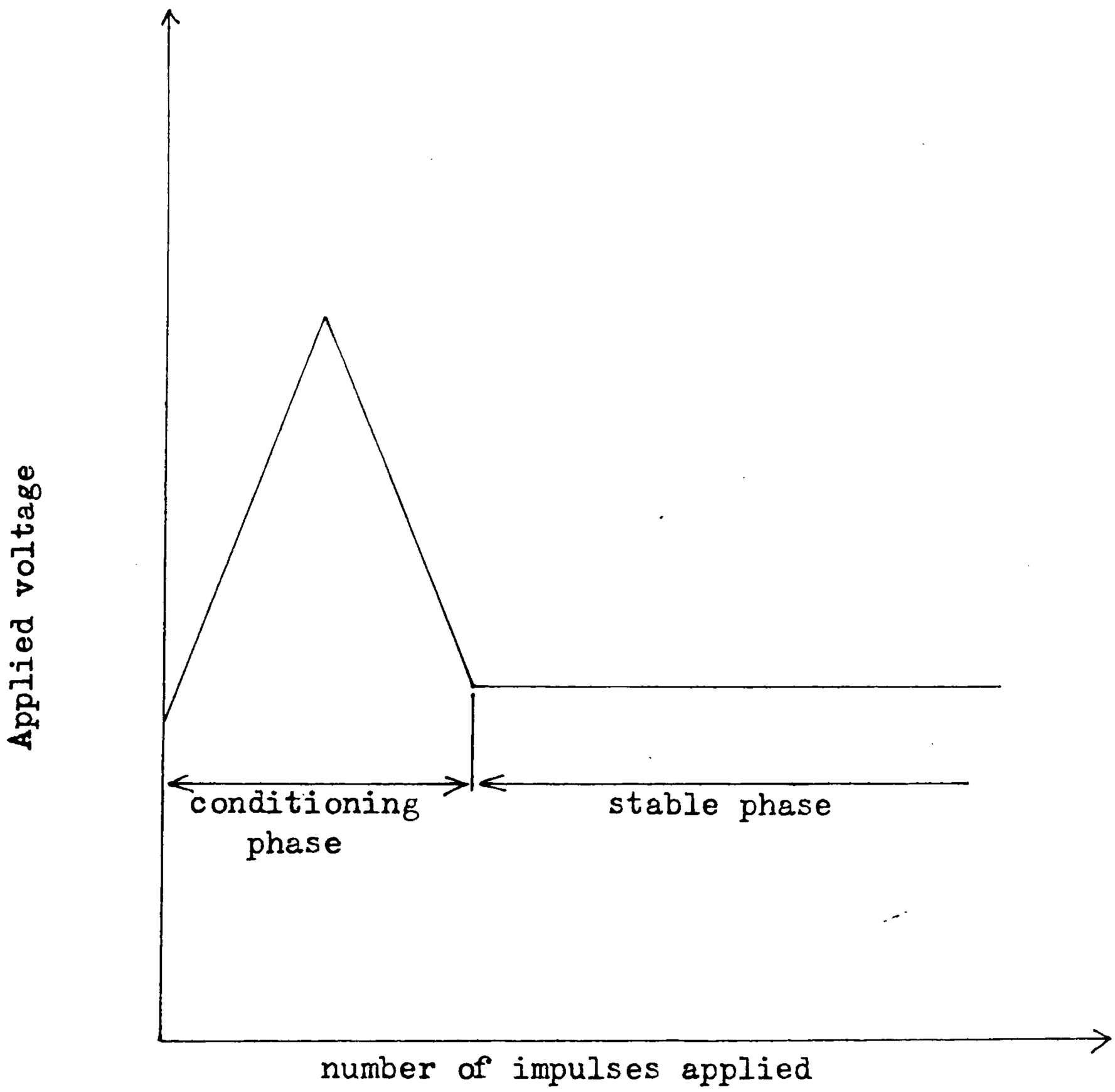

Fig. 6.3 Typical 'Up & Down' response of a segmented strip during conditioning.

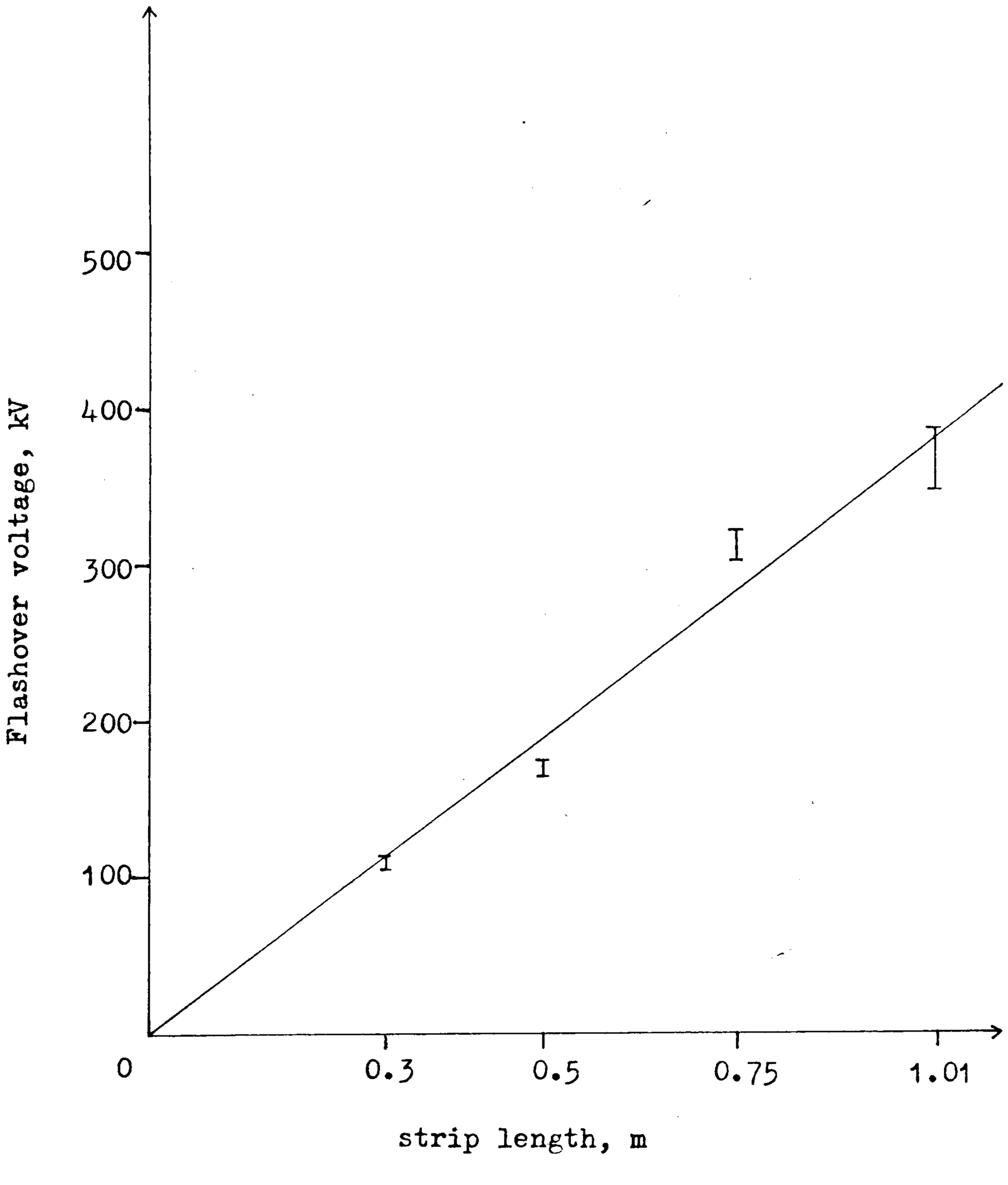

Fig. 6.4 Flashover voltage versus strip length in a uniform field.

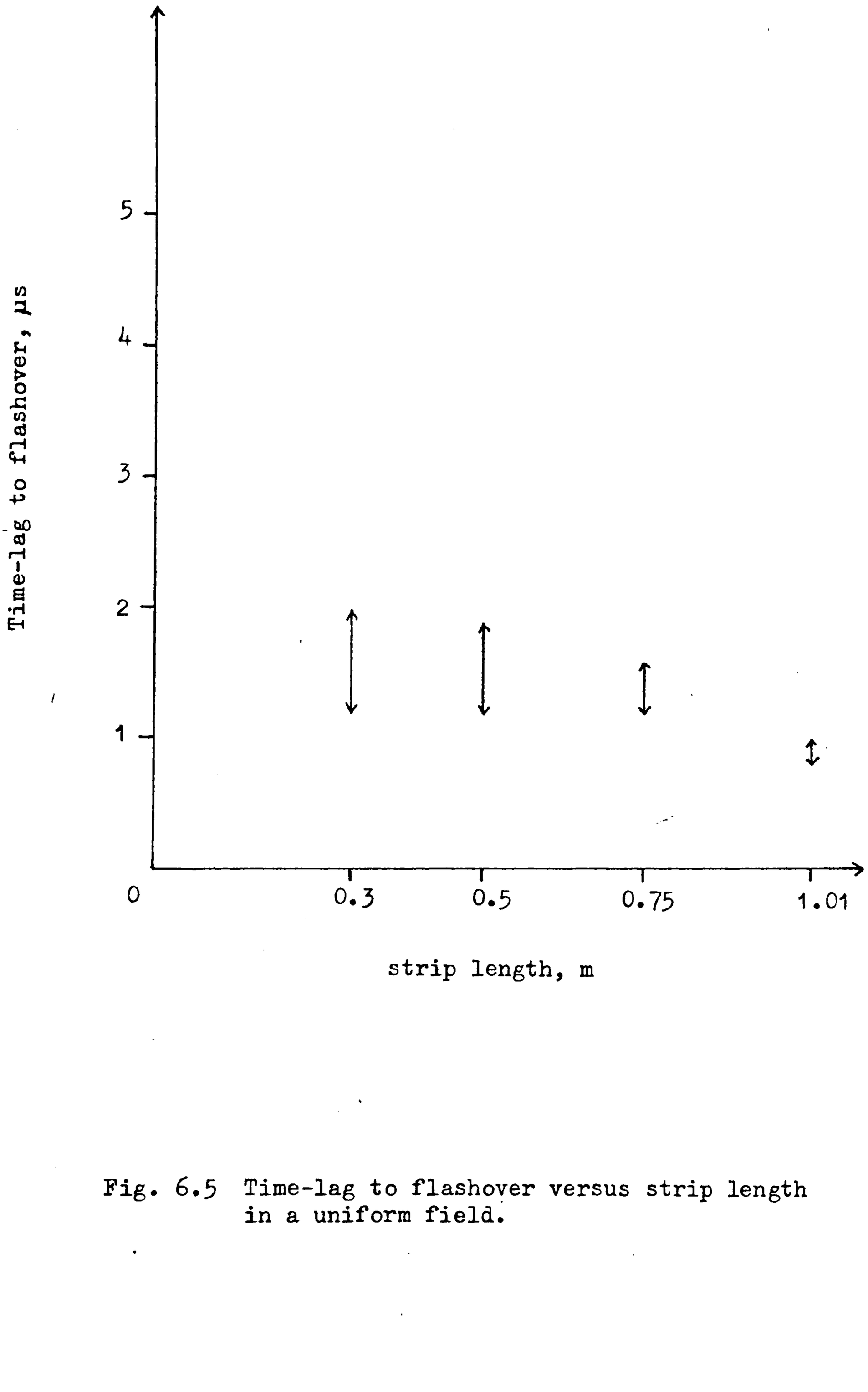

Fig. 6.5 Time-lag to flashover versus strip length in a uniform field.

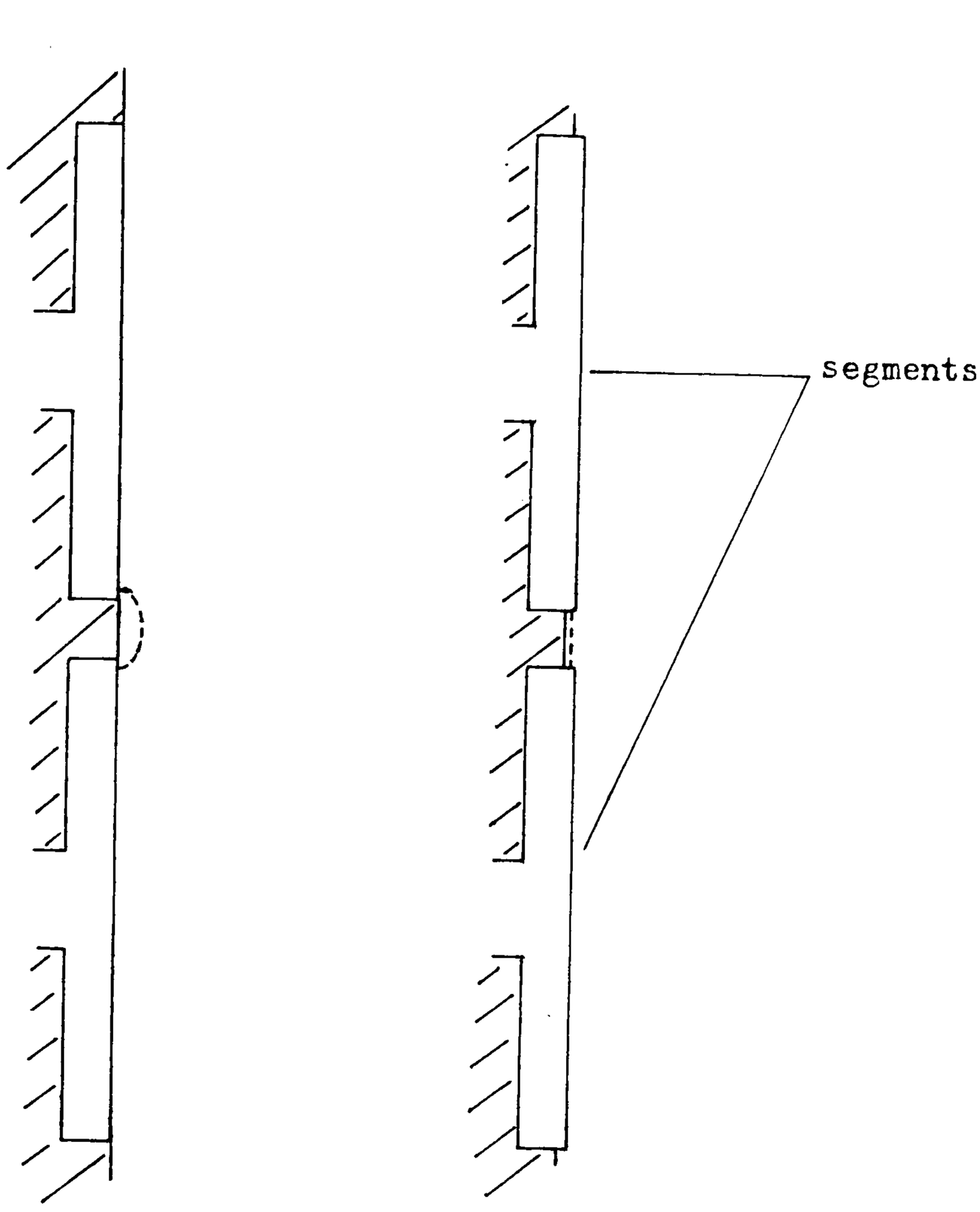

Fig. 6.6 Profile of an intersegment gap in a new segmented strip and a conditioned segmented strip.

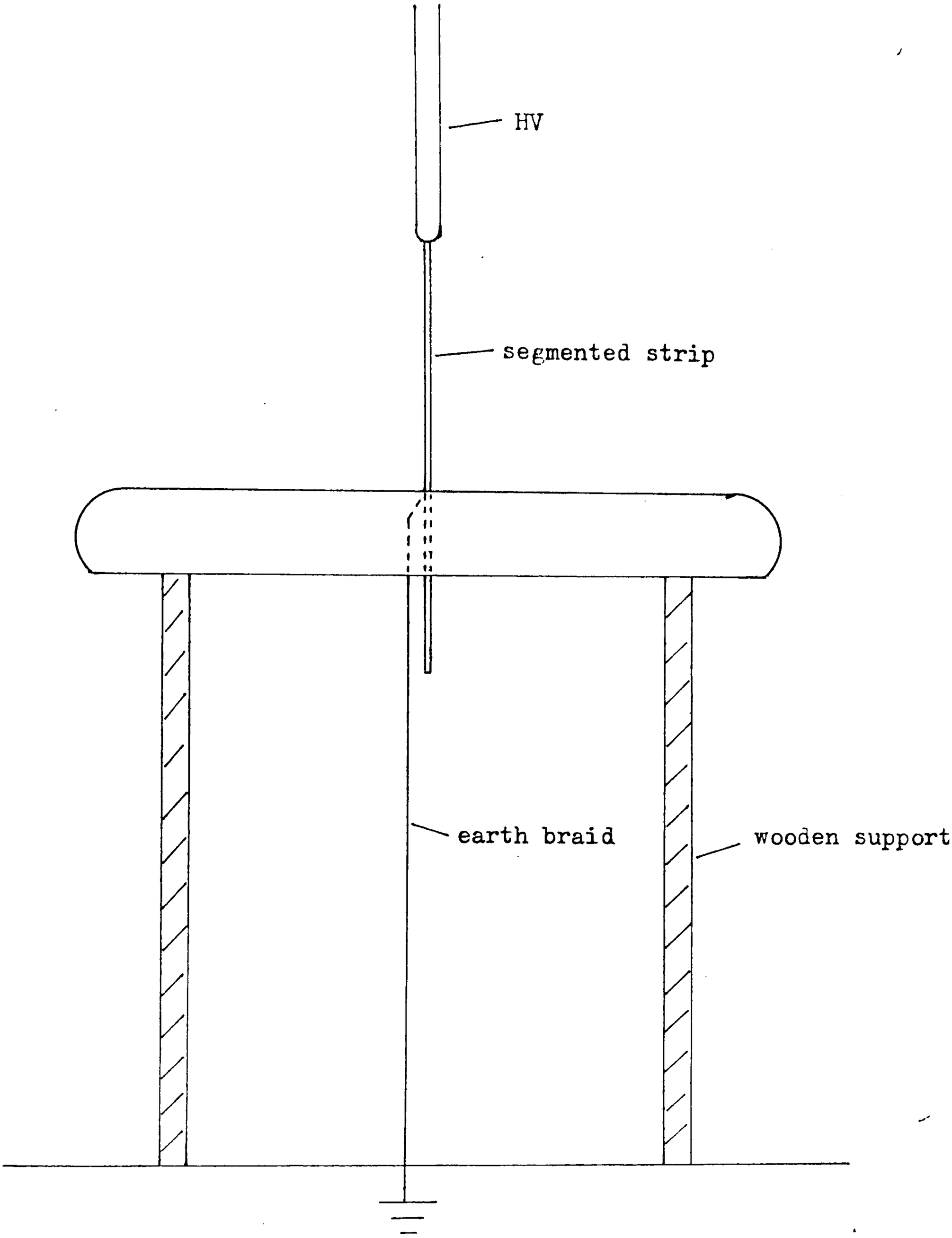

Fig. 6.7 Experimental arrangement for a strip bridging a rod/plane gap.

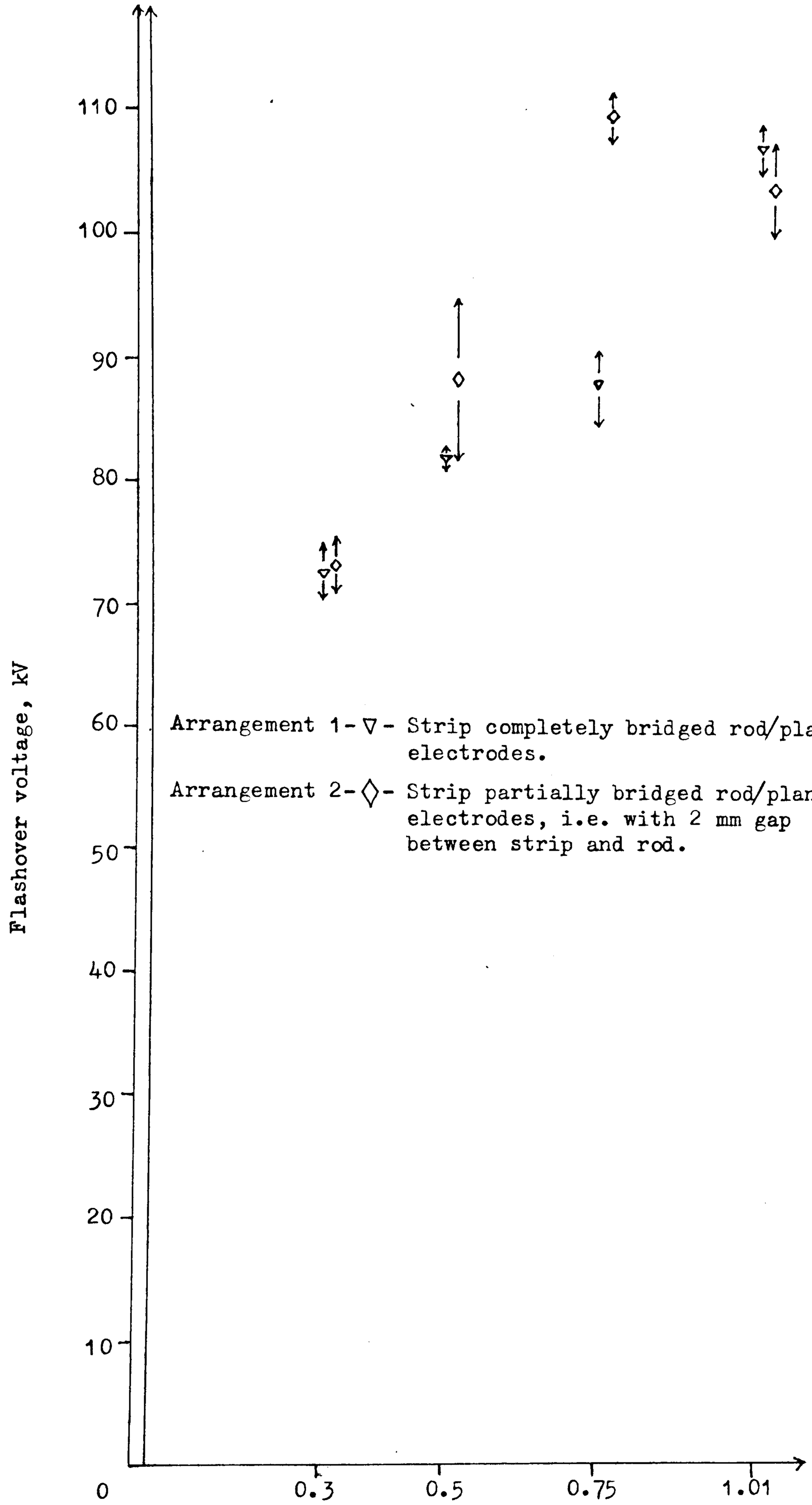

Fig. 6.8 Variation of flashover voltage with strip length. (strip bridging rod/plane electrodes)

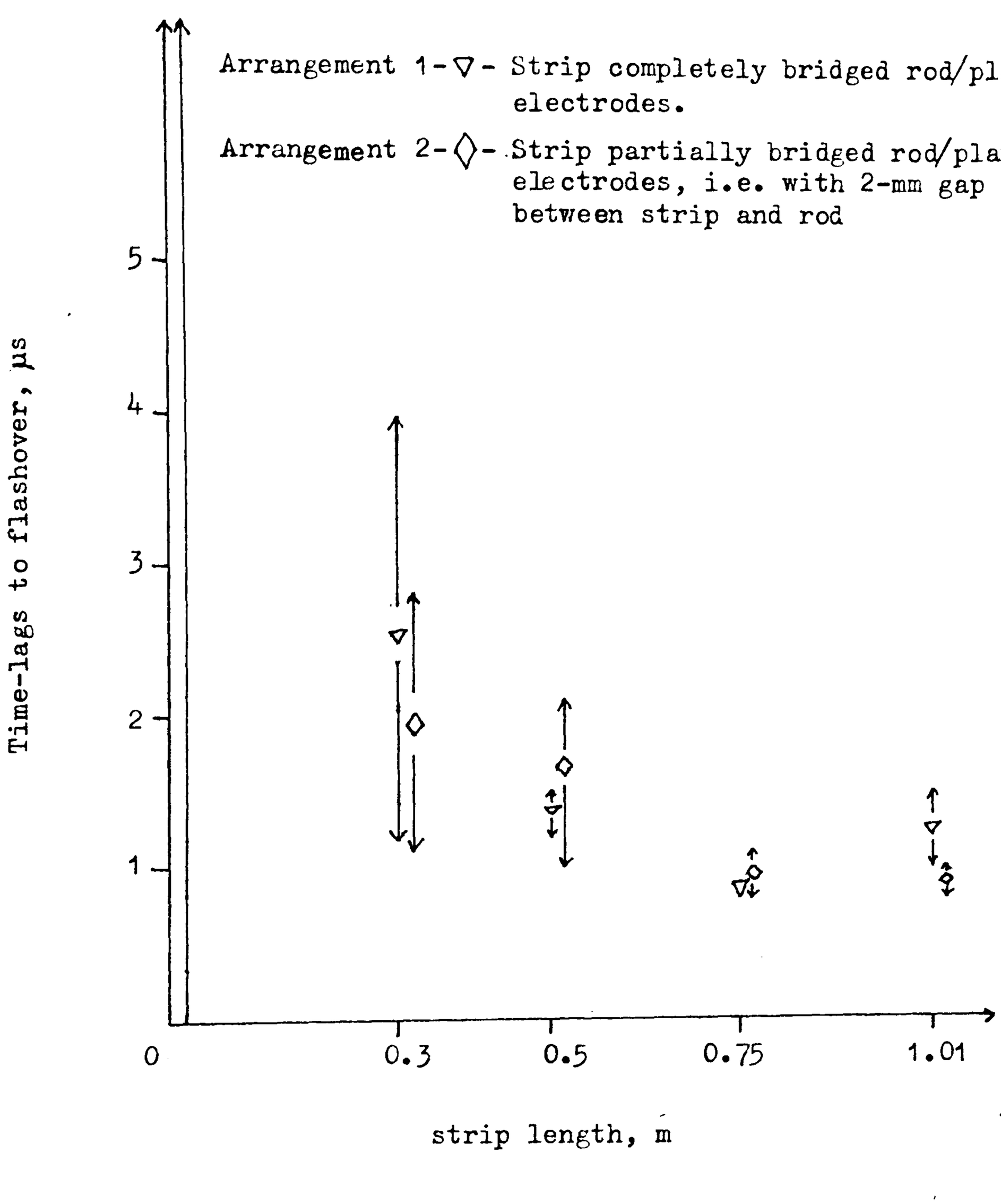

Fig. 6.9 Variation of time-lags to flashover with strip length (strip bridging rod/plane electrodes).

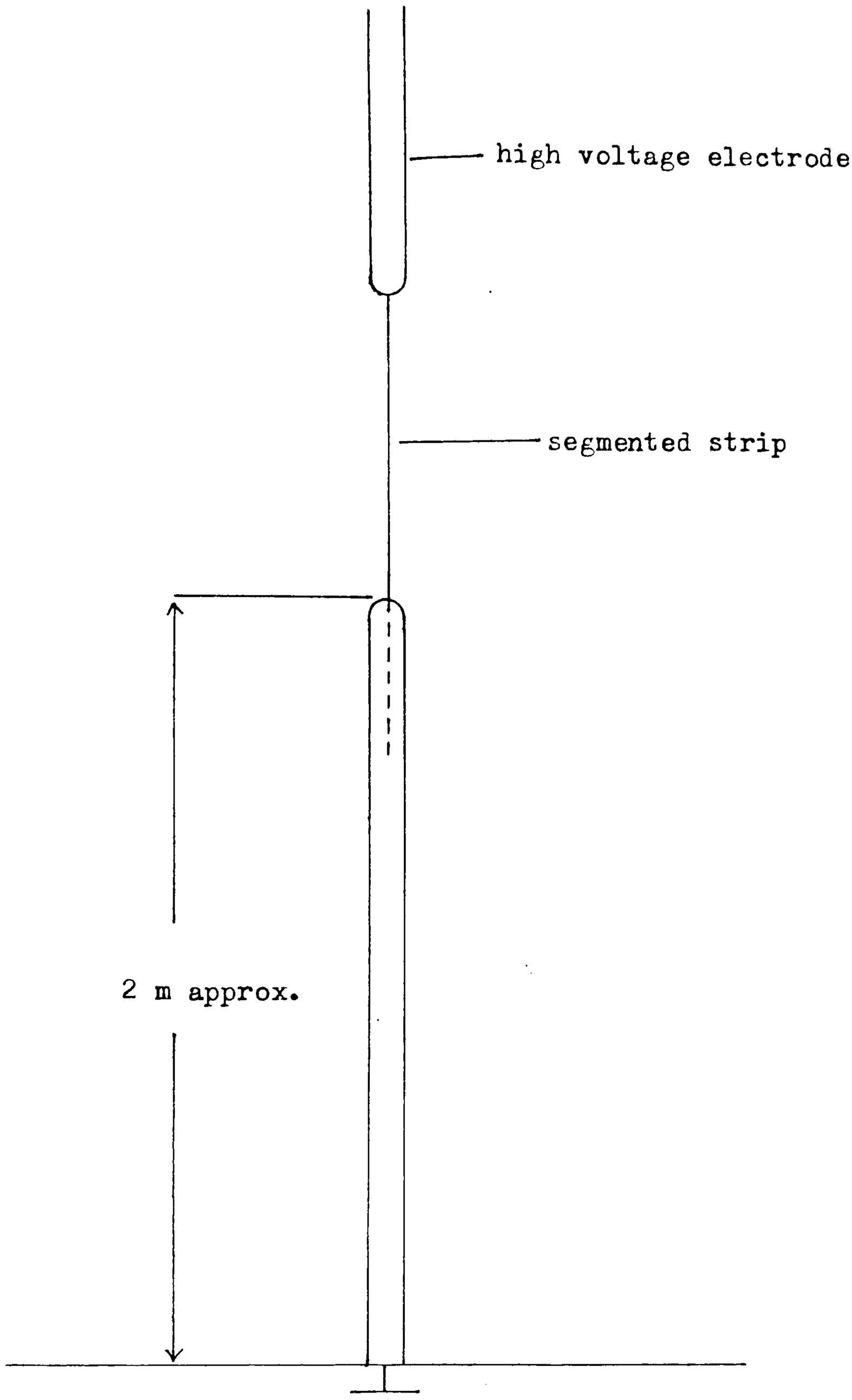

Fig. 6.10 Experimental arrangement.

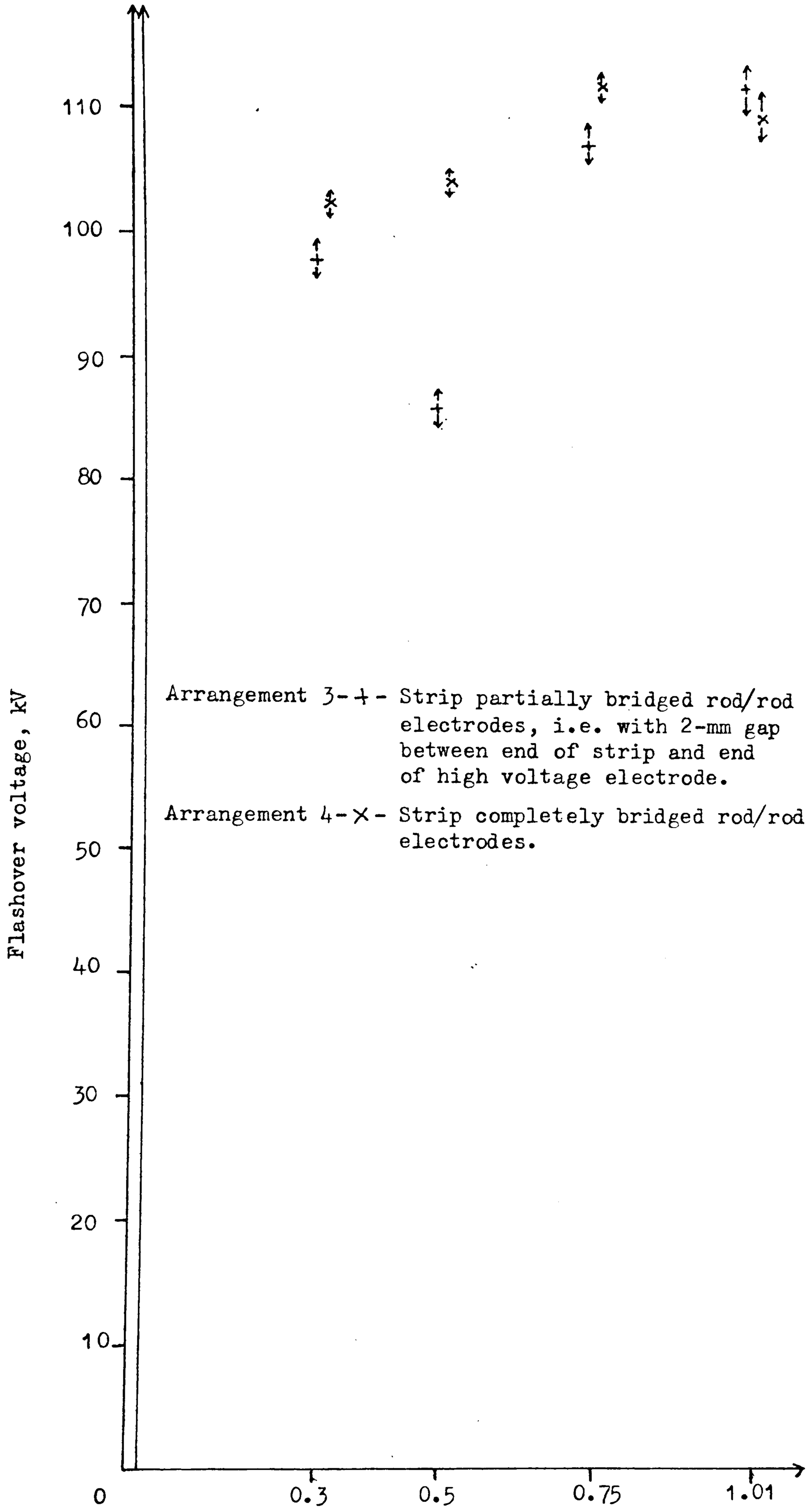

Fig. 6.11 Variation of flashover voltage with strip length. (Strip bridging rod/rod electrodes)

Arrangement 3-+- Strip partially bridged rod/rod electrodes, i.e. with 2-mm gap between end of strip and end of high voltage electrode.

Arrangement 4-X- Strip completely bridged rod/rod electrodes.

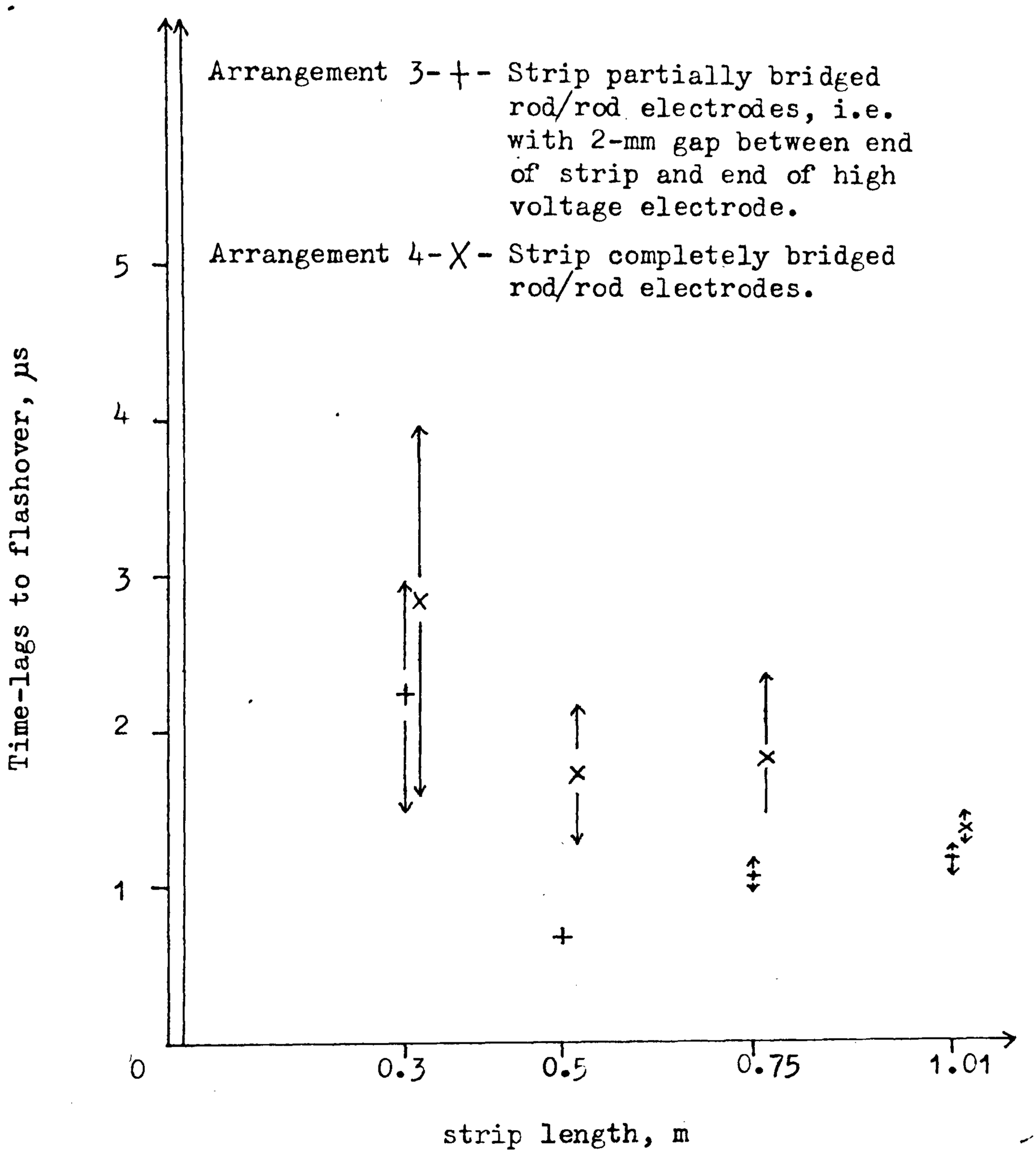

Fig. 6.12 Variation of time-lags to flashover with strip length. (Strip bridging rod/rod electrodes)

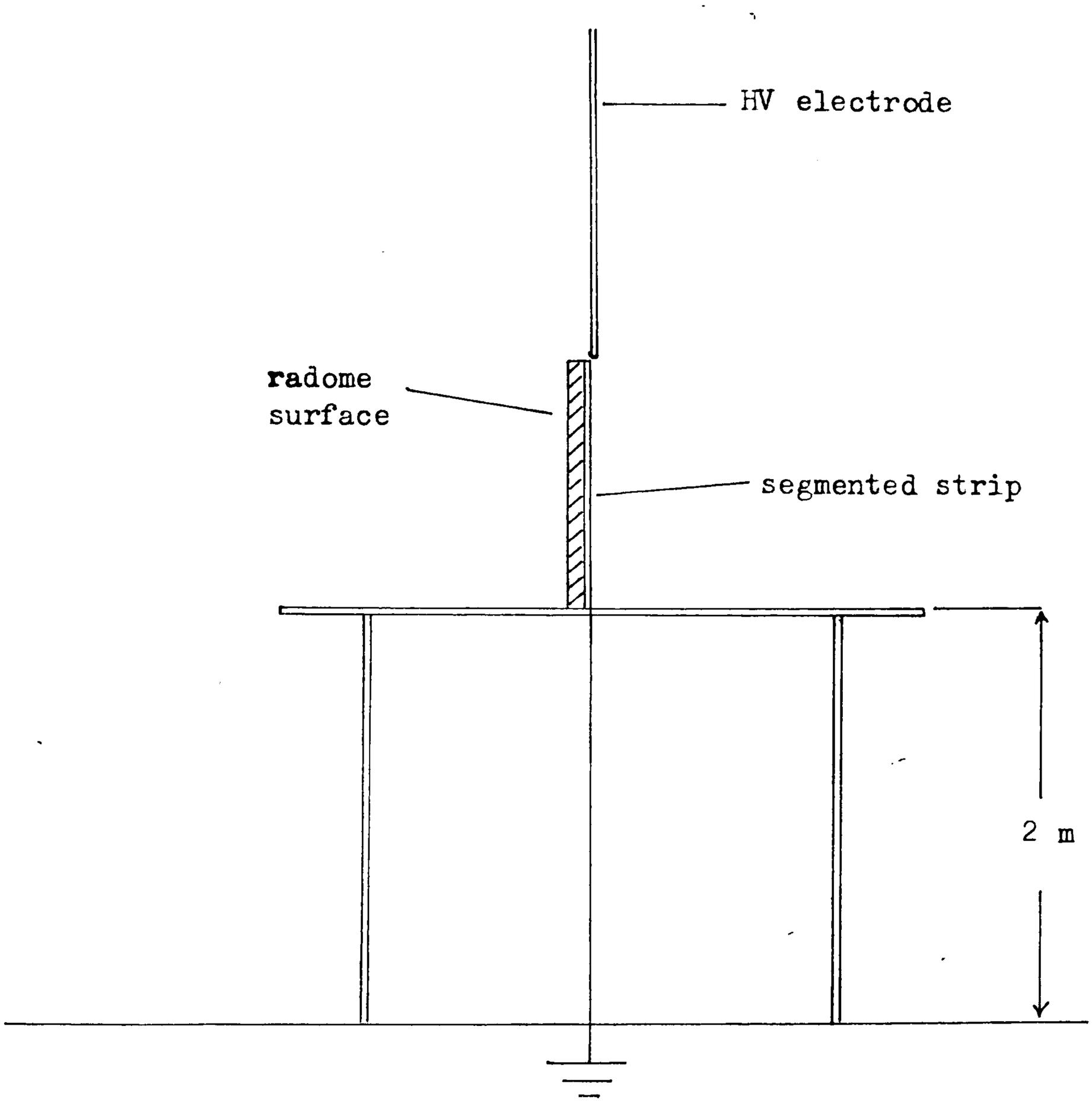

Fig. 6.13 Experimental arrangement used by Plumer & Hoots for obtaining flashover voltage/ strip length relationship.

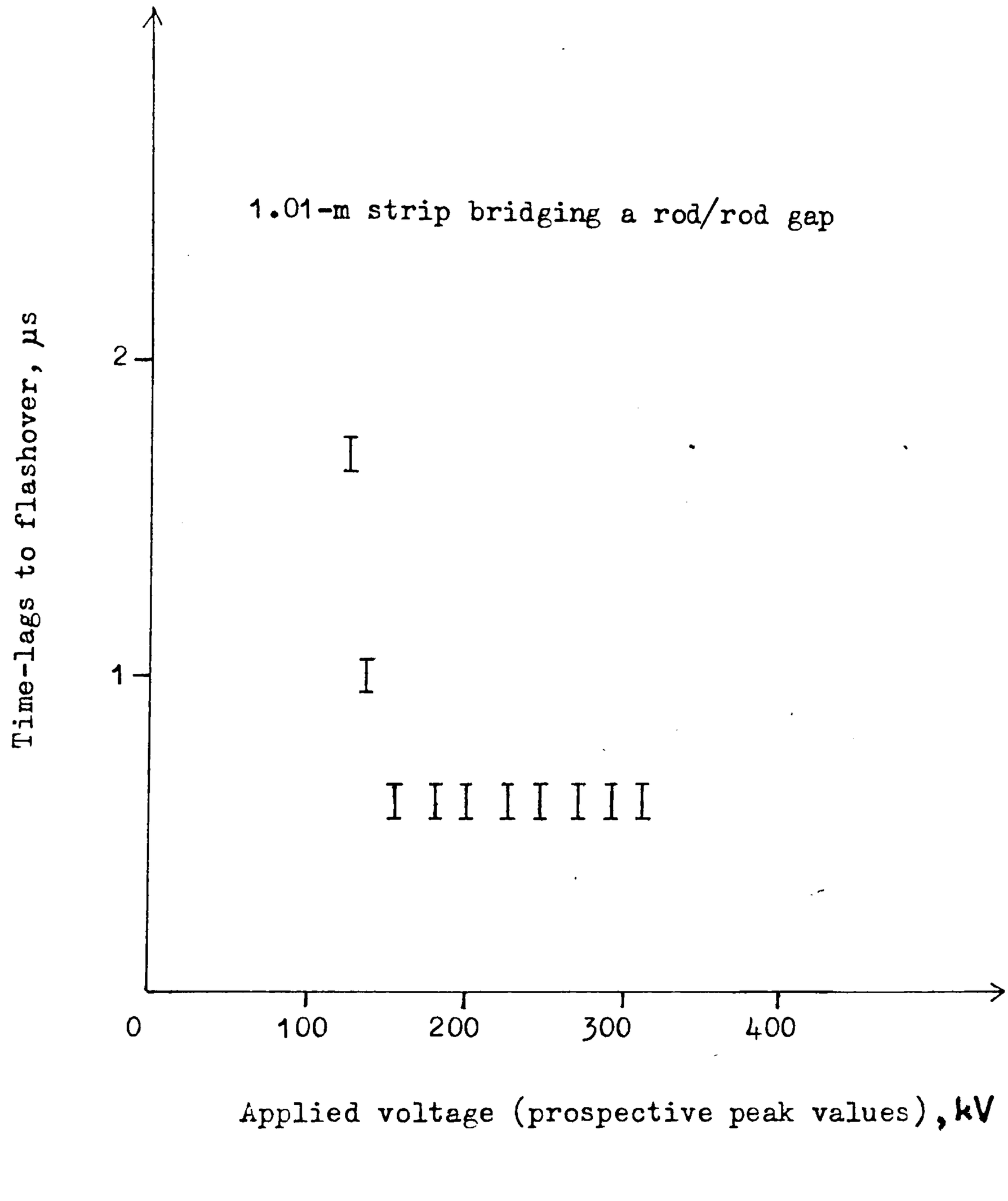

Fig. 6.14 Effect of overvoltages on time-lags to flashover.

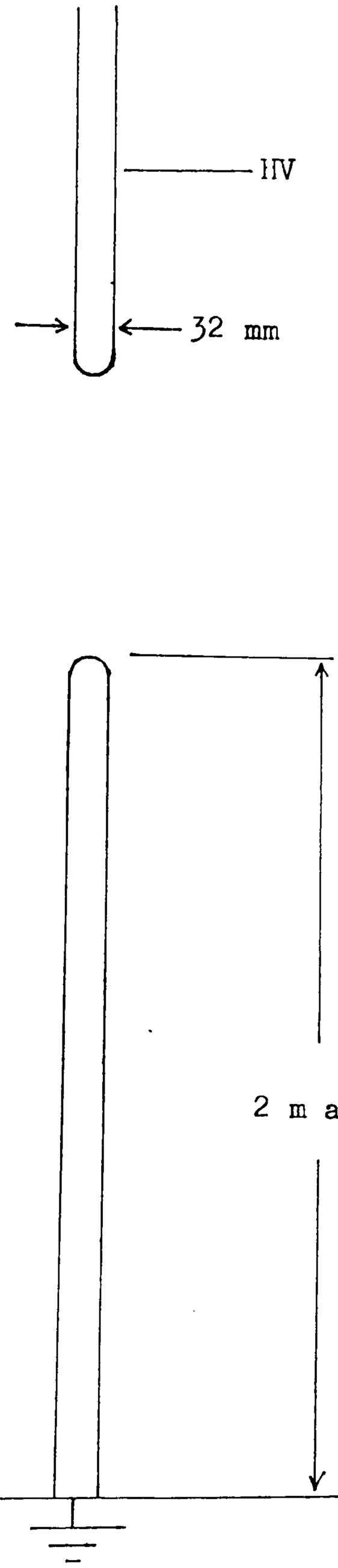

Fig. 6.15 Experimental arrangement.

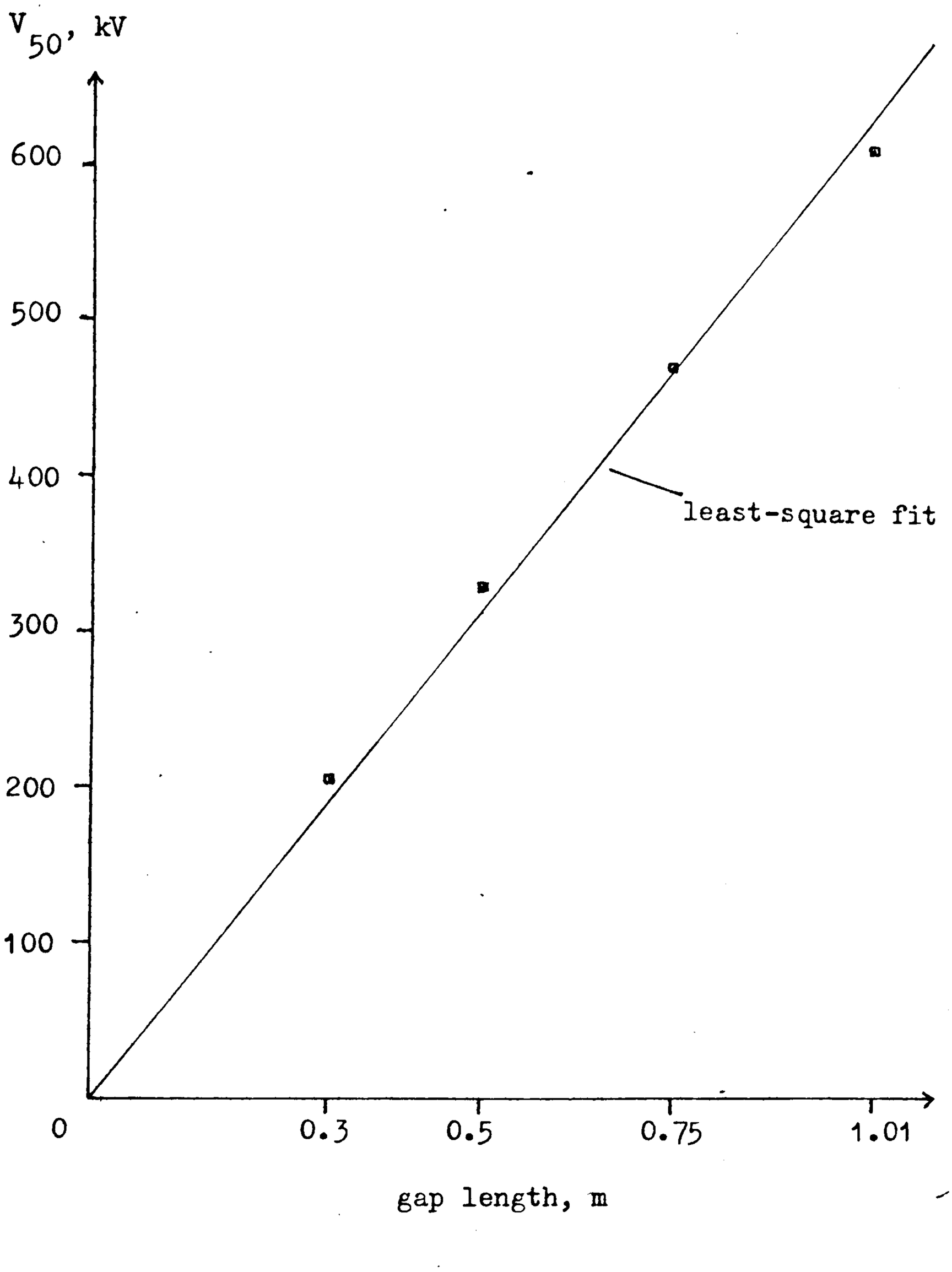

Fig. 6.16 Plot of V_{50} against gap length in a rod/rod configuration.

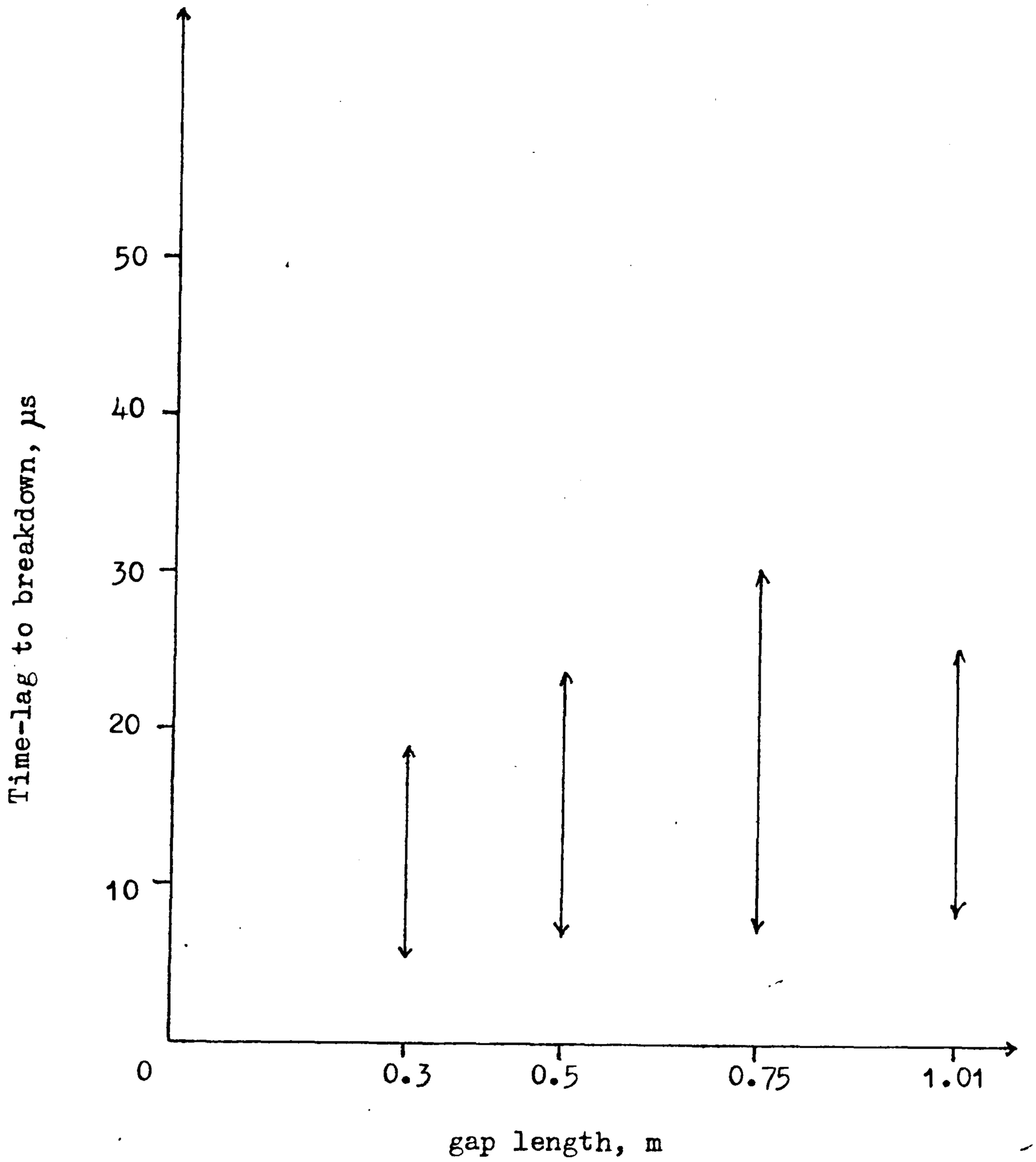

Fig. 6.17 Plot of time-lag to breakdown against gap length in a rod/rod configuration.

● — strip bridging parallel plane air gap but using maximum flashover voltage values
□ — rod/rod air gap
○ — strip bridging parallel plane air gap
× — strip bridging rod/rod air gap
▽ — strip bridging rod/plane air gap

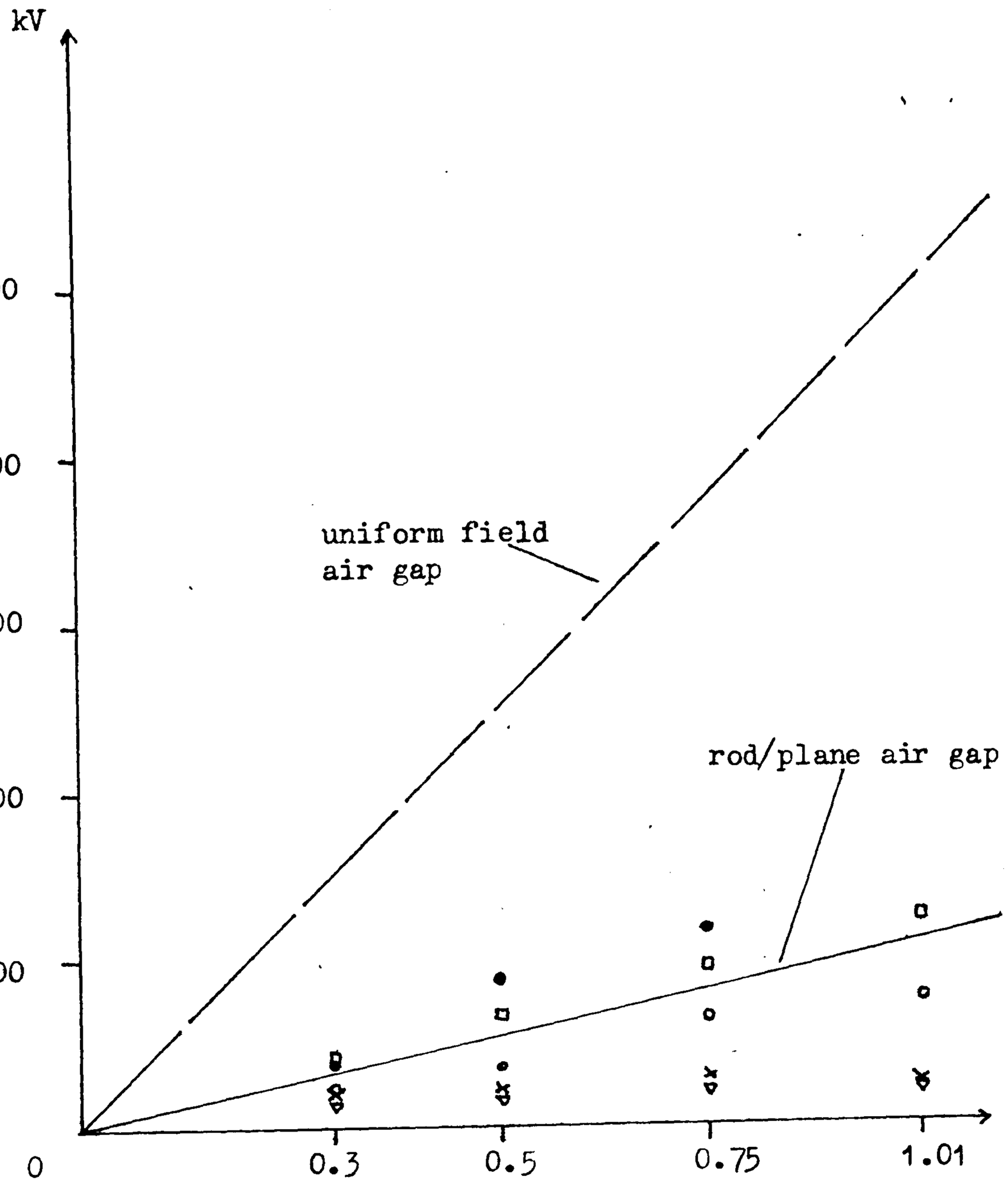

Fig. 6.18 Comparison of flashover/breakdown characteristics.

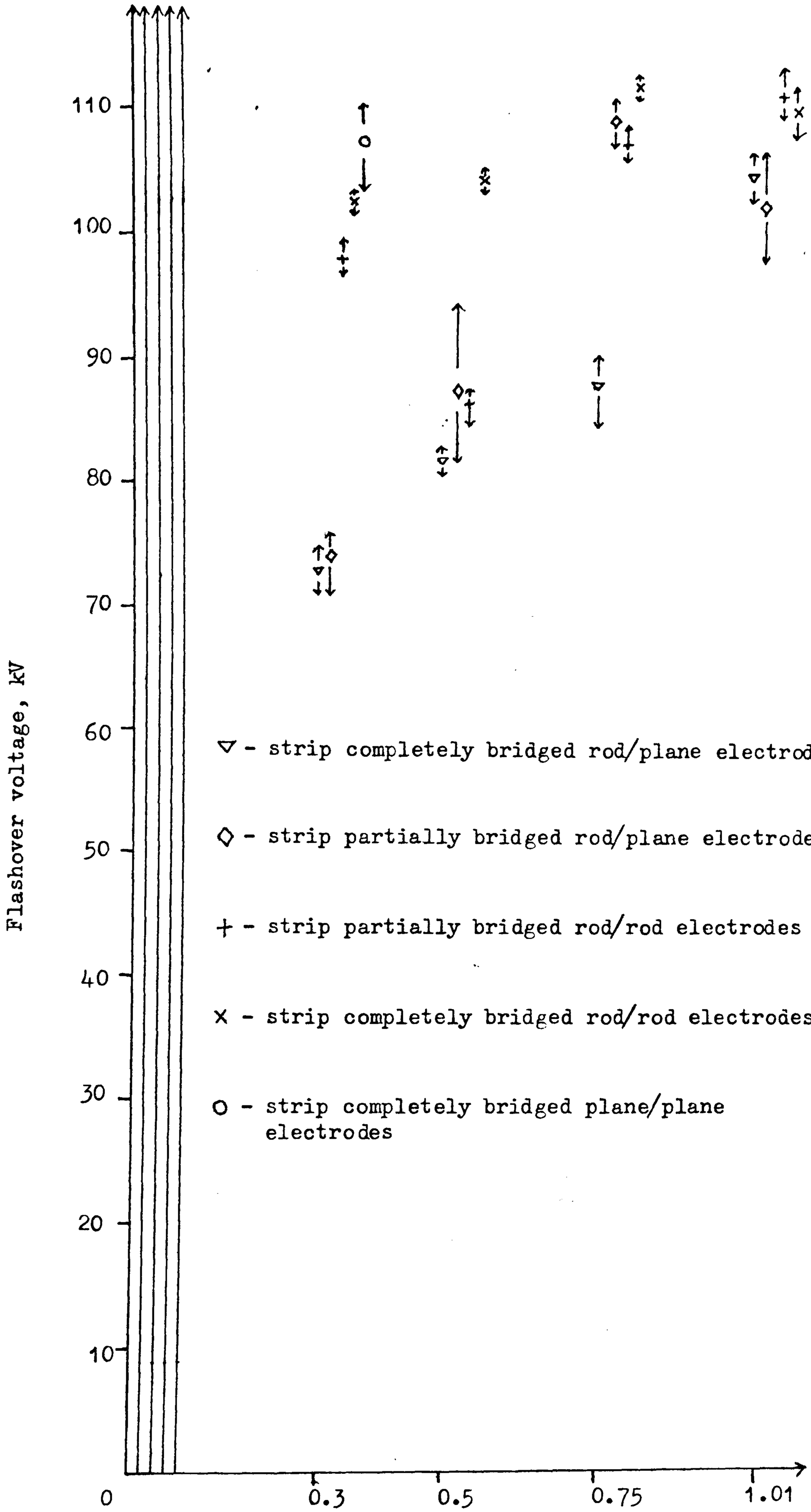

Fig. 6.19 Summary of flashover voltage measurements for a segmented strip.

Fig. 6.20 Streak record at 1 ns/mm

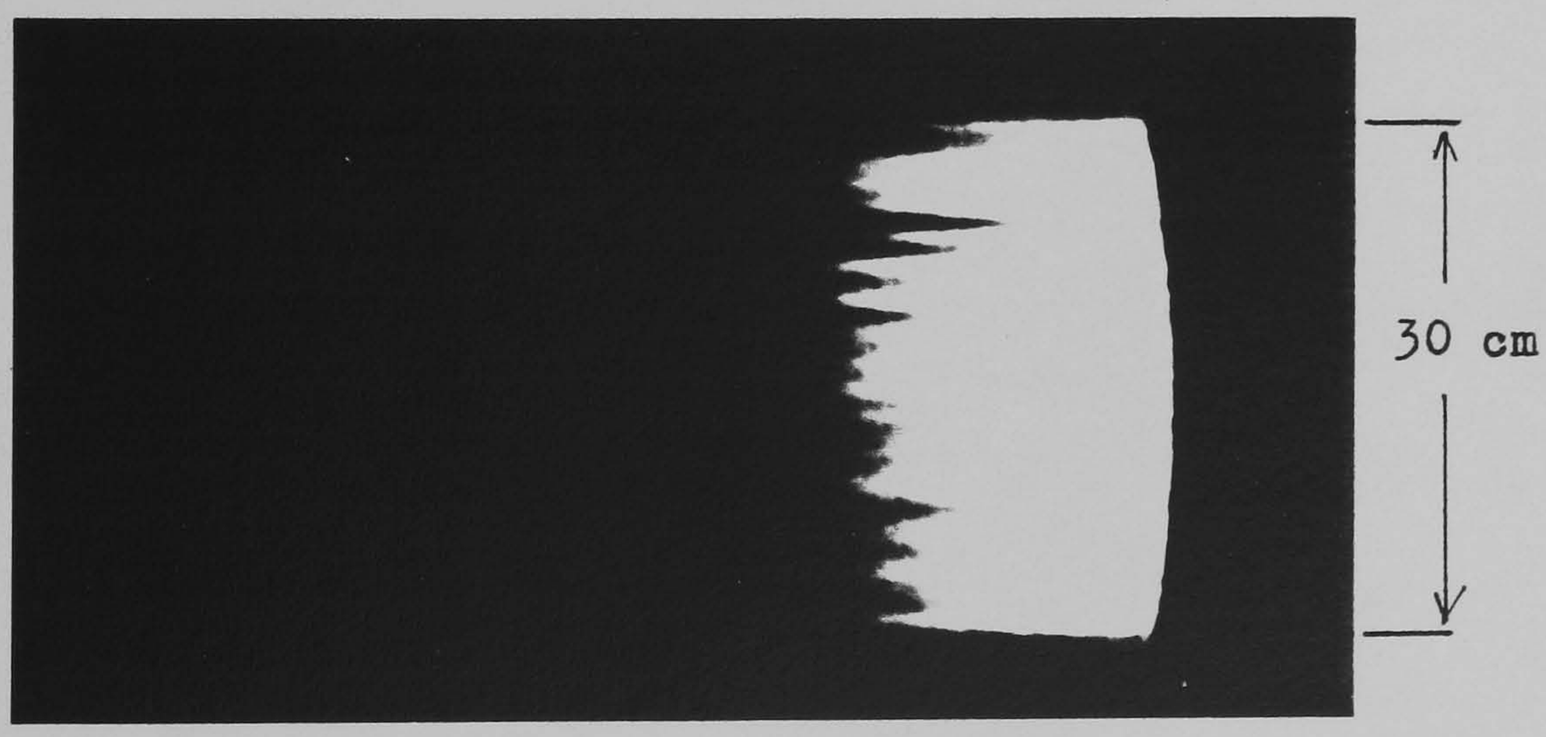

Fig. 6.21 Streak record at 2 ns/mm

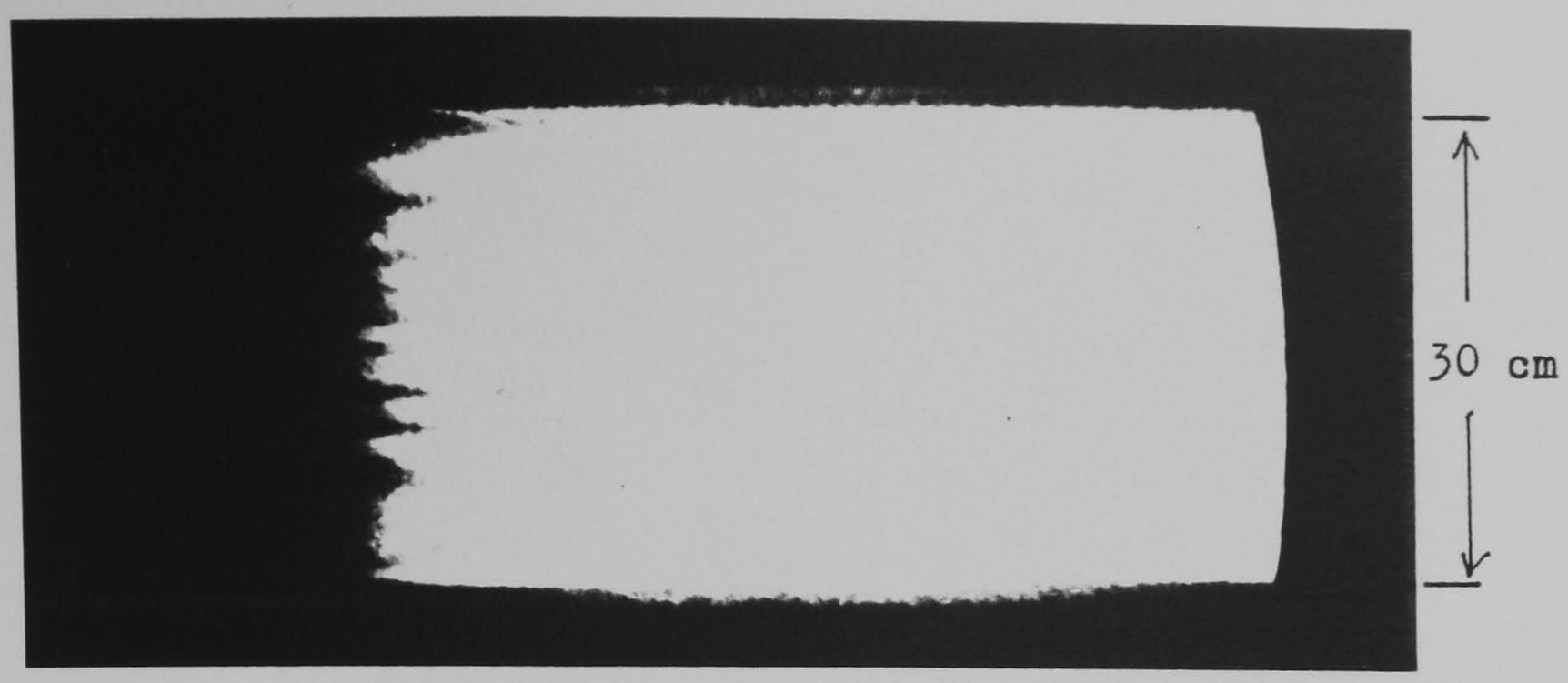

Fig. 6.22 Streak record at 2 ns/mm

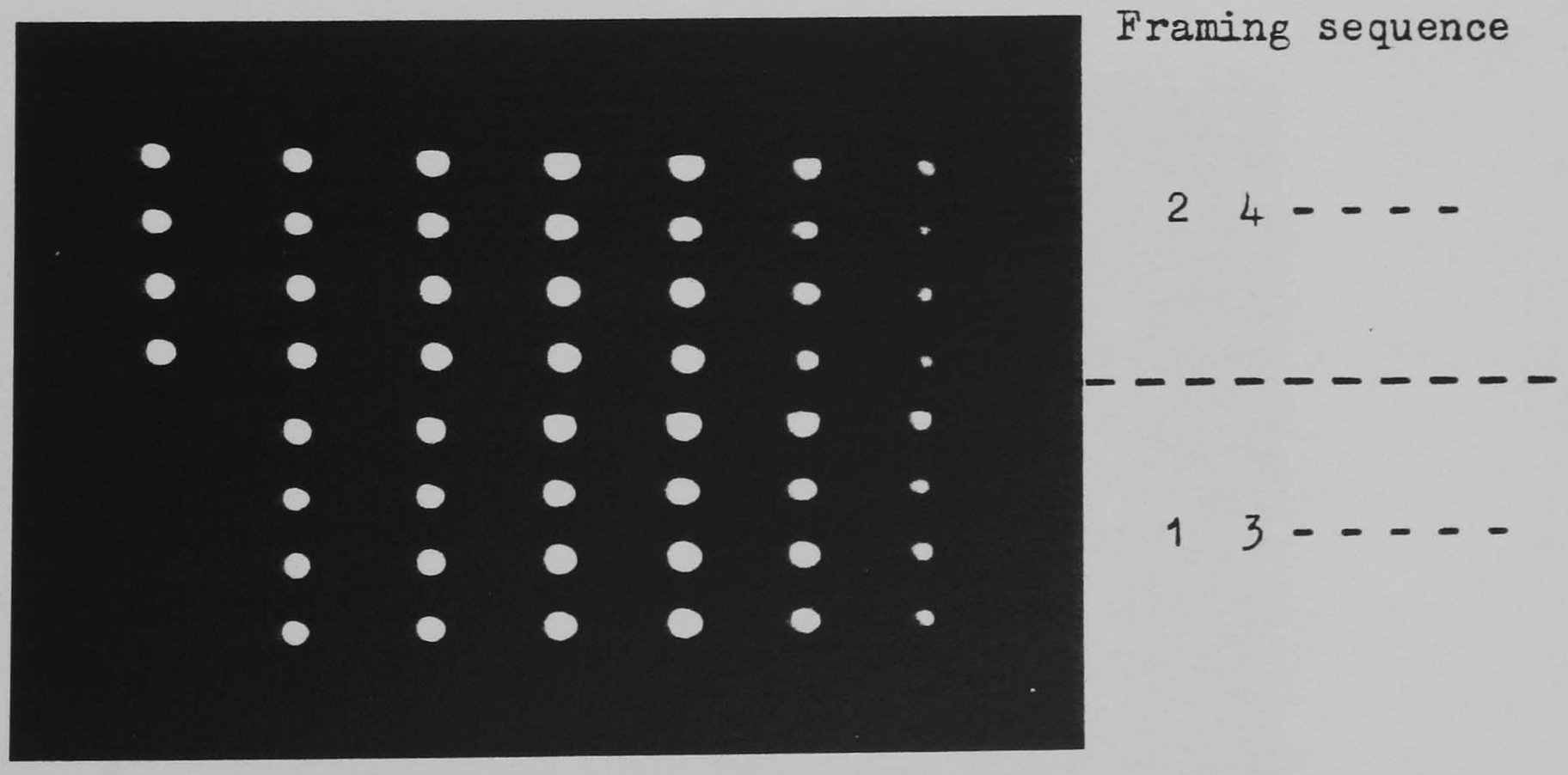

Fig. 6.23 Framing record of 4 gaps (typical)

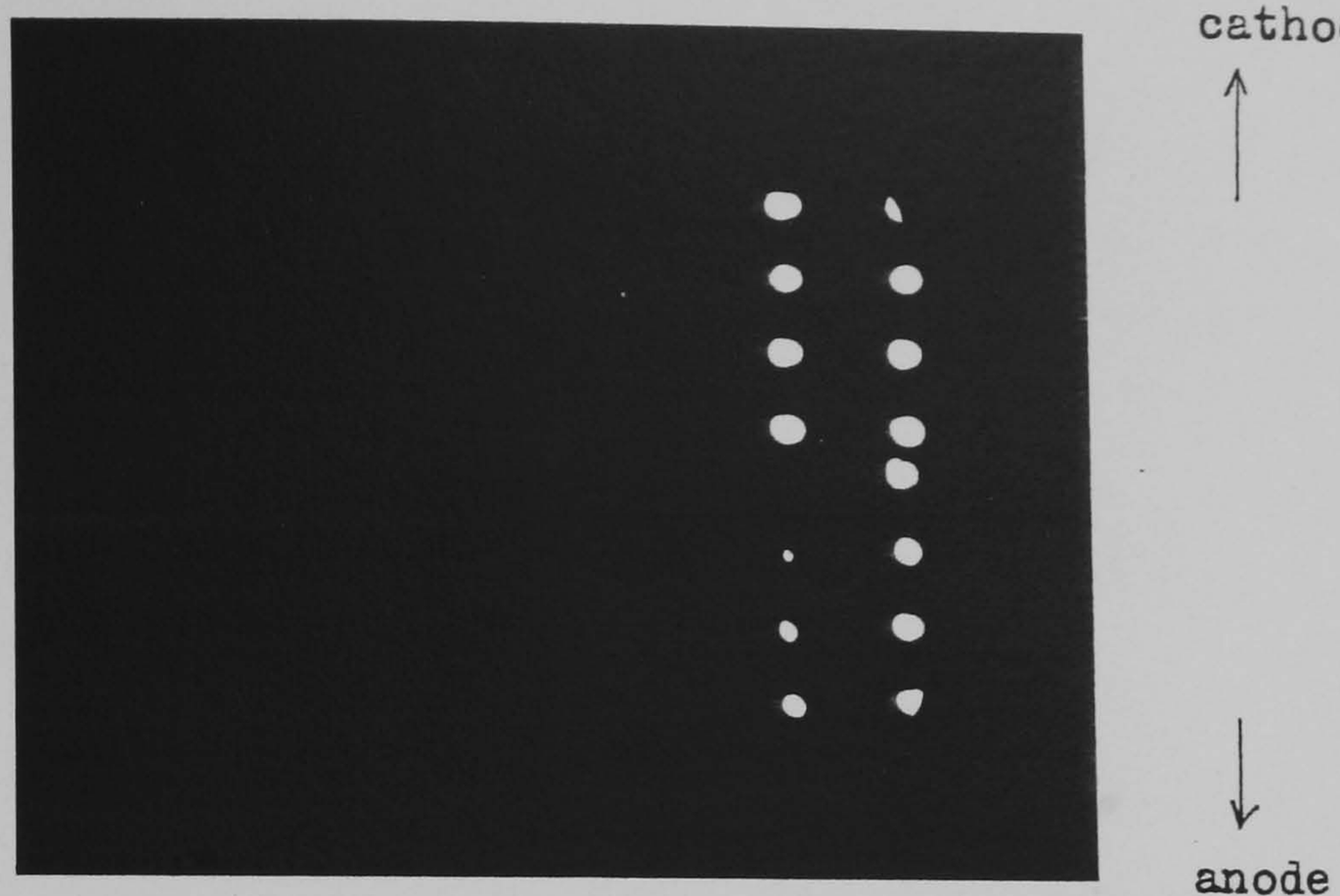

Fig. 6.24 Framing record at 2 X 10^7 frames/second showing anode to cathode direction of discharge propagation

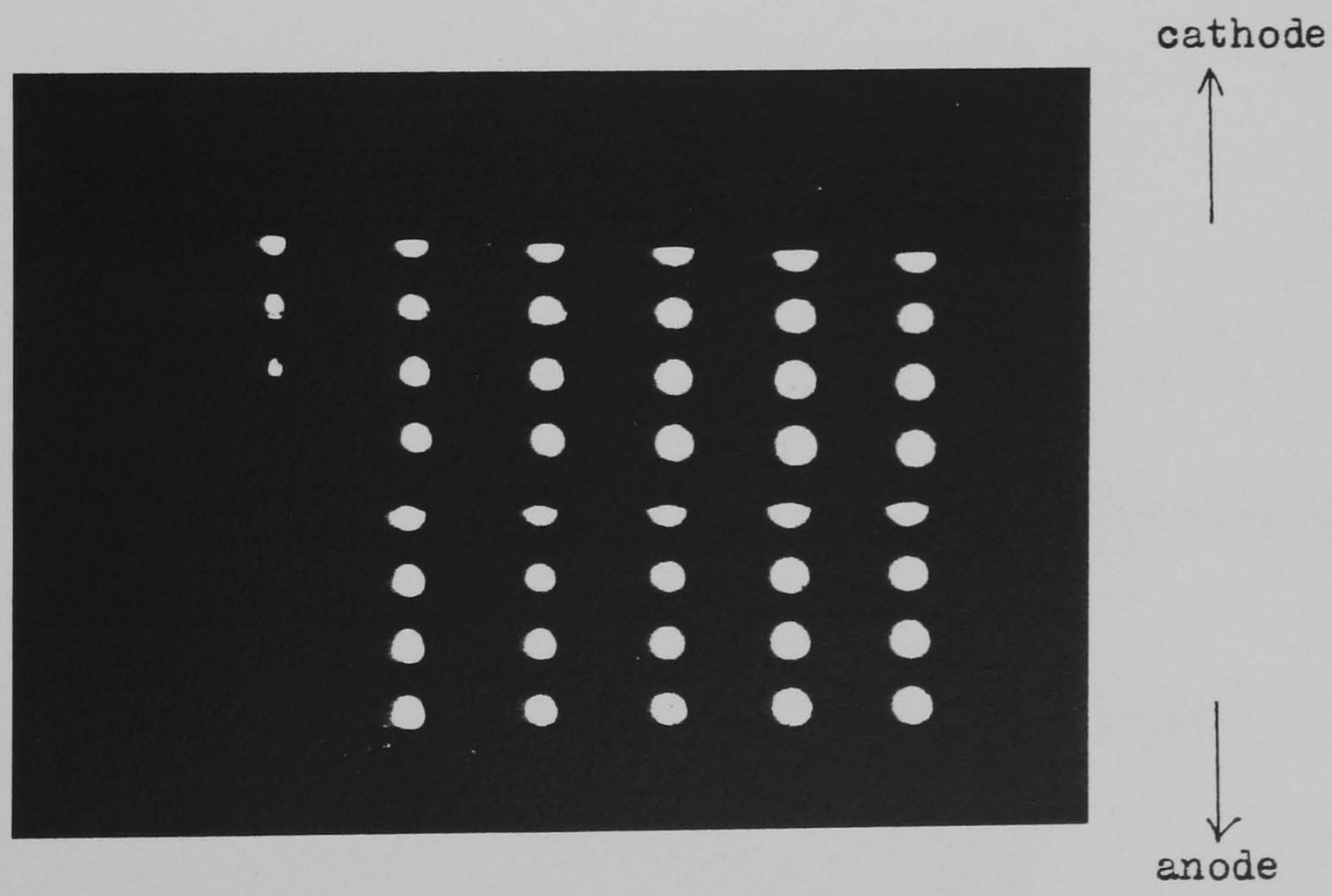

Fig. 6.25 Framing record at 2 X 10^7 frames/second showing cathode to anode direction of discharge propagation

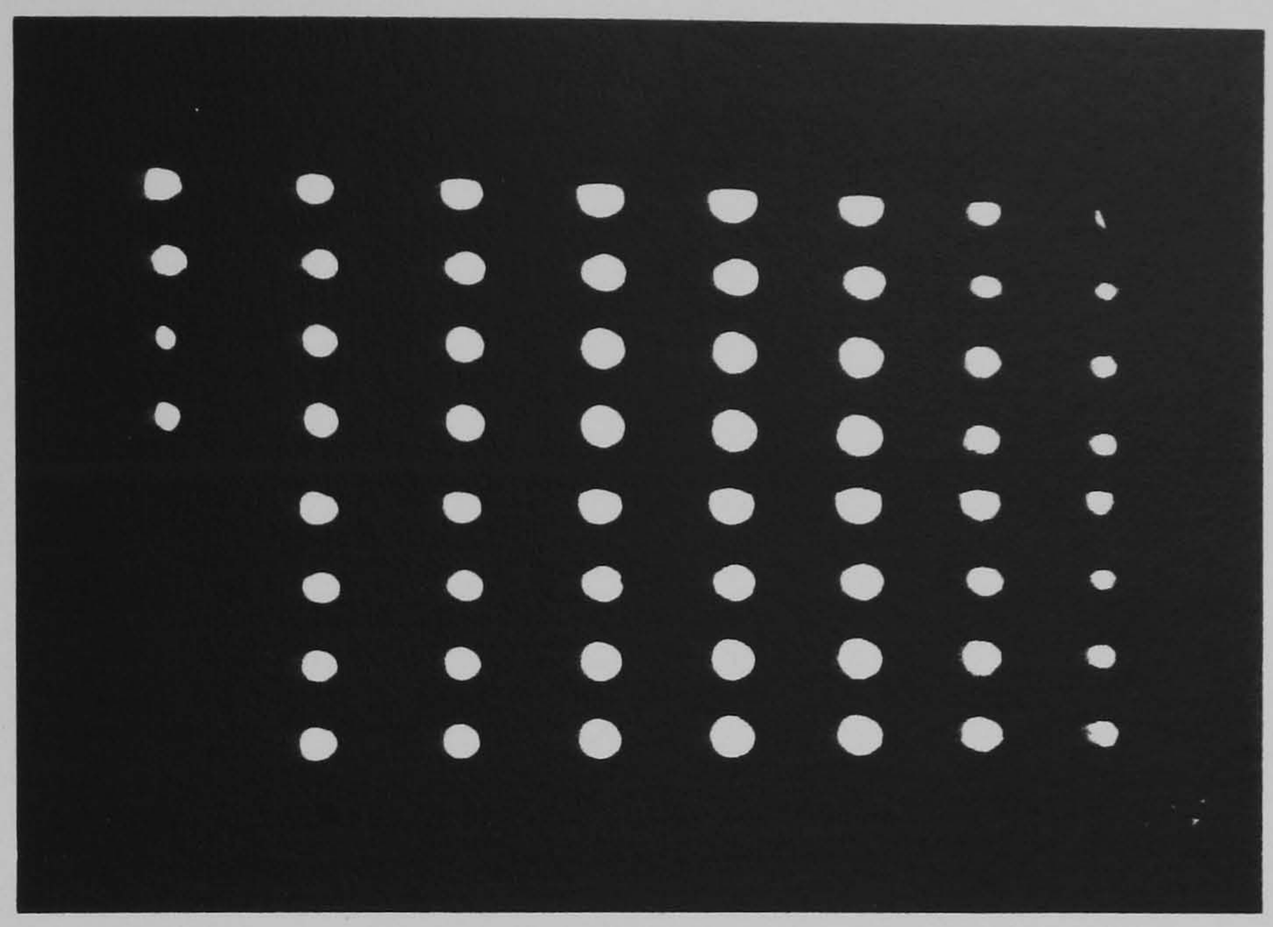

Fig. 6.26 Framing record at 2 X 10^7 frames/second showing neither anode to cathode direction of discharge propagation nor vice versa

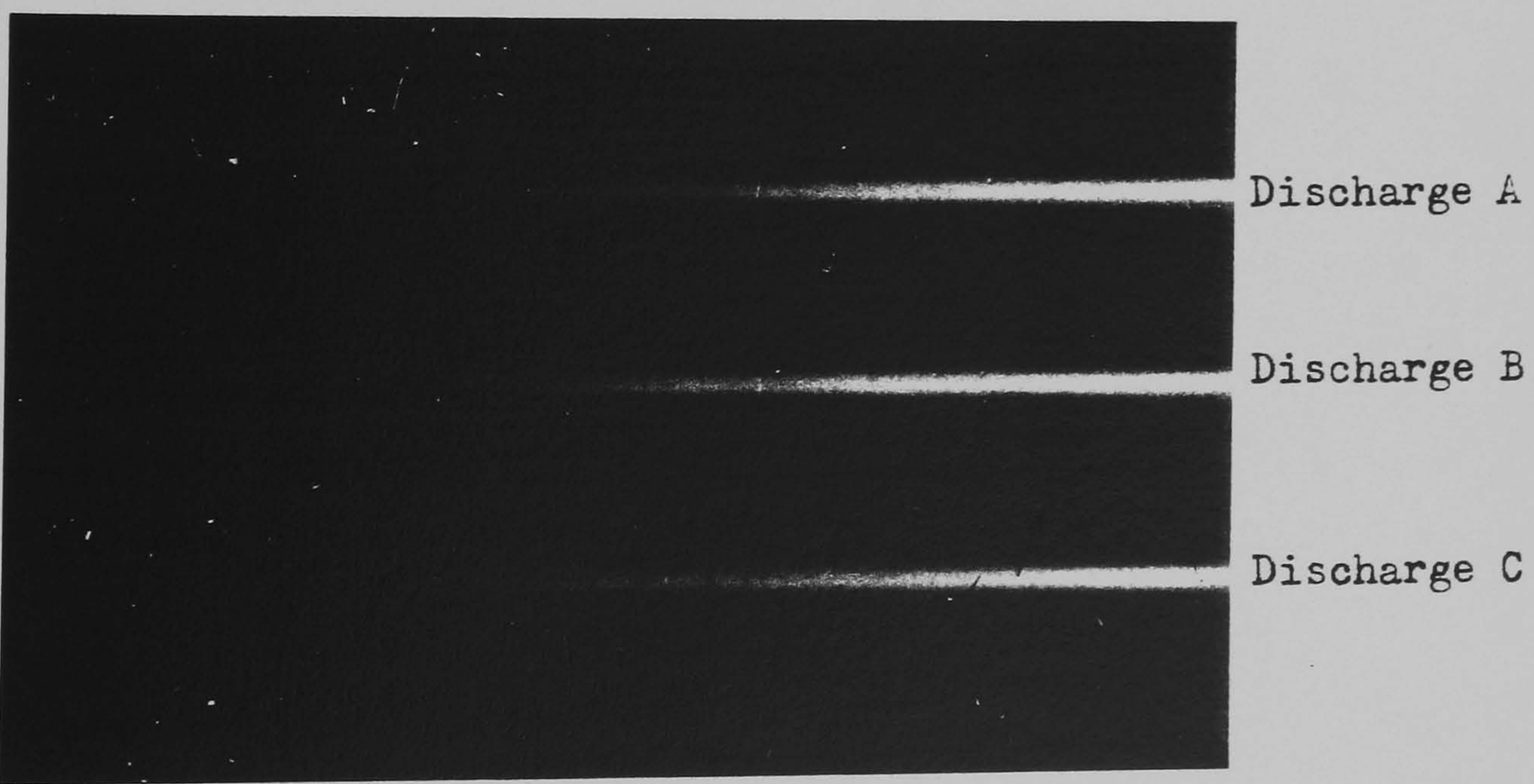

Fig. 6.27 Streak record of 3 gaps at 1 ns/mm

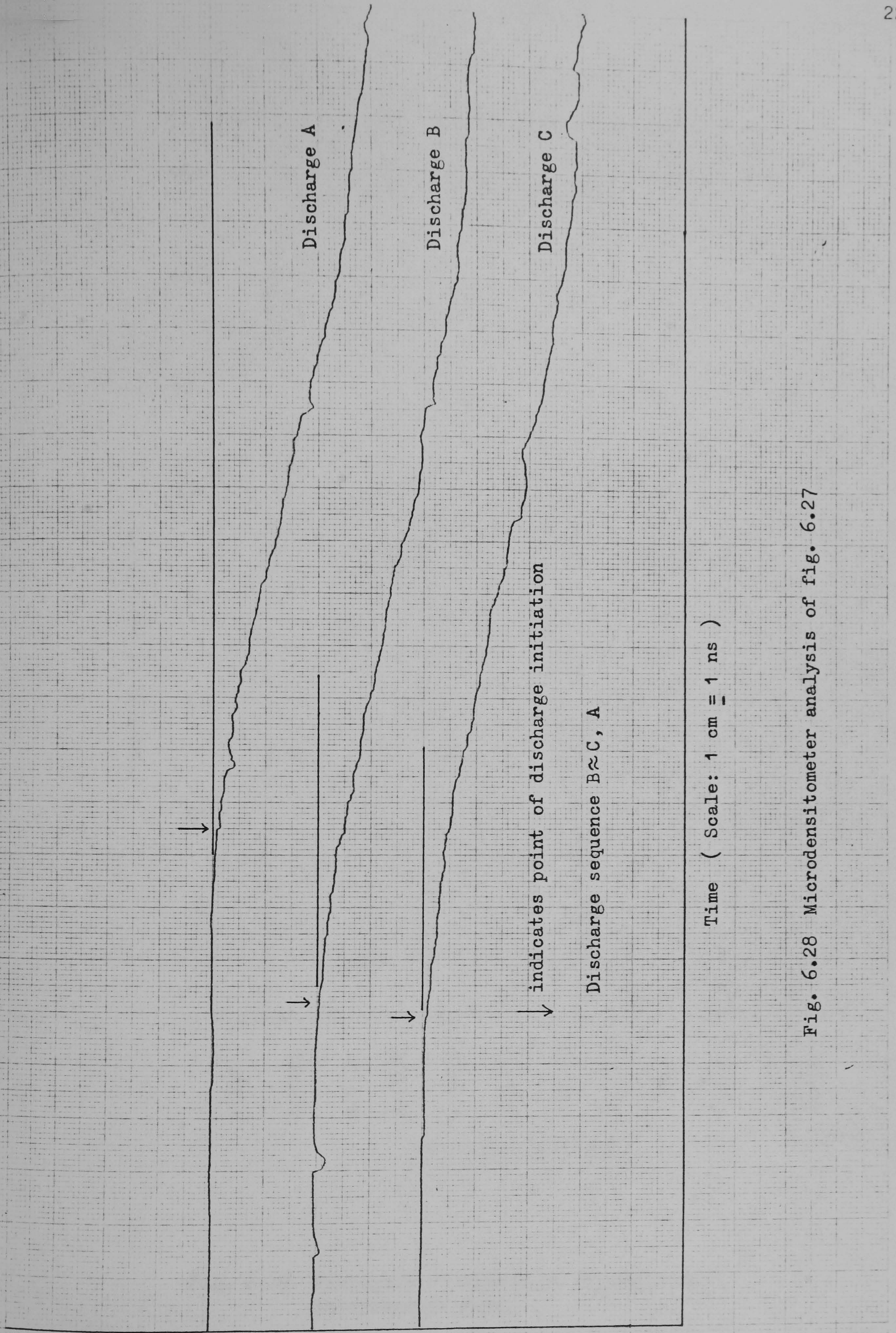

Fig. 6.28 Microdensitometer analysis of fig. 6.27

≈ Used to indicate that the sequence cannot be accurately determined as the time delay between the discharges associated with the symbol fell within the range of uncertainty

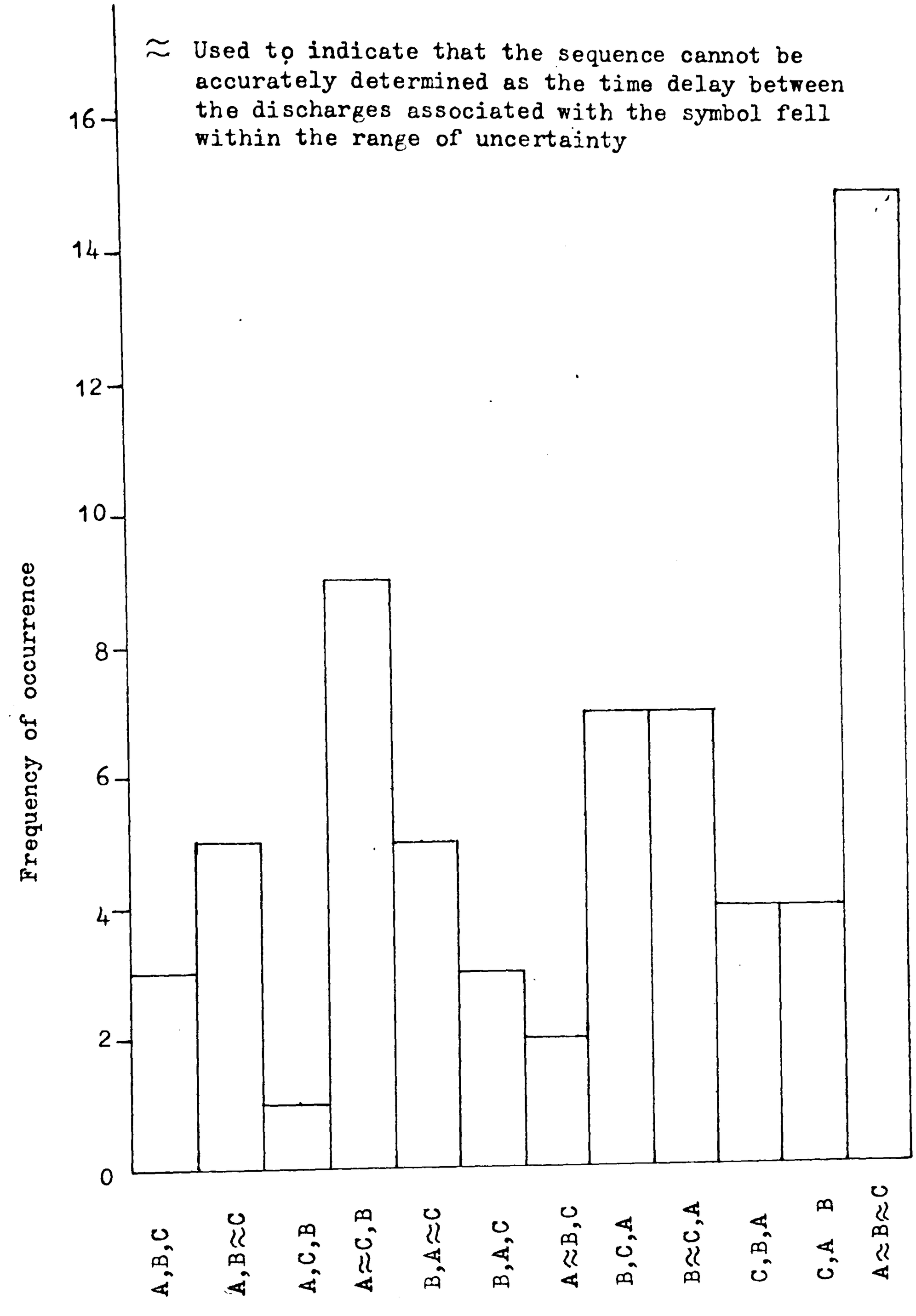

Fig. 6.29 Histogram of discharge sequence for 3 intersegment gaps.

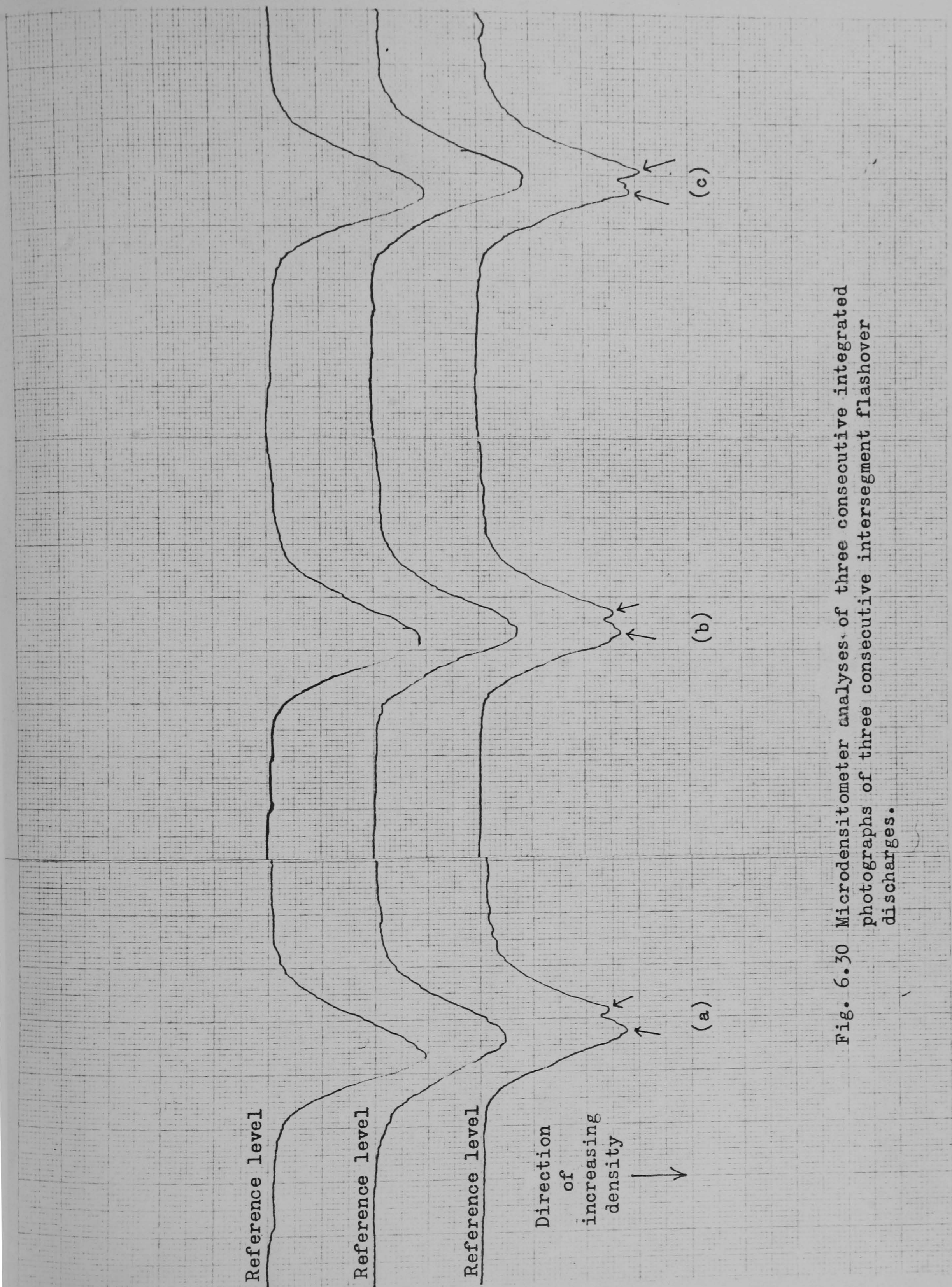

Fig. 6.30 Microdensitometer analyses of three consecutive integrated photographs of three consecutive intersegment flashover discharges.

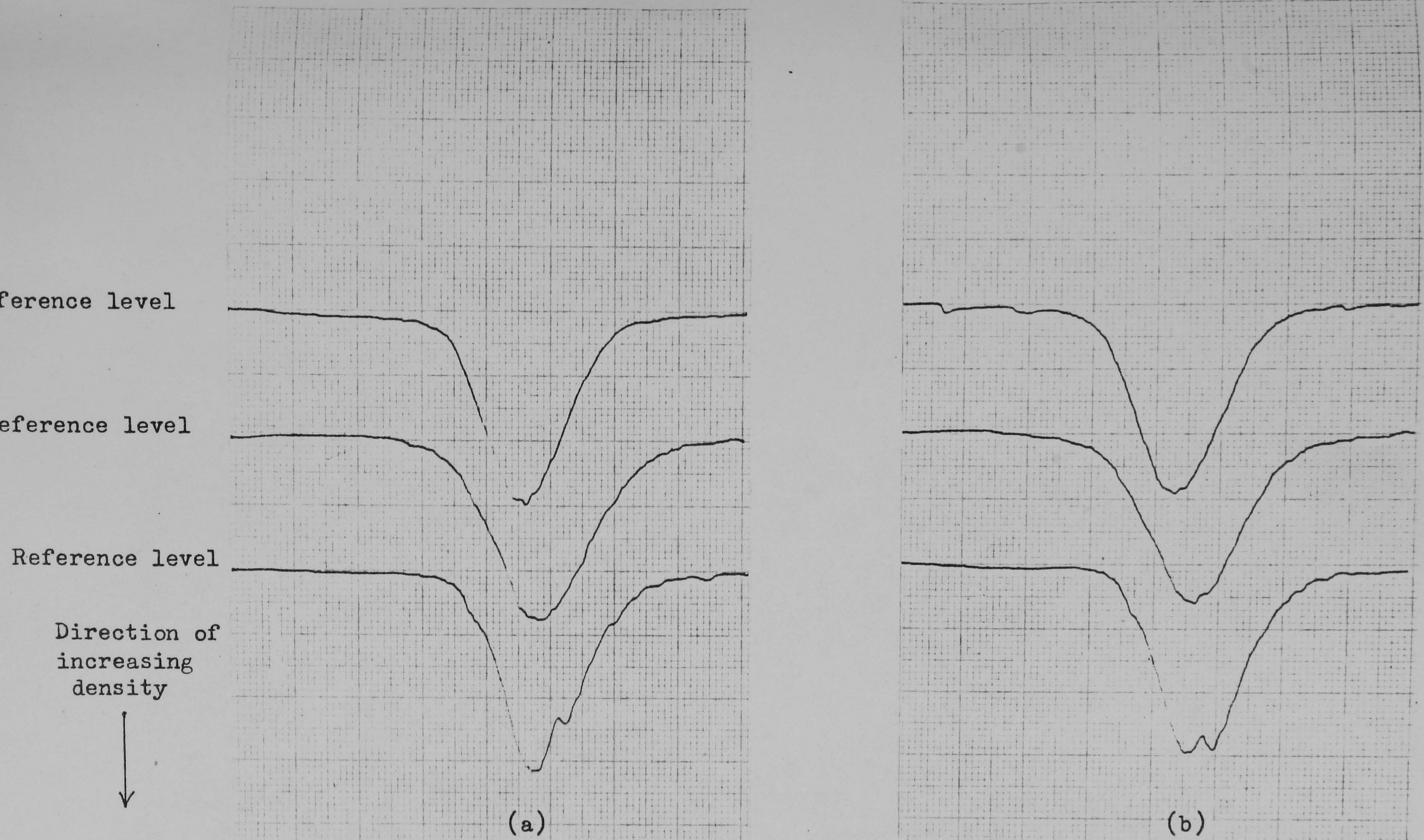

Fig. 6.31 Microdensitometer analyses of two consecutive integrated photographs of three consecutive intersegment flashover discharges.

For all waveforms, vertical scale = 220 mA/division

horizontal scale = 1 μs/division

Fig. 6.32 Current waveform with superimposed oscillations.

Fig. 6.33a Damped current waveform with 28 ohms damping resistor.

Fig. 6.33b Damped current waveform with 130 ohms damping resistor.

Fig. 6.33c Damped current waveform with 400 ohms damping resistor.

Fig. 6.33d Damped current waveform with 1 k ohms damping resistor.

Fig. 6.33e Damped current waveform with 1.5 k ohms damping resistor.

Fig. 6.33f Damped current waveform with 4 k ohms damping resistor.

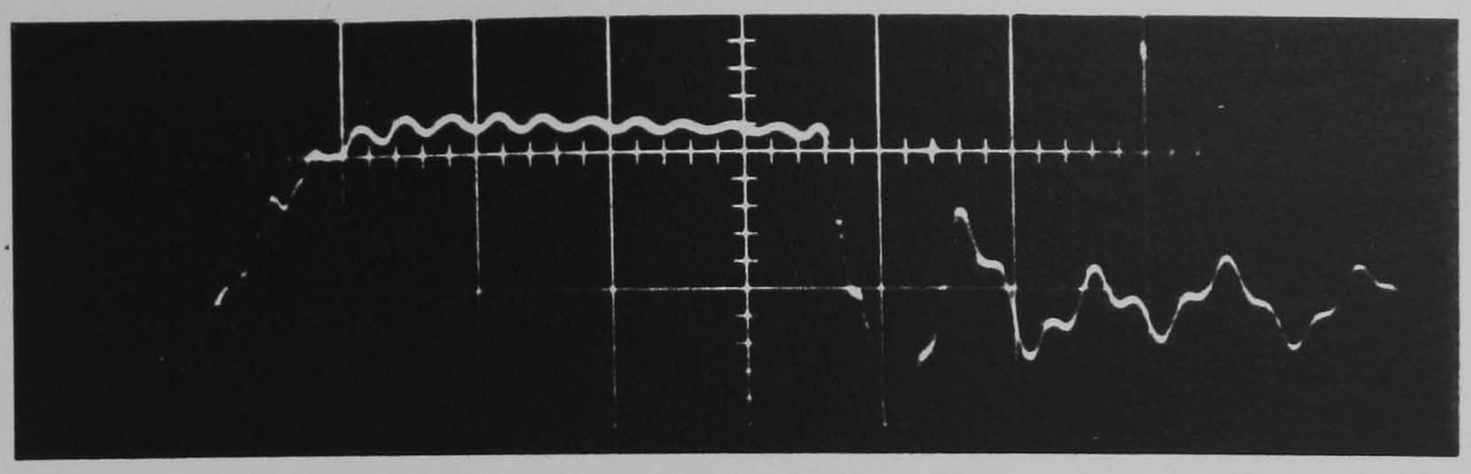

Fig. 6.32

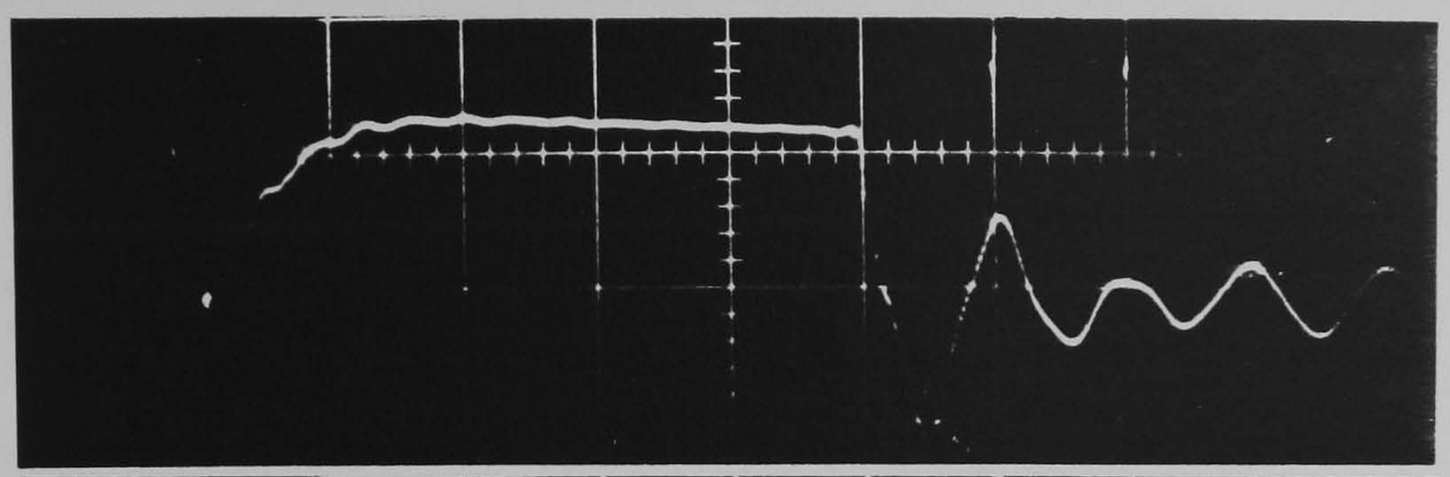

Fig. 6.33a

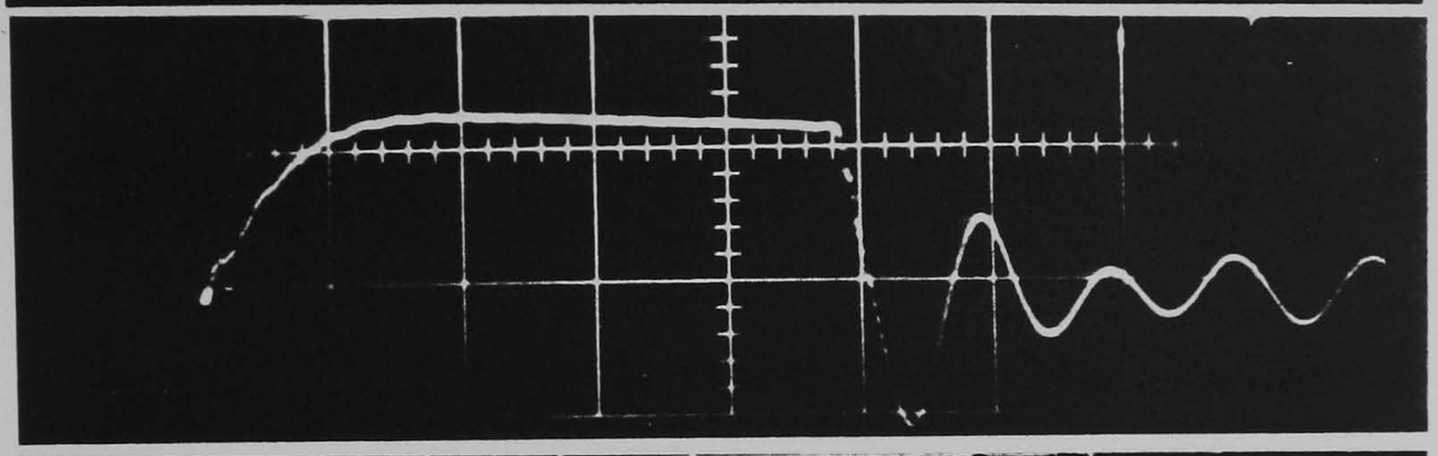

Fig. 6.33b

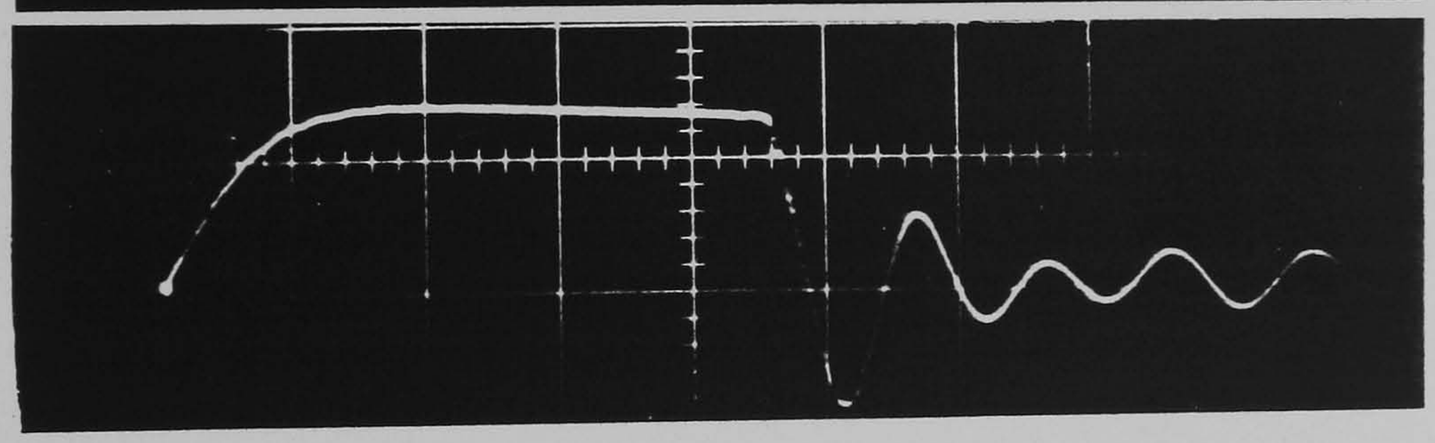

Fig. 6.33c

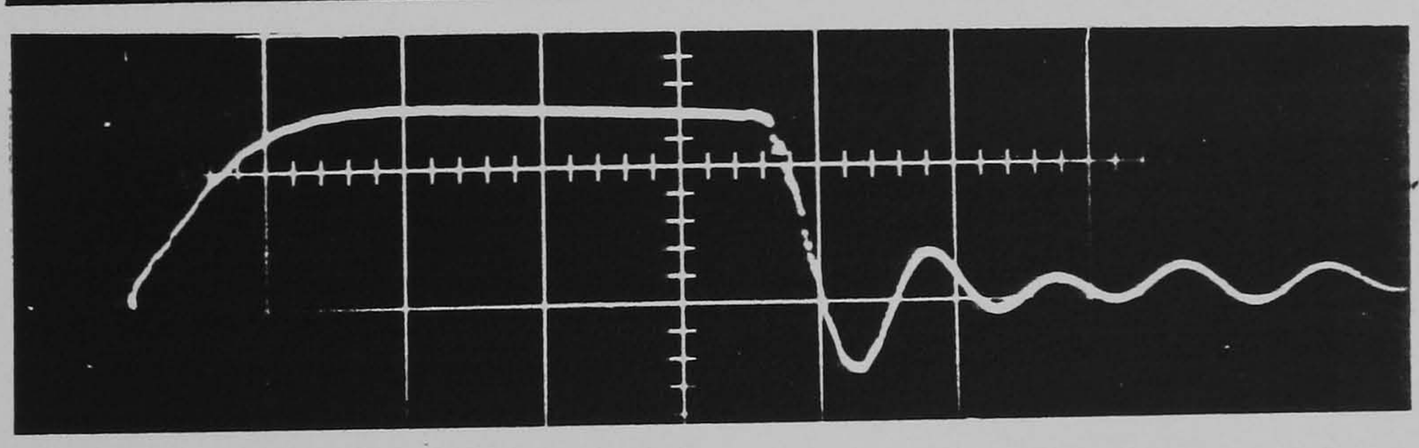

Fig. 6.33d

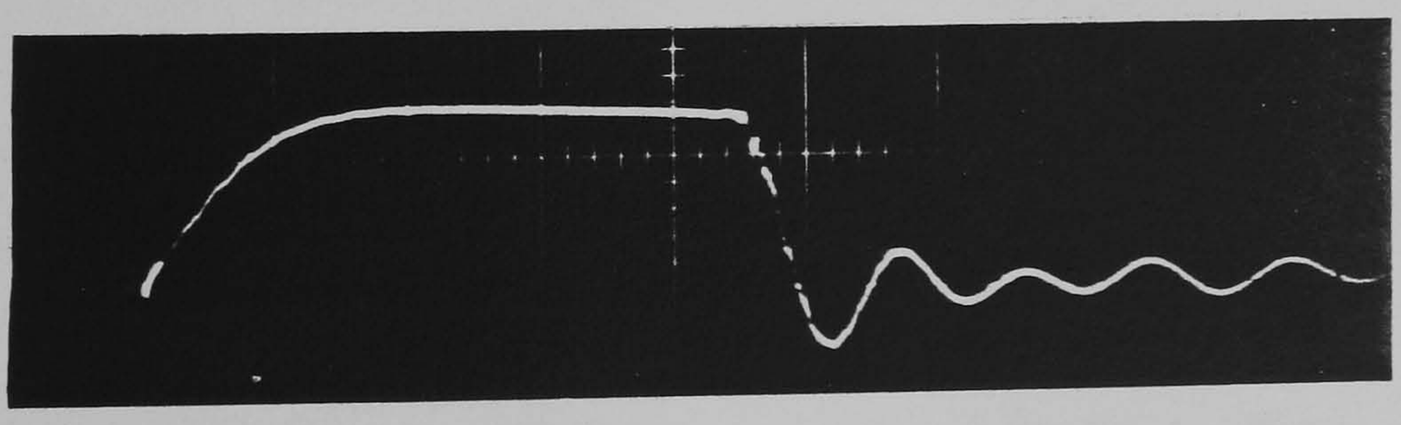

Fig. 6.33e

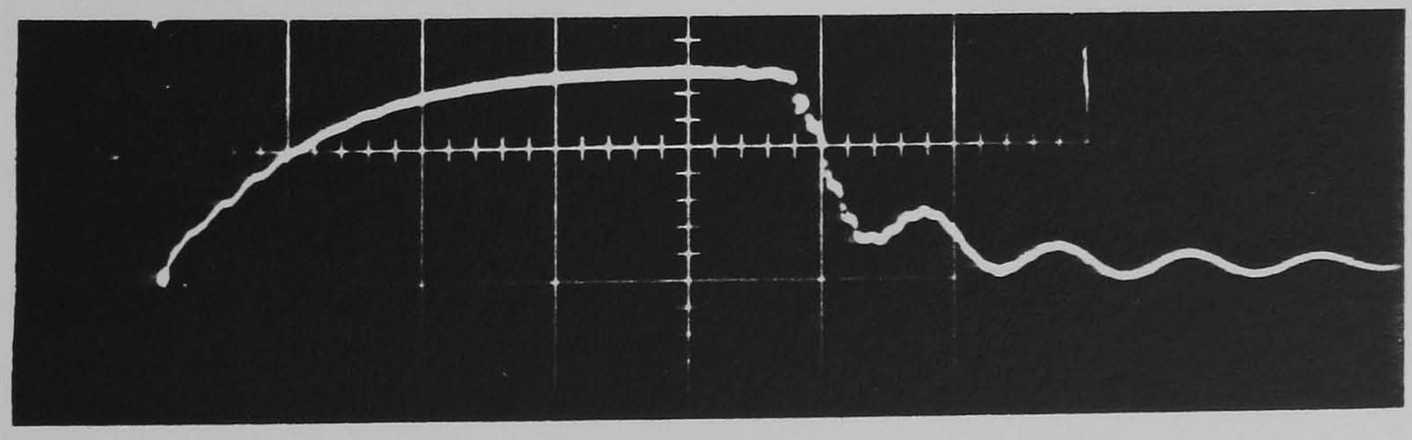

Fig. 6.33f

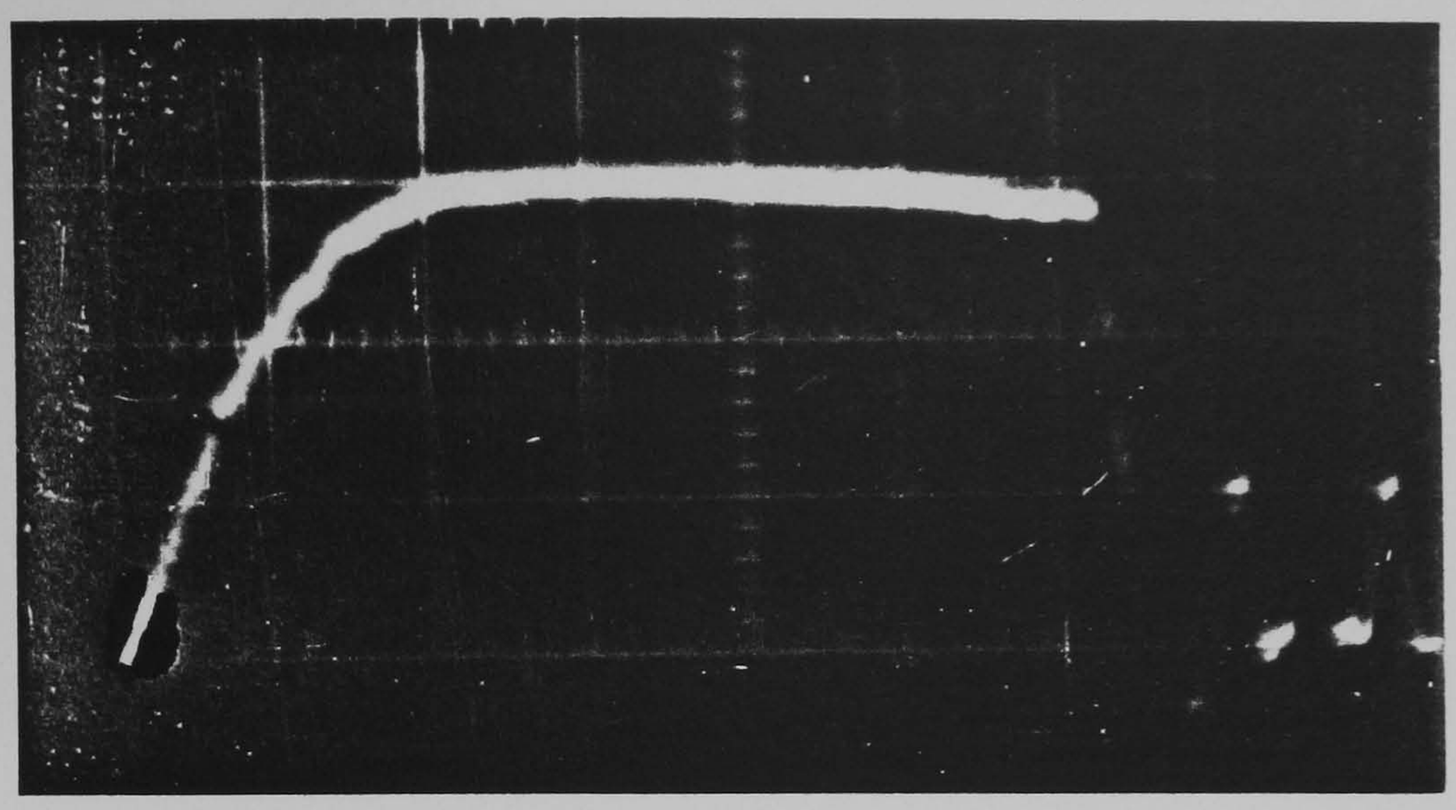

Fig. 6.34 Resistive layer current waveform (no discharge development)
Applied voltage = 96 kV peak
Vertical scale = 220 mA/division
Horizontal scale= 1 μs/division

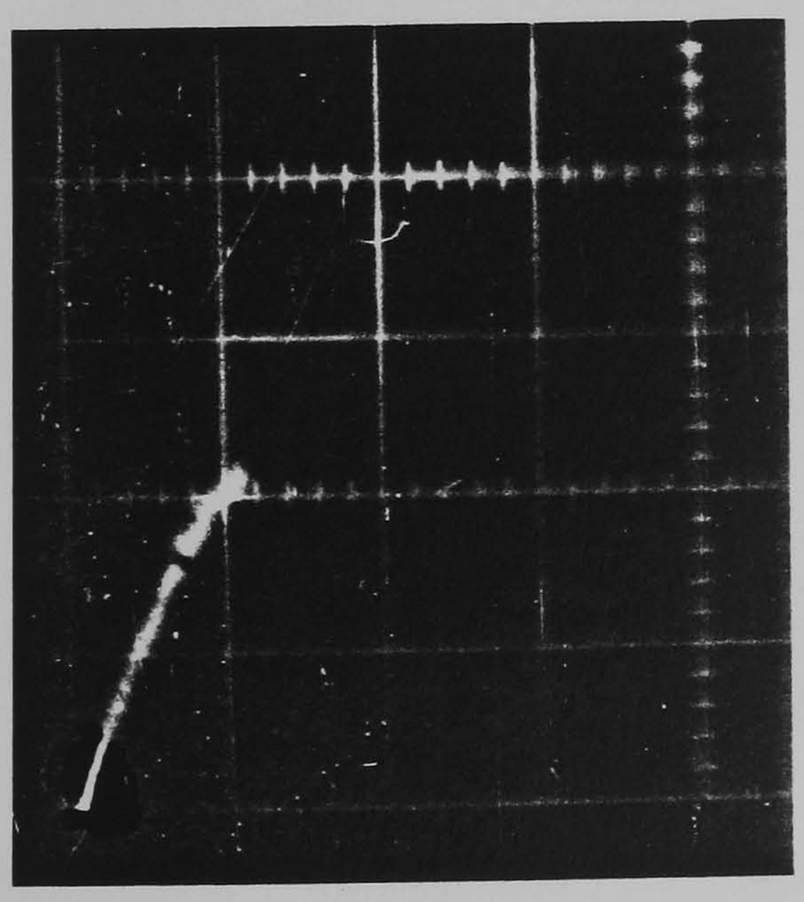

Fig. 6.35 Total current waveform with gap current discharge development time < 0.1 μs

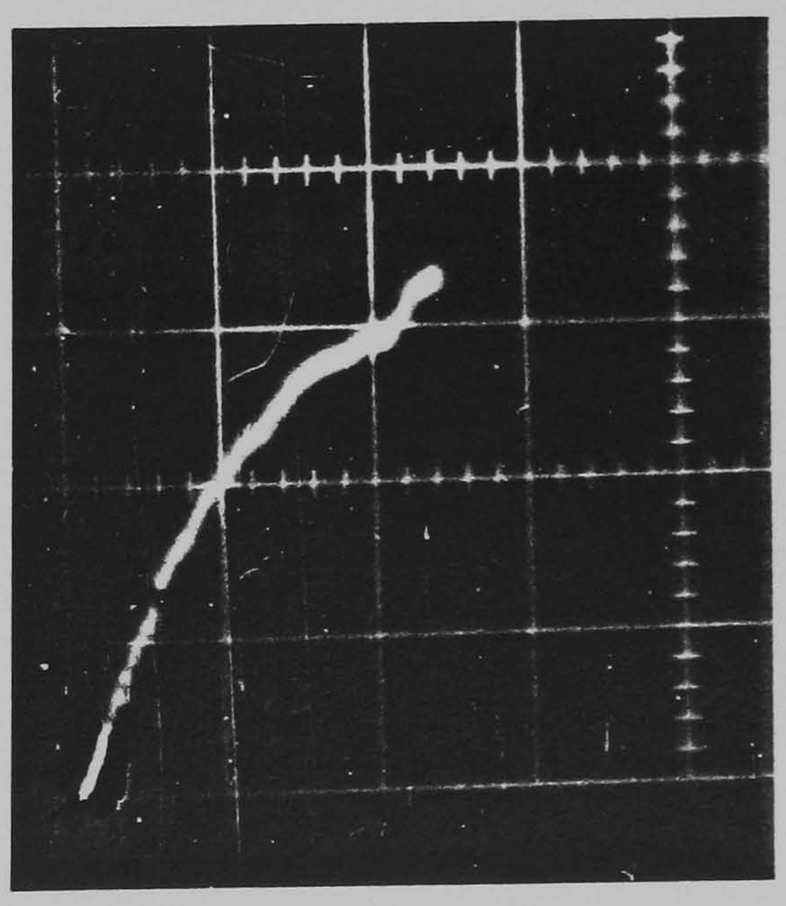

Fig. 6.36 Total current waveform with gap current discharge development time ≃ 0.8 μs

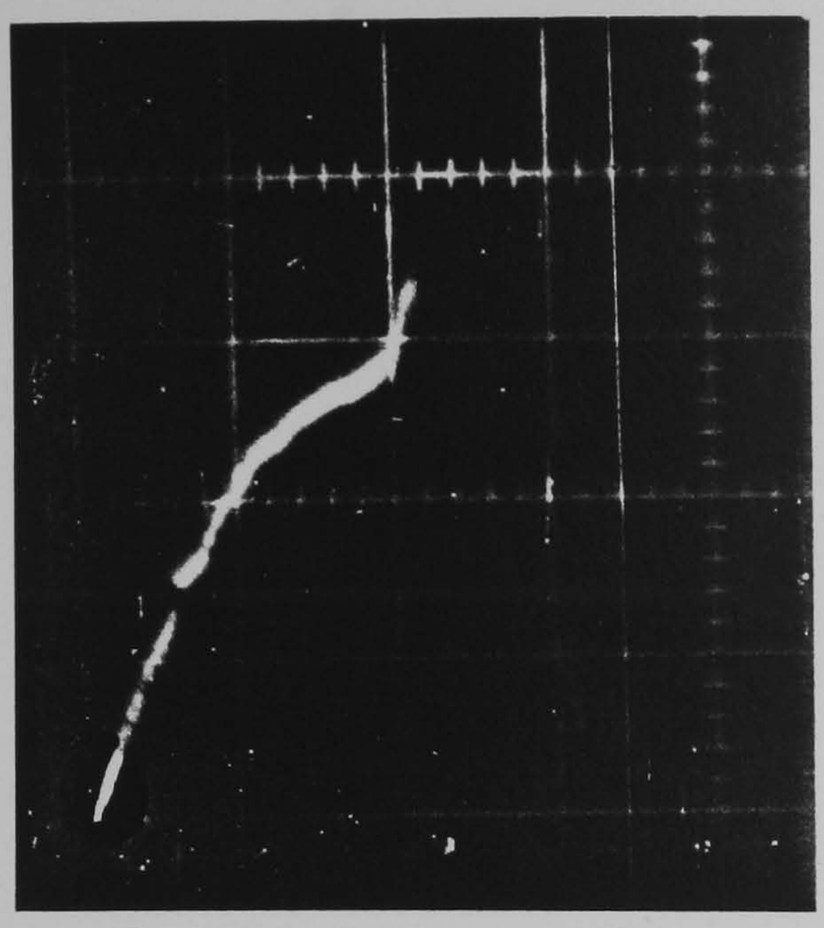

Fig. 6.37 Total current waveform with gap current discharge development time ≃1.1 μs

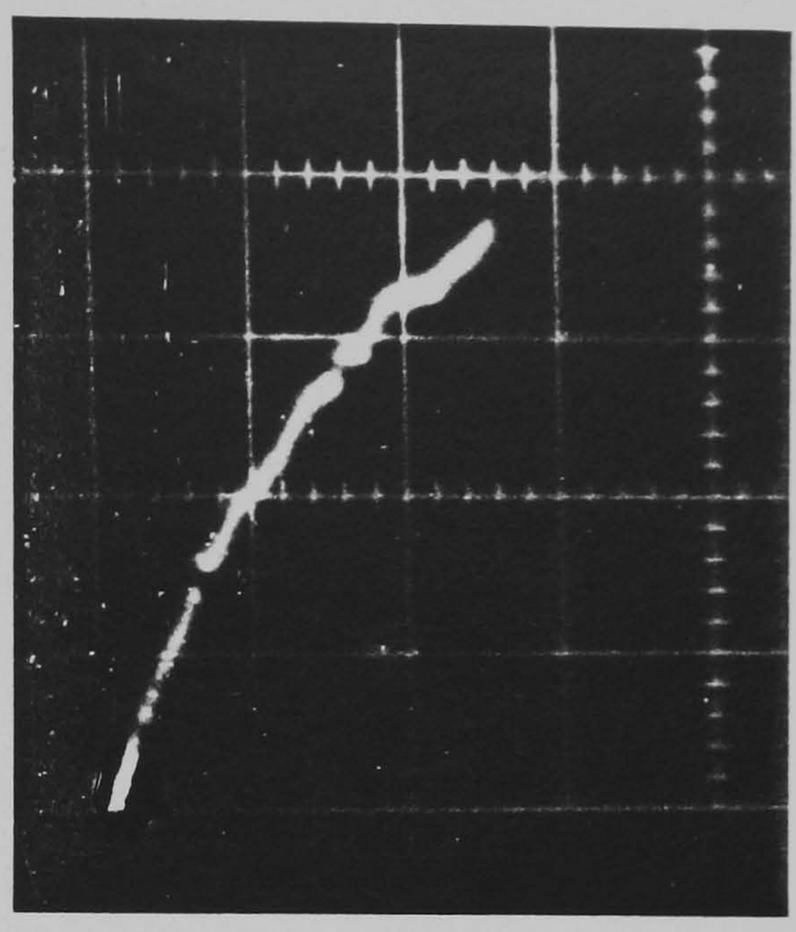

Fig. 6.38 Total current waveform with gap current discharge development time ≃ 1.2 μs

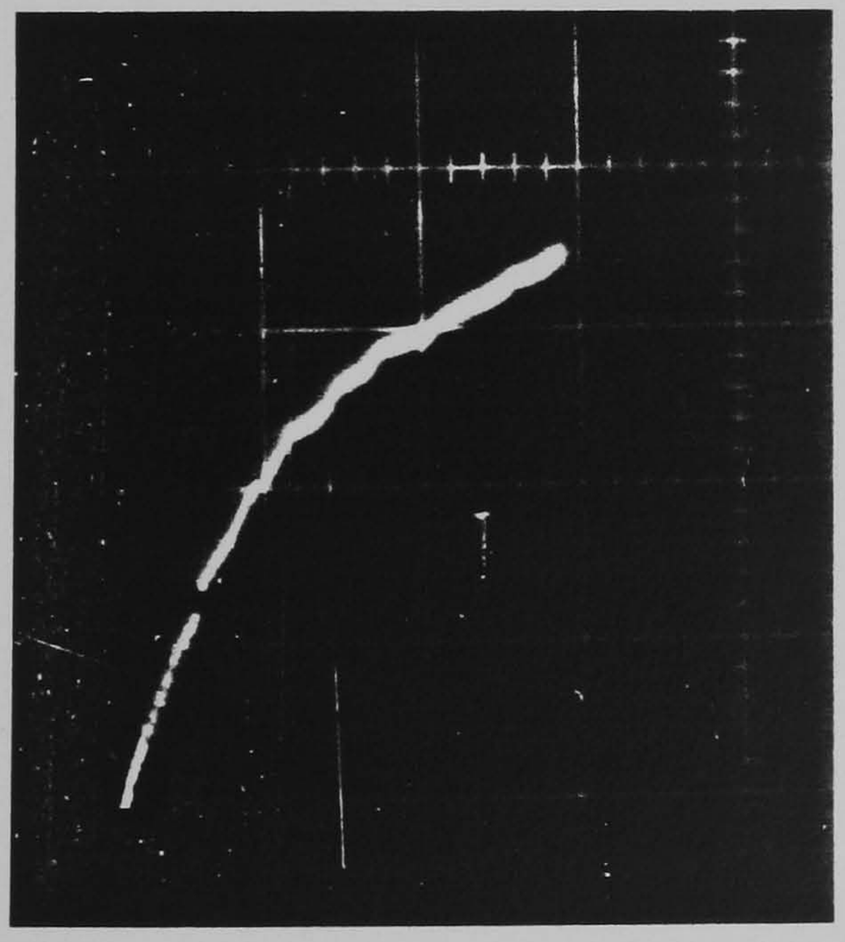

Fig. 6.39 Total current waveform with gap current discharge development time ≃ 1.9 μs

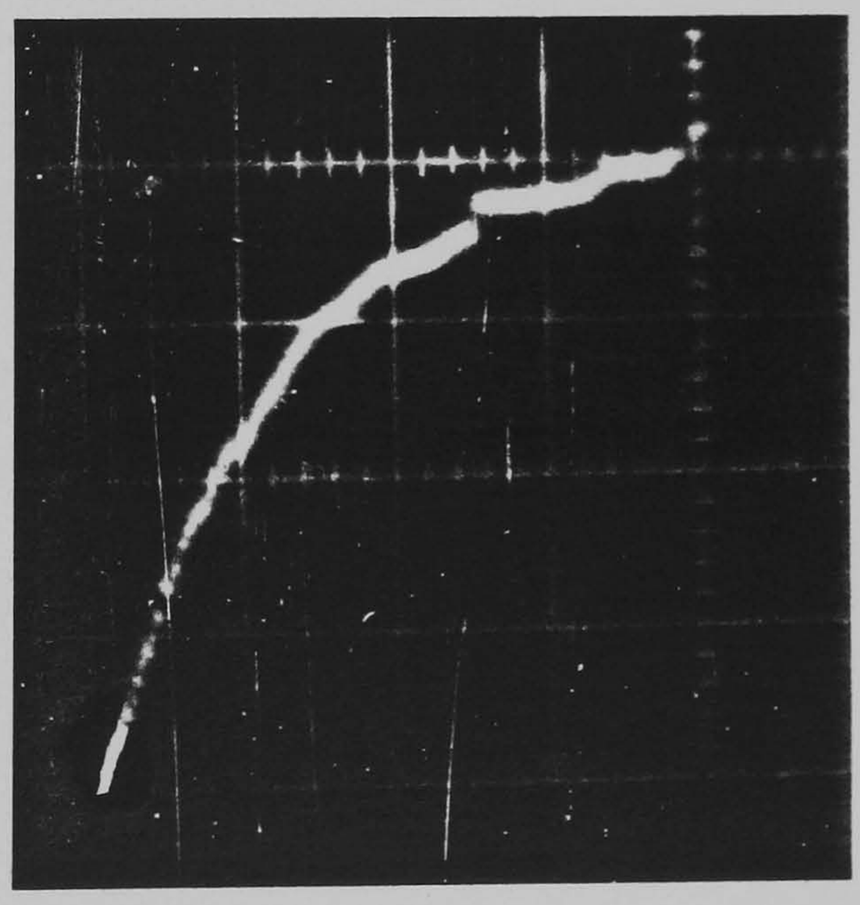

Fig. 6.40 Total current waveform with gap current discharge development time ≃ 3 μs

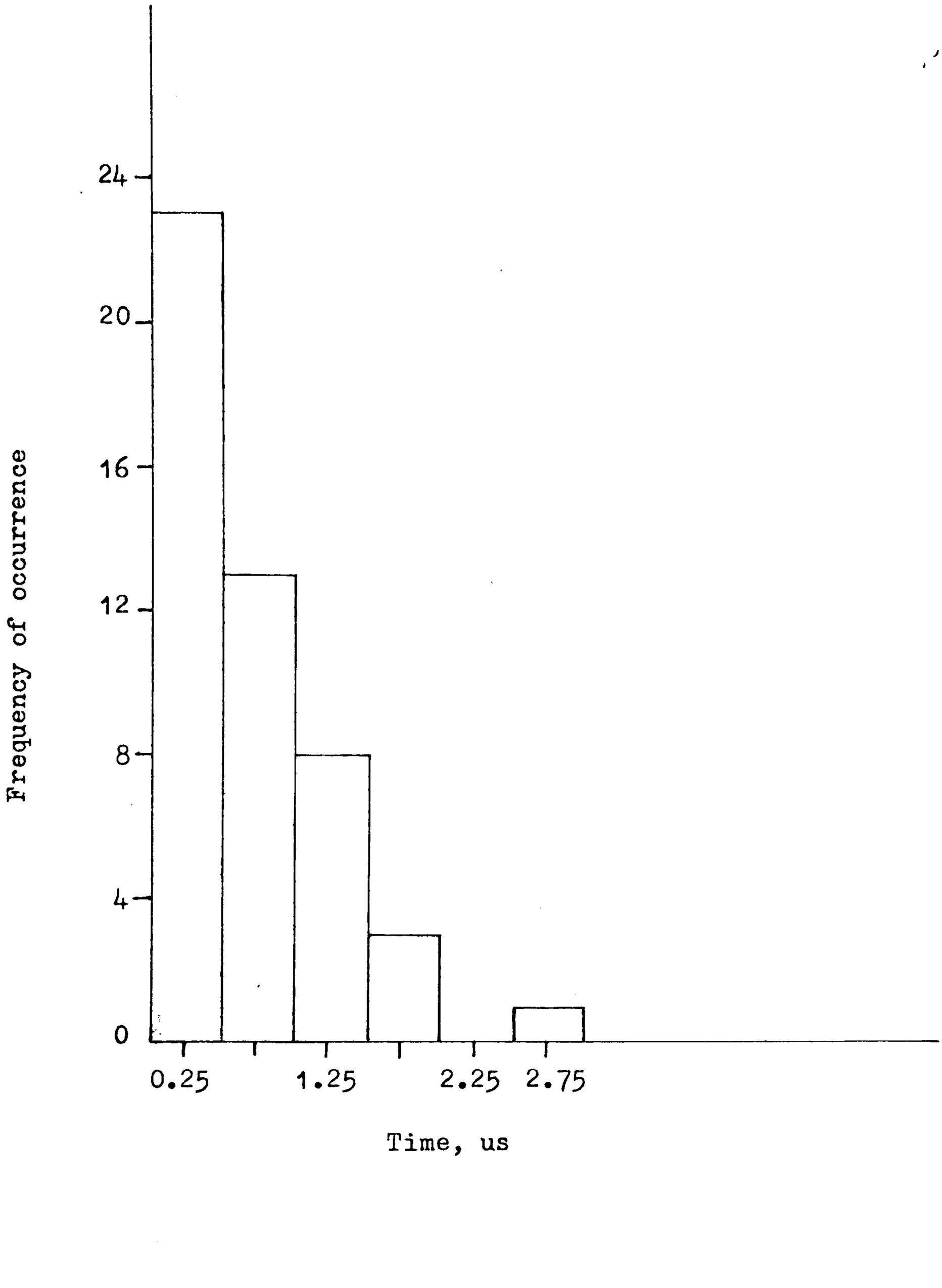

Fig. 6.41 Histogram of gap current discharge development times.

All current waveforms show the occurrence of isolated intersegment discharges.
Vertical scale = 220 mA/division
Horizontal scale = 1 μs/division

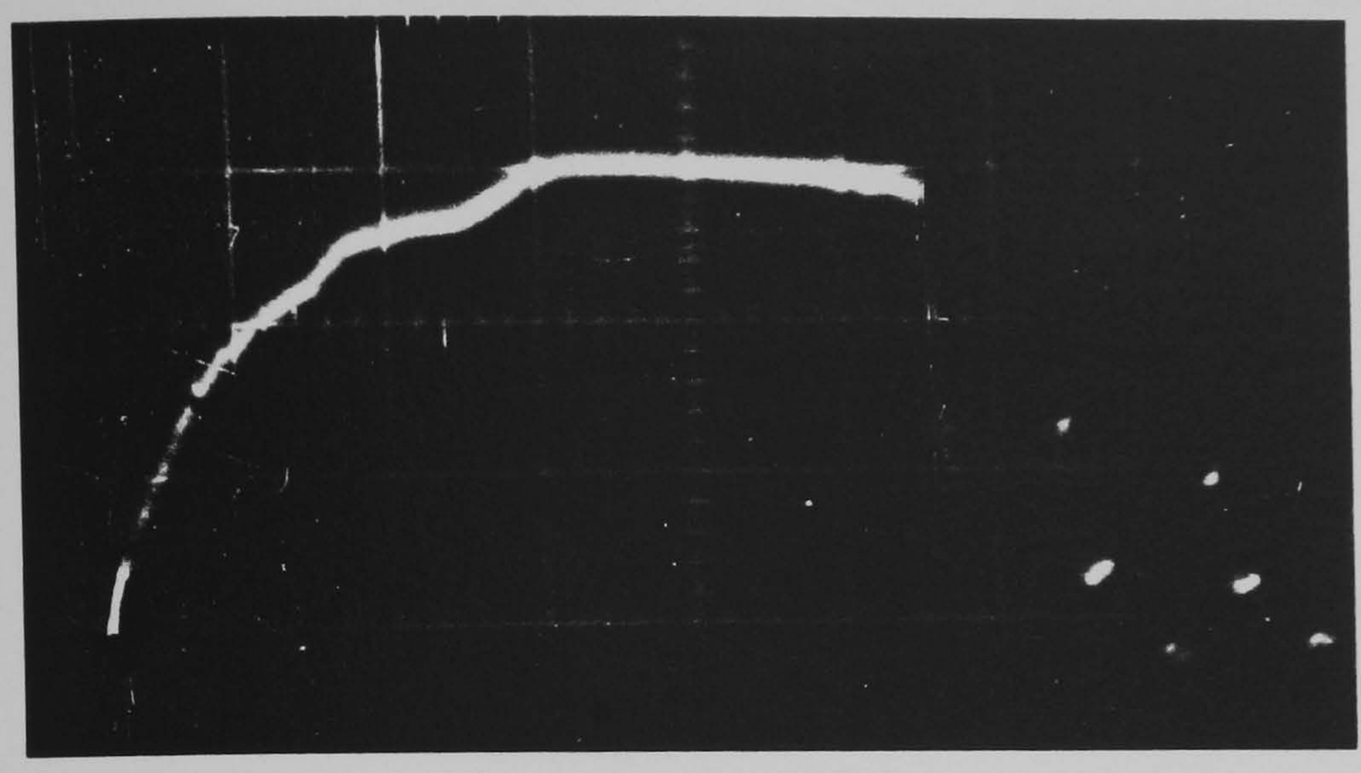

Fig. 6.42
Applied voltage=90 kV

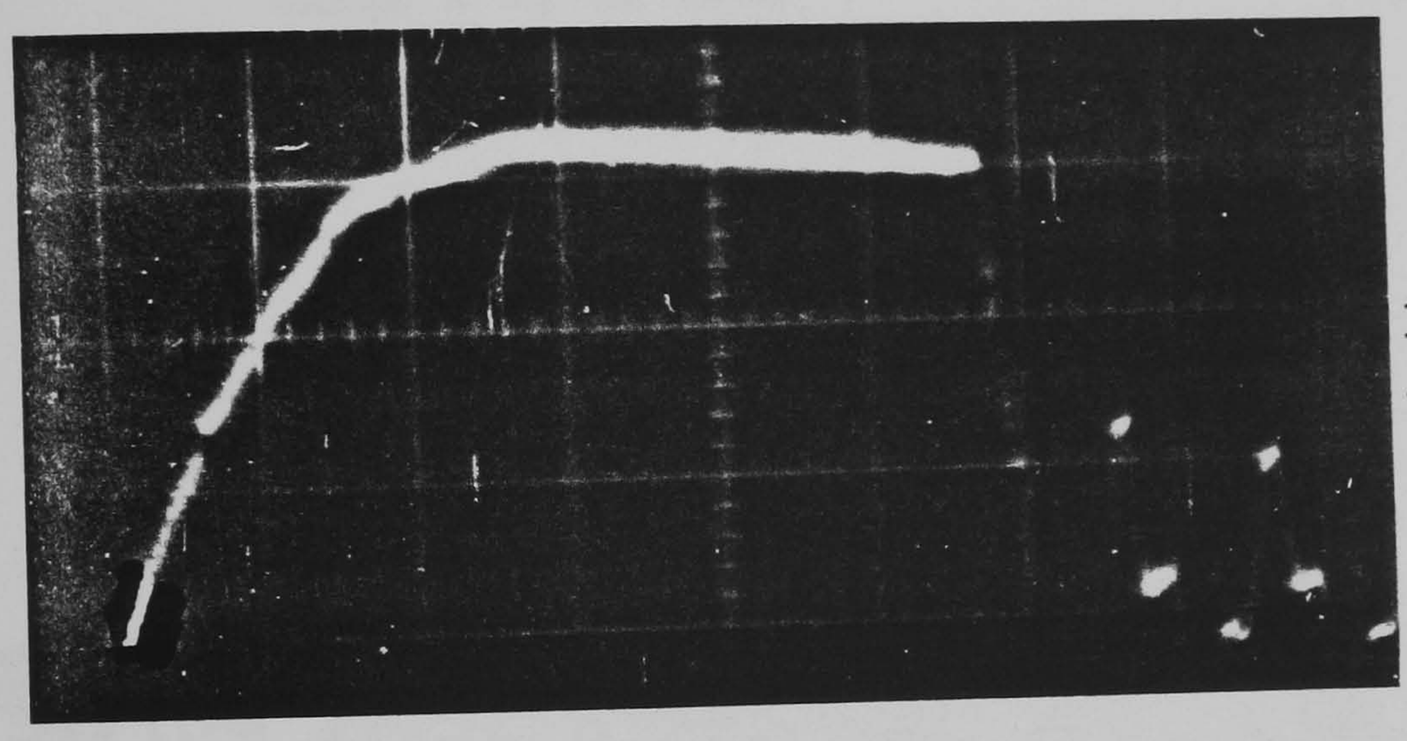

Fig. 6.43
Applied voltage=94 kV

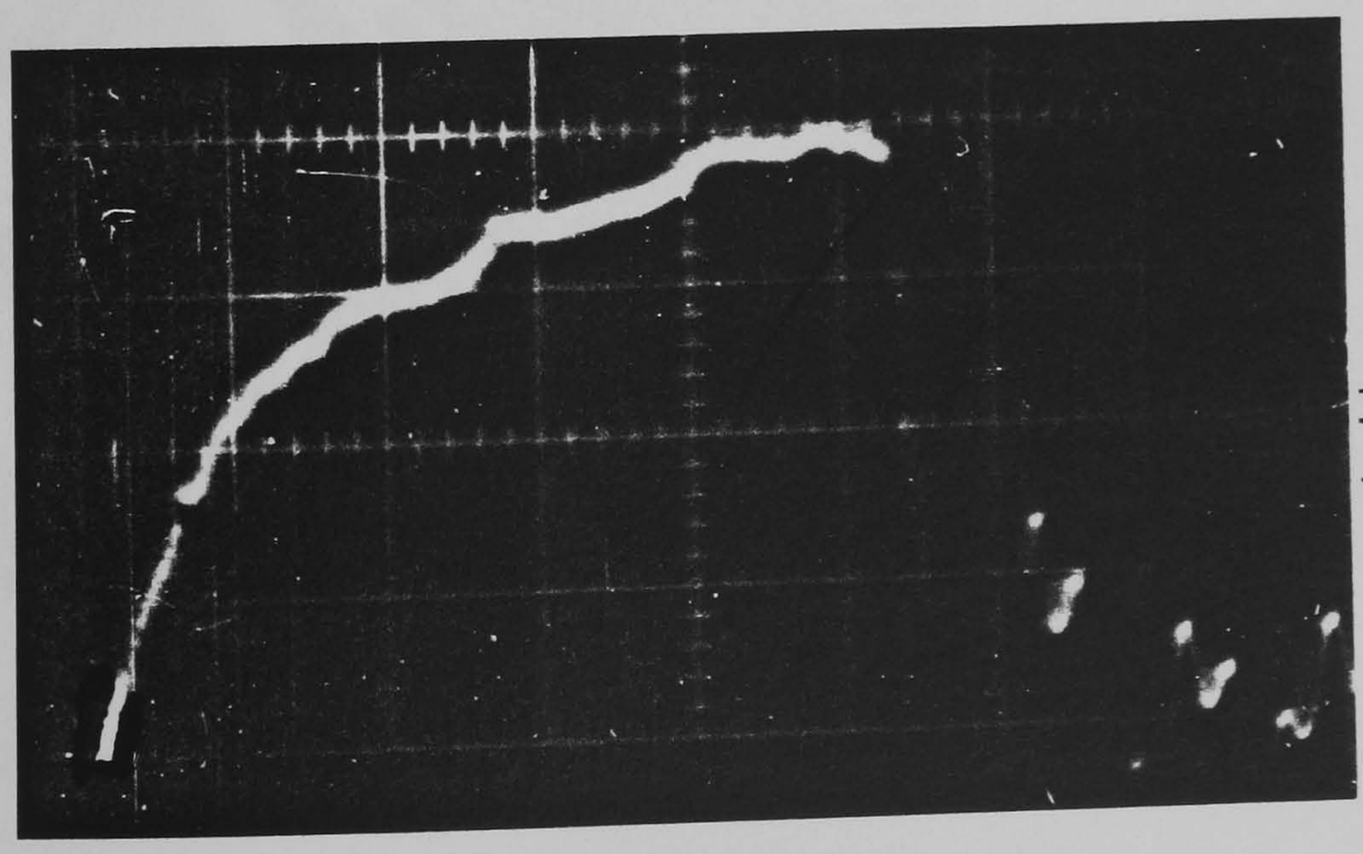

Fig. 6.44
Applied voltage=102 kV

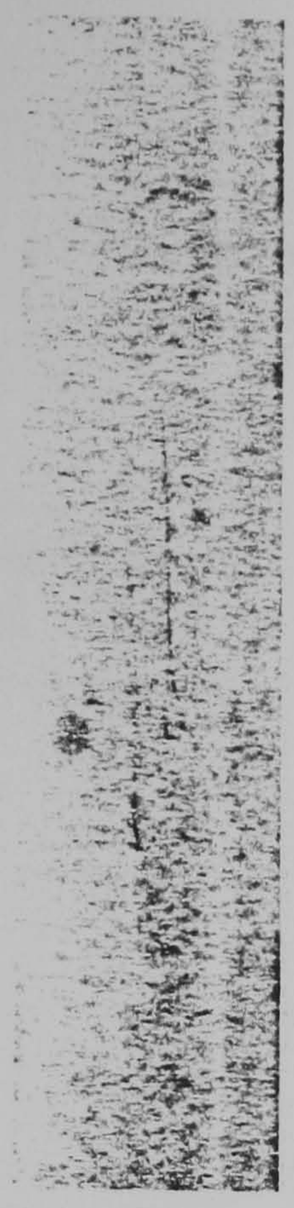

Fig. 7.1 Photograph of Dayton-Granger strip, 0.1 mm thick X 13 mm wide

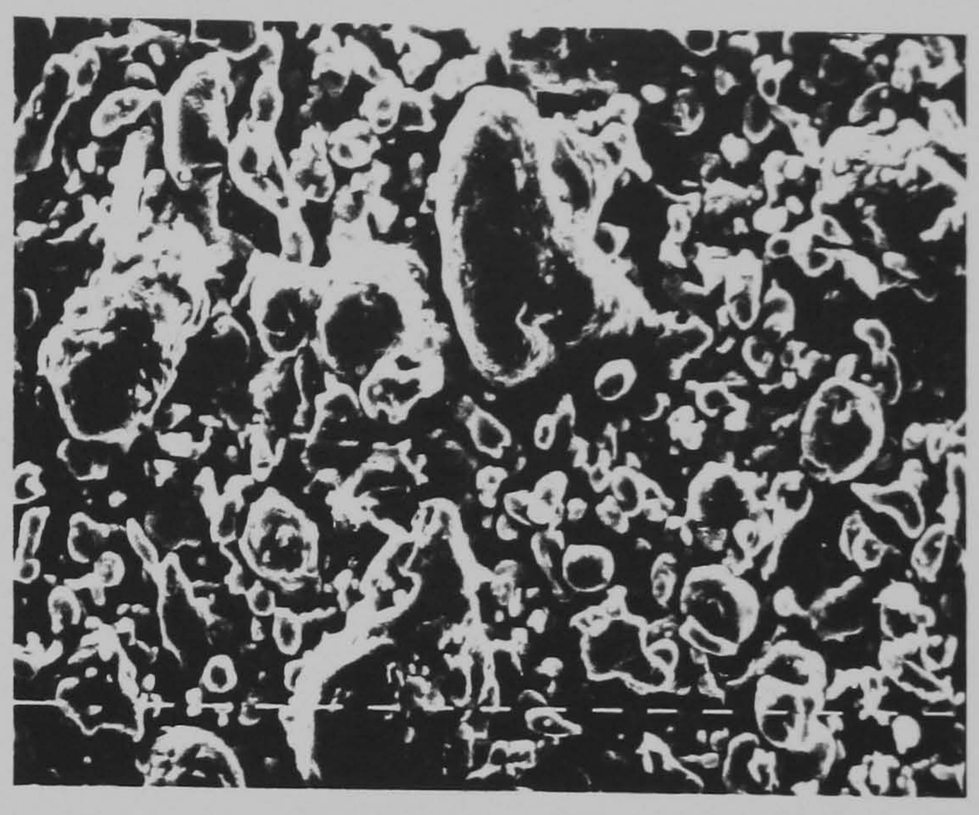

Fig. 7.2 SEM photograph of unused strip shown with 10-micron markers

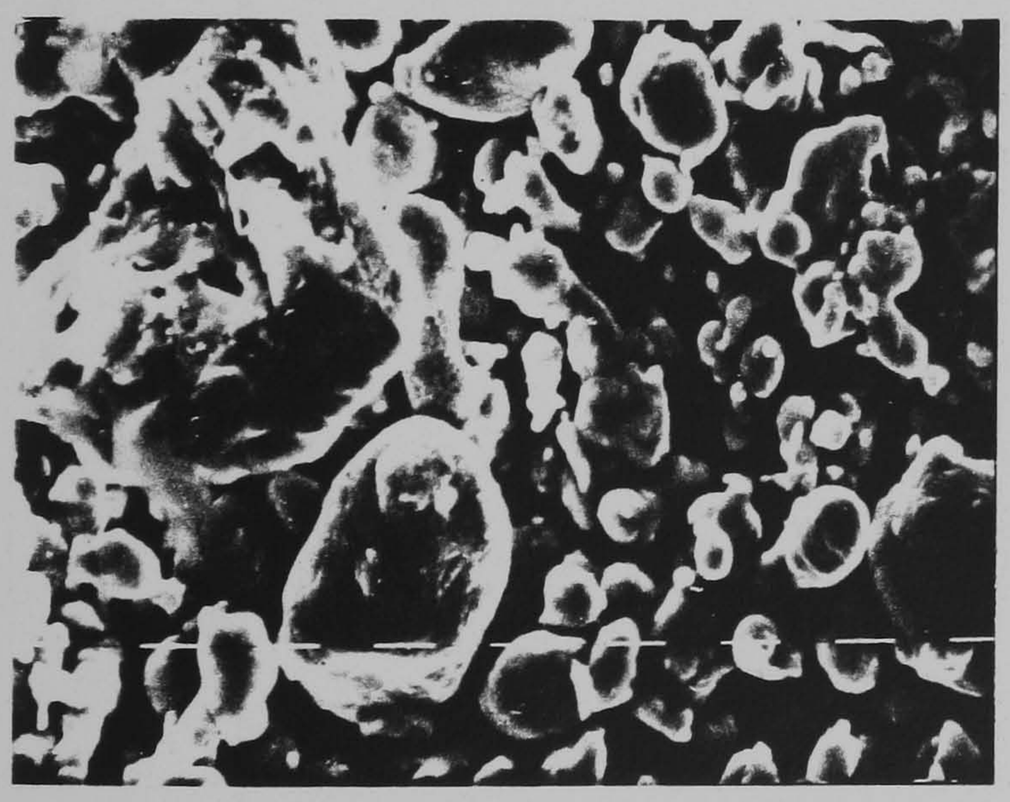

Fig. 7.3 SEM photograph of unused strip shown with 10-micron markers

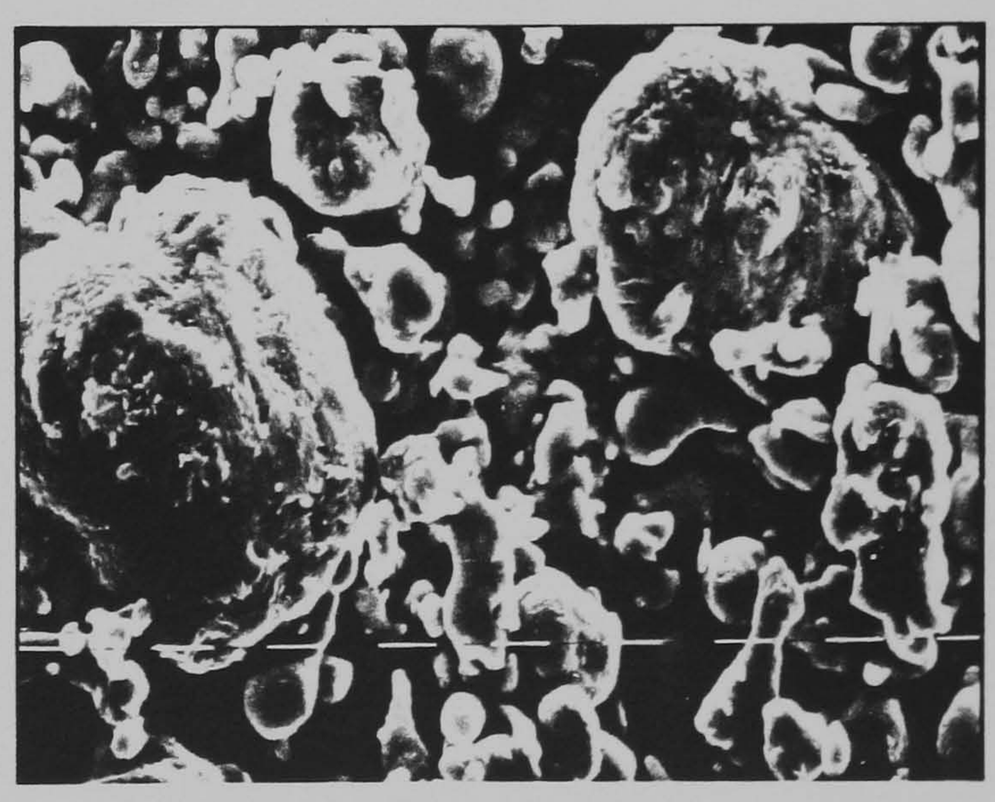

Fig. 7.4 SEM photograph of unused strip shown with 10-micron markers

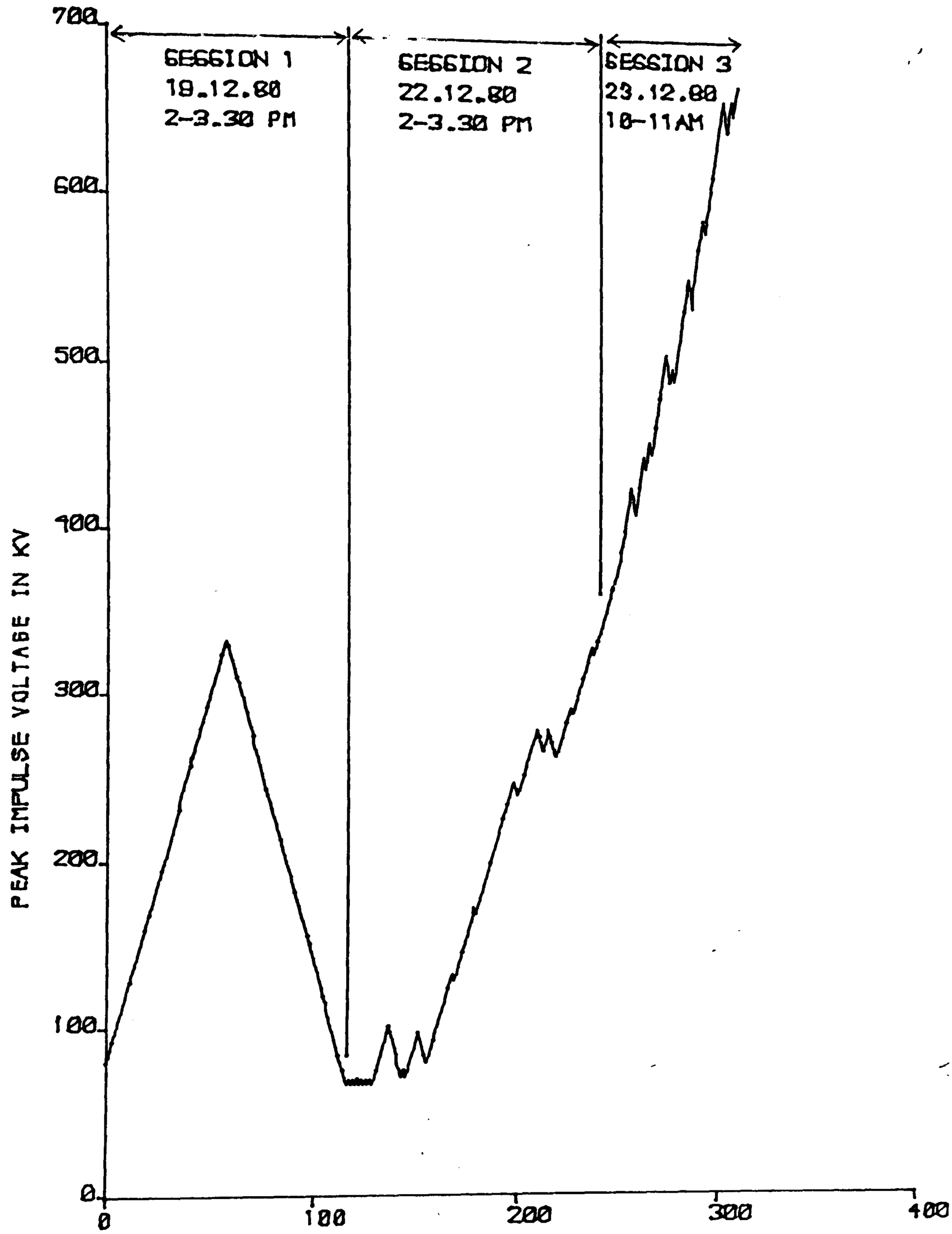

FIG. 7.5 UP & DOWN TEST RESULTS-1.01M DAYTON-GRANGER STRIP
STRIP NOT MOUNTED ON TUBE

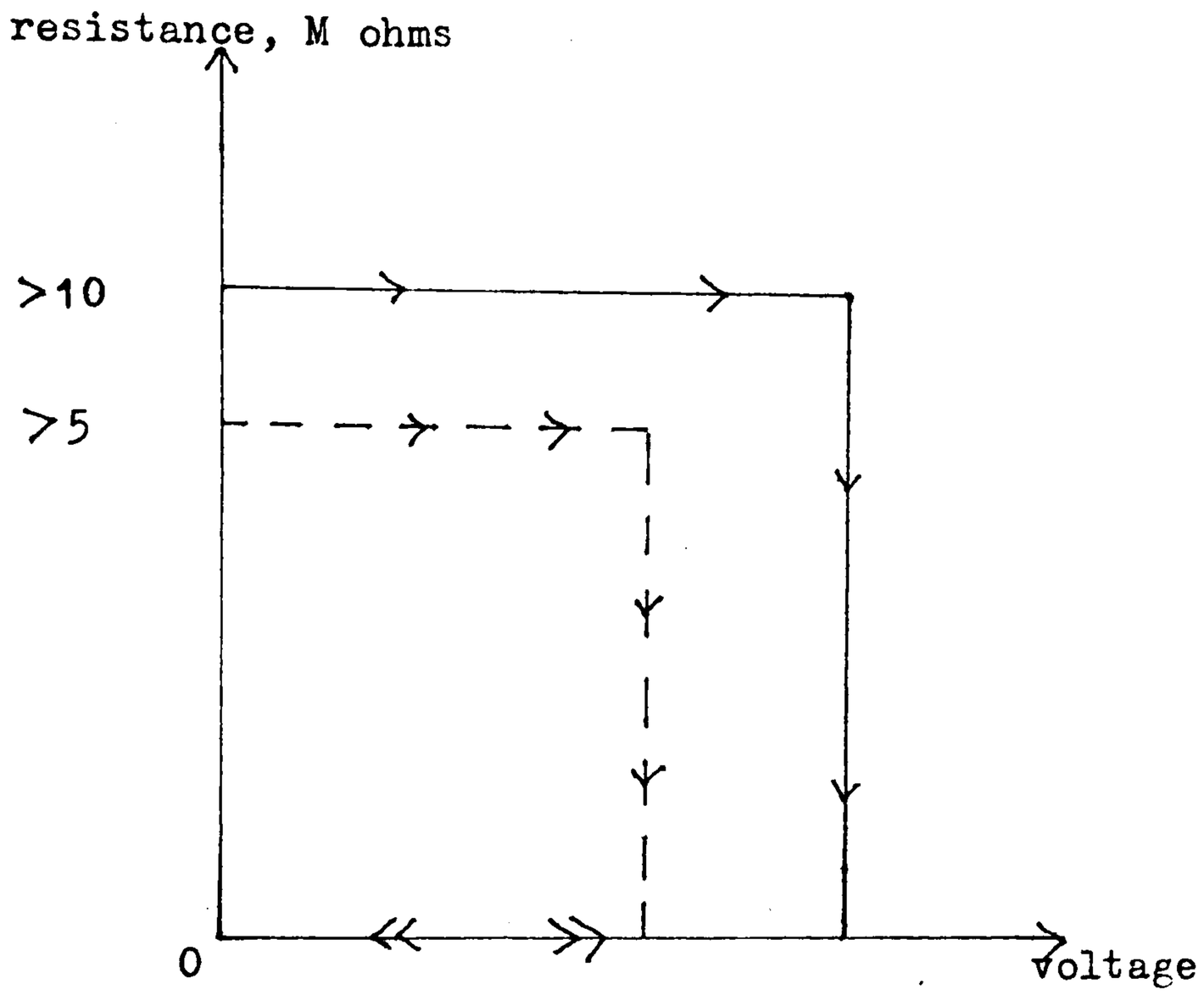

Fig. 7.6 Resistance of a strip as measured by a Megger-insulation-tester.

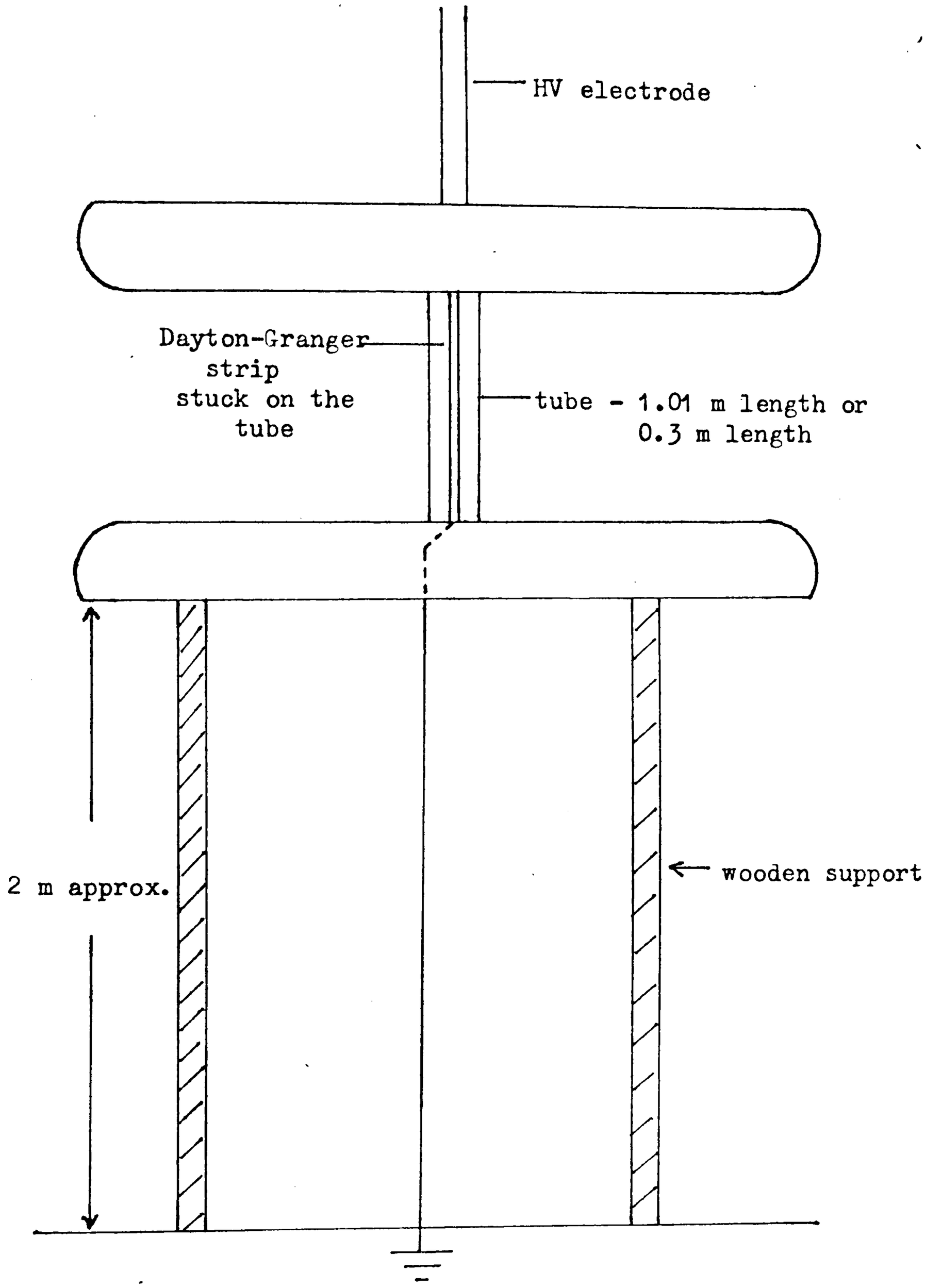

Fig. 7.7 Experimental arrangement for 'Up & Down' test on Dayton-Granger strip.

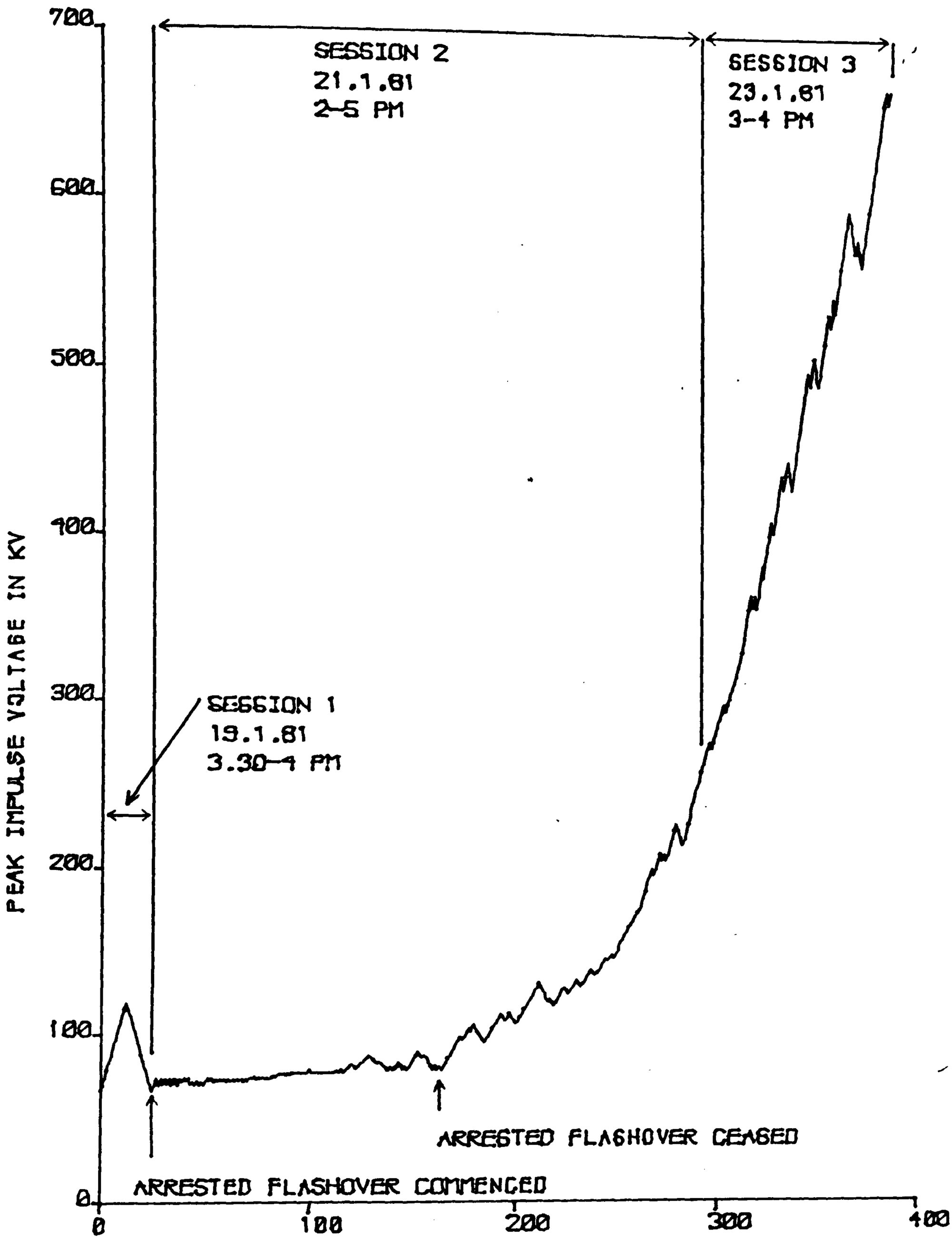

FIG. 7.8 UP & DOWN TEST RESULTS-1.01M DAYTON-GRANGER STRIP STRIP MOUNTED ON TUBE

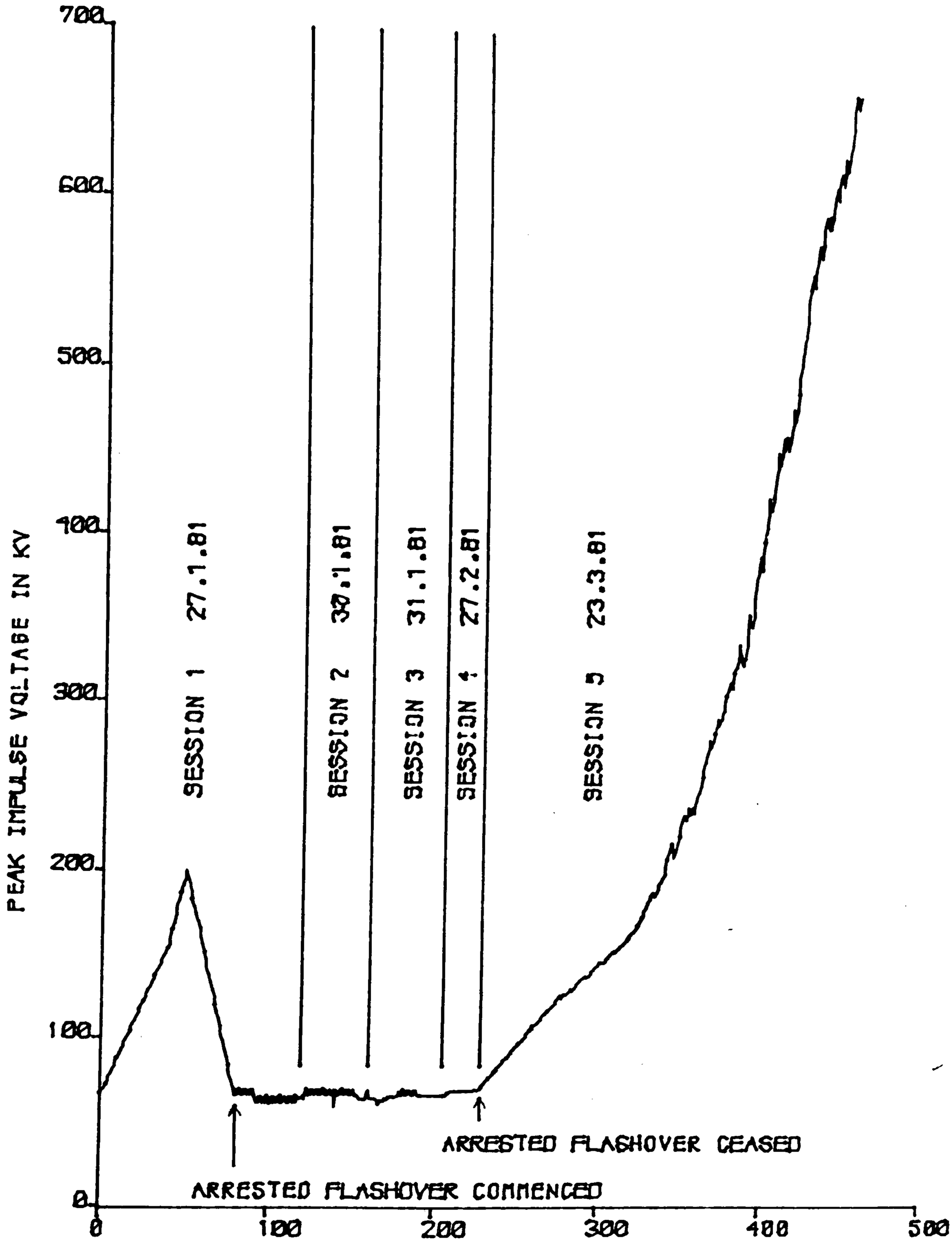

FIG.7.9 UP & DOWN TEST RESULTS-1.01M DAYTON-GRANGER STRIP STRIP MOUNTED ON TUBE

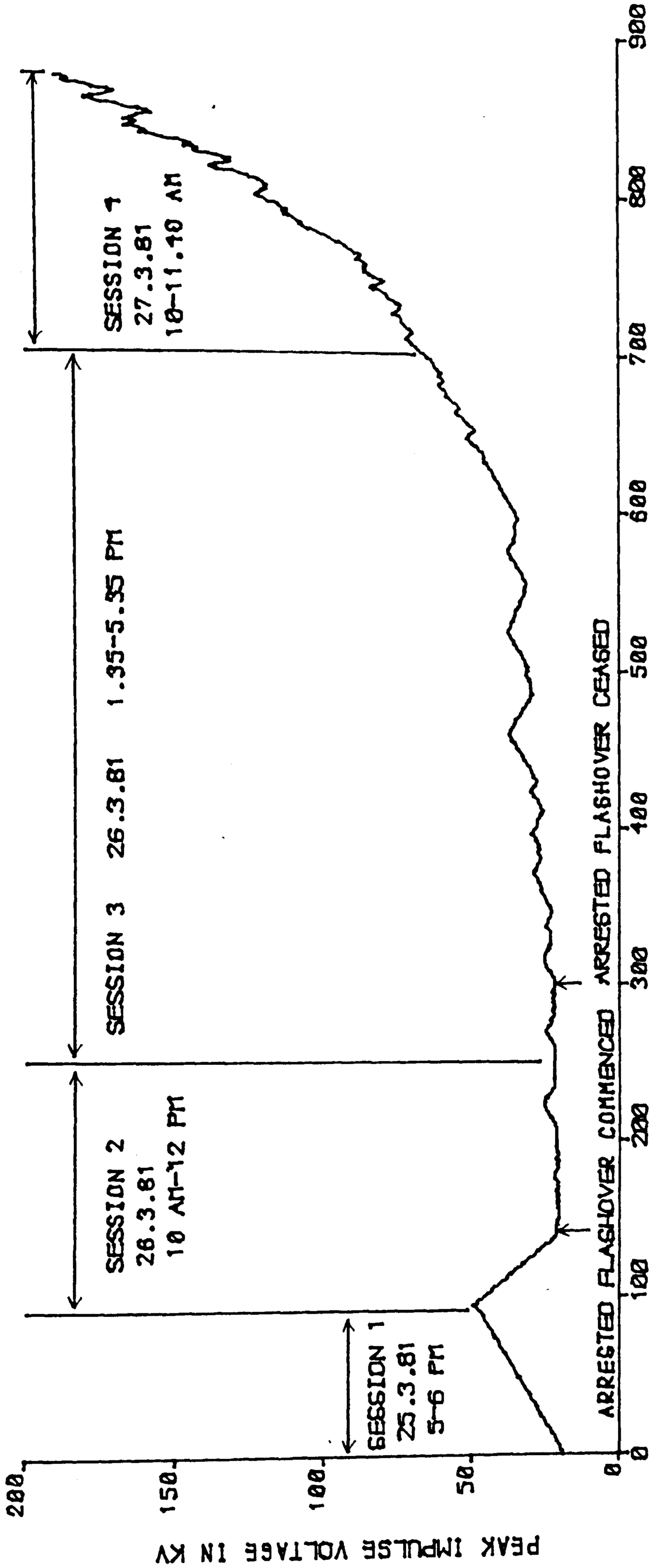

FIG.7.10 UP & DOWN TEST RESULTS-0.3M DAYTON-GRANGER STRIP MOUNTED ON TUBE

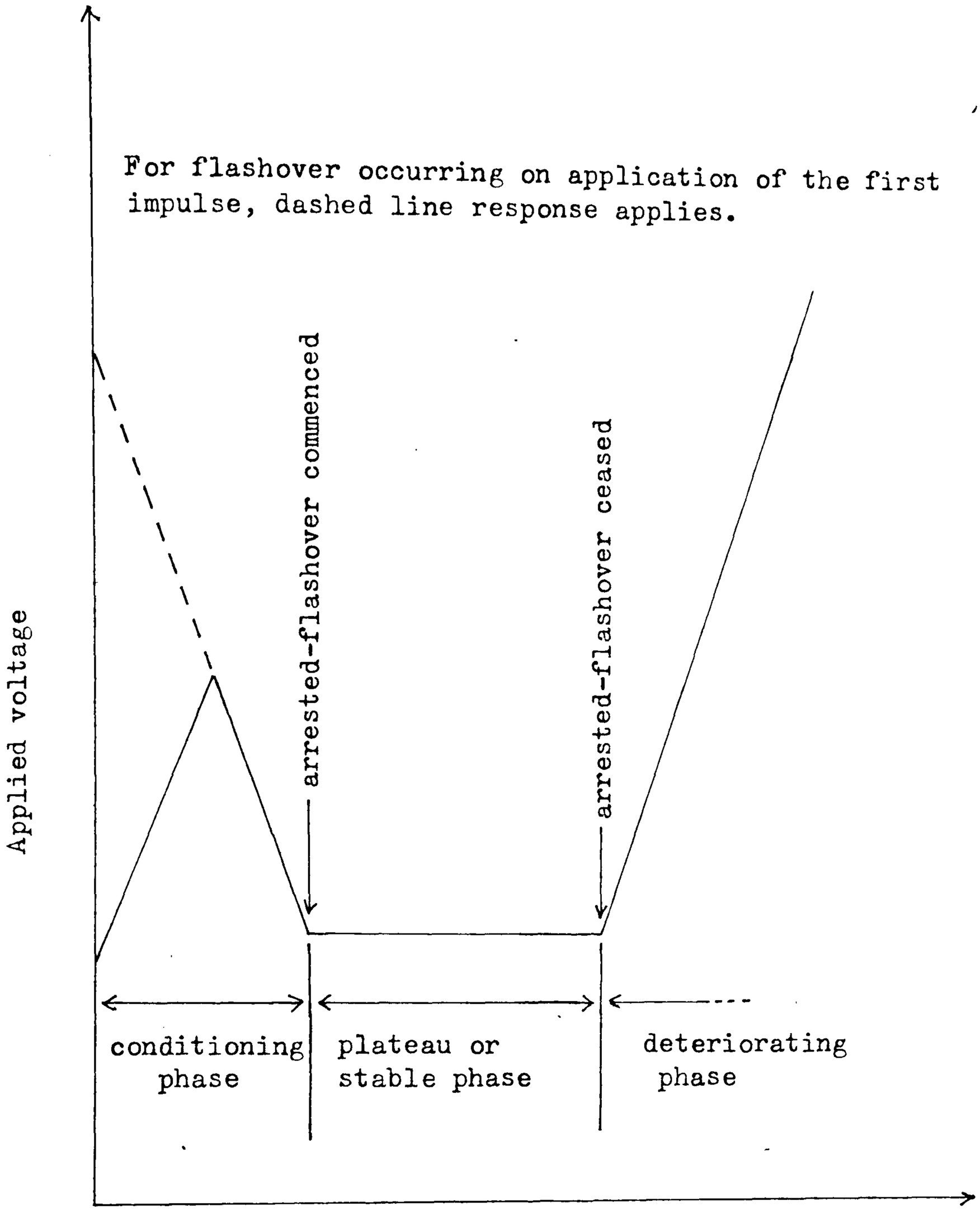

Fig. 7.11 Generalised conditioning characteristics for a Dayton-Granger strip.

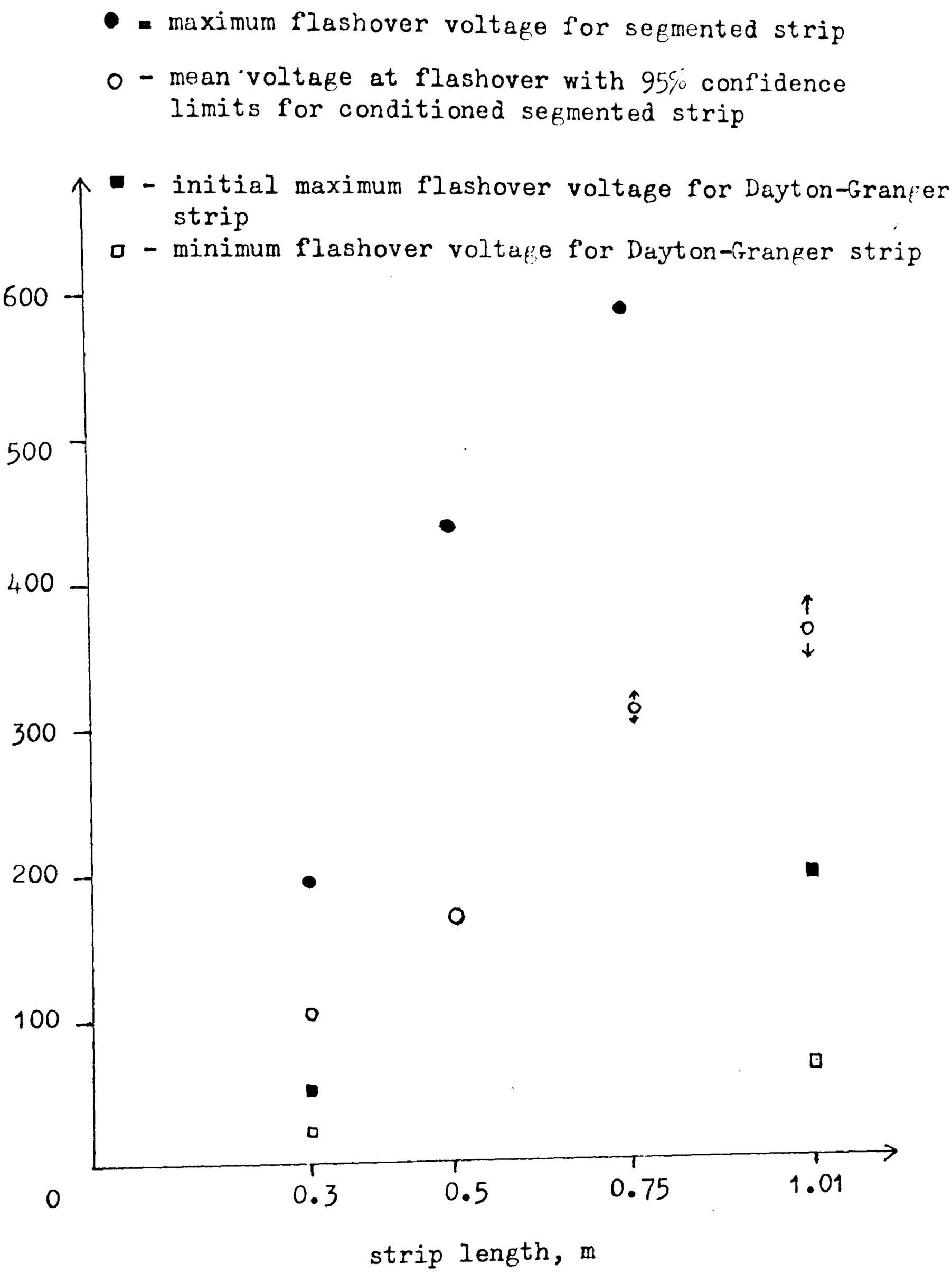

Fig. 7.12 Comparison of flashover characteristics between segmented strip and Dayton-Granger strip.

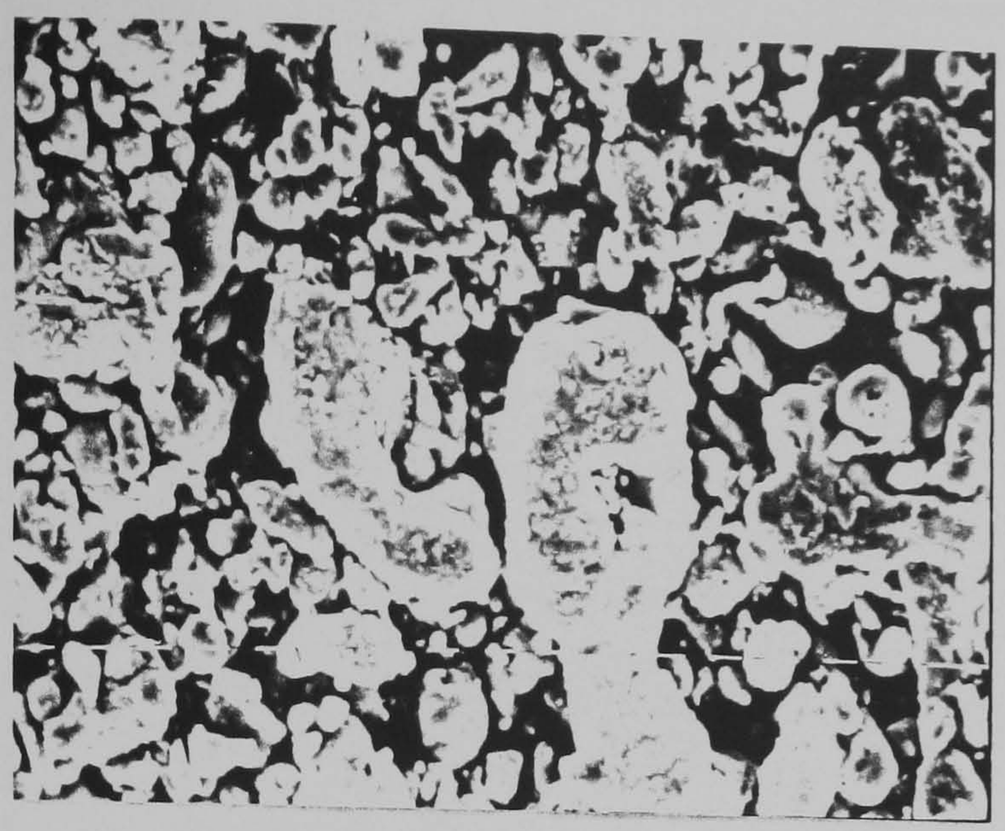

Fig. 7.13 SEM photograph of used strip shown with 10-micron markers

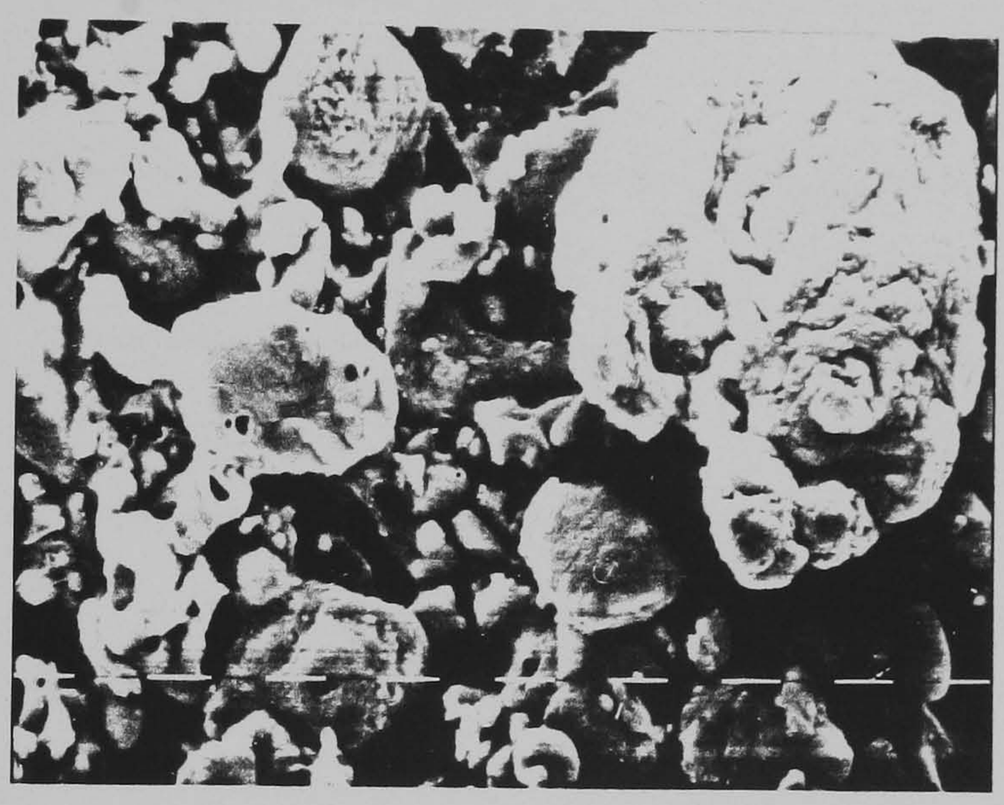

Fig. 7.14 SEM photograph of used strip shown with 10-micron markers

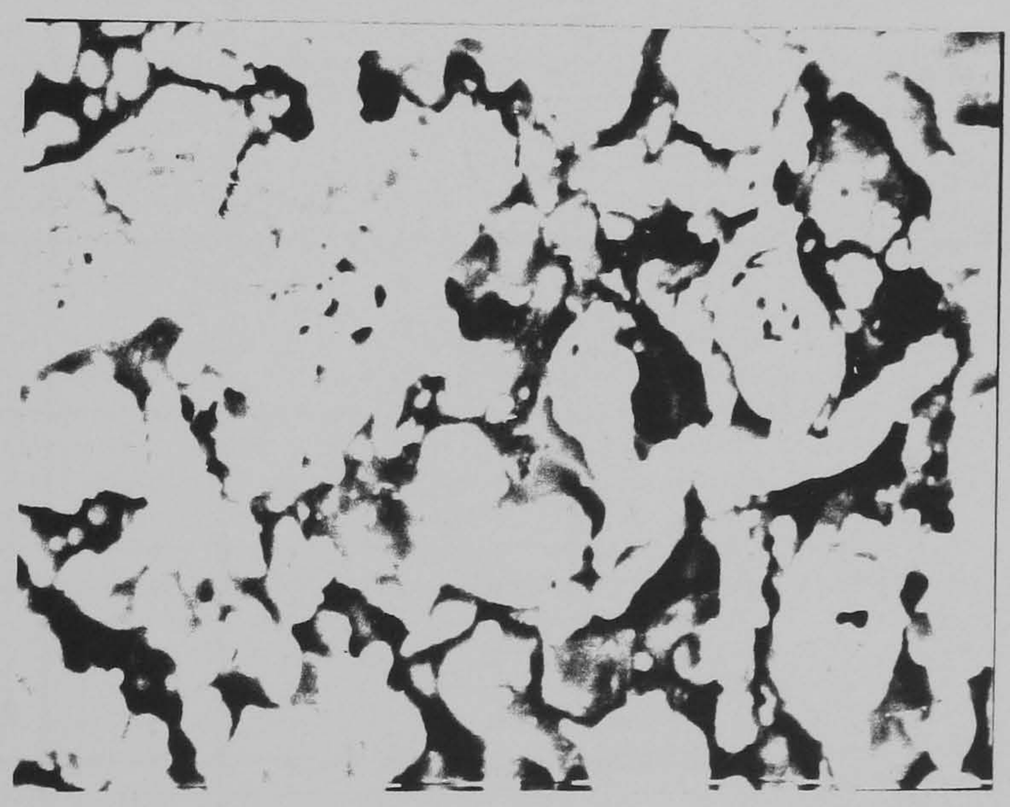

Fig. 7.15 SEM photograph of used strip shown with 10-micron markers

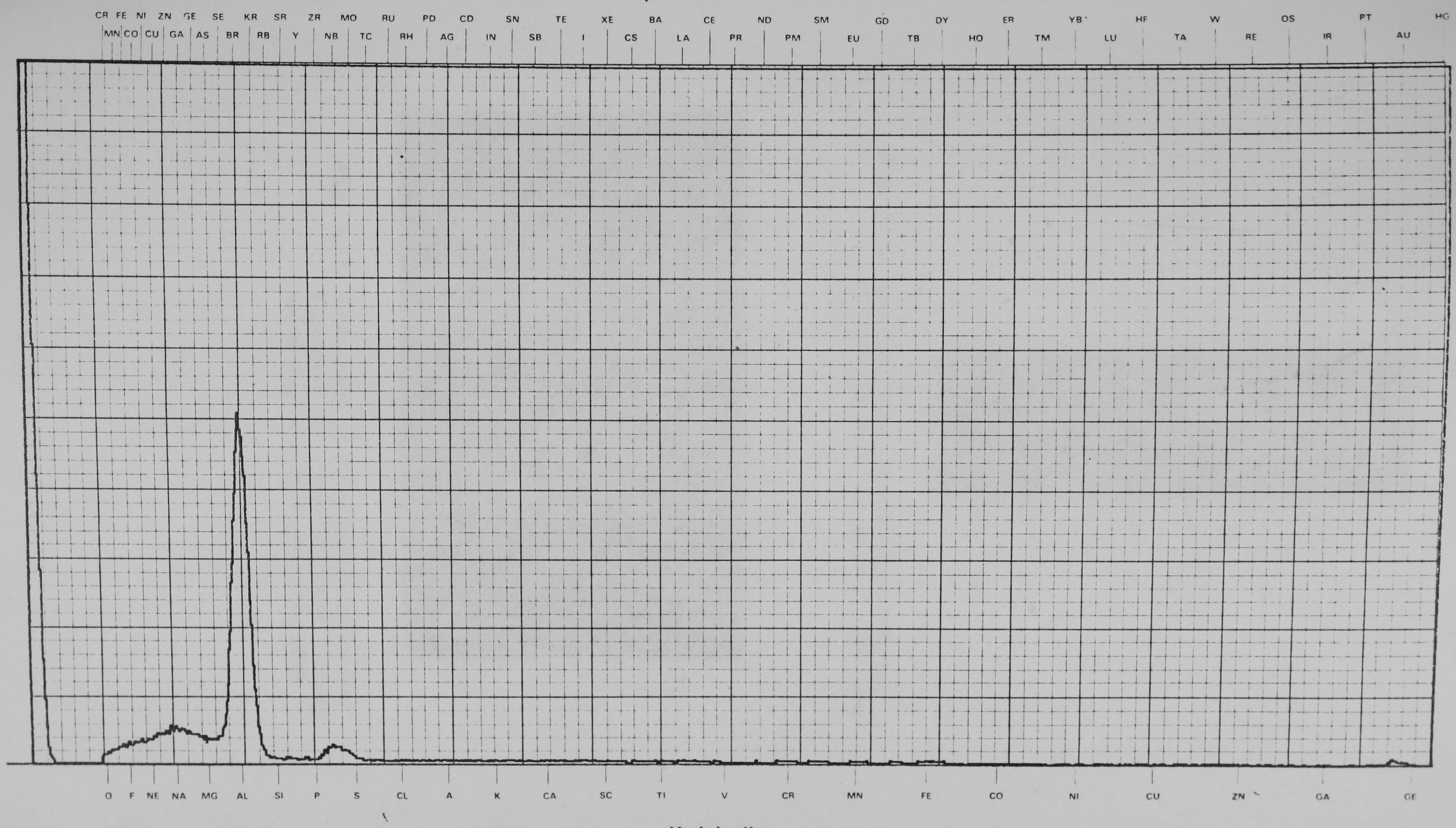

Fig. 7.16 X-ray analysis of a Dayton-Granger strip surface after having undergone flashovers.

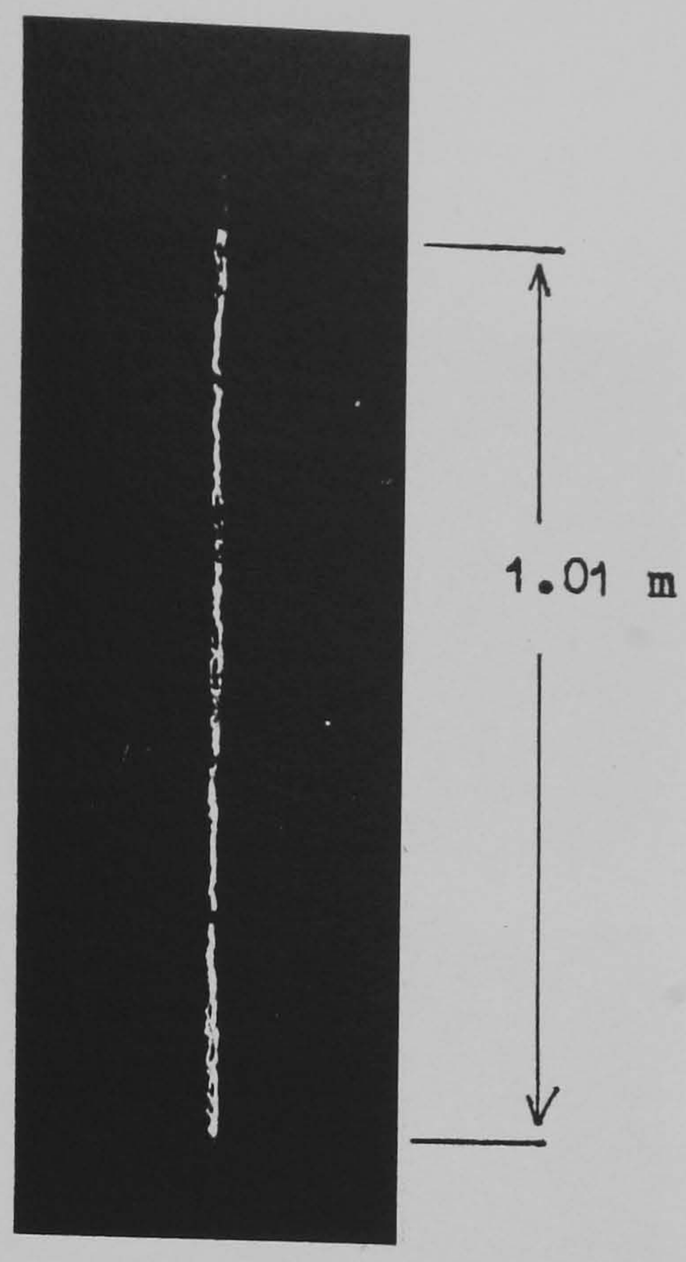

Fig. 7.17 Photograph of arrested-flashover for strip length of 1.01 m, using high speed film

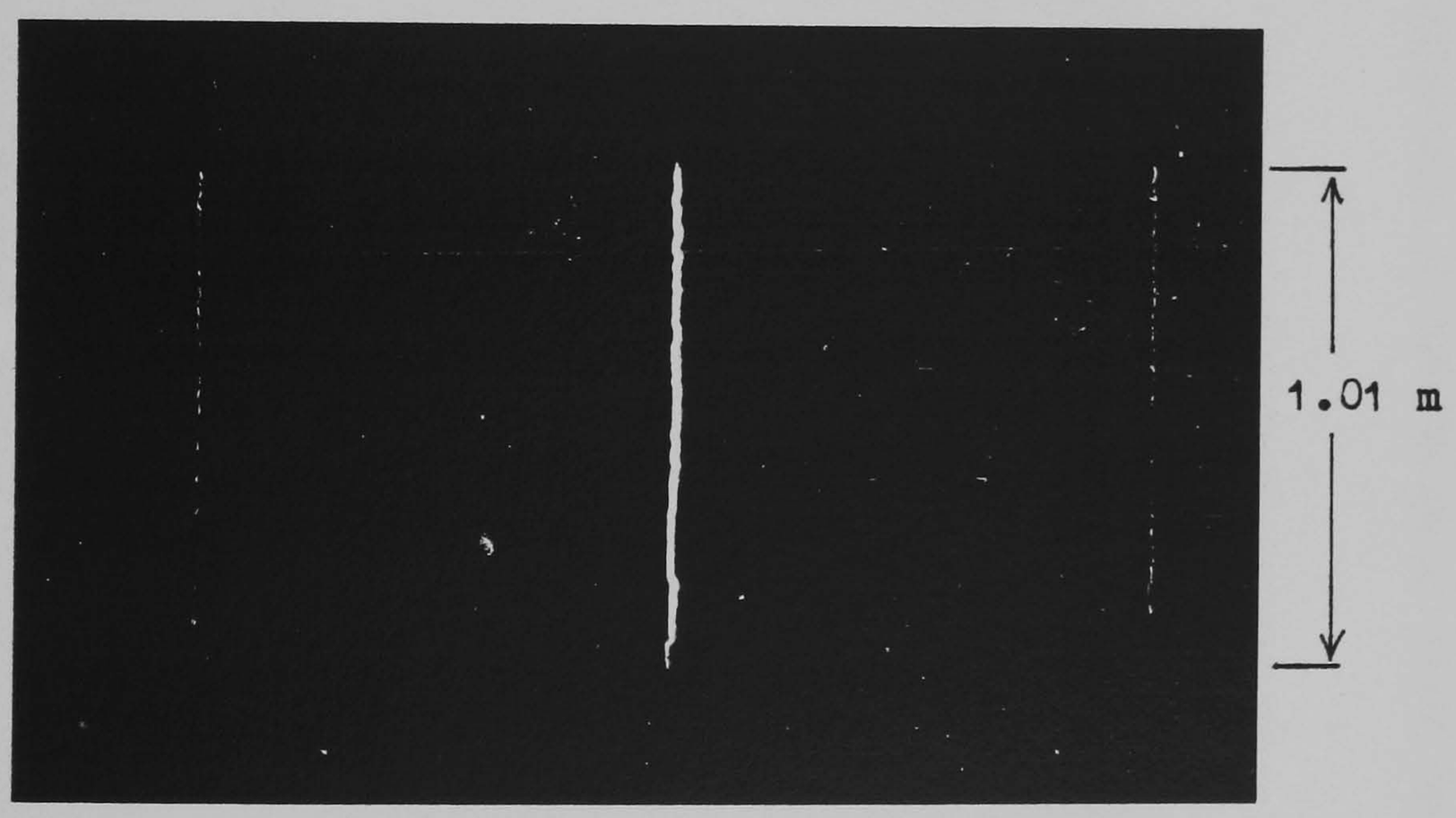

Fig. 7.18 Photograph of arrested-flashover and flashover for strip length of 1.01 m, using high contrast recording film

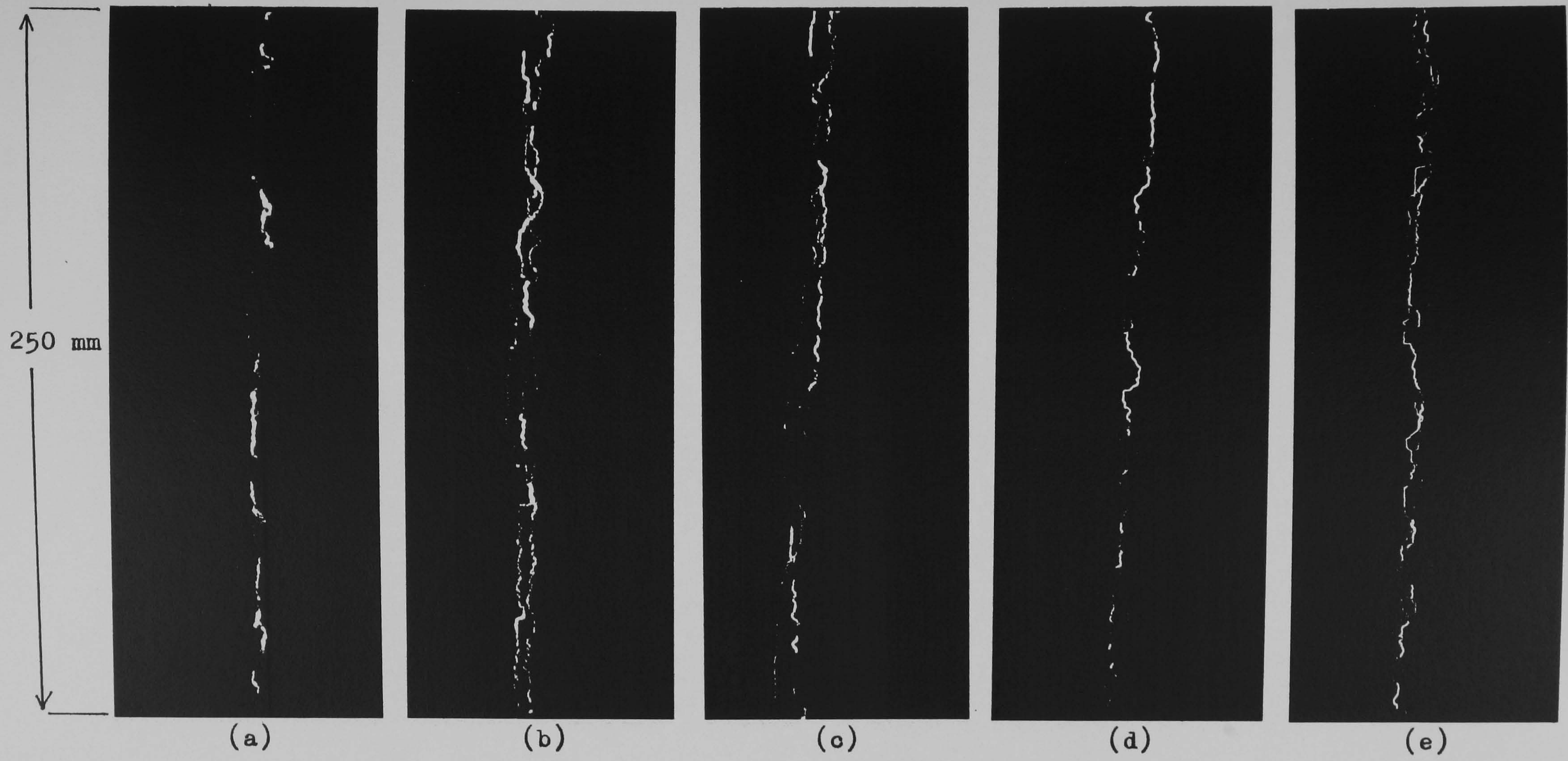

Fig. 7.19 Photograph of arrested-flashover.

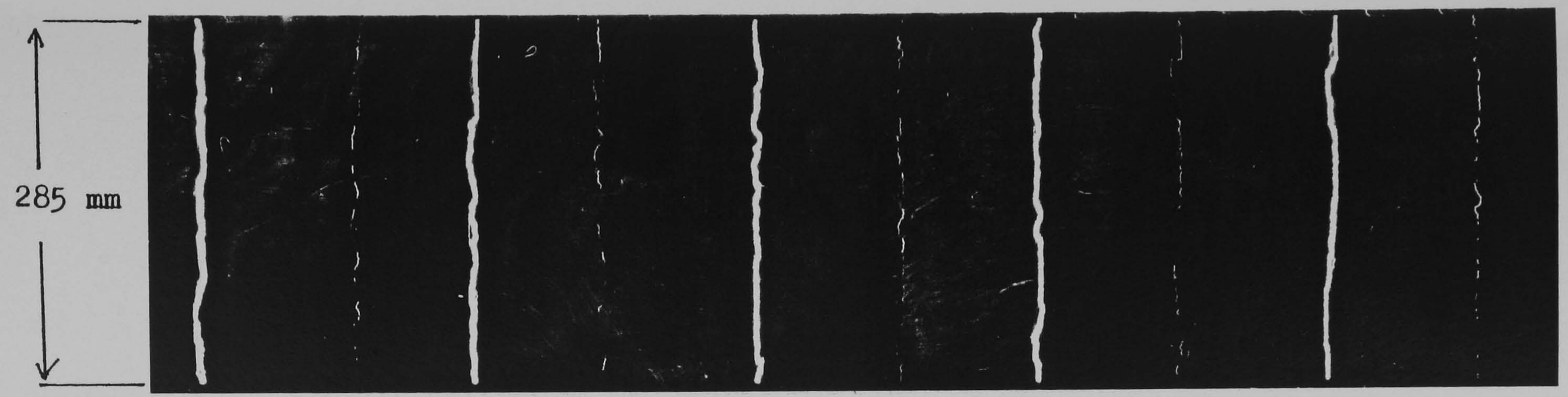

Fig. 7.20 Photographs of flashover and arrested-flashover. Chronological sequence is from left to right.

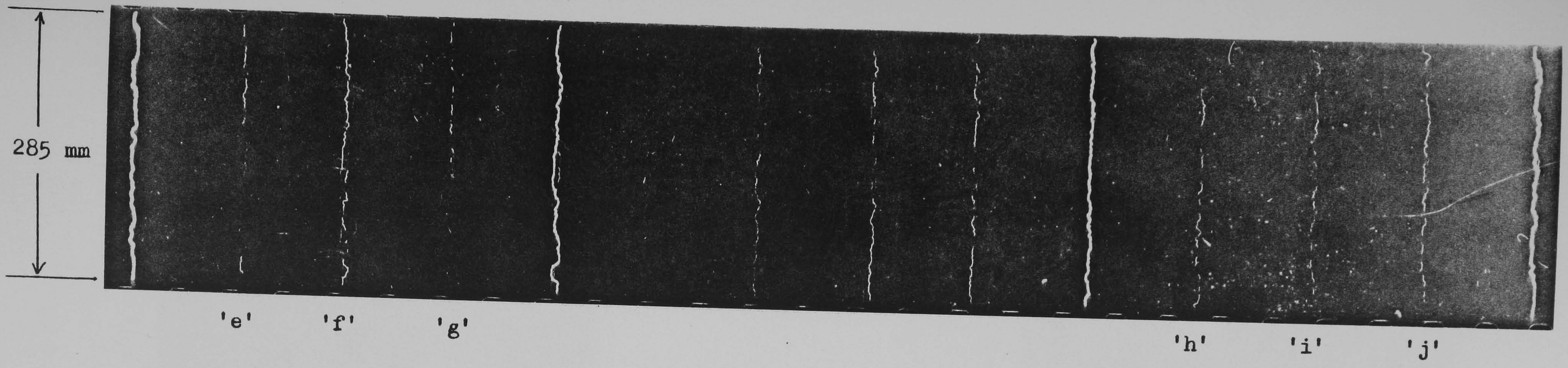

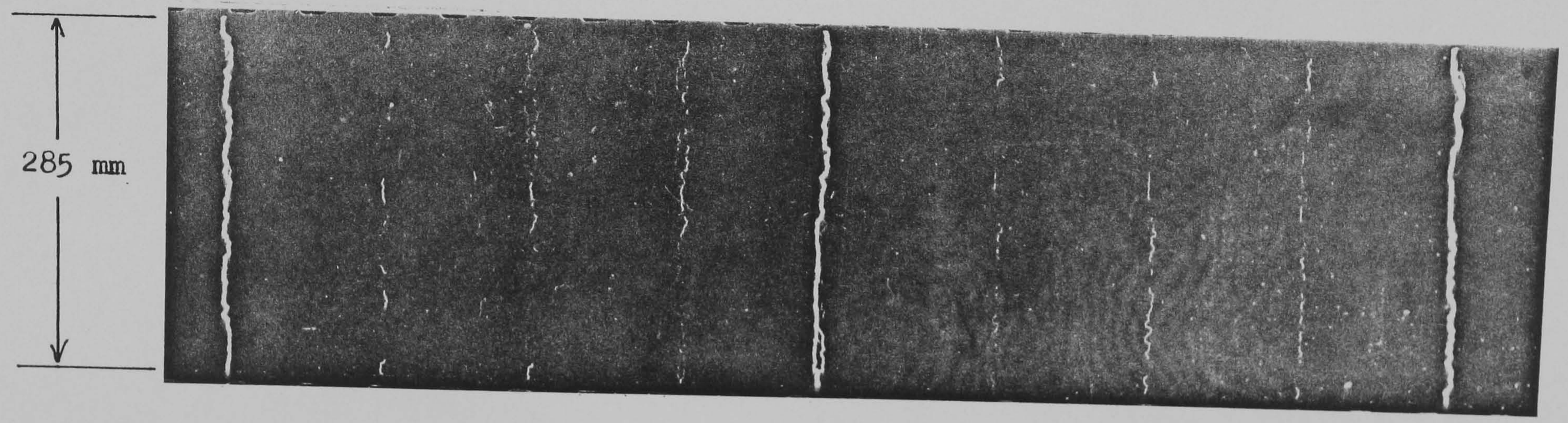

Fig. 7.21 Photographs of a few arrested-flashovers preceding a flashover. Chronological sequence is from left to right.

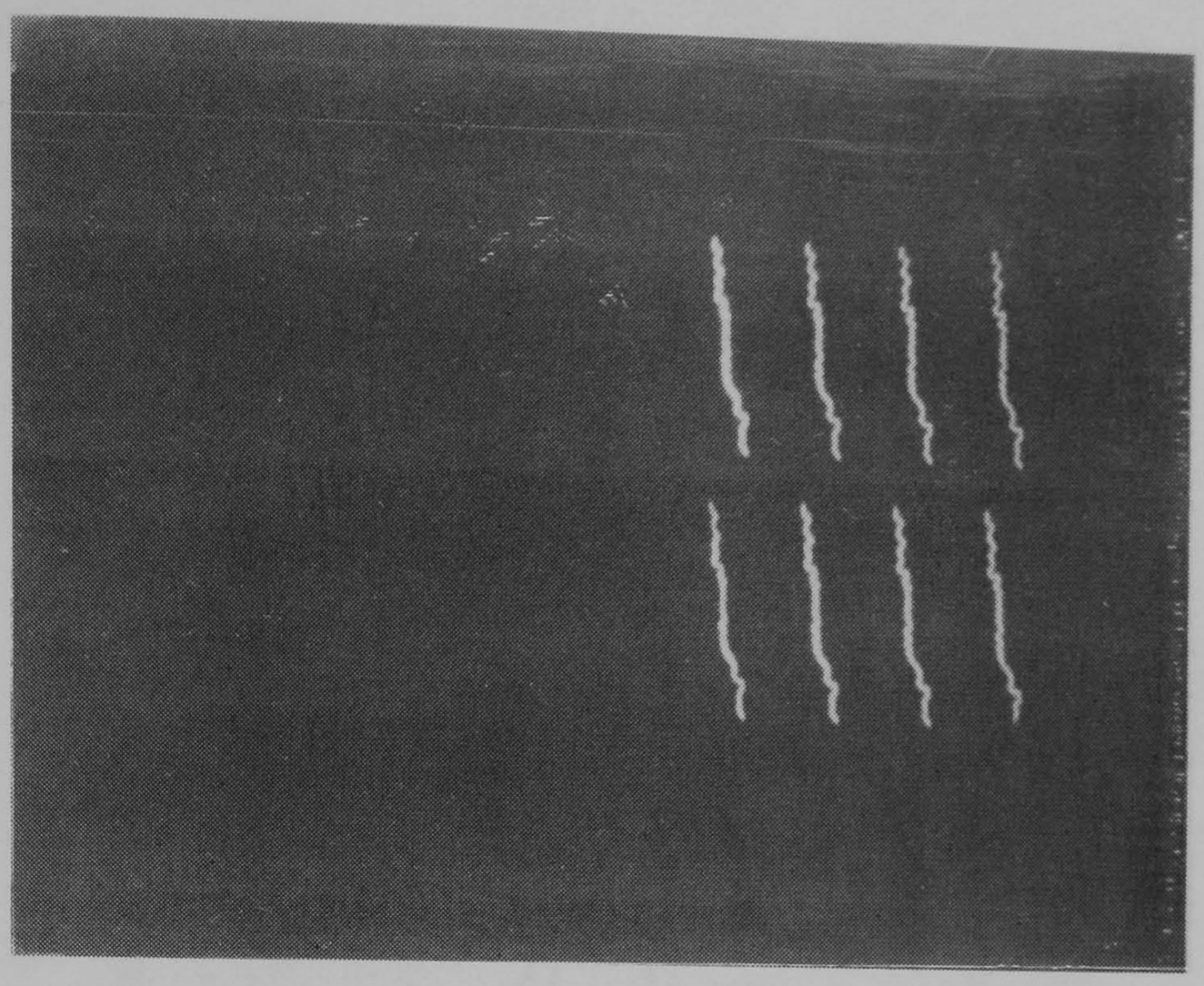

Fig. 7.22 Time-resolved photograph of discharge at 2×10^6 frames per second
Exposure duration/frame = 100 ns

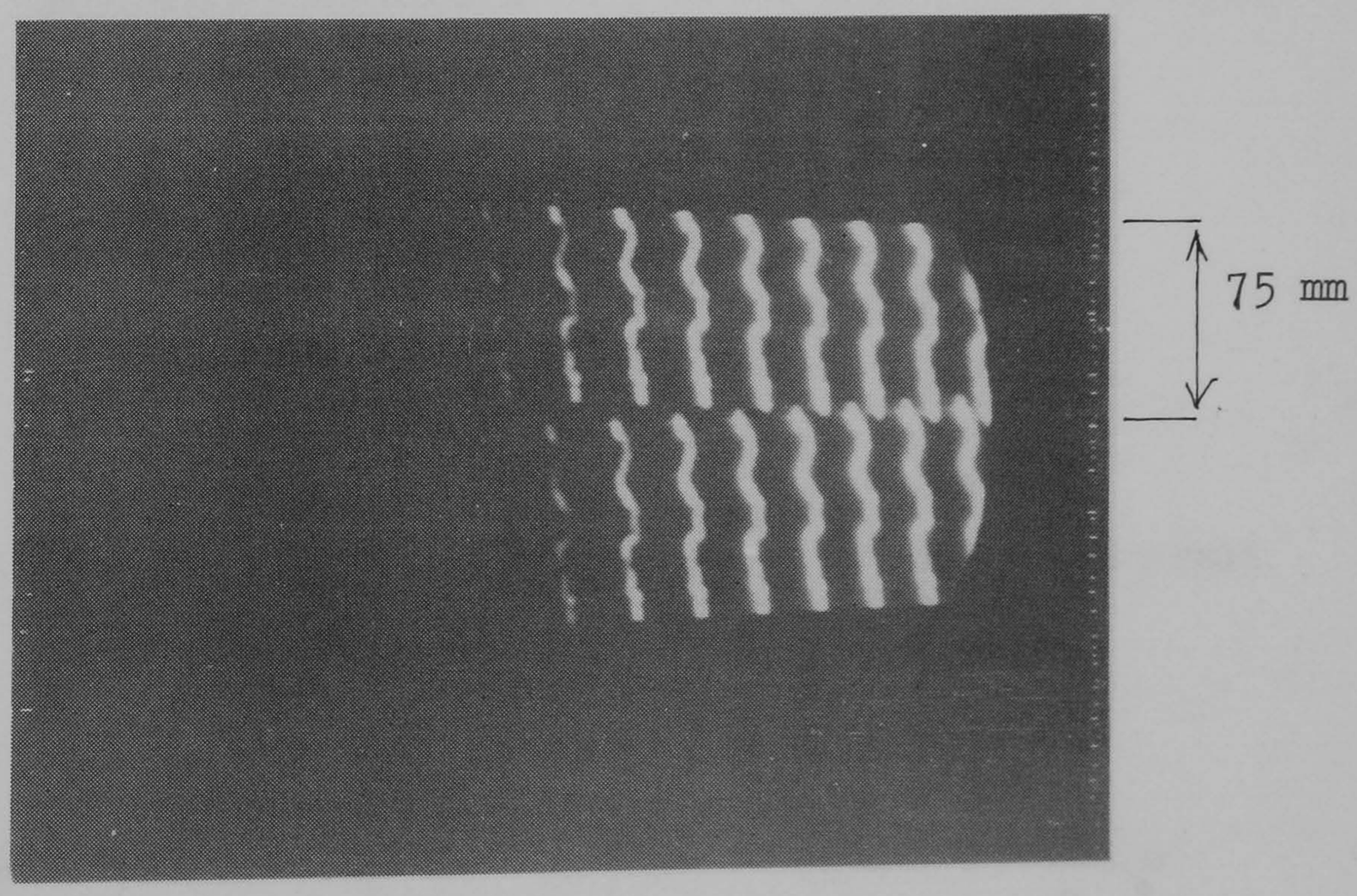

Fig. 7.23 Time-resolved photograph of discharge at 2×10^7 frames per second
Exposure duration/frame = 10 ns

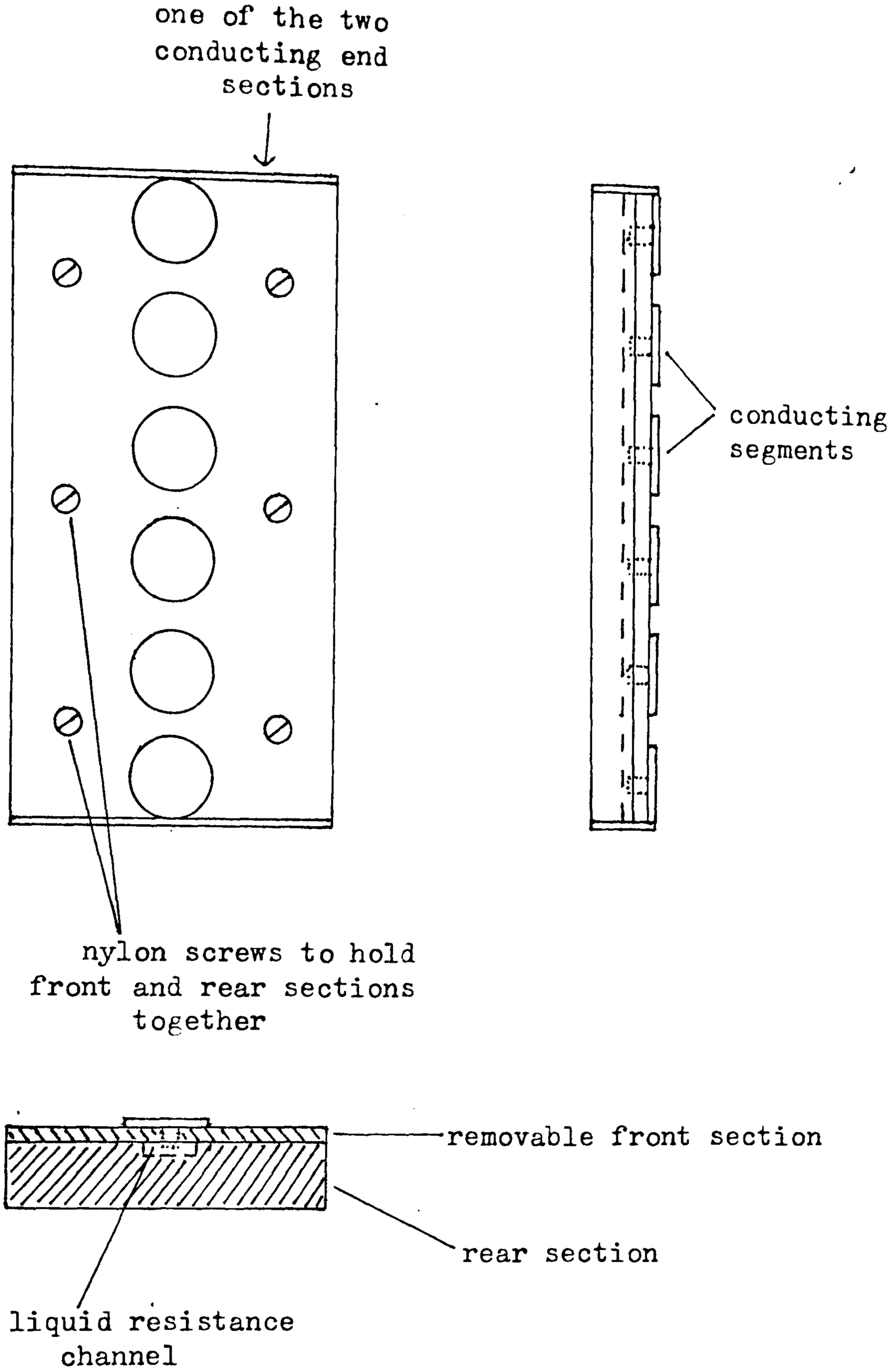

Note: Gaskets or sealing rings could be used to prevent leaks from the liquid-resistance channel.

Fig. 8.1 Proposed design of a model segmented strip.

Appendix 2.1

July 16, 1963 M. P. AMASON Re. 25,417

LIGHTNING ARRESTOR FOR RADOMES

Original Filed June 11, 1959

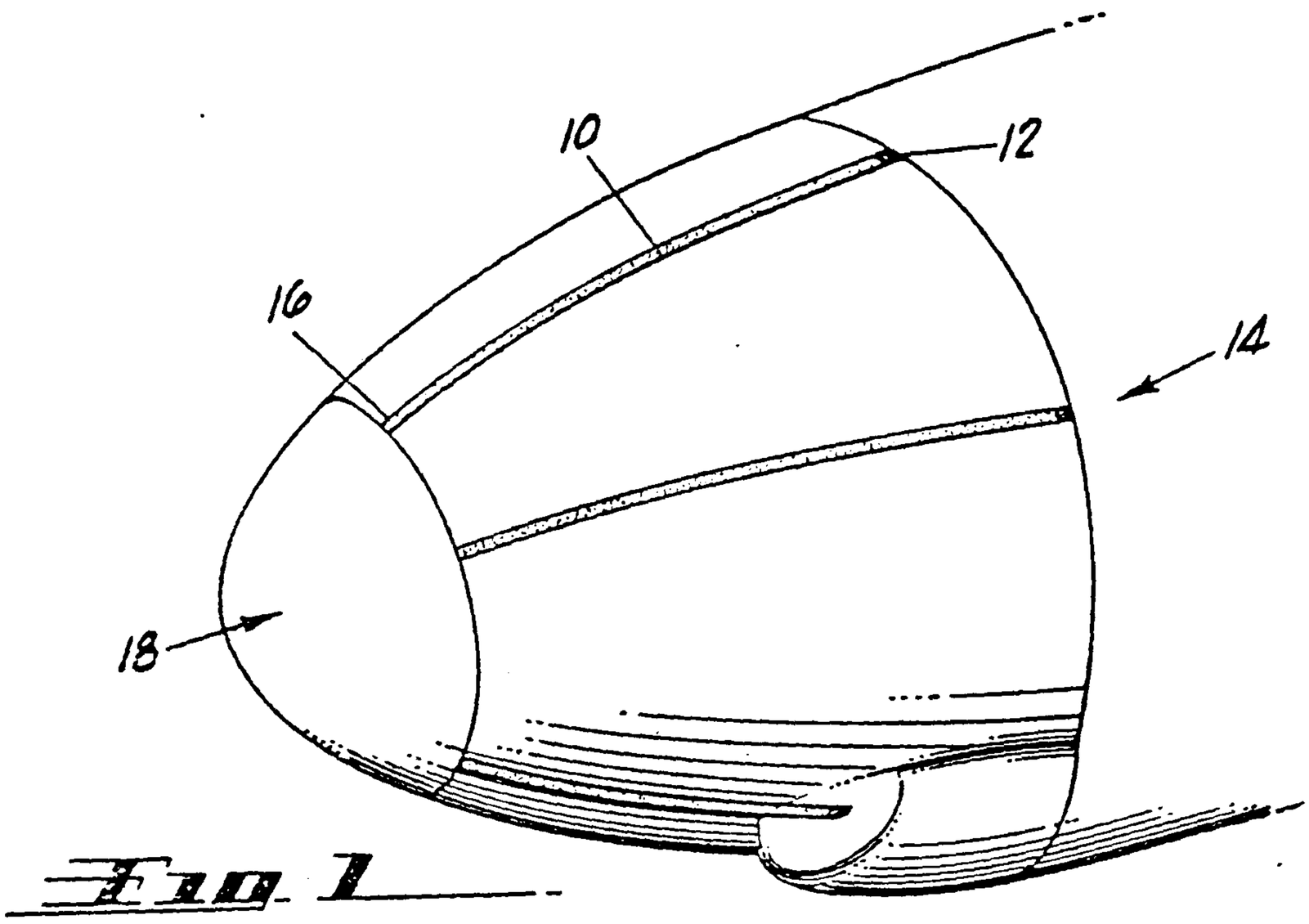

Fig. 1

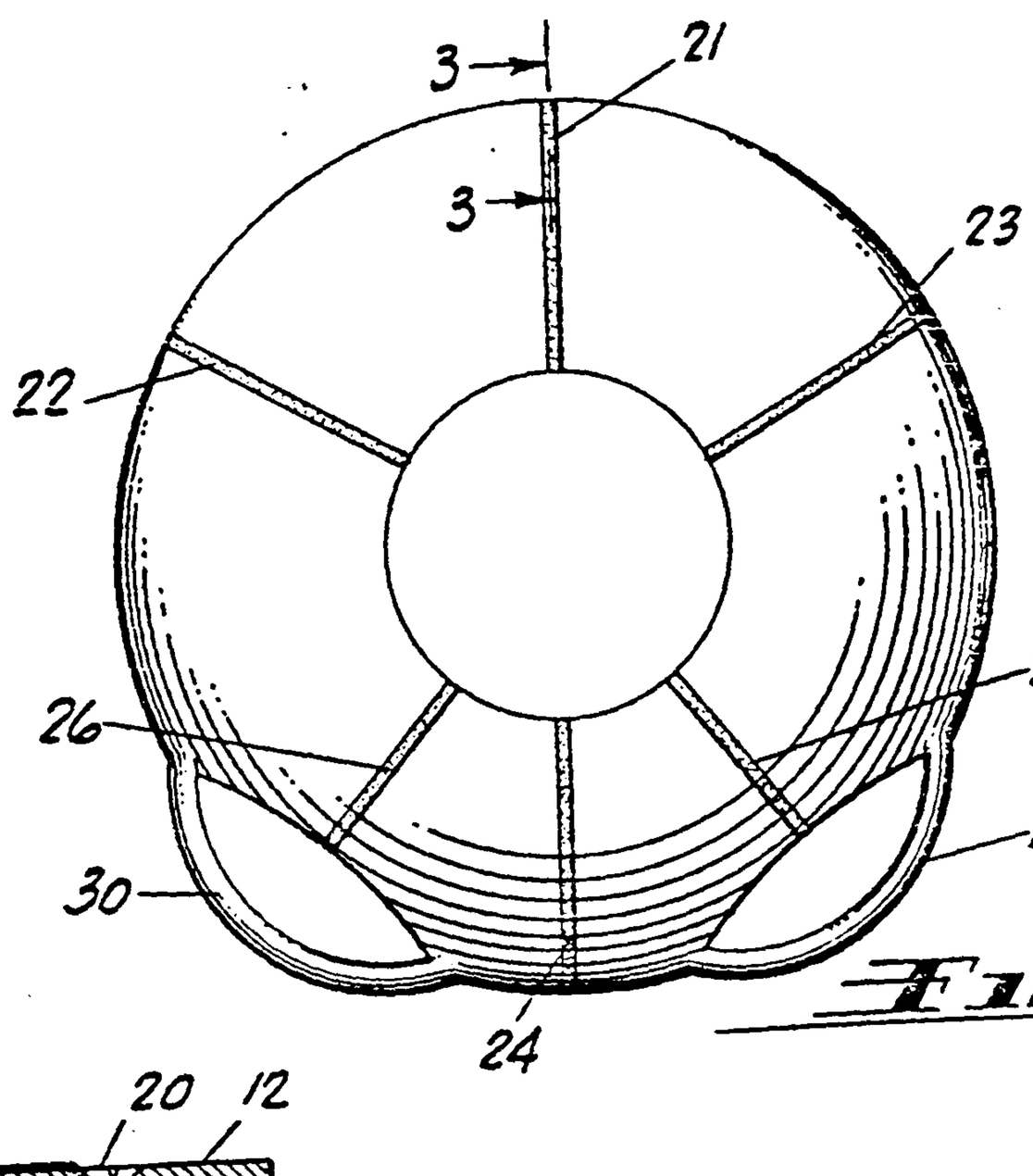

Fig. 2

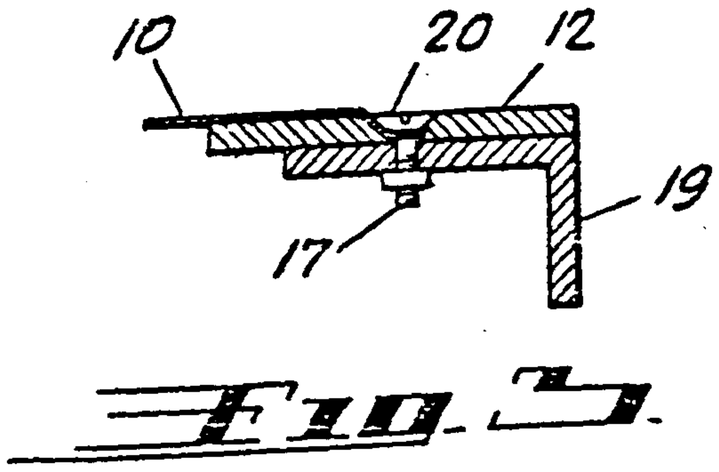

Fig. 3

INVENTOR.
MYRON P. AMASON
BY
Edwin Coates
ATTORNEY.

United States Patent Office

Re. 25,417

Reissued July 16, 1963

1

25,417

LIGHTNING ARRESTOR FOR RADOMES

Myron P. Arnason, Reseda, Calif., assignor to Douglas Aircraft Company, Inc., Santa Monica, Calif.

Original No. 2,982,494, dated May 2, 1961, Ser. No. 819,764, June 11, 1959. Application for reissue May 22, 1962, Ser. No. 197,200

6 Claims. (Cl. 244—1)

Matter enclosed in heavy brackets [ ] appears in the original patent but forms no part of this reissue specification; matter printed in italics indicates the additions made by reissue.

This invention relates to lightning protection systems and more particularly to a lightning protection system for use on general purpose radomes or plastic sections on airplanes.

Approximately 37% of the lightning strikes on an airplane while in flight are on the nose section. Generally mounted in the nose section of an airplane is the radar and other directional equipment. To protect this equipment from damage it is generally enclosed within a molded plastic enclosure called a radome. The preferred material for the construction of a radome consists of laminations of a glass fiber and resin combination. The use of laminations of glass fiber and resin has been found desirable because of their high strength properties and their relatively low interference with the electrical operation of the enclosed equipment.

When a [lighting] *lightning* stroke step leader nears an aircraft, an intense electric field is set up and streamers produced by this field leave the aircraft from high gradient points to meet the step leader. High gradient points in the nose region occur along the edges of the radar antenna and mounting structure. Streamers may initiate from these edges inside the radome, puncture the radome at several places, and connect with the main stroke. While the streamers produce only pinholes, the main stroke to which they connect may pass down the streamer and through the radome, and cause extensive damage.

Since the radome's dielectric strength is not great enough to withstand puncture, and if puncture occurs, the radome may be seriously damaged, it is necessary to provide the radome with a protective system.

A wide variety of lightning protection problems are presented by the different types of radomes and radars in use. Radars utilize many different modes of transmission, frequencies and types of antennas. Radomes have many different types of wall construction, shapes, sizes and external coatings. These make the development of a universal protection system for all radomes difficult. For this reason, the radome protection problem should be approached according to the type of radome such as, Type I—General purpose microwave, Type II—Directional guidance, Type III—Broad-band, Type IV—Low reflection and Type V—Low frequency. This invention is concerned generally with lightning protection for type I, general purpose radomes used with search and weather type radars which have no severe requirements on directional accuracy or low reflections.

Lightning protection systems, which have been developed for aircraft plastic sections, in general may be classified as stroke guiding systems, exposed grounded metal buttons, stroke diverting rods, graded resistance, and external conductors. The stroke guiding system is used on canopy type enclosures. It utilizes the dielectric strength of materials such as the acrylics to withstand puncture for a brief interval until an external surface flashover occurs to lower the potential across the dielectric. The physical and electrical characteristics of the acrylics prevent their use in radome construction. Also, since the basic radome construction has a relatively low dielectric strength this method will not work. Exposed grounded

2

metal buttons, although successful where the ground lead is not installed parallel to the inside surface of low dielectric materials, are not practical for this application since the moving antenna would interfere with a non-parallel lead. Although the stroke diverting rod system has proven to be very successful on other extremities of the aircraft such as wing and tail tips, it is not applicable to the nose of the aircraft. Graded resistance systems at present require further development in the fields of increased resistance to rain erosion and radar transmission loss. The external conductor system is made up of a network of external conductors which form a shielding cage over the nose area and reduce the tendency for streamer formation from points inside the radome. The cage also provides points from which external streamers may initiate as well as intercepting any main strokes in the vicinity of the radome. Thus, the external conductor type of lightning protection system proves to be the most advantageous for use on the radome since it obviates the difficulties encountered in the above mentioned systems.

The external conductor type of electricity discharge system is old in the art. It has been used for many years to dissipate the electrostatic or precipitation static electrical charges accumulated from rain, mist, and snow on the aircraft external surface or the electrostatic charge developed by the friction of the air on the surfaces of the airplane. These charges interfere with the operation of the radio apparatus, ignite combustible gas escaping from the motor feed system or potentially could set the airplane on fire.

One such electrostatic discharge system uses long lead wires extending in parallelism along the axis of the airplane in contact with the external surface. There are short collecting terminals branching off from the lead wires and disposed parallel to each other. Another system uses spaced longitudinally arranged conducting layers secured to the exterior of a plastic loop antenna shell. These layers are aligned parallel to the aerodynamic currents around the shell when in flight. Substantially the entire surface of the shell is covered with the conducting layers providing only enough open regions to minimize eddy current losses resulting from the covering of the enclosure. By arranging the layers in a streamline configuration the wind currents which pass about the shell during flight always exert a pressure on the layers in a manner assisting to press them firmly in their position on the shell, rather than in any other direction to dislodge them. Because of this aerodynamic assist, the layers are simply pasted on the surface, without great concern as to the permanency of the binding action of the adhesive. A further method employs two sets of parallel conductors which are set in grooves in the surface to substantially enclose the conductors. Each conductor is open at one end with its other end connected to ground, providing a Faraday method of shielding that permits the electromagnetic waves of a radio direction finder to penetrate therethrough but substantially stopping electrostatic penetration. The strips are pasted or directly plated on the surface and are electrically connected by an interconnecting strip which extends across all the longitudinal strips for connecting the layers to ground potential.

From the above mentioned systems, it is noted that external conductors on the surface of an aircraft have been used exclusively to dissipate electrostatic charges. These conductors have been arranged to substantially cover the surface, and their configurations have been designed to provide a continuous path to ground from any point on the system; thereby connecting large groups or all of the conductor path to one ground potential connector. The system configurations generally follow and conform to the motion of the aerodynamic air currents which flow over the aircraft surfaces. These systems

either mount the conductors above the surface, loosely bond the conductor to the surface, plate the conductor on the surface, or imbed the conductor in grooves in the surface.

As will be discussed more fully in subsequent paragraphs a lightning arresting system which substantially covers a general purpose radome interferes so radically with radar transmission that the utility of the radar is completely destroyed. Therefore, a system must be used that provides the maximum protection to the radome for the least electrical interference with the radar transmission. Further to provide this condition, each individual segment of the system must be independently grounded, so that a strike to the system will not destroy the whole system or a major portion of it. By grounding each segment of the system individually, a charge of lightning is conducted directly to a conductor of relatively larger size and there it is dissipated without damaging other portions of the system. To reduce the aerodynamic drag the layers must be small, and cannot be mounted above the surface. Yet they cannot be imbedded within the surface. It has been found impractical to imbed large conductor bars in radome surfaces because of the necessity to contour the surface. While small conductors could be imbedded, the damage caused to the surrounding radome area when they are contacted by the main stroke of lightning makes such an installation impractical. As discussed above, large conductors cannot be mounted above the surface, nor can large or small conductors be imbedded in the surface. The system must be made from flat, small conductors which are mounted directly on the radome surface. These conductors must be mounted in such a fashion as to withstand aerodynamic forces, yet must be able to be readily disassociated from the surface when contacted by the main stroke of lightning so that the adjacent radome surface will not become damaged.

The necessity for protecting Fiberglas housings depends upon the necessity of protecting the enclosed equipment. In many cases the equipment may require little electrical protection as it may be essentially grounded to the aircraft skin with adequate conductor sizes as, for example, radar antennas. Therefore, as discussed previously, the primary reason for the installation of a lightning arrestor on a laminated Fiberglas radome is not for protection of the equipment contained within but for the protection of the radome itself. While external conductor systems have been used before for protection, their use has been limited to a protection system which is not compatible with the requirements of a jet aircraft. The present invention resides in the use of a novel type of external conductor arranged in a novel configuration to achieve a novel and unexpected result.

The external conductor system for lightning protection for a general purpose radome has been used before. This system incorporates the use of a conducting bar attached to the surface to be protected. It has been found through experimentation and extensive field use that external conductors having a cross section of 20,000 circular mils were the minimum size conductor that would not be seriously damaged when intercepted by the main stroke of lightning. As mentioned above, a conductor of this size would not be compatible for use on a general purpose radome of the type used on jet airplanes in that, if it were installed on the external surface of the radome, it would cause excessive aerodynamic drag. On the other hand, if a large conductor were installed flush with the outside skin of the radome it would introduce major complications to the radome design. Because of the foregoing, it was necessary to conceive and develop a system using the minimum size conductor that would protect the radome from [dammage] *damage* if the aircraft intercepted a main stroke in the vicinity of the radome.

Previously, a conductor of 20,000 circular mils was considered by persons skilled in this art to be the minimum size conductor that would give the desired protection and yet not be seriously damaged when intercepted by the main stroke of lightning. However, it has been found that, by the use of the present invention, a novel configuration and use of a conventional basic material has produced a novel and completely unexpected result.

In its presently preferred form the invention consists of a network of external conductor paths which form a shield cage over the radome surface. The conductor paths are metal foil strips adhesively placed on the radome surface according to a specific design to provide the maximum protection to the radome for the least electrical interference with the equipment contained within the radome. Each strip is complete within itself because it is individually grounded at one end to the airplane fuselage.

Other advantages of the invention will hereinafter become more fully apparent from the following description of the annexed drawing, which illustrates a preferred embodiment, and wherein:

FIG. 1 is a fragmentary perspective view of an aircraft type radome and a portion of an airplane fuselage illustrating a typical installation of this invention;

FIG. 2 is a front elevational view of an aircraft type radome illustrating a typical installation of this invention; and

FIG. 3 is a portion of the cross sectional view taken at 3—3 in FIG. 2 showing the grounding connection of the conductor paths.

Referring now to FIGS. 1 and 2, the lightning protection system includes a plurality of conductor paths **10** which are arranged in a cage configuration to give the maximum lightning protection with the least hindrance to the antenna system contained within the radome. The conductor paths **10** are metal foil strips, adhesively bonded on the surface of the radome either by pressing directly onto the surface suitable metallic tape with a high temperature resistive, pressure sensitive backing or by first placing a high temperature resistive, pressure sensitive adhesive on the surface and pressing the foil strips into the adhesive. Either method produces the desired mounting of the foil strips, but it has been found more desirable to use the adhesive backed metallic tape. For each of installation, the tape need only be pressed onto the surface of the desired location, thereby eliminating the difficulties of first applying the adhesive to the surface and then pressing on the foil strips.

In the presently preferred embodiment of the invention an aluminum alloy tape, approximately ⅜ of an inch wide, is used. This tape has a high temperature resistive, pressure sensitive adhesive backing and has a thickness of approximately .003 of an inch. It is commercially known as "Scotch 425." The invention is not specifically limited to foil strips ⅜ of an inch wide. It would still be within the scope of the invention to use foil strips that varied from ⅛ inch to several inches in with. However, for ease of application, and least radar obscuration a foil strip ⅜ of an inch wide has proven to be the most effective.

As described above, in the presently preferred embodiment of the invention an aluminum alloy tape is utilized as the conductor path. It is to be understood that the invention is not specifically limited thereto, any metallic tape or metal foil strip of like size and dimension can be utilized as well.

The conductor paths **10** are arranged on the surface in a fore and aft direction so that no point on the radome surface is farther distant than 18 inches from the nearest conductor path **10** or the metallic airplane fuselage **14**. From the standpoint of efficient operation of the radar it is desirable that no more than fifty percent of the radome surface be covered with the conductor paths. Said paths **10** extend forward of the radome base **12** to a point **16** just aft of the radome rain erosion boot **18**.

Referring now to FIG. 3, to provide a means of grounding each conductor path **10** near the base of the radome

12 they are connected under the head 20 of an adjacent radome attaching flange bolt 17. The radome attaching flange 19 makes contact through the mounting hinge and radome latches (not shown) with the airplane fuselage, thus providing a ground path for the lightning arrestor system. Since each conductor path 10 is individually grounded, the main stroke of lightning intercepting one of these paths will be conducted to ground by that path and in no way will it affect any other portion of the system.

Since the exact configuration of the conductor path cage will depend upon the contour of the specific radome to which it is applied, and the nature of the antennas carried within the radome, for sake of clarity in this description a typical installation will be described.

Referring to FIG. 2, revolving within the radome is a radar antenna, and in some instances located beneath the radar antenna is the glide [scope] *slope* antenna. For the best results it has been found that three glide [scope] *slope antenna* protective conductor paths 24, 26, 28, should be placed on the lower portion of the radome surface. To minimize the distortion of the glide [scope] *slope* antenna pattern conductor paths 26, 28 are placed fore and aft of the radome along the axis of symmetry of each of the dual air scoops 30, 32 respectively. The third conductor path 24 is mounted centrally between paths 26, 28, thus forming a cage configuration so that all points on the radome surface adjacent the glide [scope] *slope* antenna are less than 18 inches from the nearest conductor path or the airplane fuselage.

To protect the surface of the radome above the radar antenna three radar protective conductor paths 21, 22, 23 are placed on the upper radome surface. To produce minimum obscuration of the radar transmission a conductor path 21 is mounted fore and aft of the upper surface of the radome along the vertical plane of symmetry of the radome. Conductor paths 22, 23 are mounted radially adjacent path 21 and are arranged to produce a configuration so that no point between said paths is farther distant than 18 inches from the nearest path or the airplane fuselage.

To provide a protective system which provides during operation of the system the least destruction or consumption of its components each glide [scope] *slope antenna* protective conductor path and each radar protective conductor path respectively is grounded at its aft point on the radome surface to an adjacent radome attaching flange bolt 17. The radome attaching flange makes contact through the mounting hinge and radome latches with the airplane fuselage. This individual grounding of each path to the radome attaching flange provides for each strip a relatively large conductor path through which the lightning charge is dissipated, thereby preventing the lightning charge from damaging other segments of the system.

After installation of the conductor paths the surface of the radome is covered with a catalyzed epoxy paint, or a paint of a similar type. This protective coating of paint is applied chiefly as a means of protecting the radome surface from rain erosion.

When the main stroke of the lightning strikes a portion of the conductor path, the conductor path at the point of contact and a portion of the path between the point of contact and the fuselage is disintegrated much like an overloaded fuse. This disintegration causes no damage to the radome surface and simply necessitates an installation of a new section of conductor. Since each conductor path is connected separately to ground with no interconnection between the individual conductor paths, only that conductor which has been contacted by the lightning will be destroyed. This means that only that conductor will have to be placed since the others have not been affected.

The disintegration property of this lightning arrestor system is considered by experts in the lightning arrestor

field to be a novel and completely unexpected result. As discussed above, bars of 20,000 circular [mills] *mils* and larger have been mounted on the surface of a radome to provide lightning protection. Because of the size of these bars and the excessive aerodynamic drag developed by them at high speeds they have proven incompatible with the needs of a high speed jet aircraft. The above mentioned bars are the minimum size that will not disintegrate upon contact with the main stroke of lightning. Therefore, as the conductor size is reduced there is the problem of distintegration to consider. To use this property of disintegration to advantage in the above described presently preferred embodiment of the lightning arrestor system the adhesive backed metallic tape is adhesively secured to the radome with a light bond and then is covered with a thin coating of catalyzed epoxy paint. The bonding of the tape to the radome surface and the thin coating of paint prevent excessive aerodynamic drag developed by the tape, but is such that when the tape is contacted by the main stroke of lightning the tape along the point of contact will be exploded from in contact with the radome, providing an ionized trail of metallic ions. It is this ionization trail that conducts the subsequent long discharge of the main stroke of lightning over the radome surface.

The explosion of the tape ionizes the metallic portion thereof but does not appreciably disturb the adhesive bonding material. The explosive ionization of the metallic portion of the tape dissipates a portion of the energy of the lightning charge through the development of the heat necessary to produce the ionization. After the explosive ionization, the adhesive bonding material remains in contact with the radome surface and provides an additional protective coating of insulation against the long discharge of the lightning. Had the tape been embedded in the radome surface or permanently bonded thereto, the tape would not have been able to explode from in contact with the surface and the contact of the main stroke of lightning would have caused excessive damage to the radome area surrounding the tape at the point of contact. For this reason a weaker, but yet effective bond is provided which enables the tape to pull loose from the radome surface under the explosive action of the lightning strike but permits the adhesive bonding material to remain in contact with the surface and provide the insulation blanket.

To provide an adhesive bonding agent that displays the necessary resistance to the explosive-heat reaction resulting from the explosion of the metallic portion of the tape a pressure sensitive adhesive of the high temperature resistive type is utilized as the bonding agent. As described above, there are available commercially, adhesive backed metallic tapes which contain adhesive backing of the desired type to produce this novel, unique lightning arresting system.

The preceding description has been limited to use of the invention to protect aircraft radomes. It is desired to point out, however, that the invention should not be limited to this application, since it has applicability as a protection system for all types of vehicles that move through the air as well as all kinds of housings and enclosures.

Although the now preferred embodiment and methods of the present invention have been illustrated and described it is to be understood that the invention need not be limited thereto for it is susceptible to change in form, detail and application, within the scope of the appended claims.

I claim:

1. In combination with a plastic [aircraft] section *of an aircraft fuselage*, a lightning arrestor, comprising: at least one conductor path of lightning ionizable material adhesively fastened to the plastic aircraft section exterior providing maximum lightning protection for the minimum electrical interference; each path being adapted to have

a portion thereof completely transmuted by a lightning strike thereto into an ion trail outwardly disposed from said plastic section to conduct away from said section the energy of said lightning strike; at least one grounding means adapted to ground said conductor paths individually to the aircraft fuselage.

2. In combination with a plastic [aircraft] section *of a metallic aircraft*, a lightning arrestor comprising: a plurality of conductor paths adhesively attached to the external surface of the section in a fore and aft direction and at intervals with no point on said section further distant than eighteen inches from an adjacent conductor path or a metallic part of the *aircraft* [airplane fuselage], said paths covering no more than fifty percent of the surface area of said section, each path being adapted to have a portion thereof completely transmuted by a lightning strike thereto into an ion trail outwardly disposed from said section to conduct away from said section the energy of said lightning strike; and means connected to each of said conductor paths for grounding each strip individually to the aircraft [fuselage].

3. In combination with a plastic [aircraft] section *of a metallic aircraft fuselage*, such as a radome section, a lightning arrestor comprising: a plurality of strips of adhesive backed metallic tape placed on the external surface of the section in a fore and aft direction and at intervals with no point of said section further distant than eighteen inches from an adjacent strip of said tape or metallic part of the [airplane] fuselage, said strips covering no more than fifty percent of the radome surface, each strip being adapted to have a portion thereof completely transmuted by a lightning strike thereto into an ion trail outwardly disposed from the external surface of said section to conduct away therefrom the energy of said lightning strike; and, means connected to each of said strips of tape for grounding each strip individually to the aircraft fuselage.

4. In combination with a plastic [aircraft] section *of a metallic aircraft*, a lightning arrestor comprising: a plurality of strips of adhesive material having a high heat resistance laterally spaced from each other and longitudinally arranged on the surface of said section; and a strip of lightning ionizable material mounted on each of said strips of adhesive material and adapted to be completely explodably disassociated therefrom by a lightning strike to form an ion trail outwardly disposed from the surface of said section for conducting away from said section the energy of said lightning strike; each of said strips of ionizable material being individually grounded to a metallic portion of the aircraft.

5. A lightning arrestor in combination with a plastic [aircraft] radome *of an aircraft* [enclosing], *said radome being adapted to enclose* a plurality of metallic members, comprising: a plurality of strips of adhesive backed metallic tape placed on the external surface of said radome [adjacent to the edge surfaces of said metallic members] in a fore and aft direction thereby defining a cage, said cage covering no more than fifty percent of the radome surface, each strip being adapted to have a portion thereof completely transmuted by a lightning strike thereto into an ion trail outwardly disposed from said radome; and means connected to each of said strips to ground each strip individually to the aircraft [fuselage]; whereby said cage prevents high field concentration from forming on said metallic members when said aircraft flies between oppositely charged cloud masses so that a lightning stroke nearing the radome surface will ionize a portion of one of said strips into an ion trail for conducting away from the radome the energy of said lightning strike.

6. In combination with a plastic [aircraft] section *of an aircraft*, a lightning arrestor, comprising: ionizable means associated with the exterior surface of said section and adapted to have a portion of said ionizable means completely transmuted by a lightning strike thereto into an ion trail adjacent to the exterior surface of said section to conduct away therefrom the energy of said lightning strike; and means associated with said ionizable means for grounding it to the aircraft [fuselage].

References Cited in the file of this patent
or the original patent

UNITED STATES PATENTS

367,435	O'Brien	Aug. 2, 1887
443,048	Hodges	Dec. 16, 1890
796,760	Price	Aug. 8, 1905
1,419,261	Howard	June 13, 1922

Appendix 2.2

Dec. 10, 1968 M. P. AMASON ET AL 3,416,027

RADOME LIGHTNING PROTECTION MEANS

Filed March 10, 1967

Fig 1

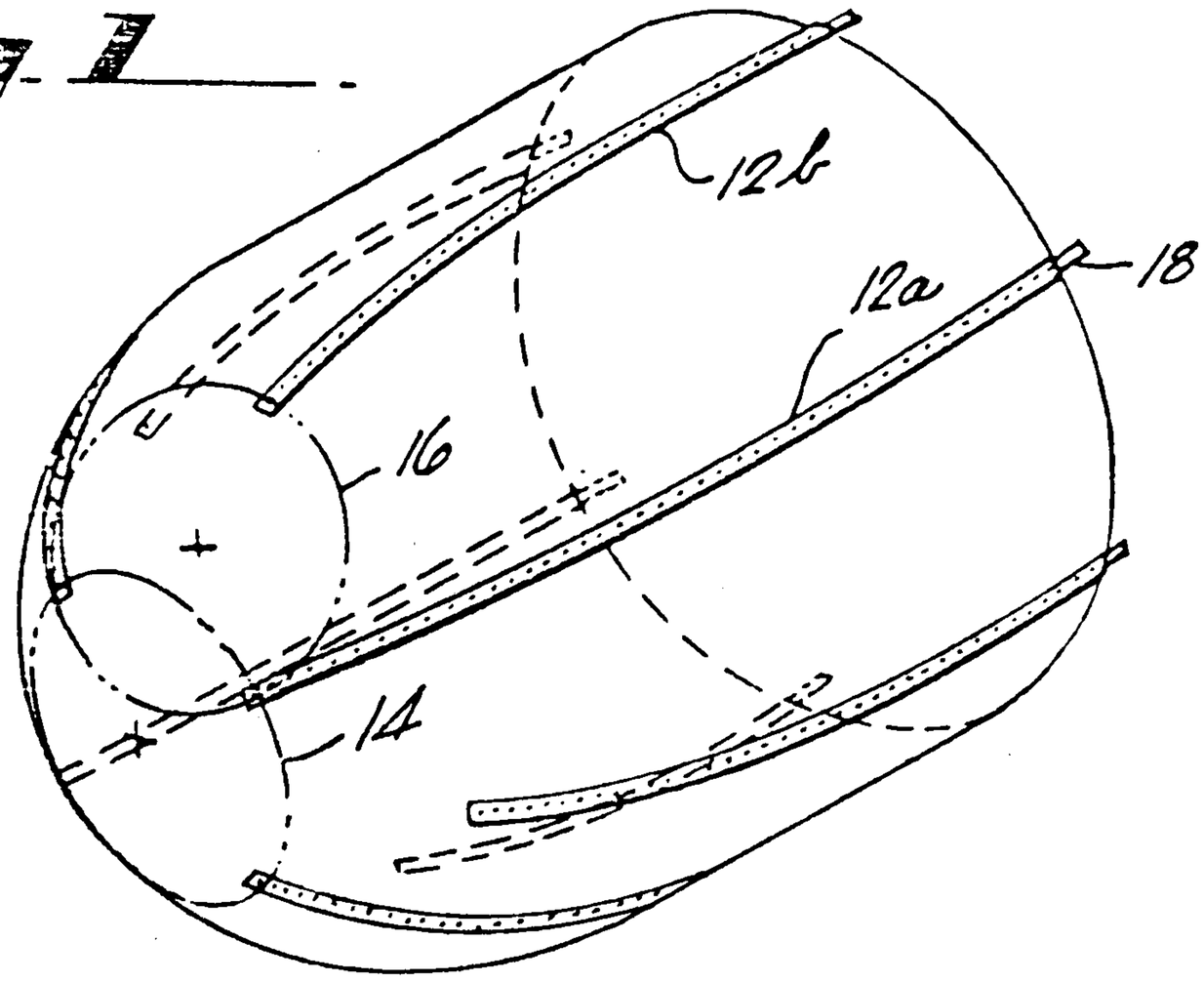

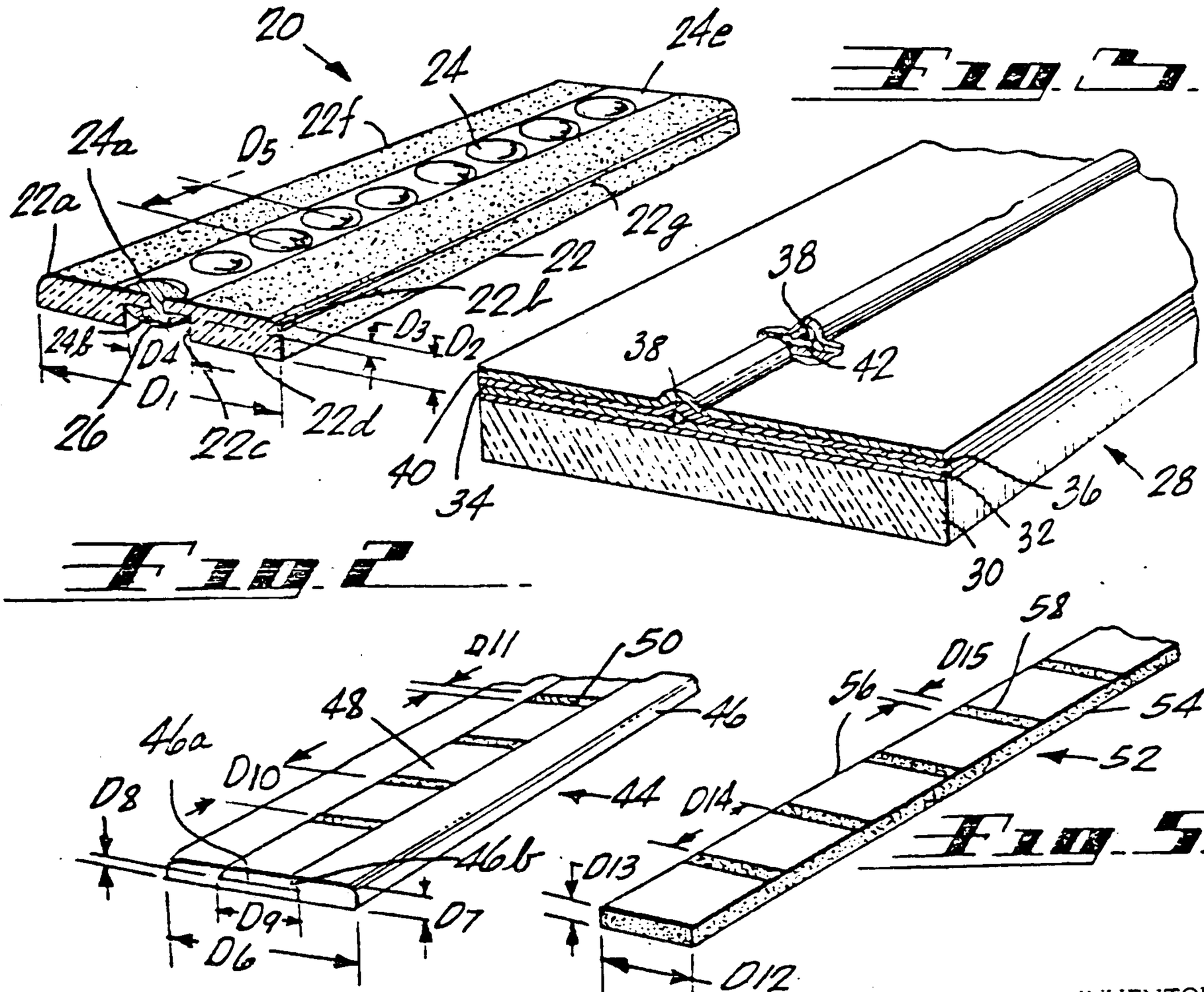

Fig 2

Fig 3

Fig 5

Fig 4

INVENTORS
MYRON P. AMASON
GEORGE J. CASSELL
BY
Mark N. Jeu
-AGENT-

United States Patent Office

3,416,027

Patented Dec. 10, 1968

3,416,027

RADOME LIGHTNING PROTECTION MEANS

Myron P. Amason, Reseda, and George J. Cassell, Huntington Beach, Calif., assignors, by mesne assignments, to McDonnell Douglas Corporation, Santa Monica, Calif., a corporation of Maryland

Filed Mar. 10, 1967, Ser. No. 622,141
12 Claims. (Cl. 315—36)

ABSTRACT OF THE DISCLOSURE

A number of lightning protection strip assemblies are installed in a selected configuration on a radome for protection thereof from lightning strokes. Each strip assembly includes a series of spaced metallic segments connected by appropriate resistance material. The metallic segments have a maximum dimension less than approximately ⅛ of a wave length of the highest operating frequency of the antennas located within or adjacent to the radome, and the connecting material has a strip resistance above approximately 80,000 ohms per foot. Such strip assemblies produce a radar transparent, radome lightning protection system which can withstand repeated lightning strikes thereon.

Background of the invention

Our present invention pertains to the field of lightning protection systems and more particularly to lightning protection means for radomes and the like.

A previously devised lightning protection system which is widely used on aircraft radomes comprises a series of continuous, metallic foil strips adhesively fastened to the exterior surface of a radome and grounded at the ends near the base of the radome. When a foil strip is first contacted by a main stroke of lightning, the strip will disintegrate along the path of contact, and will be exploded away from the radome to provide an ionized trail over the radome surface. It is this ionization trail which conducts the subsequent, relatively long discharge of the main stroke of lightning over the surface of the radome. Such a lightning protection system is shown, described and claimed in the reissue Patent No. Re. 25,417 of Myron P. Amason, reissued on July 16, 1963, and entitled, Lightning Arrestor for Radomes.

The continuous, metallic foil strips used in the lightning protection system described above re-radiate when inserted in the field of a radar antenna, causing an increase in side lobe level of the antenna radiation pattern, a loss in radar range and significant pattern distortion. Although this degradation in antenna pattern is within acceptable limits for many antennas, it is desirable to provide a radome lightning protection system of very low degradation effect and which is acceptable for use with any antenna.

Further, while the lightning protection system utilizing the continuous metallic foil strips provide adequate lightning protection for radomes against a single stroke of lightning thereon, it is obviously unsuitable where repeated stroke protection is required without having to replace after each stroke the strips vaporized by lightning. Accordingly, it is also desirable to provide a lightning protection system which is always capable of sustaining and transferring the energy of repeated strikes of lightning thereon.

Summary of the invention

Briefly, and in general terms, our invention broadly comprises a lightning protection strip assembly which includes a series of spaced metallic or conductive segments connected by appropriate resistance material. A number

of these strip assemblies are used to protect a radome by installing the strip assemblies on the radome in an appropriate configuration. The installed strip assemblies are radar transparent and can withstand repeated strikes of lightning thereon while giving proper and adequate protection of the radome on which the strip assemblies are mounted. This is accomplished by providing strip assemblies having metallic or conductive segments of a maximum dimension which is less than approximately ⅛ of a wave length of the highest operating frequency of the antenna, or antennas, housed within the radome, and by providing material having a strip resistance above approximately 80,00 ohms per foot connecting the metallic segments in each strip assembly.

The spaced metallic segments can, of course, be larger than ⅛ of a wavelength of the highest operating antenna frequency but this would cause a commensurately higher degree of antenna pattern degradation. Similarly, connecting materials with resistances less than 80,000 ohms per foot of strip length can be used for certain applications. However, the lower resistances may cause the transferred lightning discharge energy to remain almost entirely in the resistance material and result in an explosion which destroys the strip assembly. Too low a resistance will, of course, also short or connect the metallic segments together and form a substantially continuous conductive strip which re-radiates in the antenna field to produce the subsequent, undesirable, antenna radiation pattern distortion.

Brief description of the drawing

Our invention will be more fully understood, and other advantages and features of the invention will become apparent from the following detailed description of certain preferred embodiments of the invention. The detailed description is to be taken in conjunction with the accompanying drawing, in which:

FIGURE 1 is a perspective view of an aircraft nose radome having lightning protection strip assemblies in accordance with this invention installed thereon;

FIGURE 2 is a fragmentary perspective view of a first illustrative embodiment of the invention;

FIGURE 3 is a fragmentary perspective view of a second illustrative embodiment thereof;

FIGURE 4 is another fragmentary perspective view of a third illustrative embodiment thereof; and

FIGURE 5 is another fragmentary perspective view of a fourth illustrative embodiment thereof.

Detailed description of the preferred embodiments

FIGURE 1 shows a radome **10** which forms, for example, the forward part of the nose of an airplane (not shown). Lightning protection means according to our invention and including strip assemblies **12***a* and **12***b* are installed on the radome **10** in an arrangement or configuration as illustrated in FIGURE 1. The strip assemblies **12***a* and **12***b* are preferably bonded to the outer surface of the radome **10** longitudinally thereon and are spaced circumferentially about it. The strip assemblies can, of course, be structurally bolted to the radome **10**. However, such attachments should be limited to a minimum of places on the radome **10** since the drill holes required to accommodate the attachments must be carefully and completely sealed after installation. The longer strip assemblies **12***a* terminate at their forward ends approximately on the periphery of a circle **14**. The shorter strip assemblies **12***b* terminate at their forward ends approximately on the peripheries of respective circles, such as circle **16**, which each pass through the forward ends of a corresponding shorter strip assembly **12***b* and its two adjacent longer strip assemblies **12***a*. The arrangement or configuration of strip assemblies **12***a* and **12***b* on the

radome 10 is generally designed to provide full protection for a nose radome of an airplane with minimum drag or resistance to air and rain flow thereover.

The aft ends of the strip assemblies 12*a* and 12*b* are grounded at the base of the randome 10 to aircraft structure by connecting straps 18 or any other suitable connection means such as hinges, shear pins, or attach bolts. A radome area within a radius of, for example, approximately 9 or 10 inches from any point on one of the resistively conductive strip assemblies 12*a* or 12*b* will be adequately protected from a stroke of lightning since the stroke will be drawn to the point on the conductive strip assembly rather than through the radome to a point on the antenna thus causing physical damage to the radome and antenna. Accordingly, the radius of the circle 14 should not be greater than approximately 9 or 10 inches in order that the radome area within the circle 14 will be adequately protected. Similarly, the radius of the circle 16 should not exceed approximately 9 or 10 inches for the same reason. Other arrangements or configurations of resistively conductive strip assemblies similar to strip assemblies 12*a* and 12*b* can, of course, be provided on radomes of various shapes and sizes.

FIGURE 2 shows one illustrative embodiment of the lightning protection means according to this invention. A lightning protection strip assembly 20 includes a generally rectangular strip 22, and a series of metallic segments in the form of conductive buttons 24 affixed thereto and connected by resistance material 26. The strip 22 has rounded upper corners 22*a* and 22*b*, and a central lower channel 22*c* which extends the length of the strip 22. The channel 22*c* in this example has a rectangular cross section which is open along the lower face 22*d* of the strip 22. The buttons 24 can be rivets, for example, which are centrally riveted to the strip 22 such that the heads 24*a* are secured against the upper face 22*e* and spaced uniformly along the length of the strip 22. The lower ends 24*b* of the rivets or buttons 24 are compressively deformed within channel 22*c* to fasten the rivets 24 to the strip 22. The resistance material 26 is formed by brushing the material in liquid condition over the lower ends 24*b* of the rivets 24 to cover and connect the lower ends 24*b* fully in the channel 22*c*. The number of coats applied determines the resistance of the material 26. The upper side surfaces 22*f* and 22*g* along the strip 22 are preferably coated with neoprene to provide rain erosion protection therefor where required.

The resistance material 26 assists in the initiation and establishment of an ionization channel or path adjacent to the strip assembly 20 during a lightning strike when the strip assembly 20 is installed on a radome. The resistance material 26 also helps prevent corona discharge and sparking between the metallic segments or conductive buttons 24 during electrostatic and tribolectric charging (transfer of charge by particle impingement) of the spaced metallic segments. This, of course, prevents the invention from generating radio frequency noise which interferes with communication systems aboard the aircraft mounting the radome. In order to accomplish the foregoing functions, the resistance material 26 must have a sufficiently high strip resistance but obviously not so high as to approach that of an insulating material which would effectively separate electrically the metallic segments or conductive buttons 24.

The resistance material 26 is selected from appropriate materials by considering (1) the basic environmental characteristics of the material, (2) the electrical resistance or resistivity of the material, (3) the shape, size and spacing of the metallic segments used and (4) the overall length of the lightning protection strip assemblies.

In connection with the environmental characteristics of the resistance material, the selected material must, of course, perform satisfactorily where applicable in regards to its structural, thermal, electrical and weathering (rain durability, for example) properties in an operating aircraft's environment. It is desirable for the resistance material to have an electrical resistance or lineal resistivity above approximately 80,000 ohms per foot of strip length in order to initiate and establish an external ionization channel or path adjacent to a strip assembly during a lightning strike. As mentioned previously, lower resistances may result in an explosion or vaporization of the resistance material and thus destroy the strip assembly. If the resistance material has too low a resistance, re-radiation occurs when the strip assembly is located in the field of an antenna and causes undesirable distortion of the antenna radiation pattern.

The size and shape of the metallic segments in a strip assembly are physically limited essentially by the type of material used, and primarily limited by its permissible electrical size in terms of wave length. For radar transparent, radome lightning protection strip assemblies, the maximum dimension of the metallic segments should be less than approximately ⅛ wave length at the highest antenna operating frequency. The spacing between the metallic segments should be great enough to prevent sparking during maximum p-static (precipiation-static) charging rates and close enough together to establish ionization or arcing between segments during lightning strikes. Such spacing is, of course, also a function of the resistance material used to connect the metallic segments as discussed above.

Where long lightning protection strip assemblies are required, it is desirable to have various sections of the strip assemblies fabricated using respective resistance materials of different resistances. The section of the lightning protection strip assembly farthest from ground should, in most cases, have the righest resistance. The purpose of this is to develop a reasonably high voltage across a relatively small outer section rather than over the total length of the strip assembly and thus aid in the initiation of an external ionization channel or path in which arcing takes place during a lightning strike.

A lightning protection strip assembly 20 which can be used with antennas operating at or below approximately 10 gHz. (10 gigahertz or 10 kilomegacycles per second) can have the strip 22 fabricated from Fiberglas laminate material, the conductive buttons 24 can be MS20470A3 rivets, the resistance material 26 can be formed of type R–15SD resistive coating which is available from Electro Science Company of Philadelphia, Pennsylvania, and the side surfaces 22*f* and 22*g* can be coated with MIL–C–7439, Class 1, neoprene. Labeled illustrative dimensions indicated in FIGURE 2 includes D1=0.750, D2=0.100, D3=0.040, D4=0.200 and D5=0.208 (typical) inch.

It should be clearly understood, of course, that the particular types of materials and specific dimensions listed above are provided for illustrative purposes only. and are not intended to limit the scope of our invention in any manner. This is also true for any of the various types of materials and specific dimensions subsequently given.

The resistance material 26 covering and connecting the lower ends 24*b* of the rivets or buttons 24 has a selected strip resistance or lineal resistivity which is normally constant in ohms per foot of strip length. However, the resistance material 26 can be made to vary in resistance along the length of the strip 22. For example, the resistance of the material can be progressively reduced with distance from the forward end of one of the strip assemblies 12*a* and 12*b* in FIGURE 1 towards the aft end at the base of the radome 10. This progressive reduction in resistance or resistivity with distance from the forward end of a strip assembly can be varied in a continuous manner or in discrete increments. The electrical protection strip assemblies 12*a* and 12*b* are preferably made variable in resistance or resistivity with distance where the lengths of the strip assemblies are relatively long; e.g., approximately 8 or 9 feet and over.

It is, of course, simpler and more economical to fabricate the strip assemblies 12*a* and 12*b* with resistance ma-

terial which varies in resistance in discrete increments rather than in a continuous manner. In fact, separate strips such as strip 22 having resistance material 26 of constant resistance can be used to form a strip assembly by electrically connecting contiguous ends of adjacent strips together. In a strip assembly which is, for example, 12 feet long, three major sections each 4 feet long and having resistance material 26 of respectively constant resistances can be used. The resistances of the sections preferably differ progressively in powers of 10. Thus, the forward section of the exemplary strip assembly can have a resistance material 26 having a strip resistance of 8 megohms per foot, that of the intermediate section can have a resistance of 800 kilohms per foot and that of the aft section can have a resistance of 80,000 ohms per foot.

FIGURE 3 shows another embodiment of this invention. A lightning protection strip assembly 28 includes a lower base strip 30, a thin layer 32 of non-conductive neoprene thereon, followed by a resistively conductive layer 34 of neoprene, which embeds therein a series of spaced metallic wire segments 38, then by another resistively conductive layer 36 of neoprene and finally by a top cover layer 40 of non-conductive neoprene. Small gaps 42 are produced between the wire segments 38 during the process of fabricating the strip assembly 28. The base strip 30 can be, in certain instances, part of a radome itself.

The strip assembly 28 is illustratively fabricated by utilizing a Fiberglas laminate base strip 30 of appropriate length and applying thereon a layer 32 of Class 1 neoprene followed by a layer 34 of Class 2 neoprene. While this layer 34 is still tacky, copper wire segments 38 approximately ⅛ wave length long are pressed into the tacky layer 34 end to end centrally down the length of the strip 30. Another layer 36 of Class 2 neoprene is then applied over the layer 34 and the embedded wire segments 38. A top cover layer 40 of Class 1 neoprene is then applied over the layer 36. The ends of the wire segments 38 are separated by small gaps 42 so that the segments 38 are only connected by the resistively conductive layers 34 and 36.

A radome transparent, lightning protection strip assembly 28 which is suitable for use with antennas operating at or below approximately 10 gHz. can be fabricated, for example, with Fiberglass laminate 1/16 x ¾ inch stock for the base strip 30, Class 1 neoprene 0.010 inch thick for the layers 32 and 40, Class 2 neoprene 0.010 inch thick for the layers 34 and 36, and No. 26 copper wire for metallic segments 38 which are 0.150 inch long with gaps 42 of approximately 0.020 inch therebetween.

FIGURE 4 illustrates another embodiment of a strip assembly 44 which includes a base strip 46 having a channel 46*a* with inwardly beveled sides 46*b* to accommodate and retain metallic plate segments 48 that are spaced from each other by separating resistance material 50. The channel 46*a* is open and extends centrally along the upper face of the base strip 46. The plate segments 48 have beveled sides which complement the beveled sides 46*b* of the channel 46*a*. The beveled sides of the channel 46*a* and of the plate segments 48 are inclined inwardly toward the center of the strip 46 at angles of, for example, 60 degrees from vertical.

As in the previous examples, a radome transparent, lightning protection strip assembly 44 which is suitable for use with antennas operating at or below approximately 10 gHz. can be fabricated, for example, with Fiberglas laminate material for the base strip 46, 0.032 inch thickness sheet aluminum for the plate segments 48 and type R–14 resistive coating for the resistance material 50. Labeled illustrative dimensions indicated in FIGURE 4 include D6=0.750, D7=0.100, D8=0.060, D9=0.250, D10=0.150 and D11=0.020 (typical) inch.

FIGURE 5 shows another exemplary embodiment of a strip assembly 52 which includes base strip 54, metallic sprayed segments 56 and protective coatings 58 provided between the sprayed segments 56 and, if desired, on the sides of the base strip 54. The base strip 54, in this example, is a generally rectangular cross section strip of suitable length and made of appropriate resistance material. The sprayed segments 56 are obtained by providing a layer of spray metal less than approximately 0.003 inch thick on the base strip 54 on longitudinally spaced rectangular areas on the upper surface thereof.

The base strip 54 is illustratively a type 2 resistance strip manufactured and sold by International Resistance Company of Philadelphia, Pennsylvania. The sprayed segments 56 can be formed from type E-Kote 40 spray metal which is available from Epoxy Products, Inc. of Irvington, NJ. The coatings 58 can be Class 1 neoprene, for example, applied on the upper surface of the base strip 54 between the sprayed segments 56 to provide rain erosion protection for such areas where desired. These coatings 58 can be approximately 0.010 inch thick.

A satisfactory radome transparent, lightning protection strip assembly 52 which is suitable for use with antennas operating at or below approximately 10 gHz. can have dimensions as labeled in FIGURE 5 wherein D12=0.250, D13=0.027, D14=0.150 and D15=0.020 (typical) inch. As is the case with the other lightning protection strip assemblies, the strip assembly 52 is preferably bonded onto a radome surface in an appropriate configuration, rather than being structurally bolted thereto.

Although our lightning protection means is intended to be used primarily on aircraft radomes, it can be obviously adapted for use on ground radomes, shipboard radomes, and other structures. The strip assemblies can also be curved or otherwise shaped or molded, and it is to be understood that the particular embodiments of our invention described above and shown in the drawing are merely illustrative of, and not restrictive on, the broad invention and that various changes in design, structure and arrangement may be made without departing from the spirit and scope of the appended claims.

We claim:

1. Lightning protection means comprising:
a series of spaced conductive segments having at least a portion of each of said segments located closely to a potential lightning producing environment; and
resistance material connecting said segments in series, the spacing of said segments and the resistance of said material being selected to prevent corona discharge and sparking between said segments during any electrostatic and triboelectric charging thereof and to initiate and establish ionization between said segments during one and more lightning strikes thereon, whereby generation of radio frequency noise through any electrostatic and tdiboelectric charging is prevented and travel in and damage to said material by a main, high current, portion of each lightning strike are prevented, respectively.

2. The invention as defined in claim 1 wherein said segments have a maximum dimension less than approximately ⅛ of a wave length of the highest operating frequency of an associated antenna, and said resistance material has a resistance above approximately 80,000 ohms per foot and below approximately 800 megohms per foot of length in a direction generally along said segments connected resistively in series.

3. The invention as defined in claim 1 wherein said segments include metallic buttons.

4. The invention as defined in claim 1 wherein said segments include lengths of metallic wire.

5. The invention as defined in claim 1 wherein said segments include metallic plates.

6. The invention as defined in claim 1 wherein said segments include spray metal portions.

7. Lightning protection means comprising:
a series of spaced conductive segments; and
resistance material connecting said segments in series, said resistance material being variable in resistance

with distance in a direction generally along said segments connected resistively in series.

8. Lightning protection means comprising:

a nonconductive strip having a lower channel extending along the length thereof;

a series of spaced conductive segments, said segments having a maximum dimension less than approximately ⅛ of a wave length of the highest operating frequency of an associated antenna and including metallic buttons affixed to an upper surface of said strip with lower ends of said buttons positioned within said channel; and

resistance material connecting said segments in series, said resistance material having a resistance above approximately 80,000 ohms per foot and located in said channel covering and connecting the lower ends of said buttons.

9. The invention as defined in claim 7 wherein the resistance of said resistance material varies continuously with distance in a direction generally along said segments connected resistively in series.

10. The invention as defined in claim 7 wherein the resistance of said resistance material varies in discrete increments with distance in a direction generally along said segments connected resistively in series.

11. The invention as defined in claim 1 wherein said segments have a maximum dimension less than approximately ⅓ of a wave length of the highest operating frequency of an associated antenna, and said resistance material has a resistance above approximately 40,000 ohms per foot and below approximately 500 megohms per foot of length in a direction generally along said segments connected resistively in series whereby a small amount of distortion could be produced in the radiation pattern of said associated antenna.

12. The invention as defined in claim 1 further comprising a radome structure for housing said associated antennas and including a plurality of said lightning protection means thereon, said segments each having a selected maximum dimension and spacing therebetween to prevent said segments from re-radiating effectively at the operating frequencies of said associated antennas, and said resistance material having a selected resistance above approximately 10,000 ohms per foot and below approximately 500 megohms per foot to provide radio frequency isolation between said segments and produce arcing across the spacings between said segments during the initial phases of each lightning strike to create an ionized path adjacent thereto for the main, high current, portion of the lightning strike to follow.

References Cited

UNITED STATES PATENTS

958,454	5/1910	Wirt	313—325 X
2,891,194	6/1959	McStrack	315—36

FOREIGN PATENTS

578,664	7/1946	Great Britain.

JAMES W. LAWRENCE, *Primary Examiner.*

U.S. Cl. X.R.

313—308, 325; 315—59, 189, 324; 317—69, 70

Appendix 4.1

Action integral of a double exponential wave

An applied impulse voltage, v, is given by

$$v = V_k(e^{-at} - e^{-bt}) \text{ where } a=1/T_d \; ; \; b=1/T_r \; ; \; V_k = \text{constant}$$

T_d = time constant of decaying exponential

T_r = time constant of rising exponential

and $a \ll b$

With no flashover, current through the segmented strip is proportional to the voltage impressed - neglecting intersegment capacitance and capacitance to ground.

Therefore,

$$I \propto V_k(e^{-at} - e^{-bt})$$

$$\text{and the action integral} = \int_o^t I^2 \, d\tau$$

$$\propto \int_o^t V_k^2(e^{-2a\tau} - 2e^{-(a+b)\tau} + e^{-2b\tau}) \, d\tau$$

$$\propto V_k^2 \left[\frac{e^{-2a\tau}}{-2a} + \frac{2e^{-(a+b)\tau}}{a+b} - \frac{e^{-2b\tau}}{2b} \right]_o^t$$

$$\propto V_k^2 \left[\frac{2e^{-(a+b)t}}{a+b} - \frac{e^{-2at}}{2a} - \frac{e^{-2bt}}{2b} + \frac{1}{2a} - \frac{2}{a+b} + \frac{1}{2b} \right]$$

$$\propto V_k^2 \left[\frac{2e^{-(a+b)t}}{a+b} - \frac{e^{-2at}}{2a} - \frac{e^{-2bt}}{2b} + \frac{(a-b)^2}{2ab(a+b)} \right]$$

For a unit magnitude 1/50-μs current wave,

$$V_k = 1.036$$

$$a = 0.0146 \times 10^6$$

$$b = 2.56 \times 10^6$$

then the action integral for the full impulse current

$$= \frac{V_k^2(a-b)^2}{2ab(a+b)}$$

$$= 36.13 \times 10^{-6} \; A^2s$$

For a unit magnitude 250/2500-μs current wave,

$$V_k = 1.1035$$

$$a = 0.0314 \times 10^4$$

$$b = 0.016 \times 10^6$$

Appendix 4.1 (continued)

The action integral up to the crest of the wave is obtained by substituting t = 250 μs into the equation.

Thus, the action integral = 173×10^{-6} A^2s

This value is about 5 times the action integral of a full lightning impulse. Since the applications of full lightning impulses result in damage to a segmented strip, then the applications of switching impulses will inevitably result in damage to the strip even if flashover were to occur before the time-to-crest in a series of tests at the V_{50} level.

Appendix 4.2

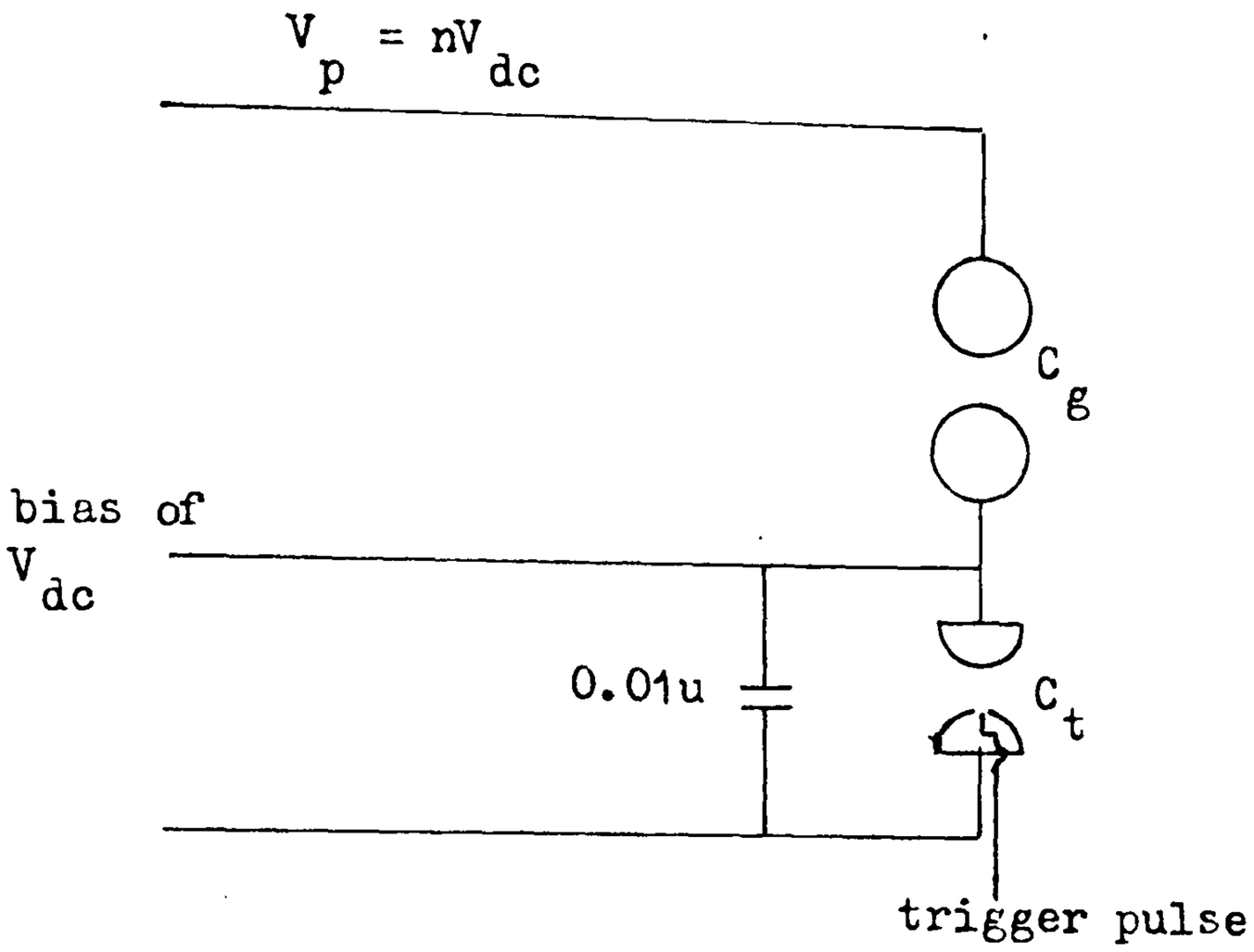

Let the capacitance of the upper gap be C_g in pF.

Total capacitance of lower gap $\simeq$ 0.01 uF because capacitance of triggered gap, C_t, $\ll$ 0.01 uF.

Under impulse conditions, the maximum instantaneous voltage across the lower gap

$$\simeq \left(\frac{C_g}{C_g + 10000}\right) V_p + V_{dc}$$

$$\simeq \frac{C_g nV_{dc}}{C_g + 10000} + V_{dc}$$

Therefore, maximum increase $\simeq \frac{nC_g V_{dc}}{C_g + 10000}$

maximum percentage increase $\simeq \frac{100nC_g}{C_g + 10000}$ %

For a plane electrode gap, $C_g \simeq \frac{A\epsilon_o}{d} \simeq$ 700 pF for a gap of 1 cm and an electrode of 1 m diameter.

Using a breakdown stress of 30 kV/cm and a minimum applied voltage of 90 kV, the maximum value of $C_g \simeq$ 230 pF.

Appendix 4.2 (continued)

Therefore, if n = 9 or 7,

maximum percentage increase $\simeq$ 20% or 16% respectively.

As the actual value of C_g would be higher, the percentage overvoltage would be greater than 20 or 16 respectively. This would definitely cause a self-breakdown of the lower gap. As the capacitance of a sphere gap[83], using 1-m diameter spheres and having a 3-cm gap, is at least 5 times smaller, the maximum percentage increase would be reduced considerably. For example, taking the capacitance of a 3-cm sphere gap as 40 pF, the maximum percentage increase for n = 9 or 7 is 3.6 or 2.8 respectively.

Appendix 4.3

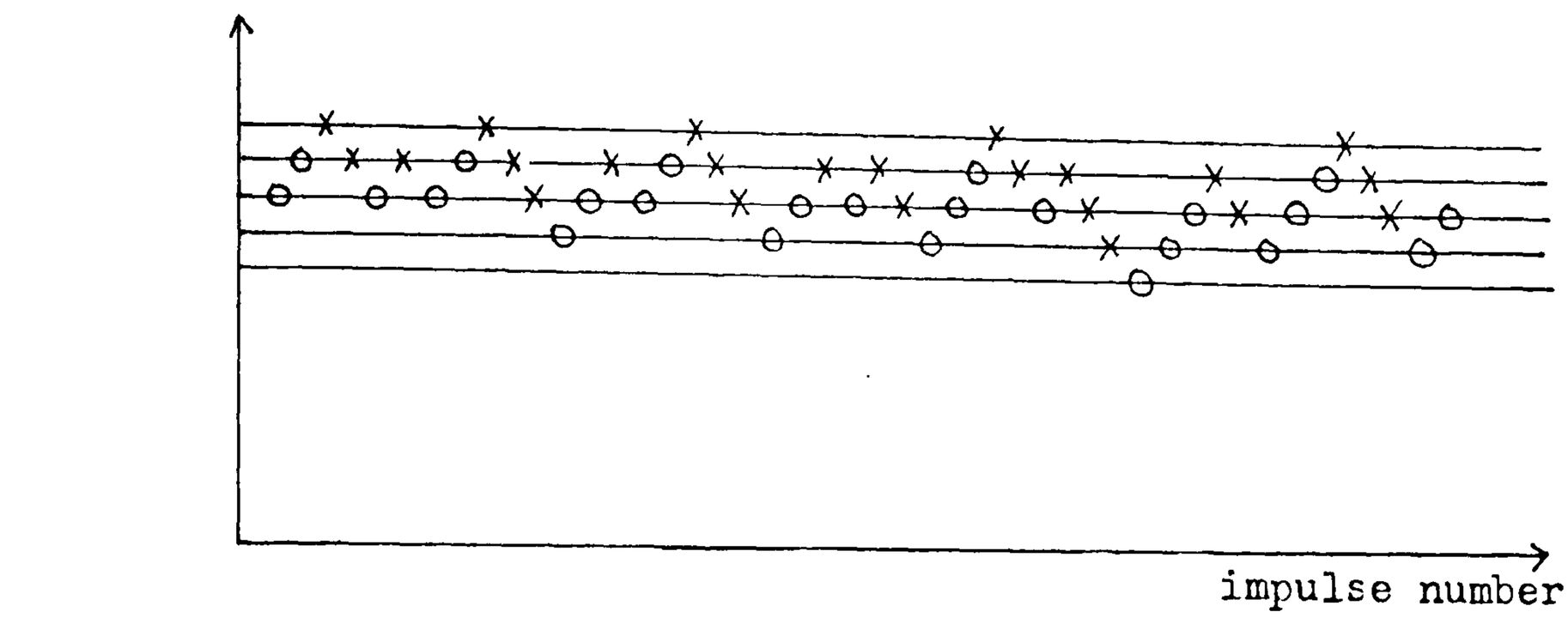

In the calculation of the 50% flashover voltage, V_{50}, normal distribution of the results is assumed.

Flashovers are denoted by crosses and withstands by noughts.

Only the number of flashovers or the number of withstands are used depending on which is the smaller total.

Let N denote the smaller total and let n_o, n_1, n_2, ... n_k denote the frequencies at each level for this less frequent event where n_o corresponds to the lowest level and n_k the highest level on which the event occurs.

The estimate of the mean and standard deviation are made using the moments

$$A = \sum_{i=0}^{k} i\, n_i$$

and $$B = \sum_{i=0}^{k} i^2 n_i$$

The mean is then given by

$$V_{50} = y_o + \delta\left[\frac{A}{N} \pm 0.5\right]$$

where y_o is the applied voltage at the lowest level on which the less frequent event occurs,

δ is the step-change in applied voltage and the plus sign is used when the analysis is based on the withstands,

and the standard deviation, s, by

Appendix 4.3 (continued)

$$s = 1.62\delta \left[\frac{NB - A^2}{N^2} + 0.029 \right]$$

and is fairly accurate when $\frac{NB - A^2}{N^2} > 0.3$

To obtain the confidence intervals, C.I.,

$$C.I. = V_{50} \pm z\, s_m$$

where $z = 1.96$ for a 95% confidence interval

and s_m = standard deviation of the mean

$$= Gs/\sqrt{N}$$

where G is a correction factor based on δ/s and given graphically in Dixon and Mood[74].